Deformation Behaviour of Pharmaceutical Excipients and Compressed Tablets

by

Peter John Rue

A thesis presented for the degree of

DOCTOR OF PHILOSOPHY

of the

University of Aston in Birmingham.

March, 1978.

Deformation Behaviour of Pharmaceutical Excipients and Compressed Tablets

by Peter John Rue

Submitted for the degree of Doctor of Philosophy, 1978.

By attaching a displacement transducer to the moving lower platten of a diametral compression testing instrument, the deformation behaviour of tablets prepared from five direct compression excipients has been studied. The resistance of the tablets to mechanical damage was determined by multiple diametral impact testing using a modified jolting volumeter. The tensile strength did not adequately characterise the mechanical properties of the compressed tablets. Better characterisation was achieved using the area under the diametral load-displacement curves calculated by numerical integration; this parameter, termed work of failure, depends on both the tensile strength and deformation behaviour of a tablet and is related to its resistance to damage as assessed by multiple diametral impact testing. A linear correlation was established between the work of failure and the number of impacts required to cause failure. Tablets of plastically deforming material possessed a higher work of failure and greater resistance to mechanical damage than tablets of brittle materials because plastic materials are able to resist crack propagation.

The deformation behaviour of tablets prior to failure was studied by loading tablets, at four rates of platten movement, to various percentages of their breaking force, followed by unloading. Using this technique the deformation of Elcema and Sta-Rx tablets was found to be considerably more strain rate dependent than the deformation of similar tablets of Emcompress or anhydrous lactose. By applying the Heckel equation to compaction data obtained at different dwell times, it was shown that the amount of consolidation during compaction of Elcema and Sta-Rx is much more strain rate dependent than the consolidation of Emcompress and anhydrous lactose. The results obtained suggest that consolidation behaviour of a powder can be deduced from the deformation of tablets during diametral loading, but such inferences are complicated by factors such as work hardening of sodium chloride which causes embrittlement of the material and the high strain rate sensitivity of Sta-Rx which alters considerably the relative amounts of plastic and elastic deformation at different strain rates.

Stress relaxation data obtained both during compaction and for tablets subjected to diametral loading could not be described by a simple Maxwell model, but the results provided useful qualitative information about plastic flow during compaction.

Using, as an example, two batches of a commercial microfine cellulose having markedly different compaction properties, the usefulness of the proposed experimental techniques is discussed. Such techniques might be suitable for establishing physico-mechanical specifications for drugs and excipients in order to minimise inter-batch variation and associated problems.

To my Parents

ACKNOWLEDGEMENTS

My sincere thanks are due to the following:-

The University of Aston, for the award of an Aston studentship

Professors M.R.W. Brown and D.G. Wibberley, for allowing me the use of the facilities of the Department of Pharmacy in which the work was undertaken.

Mr G.N. Elson, for technical assistance throughout the period of this work.

Mr H. Arrowsmith and the staff of Aston Services Ltd., for their help with the building of the diametral compression testing instrument.

Mr T. Slimak, for allowing me the use of the Mayes Universal Testing Instrument.

The Department of Mineral Engineering of Birmingham University, for the use of the helium-air comparative pycnometer.

Miss S.A. May, for help and encouragement during the preparation of this thesis.

Finally, I am grateful for the help, guidance and encouragement offered to me by my supervisor Dr John Rees throughout the period of this work.

Index

Page number

List of Figures

List of Tables

1. INTRODUCTION

1.1 The Process of Compaction

The process of die compaction in the pharmaceutical sciences has been the subject of several reviews. The most recent review relating specifically to tablet technology is that by Cooper and Rees (1972), but a chapter by Rees (1978) also covers more recent work. Some areas of compaction research relevant to the work reported in this thesis are considered in the following sections.

Much research, both of other workers and also that presented in this thesis, attempts to provide the formulation scientist with sufficient fundamental knowledge of the tabletting process to enable him to adopt a systematic approach to formulation design.

1.1.1 Mechanisms of compaction

Compaction of particulate material in a die occurs by several mechanisms as proposed by Seelig and Wulff (1947).
The mechanisms are:-

1. Rearrangement and closer packing of particles;
2. Elastic and plastic deformation of particles;
3. Bond formation, with or without fragmentation of the particles.

It is not usually possible to identify clear stages in the process since several mechanisms may occur simultaneously.

Train (1956), studying the compaction of magnesium carbonate suggested that it may be possible to distinguish stages of compaction from changes in slope of the relationship between the relative volume and the logarithm of applied pressure. Train (1956) proposed a further mechanism, being the elastic compression of the solid material itself at high pressure.

Birks and Muzaffar (1971) studied the low pressure consolidation of powder. They identified four types of re-arrangement, such as simple particulate repacking and localised melting of asperities under high local stresses. Hersey and Rees (1970) suggested that rearrangement of sodium chloride particles, at low compaction pressures may explain deviation from linearity of a Heckel plot (see section 1.4). However the re-arrangement stage was not observed for sodium chloride by Hersey, Cole and Rees (1973). According to Hersey, Rees and Cole (1973) the difference in the two observations may be attributed to the much larger, 33 mm, diameter die used by Hersey, Cole and Rees (1973) compared to the 12 mm diameter die used by Hersey and Rees (1970). Whether rearrangement occurs at low applied compaction pressures will depend on the ratio of the particle size to the die diameter and also on the packing configuration adopted by the powder as it is introduced into the die. For example, particles of a powder with poor flow characteristics may protect relatively large voids by bridging and would thus be expected to undergo considerable rearrangement at low applied pressures.

1.1.2 Inter-particulate bond formation

The formation of inter-particulate bonds during compaction

depends on the particles being brought into intimate contact so that surface forces interact. Thus the deformation and failure properties of a material will be important in the compaction process. Stewart (1950) suggests that the ease with which a particulate material forms a compact depends on the ability of the material to undergo plastic flow. Hardman and Lilley (1973), using specific surface area and pore volume measurements and also using scanning electron photo-microscopy, found that sodium chloride consolidates by plastic flow whereas coal and sucrose consolidate mainly by particle fragmentation. The strength of the sodium chloride compacts was greater than that of either coal or sucrose and these authors state that the strength of the bond between two surfaces is determined mainly by the area of intimate contact. Thus it would be expected that the plastically deforming sodium chloride would produce a strong compact. Furthermore to produce a strong compact, the region of inter-particulate contact must be clean and free from adsorbed contaminants such as oxide layers or moisture. Shotton and Rees (1966) found that an increase in moisture content decreased the crushing strength of sodium chloride tablets, presumably by reducing inter-particulate bonding.

Cole, Rees and Hersey (1975) reported that sodium chloride and potassium chloride consolidated by plastic flow whereas potassium citrate and lactose consolidated by fragmentation. The breaking strength of tablets prepared from the plastic materials was greater than that of the material which underwent fragmentation. In a study of the compaction of various polymorphic crystal forms of sulphathiazole, barbitone and aspirin, Summers, Enever and Carless (1976) found that as the yield strength of the sulphathiazole and barbitone polymorphs decreased the residual radial stress decreased and the maximum stress transmitted to the die wall increased. Conversely, as

the yield stress of the aspirin polymorphs decreased, the residual radial stress increased and the maximum radially transmitted stress decreased. These authors state that plastic flow will occur more easily in structures having high potential energy which is equivalent to a low yield stress. A high maximum radially transmitted stress is expected with a plastic material but this would be expected to be associated with a high residual radial stress. However, Higuchi, Shimamoto and others (1965) have shown that residual die wall stress decays, with time, after compaction and before ejection due to plastic flow of the material. The time required for decompression, in the work of Summers, Enever and Carless (1976), was 5 seconds. Thus during decompression, plastic flow of the sulphathiazole and barbitone occurred under the influence of the die wall stress. The relatively slow decompression allowed considerable plastic flow resulting in a value of residual die wall stress much lower than would be expected with the much shorter decompression times normally used in the tabletting process. Summers, Enever and Carless (1976) attribute the anomalous results for aspirin to work hardening (see section 1.5.4.) of the crystals which reduces the plastic flow of the material. Reducing plastic flow will decrease the maximum radially transmitted stress, but increase the residual die wall stress.

Shear forces have been shown to be important in the formation of compacts. For example Gregory, Rhys-Jones and Phillips (1959) increased the strength of coal briquettes by rotating the die during compaction, thus increasing the shear forces developed at the die wall. Train and Hersey (1960) also demonstrated the importance of shear forces. Compressing lead shot, Train and Hersey (1960) produced an intact compact, the interior of which was found to contain deformed but separate particles. The outer skin was produced by extensive plastic deformation and bonding of the lead shot in contact with the

die wall. This plastic deformation, aided by the shear forces, generated large areas of clean surface which, when in intimate contact, bonded together. Goetzel (1949) states that materials such as lead which form oxide layers very quickly, do not produce good compacts. Thus, although the lead shot used by Train and Hersey (1960) deformed plastically, little clean surface was formed, other than under the influence of shear forces, and no bonding occurred. A similar shear skin has been postulated for sodium chloride tablets by Rees and Shotton (1970).

The plastic deformation of materials can be examined either by stress relaxation experiments performed at constant strain or by measuring the change in thickness of a compact, with time, under constant load. This second method was used by Okada and Fukumori (1974) to show that potassium chloride could deform plastically whereas lactose could not. The first report of stress relaxation measurements on pharmaceutical systems was by Shlanta and Milosovich (1964). They found that materials which showed little stress relaxation formed poor tablets and that materials which showed very large relaxation also formed poor tablets. Materials which are capable of plastic flow transmit a considerably higher percentage of the applied force to the die wall than materials which do not deform plastically. Windheuser, Misra and others (1963) suggested that materials which transmit a high percentage of the applied force to the die wall tend to form good tablets, but Doelker and Shotton (1977) stated that good radial transmission alone is not sufficient to obtain good tablets, but must be accompanied by bonding properties which can absorb elastic recovery without rupture. During decompression, axial elastic recovery will occur and, combined with radial stress due to residual die wall force, may cause inter-

particulate bond rupture unless plastic flow of the bonds or particles accommodates the recovery. It is possible that the material studied by Shlanta and Milosovich (1964), which showed high stress relaxation indicating extensive plastic flow for 30 seconds after maximum force, but which did not form satisfactory tablets, could not deform plastically at the high compaction rates used by these authors to produce tablets, and thus considerable elastic recovery occurred.

Cole, Rees and Hersey (1975) studied the stress relaxation behaviour of four crystalline materials. They concluded that such measurements, together with determination of tablet strength, provide useful information concerning the compaction properties of the materials. Sodium chloride and potassium chloride were found to consolidate by plastic flow, these materials exhibiting relatively high stress relaxation after two minutes, whereas potassium citrate and lactose consolidated by particle fragmentation and exhibited relatively low stress relaxation after two minutes. Cole, Rees and Hersey comment that with a material like lactose which fragments under load, a strong compact may be expected due to bonding between newly created surface forced into close proximity. However, they found very weak compacts of lactose. They attribute this low strength to the large number of contact points which support the applied load so that the stress on each point contact is low. If, as shown by the relatively low stress relaxation, the plastic deformation of the contact is very small, the strength of the bond formed during compaction will be relatively low. Using stress relaxation measurements, David and Augsburger (1977) demonstrated the importance of plastic flow in relation to bonding. They found that, for materials which exhibited considerable stress relaxation, increasing the duration of the compression cycle increased the tensile strength

of tablets. In contrast, with materials for which the relaxation was small, the tensile strength of tablets did not change with the time of the compression cycle.

In an investigation of the physical processes of tabletting, Hiestand, Wells and others (1977) studied the stress relaxation of both the applied load and die wall force. They found that materials known to cap exhibited slower relaxation. Attempting to determine whether air entrapment could cause capping, Hiestand, Wells and others (1977), repeated their stress relaxation measurements in an evacuated die. There was no change in the general shape of the relaxation curves and these authors concluded that air escape must occur during the time required for application of force, which was between 0.4 and 0.7 seconds. Compression equipment which applies force at a rate similar to that in a high speed rotary tablet machine is required to clarify the effect of entrapped air.

1.1.3 Mechanisms of bonding

Goetzel (1949) reviewed the mechanisms of inter-particulate bonding in powders and classified them as inter-atomic forces, liquid surface cements and mechanical interlocking. In the case of most pharmaceutical powders inter-atomic or inter-molecular forces, which bond particles together, are the same forces as those which operate within the particle. Such forces include covalent bonding, van der Waals forces and hydrogen bonding. The remaining two types of inter-particulate bonding are created only between particles.

Liquid surface cements may be formed by either local melting of the material at the inter-particulate contact points or by deposition of dissolved material from liquid films around the particles. Rankell and Higuchi (1968) explained how the high stresses developed at the inter-particulate contact points could lower the melting point of the

material. A temperature increase has been seen during compaction by many workers; for example Hanus and King (1968) found that the temperature rise of sodium chloride tablets was linearly related to the compaction force and there was a linear relationship between the reciprocal of machine speed and the logarithm of tablet temperature. By inserting thermocouples through the die wall into the central region of a powder bed, Travers and Merriman (1970) were able to measure the internal temperature changes occurring during compaction and recompaction of some powders. These authors found a 16°C temperature rise for Asagran tablets and a 12°C rise for sodium chloride tablets compacted at 50 kN. However the thermal diffusivity of sodium chloride was much greater than Asagran; thus, at the relatively low rates of compaction used, the heat generated during compaction of sodium chloride will diffuse away from the high temperature areas causing a lower temperature rise than would be expected at higher rates of compaction. Recompressing the previously formed compacts, Travers and Merriman (1970) found a temperature rise lower than the initial rise, and on decompression a temperature fall was recorded. The temperature rise and fall on recompression and decompression could be reproduced indefinitely and was analogous to the adiabatic compression and expansion of a gas.

York and Pilpel (1972) studied the effect of temperature on the mechanical properties of some pharmaceutical powders and found that the tensile strength of the powders increased with an increase in temperature. The same authors later suggested (1973) that the heat generated by frictional effects during compaction, and the high temperatures at the points of contact are sufficient to cause asperity melting. As the heat diffuses away from the high temperature area or as the temperature falls on decompression, the molten material solidifies leading to the formation of solid bridges of material between the

particles. York and Pilpel (1973) suggest that the process of melting and solidification may contribute to the tensile strength of tablets, particularly where one or more of the components of the formulation has a low melting point.

Recrystallisation of dissolved materials has been shown, by Shotton and Rees (1966), to increase the strength of sodium chloride compacts. By compacting samples of sodium chloride of known moisture content and then drying some of the compacts, their wet and dry strength could be compared. In all cases Shotton and Rees (1966) found that dried compacts were stronger than their corresponding wet compact. Microscopic examination of the dried compacts showed that the increase in crushing strength was due to the recrystallisation of sodium chloride, from solution, forming solid inter-particulate bridges. Armstrong and Griffiths (1970) studying the changes in surface area of compacted powder systems found that addition of moisture to paracetamol and phenacetin granules decreased the surface area of the compact at all compaction pressures. Such a decrease in surface area indicates an increase in inter-particulate contact area which may be associated with an increase in compact strength. However, the aqueous solubility of the material must be considered and, since the solubility of phenacetin is very low, Armstrong and Griffiths (1970) state that the reduction in surface area of compacts containing moisture compared to the dry compacts is due to the moisture acting as a lubricant increasing the consolidation of the powder. This confirms earlier work by Shotton and Rees (1966) who showed that the presence of moisture decreased the force lost to the die wall during the compaction of sodium chloride. These authors attributed this to the lubricant effect of the moisture at the die wall. However, since the solubility of paracetamol is greater than phenacetin, the reduction in surface area of the paracetamol compacts containing moisture is due to both lubrication and to recrystallisation in fine cracks and around surface

discontinuities.

Mechanical interlocking may occur in some materials if the surfaces of the particles are irregularly shaped or possess projections. If plastic flow of the materials occurs the projections may become interlocked and increase the strength of the compact. However, as pointed out by Goetzel (1949), such projections need to be very strong to avoid being sheared off during compaction. It is unlikely that mechanical interlocking contributes greatly to the strength of tablets.

1.2 Direct Compression

Direct compression agents have been described by Gunsel and Kanig (1976) as inert substances which may be compacted with no difficulty even when mixed with quantities of drugs. Compared with wet granulation , direct compression mainly offers economic advantages since preparatory processing of the material is minimised, but may also be useful when the drug substance is sensitive to moisture or heat. The properties of an ideal direct compression agent have been listed by Kanig (1970), but no known material possesses them all. The desired properties are:-

1. The material should have a high fluidity or flowability.
2. It should have high compressibility.
3. It should be physiologically inert.
4. It should not show any physical or chemical changes on ageing and should be stable to heat, moisture and air.
5. It should have a high "capacity", which is defined as the amount of active ingredient which the diluents can carry in the direct compression technique.

6. It should be colourless and tasteless.

7. It should accept colourants uniformly.

8. It should be relatively inexpensive.

9. It should not interfere with the biological availability of active ingredients.

10. It should be compatible with all types of active ingredients.

11. It should have a particle size range equivalent to most active ingredients.

12. It should be capable of being reworked, without loss of flow or compressibility.

13. It should have a good pressure-strength profile.

Several investigations have examined the properties of specific direct compression agents. For example, Batuyios (1966) evaluated anhydrous lactose as a direct compression agent and found it to possess satisfactory direct compression and flow properties. The compaction properties of other forms of lactose have been examined by Fell (1972) and by Alpar, Hersey and Shotton (1970). Microcrystalline cellulose is another direct compression agent which has been widely investigated. Fox, Richman and others (1963) found that microcrystalline cellulose produces strong tablets and Reier and Shangraw (1966) noted its rapid disintegration characteristics. The direct compression properties of ten materials and their mixtures were compared by Lerk, Bolhuis and DeBoer (1974); the materials included dicalcium phosphate dihydrate (Emcompress), dextrose, directly compressible sugar and directly compressible starch. The properties of directly compressible starch have also been examined by Manudhane, Contractor and others (1969) who concluded that it has advantages over starch U.S.P. in that it produces a stronger tablet with equivalent disintegration times. However, Bolhuis, Lerk and

others (1975) found that a mixture of directly compressible starch and 0.5% w/w magnesium stearate could not be compressed into a tablet. Nevertheless, if a particular formulation requires a high disintegrant concentration, it is probably better to use directly compressible starch due to its improved compaction properties compared to ordinary starch. The disadvantages and problems associated with direct compression have been reviewed by both Khan and Rhodes (1973) and Gunsel and Kanig (1976).

One particular advantage of direct compression agents is in the study of the compaction process. Direct compression agents are usually single component systems compared with the multicomponent granulated systems and thus the compaction process is not complicated by binding agents or the effect of mixtures of materials. Jaffe and Foss (1959) used single component systems of a range of crystals to examine the compaction process and Lazarus and Lachman (1966) used potassium chloride to study the effect of particle size distribution, crystal shape, apparent bulk density and moisture content on the compaction process. Sodium chloride has also been widely used to study the processes of compaction and consolidation. For example, Shotton and Ganderton (1960) used sodium chloride tablets to examine the relationship between tablet strength and compaction force. Later Rees and Shotton (1971) studied the effect of moisture on the compaction process using sodium chloride as an ideal crystalline, particulate system. Recently, David (1974) has made a detailed study of the flow, packing and compaction properties of powders using single direct compression excipients.

1.3 Mechanical Properties of Tablets

1.3.1 Strength of tablets

The need to quantify the strength of tablets has long been recognised both in research into the compaction process and in industrial practice as a quality control parameter. As early as 1952, Higuchi, Arnold and others (1952) suggested that the resistance of tablets to mechanical wear is governed by the modulus of elasticity and tensile strength of the tablets. Later Shafer, Wollish and Engel (1956) attempted to quantify and predict the deterioration of tablets during packaging and handling by subjecting them to mutual attrition and mechanical shock in a Roche friabilator.

Probably the earliest method of assessing the strength of tablets is described by Nutter-Smith (1949a) as 'feel judgment'. Using this method the degree of firmness of the tablet was assessed by breaking the tablet between the fingers and thumb. Many technologists, even today, continue to judge tablet performance by the 'snap' or the sound emitted as the tablet breaks.

1.3.1.1 Diametral crushing

Because most pharmaceutical tablets are cylindrical in shape, the usual method of assessing the strength of tablets is to measure their resistance to diametral crushing when a force is applied to a tablet, across a diameter, until the tablet breaks. This property is often imprecisely referred to as hardness. However, true hardness is a surface property measured by the resistance to indentation under point load. The first instrument available for measuring the diametral crushing resistance was the Monsanto tester which Nutter-Smith (1949b) comments was in use as early as 1933.

Other testers such as the Strong-Cobb, Erweka and Pfizer, have been widely used by the pharmaceutical industry but, during the past decade these instruments have been criticised due to variation in measurements both between operators and between instruments. Ritchel, Skinner and Schlumpf (1969) found that the reproducibility of the results, with a definite apparatus depended on the operator; there was a significant difference in the results between operators for all the instruments tested, except the Pfizer and motorised Heberlein. Using a load transducer in place of a tablet, Brook and Marshall (1968) compared several instruments and found that variation in crushing strength values was due, in part, to inaccuracies in the instrument scale values and to varying methods of applying the load. They were able to show, for example, that spring fatigue in the Monsanto tester leads to increasing values of crushing strength as the instrument ages. These workers concluded that calibration of a particular instrument is necessary when a high degree of accuracy is required or when comparing results from different testing instruments. A further problem associated with comparison of results from different instruments is that of the effect of rate of loading. Rees, Hersey and Cole (1970) found a small increase in the crushing strength with an increase in the rate of loading. On the basis of a comparison of the Strong-Cobb and Schleuniger (Heberlein), Goodhart, Draper and others (1973) suggested that the Schleuniger tester has distinct advantages in that a uniform rate of force application is achieved, and there is less need for calibration checks. In order to overcome the variation due to rate of loading Shotton and Ganderton (1960) designed an instrument in which the load is applied via a motor driven screw and the applied force is monitored by strain gauges

bonded to a flexible spring plate. Using this equipment the strain gauge output could be continuously recorded allowing accurate measurement of breaking load.

1.3.1.2 The use of diametral compression to measure tensile strength

Carneiro and Barcellos (1953) first reported the use of a diametral compression test to measure the tensile strength of concretes and this test has since been used by other workers to determine the tensile strength of various materials such as coal (Barenbaum and Brodie, 1959), ceramics (Rudnick, Hunter and Holden, 1963), and pharmaceutical tablets of lactose (Fell and Newton, 1968).

The use of diametral compression to determine tensile strength, rather than simply crushing force, depends on the stress distribution set up within a disc under such loading. For a disc of an elastic, isotropic, homogeneous material under ideal diametral line loading, Timoshenko and Goodier (1970) showed that the tensile stresses, σ_x acting at right angles to the loaded diameter may be calculated from equation 1.1.

$$\sigma_x = \frac{2P}{\pi D t} \qquad \text{Eq. 1.1.}$$

where P = applied load

D = diameter of disc

t = thickness of disc

Under these conditions of loading there are also compressive stresses which vary in magnitude along the loaded diameter. The minimum compressive stress, σ_y is at the centre of the disc and is

given by equation 1.2.

$$\sigma_y = \frac{6P}{\pi D t} \qquad \text{Eq. 1.2.}$$

The compressive stress becomes infinitely high immediately under the line of loading and these high compressive stresses may prevent the initiation of failure in tension.

In practice ideal line loading will not be achieved and the load will be applied through a finite contact area. For a disc in diametral compression when the width of the contact area is one tenth of the specimen diameter, Peltier (1954) has shown that the tensile stress is constant over most of the loaded diameter except for the region near the loading area. Under these loading conditions the compressive and shear stresses have been considerably reduced compared to the case of line loading. It is then possible for failure to be initiated in tension and the tensile strength of the specimen may then be calculated from equation 1.1.

Rudnick, Hunter and Holden (1963) point out that the stress distribution within a specimen is controlled by the mechanical properties of both the specimen and the loading plattens. In pharmaceutical applications the specimen is relatively soft compared to the metal plattens; this will cause the tablets to deform and spread the load over an area thus reducing the shear and compressive stresses and allowing failure to be initiated in tension. If, however, the tablet has a high modulus of elasticity, line loading may be approached causing failure to be initiated in compression or shear. In this case Rudnick, Hunter and Holden (1963) suggested the use of soft padding material between the platten and the specimen. Fell and Newton (1970) adopted this technique when testing tablets of

crystalline and spray dried lactose. They found 3 pieces of blotting paper, each 0.3 mm thick, ensured tensile failure in these tablets. The various types of failure observed during diametral compression, when the correct loading conditions are not imposed, are shown in Fig. 1.1. The stress distributions producing such failure are discussed by Newton, Rowley and others (1971).

1.3.1.3 Pharmaceutical applications of diametral compression testing

Fell and Newton (1968) first applied the theory of diametral compression to the calculation of tensile strength of pharmaceutical tablets. This method of characterising tablets, rather than crushing force, has since been used by many workers including Goodhart, Draper and others (1973), York and Pilpel (1973) and David and Augsburger (1977).

Newton, Rowley and others (1971) originally suggested a correction to equation 1.1. to allow for the average porosity of the tablet. This correction is shown in equation 1.3.

$$\sigma_x = \frac{2P}{\pi Dt\ (1-e)} \qquad \text{Eq. 1.3.}$$

where e = fractional voidage

Rowe, Elworthy and Ganderton (1973) used the corrected equation to calculate the tensile strength of plastic matrix tablets. However, Newton (1974) later criticised the correction factor since it does not correct for the true area of inter-particulate contact, and does not allow for the distribution of porosity within the tablet. In response, Rowe, Elworthy and Ganderton (1974) pointed out that

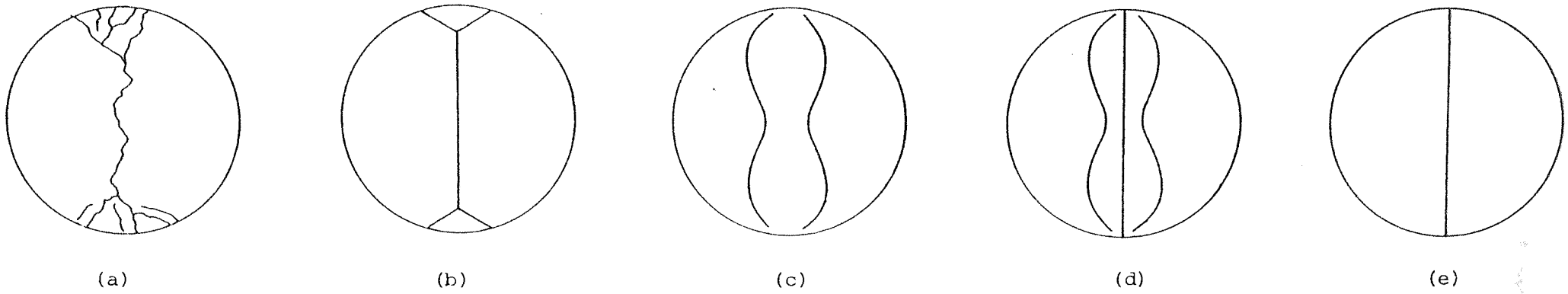

Fig. 1.1 Failure of tablets subjected to diametral loading.
(a) Compression failure locally at the loading points
(b) Failure under local shear at and near the loading points (c) Failure along maximum shear loci when point loading is applied (d)"Triple cleft" fracture (e) Ideal tensile failure (From Newton, Rowley and others, 1971).

for their particular system of non-porous, spherical, polymer particles with a very narrow size distribution, the contact area is proportional to (1-e) over the porosity range 0.1 to 0.4. They agreed however, that the use of the correction factor must be restricted to well defined particulate systems which fail at the interface created during compaction. Carless and Sheak (1975) also used equation 1.3. to calculate the tensile strength of tablets produced from sulphathiazole. However, the size distribution of the powder was larger than the polymer particles used by Rowe, Elworthy and Ganderton (1973) and little was known about the particle shape or porosity. Under these conditions the criticisms of Newton (1974) appear to be justified and the factor of (1-e) is not appropriate to calculate tensile strength.

Testing lactose tablets, Fell and Newton (1970) found a low variance in the value of tablet breaking load when the tablet failed in tension whereas, if this type of failure did not occur, there was a much larger variance. They also found that, unless failure occurred in tension, there was a significant difference in the breaking load between tablets tested with and without platten padding.

Rudnick, Hunter and Holden (1963) consider that there is no such value as true tensile strength, but that the values obtained for a particular set of experimental conditions are true for those conditions. Thus, in order to compare the tensile strength of tablets, the test conditions must be standardised. Newton, Rowley and others (1971) claim that calculation of tensile strength from the breaking load converts the value to a standard form and allows comparison of specimens of different dimensions.

1.3.1.4 Other methods of assessing tablet strength

A characteristic referred to as fracture resistance was

measured by Endicott, Lowenthal and Gross (1961) using a modified Strong-Cobb tester. In their test the tablet rested on two supports near to its circumference and the force was applied by a knife edge applied to the diameter of the tablets until failure occurred. David and Augsburger (1974) applied the theory of bending stresses in beams (see for example Jansen, Chenoweth and Parker, 1974) to a test similar to the three-point bending test of Endicott, Lowenthal and Gross (1961). Fig 1.2. shows diagrammatically the system used by David and Augsburger (1974) to test tablets by flexure. Using this flexure test, David and Augsberger (1974) calculated the tensile strength, σ_o of the tablets from equation 1.4.

$$\sigma_o = \frac{3Fb'}{4bh^2} \qquad \text{Eq. 1.4.}$$

where F = applied load at failure

b' = distance from fulcrum to fulcrum

b = tablet width

h = tablet thickness

David and Augsburger (1974) compared the tensile strength of tablets measured by both diametral compression and the flexure test and found very good agreement in the values of tensile strengths obtained from both methods. However, Rudnick, Hunter and Holden (1963) criticise the flexure test since the stress distribution developed is non-uniform.

The Roche friabilator was designed by Shafer, Wollish and Engel (1956) to quantify and predict the deterioration of tablets during packaging and handling. They found that tablets showing more than 1% loss in weight after 100 revolutions of the friabilator

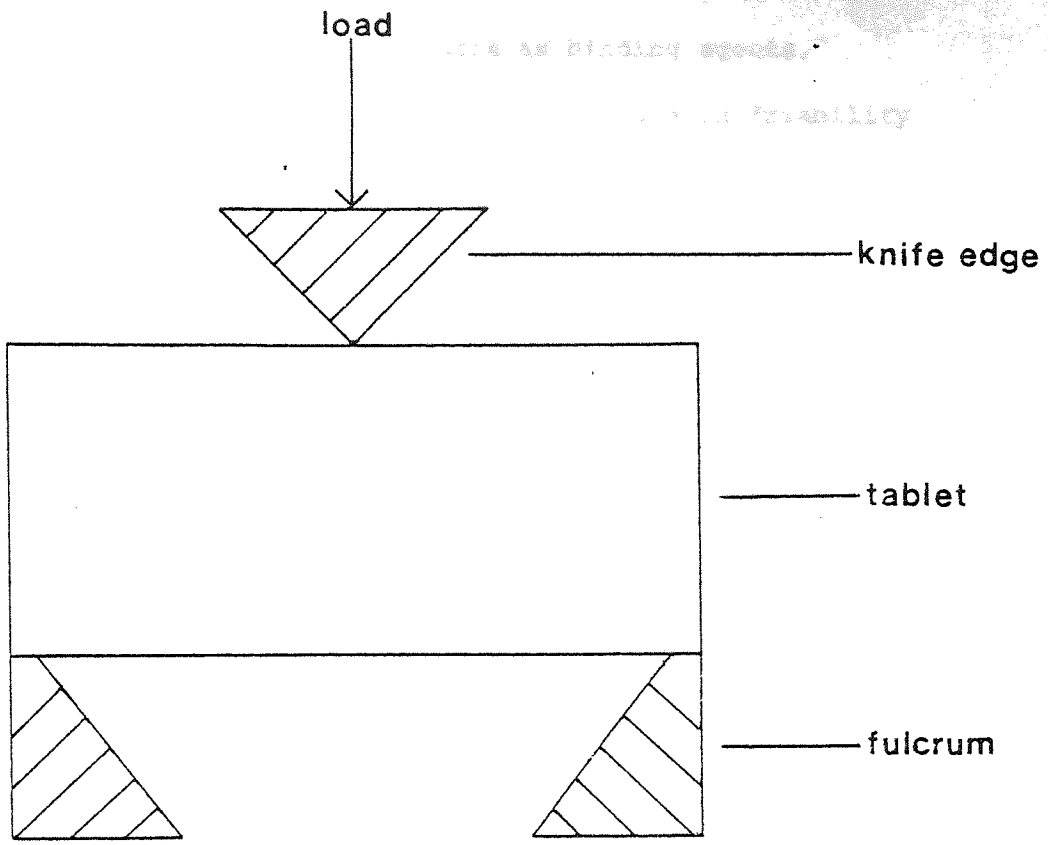

Fig. 1.2 The flexure test used by David and Augsburger (1974) to determine the tensile strength of tablets.

suffered an undesirable amount of breakage, chipping and surface loss of powder in practice. For lactose tablets containing various percentages of gelatin and acacia as binding agents, Sakr and Kassem (1972) found an exponential decrease in friability as the tablet strength increased.

1.3.2 Surface properties of tablets

Nutter-Smith (1949a) suggested that the resistance of a tablet to "wear and tear" must be influenced by the quality of the surface of a compressed tablet, but does not suggest a method of measuring surface properties. The surface property of a material, known as hardness, is commonly measured by indentation testing, whereby a small indentation is made in the surface by means of a hard steel sphere or diamond point, under a known applied load. Aulton (1977) has reviewed the use of indentation testing to determine the properties of pharmaceutical materials and has shown that this type of testing is a useful method for measuring some fundamental properties of materials, such as plasticity and elasticity. Hardness is defined as the resistance to local permanent deformation and Aulton (1977) criticised indentation testing of tablets on the grounds that the surface properties of the tablet may not be representative of its bulk internal properties. An extreme example of this was reported by Train and Hersey (1960). They showed that an intact compact may be formed from lead shot due to the high shear stresses developed at the die wall during compaction even though, within the compact, the lead shot was not bonded. Furthermore, if a material work hardens during compaction under the influence of the high shear and compressive stresses at the die wall and punch faces, the surface hardness of the tablet will be relatively high and will

not reflect the internal properties of the tablet.

1.4 Consolidation of Powder During Compaction

Changes in volume, and hence density of a powder bed subjected to a compaction force, have been widely investigated. In studying the compaction of magnesium carbonate, Train (1956) identified different mechanisms of compaction by changes in slope of the relationship between the relative volume and the logarithm of applied pressure. The mechanisms identified were rearrangement of intact particles, fracture and plastic flow of particles and finally elastic compression of the bulk compact. Many empirically derived equations have been proposed relating the volume changes to the compaction force. These equations have been reviewed by Kawakita and Tsutsumi (1966) and more recently by Kawakita and Lüdde (1970/71). Most of these equations were derived for metal powders and have found little use in pharmaceutical research. Bockstiegel (1973a) stated that compaction equations are of little practical value since such equations only fit the experimental data over a limited range of compaction pressure due to the large number of parameters which affect the compaction process but which are not represented in the equations. Furthermore, Bockstiegel (1973a) considers that compaction experiments are easy to perform and are more reliable than theoretical predictions.

One equation which has been investigated with regard to its application to pharmaceutical systems, is that derived by Heckel (1961a) who considered the compaction of powders to be analogous to a first-order chemical reaction, the pores being the reactant. The relationship proposed by Heckel (1961a) is given in equation 1.5.

$$\ln\left(\frac{1}{1-D}\right) = KP + A \qquad \text{Eq. 1.5.}$$

where D = relative density of the compact which may be calculated as the theoretical volume of the powder at zero porosity divided by the volume at pressure.

P = applied pressure

K and A are constants.

K is determined from the linear section of the plot relating ln(1/1-D) to compaction force, and A is determined by the intercept of the extrapolated linear section at zero applied pressure. A diagrammatic representation of the curves obtained by Heckel (1961a) for iron and copper powders, is shown in Fig. 1.3. The initial curved region was attributed by Heckel (1961a) to the densification which takes place by individual particle movement in the absence of inter-particulate bonding. In a discussion of a paper by Hersey, Cole and Rees (1973), Bockstiegel (1973b) stated that the Heckel equation is similar to several other powder compaction equations, the difference being that Heckel acknowledged that A is not a true constant as considered by other equations. Heckel (1961b) showed that A may be considered as the sum of two terms related to the apparent density of the powder. The two terms are: $\ln(1/1 - D_o)$, where D_o is the relative density of the loose powder at zero applied pressure, and B which is the densification which takes place by individual particle movement at low pressures before appreciable inter-particulate bonding takes place. Thus A will depend on the particle size relative to the die diameter, the size distribution of the powder, the amount of fragmentation occurring at low applied pressures and other factors which oppose consolidation of the powder such as electrostatic

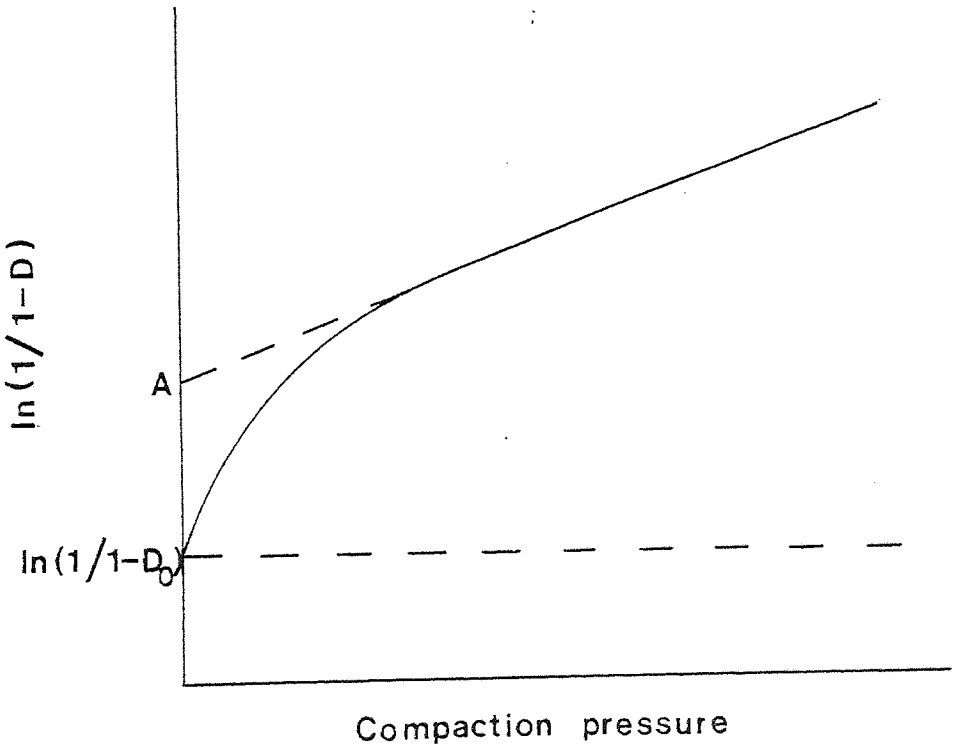

Fig. 1.3 A diagrammatic representation of the curves obtained by Heckel (1961a) for iron and copper powders.

repulsion, die wall friction and possibly entrapped air. The constant K, was shown by Heckel (1961b) to be related to the yield strength of the material, σ_o by equation 1.6.

$$K = \frac{1}{3\sigma_o} \qquad \text{Eq. 1.6.}$$

Hersey and Rees (1970) using the compaction data of Hersey, Bayraktar and Shotton (1967) found that, in a 12 mm diameter die, the Heckel plots for various particle size fractions of sodium chloride were non-linear up to an applied compaction pressure of 50 MN m^{-2}, whereas in later experiments (Hersey, Cole and Rees, 1973) using a 33 mm diameter die and various size fractions of sodium chloride, a completely linear Heckel plot was observed up to 60 MN m^{-2}. The larger diameter die used by Hersey, Cole and Rees (1973) apparently allowed close packing of the particles during die filling and so no rearrangement was seen at low pressures. Thus the curved section of the plots found by Hersey and Rees (1970), using data for a smaller diameter die, can be attributed to particle movement during rearrangement at low compaction pressures.

Using the data of Alpar, Hersey and Shotton (1970), Hersey and Rees (1970) also investigated the effect of lactose particle size on the Heckel plots. The amount of powder compacted was sufficient to produce a 4 mm thick compact at zero porosity in a 12 mm diameter die and the volume of the compacts was determined <u>after</u> ejection from the die. Under these conditions Hersey and Rees (1970) found that, above an applied pressure of 50 MN m^{-2}, the Heckel plots were identical and linear for all the size fractions studied. However, Hersey, Cole and Rees (1973) later studied the compaction behaviour of various size fractions of lactose in a

33 mm diameter die using equal volumes of bulk powder. In this study the volume of the compact was measured under load by monitoring the movement of the upper punch into the die. Under these conditions the Heckel relationship did not produce identical plots for the different size fractions of lactose. Evaluation of the slopes of the linear sections of the graphs showed that, as the mean particle size decreased, there was a tendency for the yield strength to increase. This increase in yield strength was attributed by the authors to the fact that, as the particle size is reduced, the probability of finding a crack is reduced. Fell and Newton (1971b), using crystalline lactose, found that different Heckel plots were obtained for different rates of compaction, and depending on whether the volume of a tablet was measured under load or after ejection from the die. They concluded that volume measurements made under load include an elastic component which will increase the value of ln(1/1-D) for a given compaction force, thus giving a false low value of the yield strength.

Hersey, Cole and Rees (1973) stated that the Heckel treatment of compaction data is strictly only applicable to plastically deforming systems, but that it can be used to elucidate consolidation mechanisms and to determine mechanical properties of powders such as their yield strength. Hersey and Rees (1971) reported that the two general types of Heckel plot observed might be used to differentiate between consolidation mechanisms. The two types of plot are shown in Fig 1.4. They state that type 1 plots are shown by different particle size fractions of a material which consolidates by plastic flow, whereas type 2 plots are shown by materials which consolidate by particle fragmentation. York and Pilpel (1973) demonstrated a third type of plot which is shown in

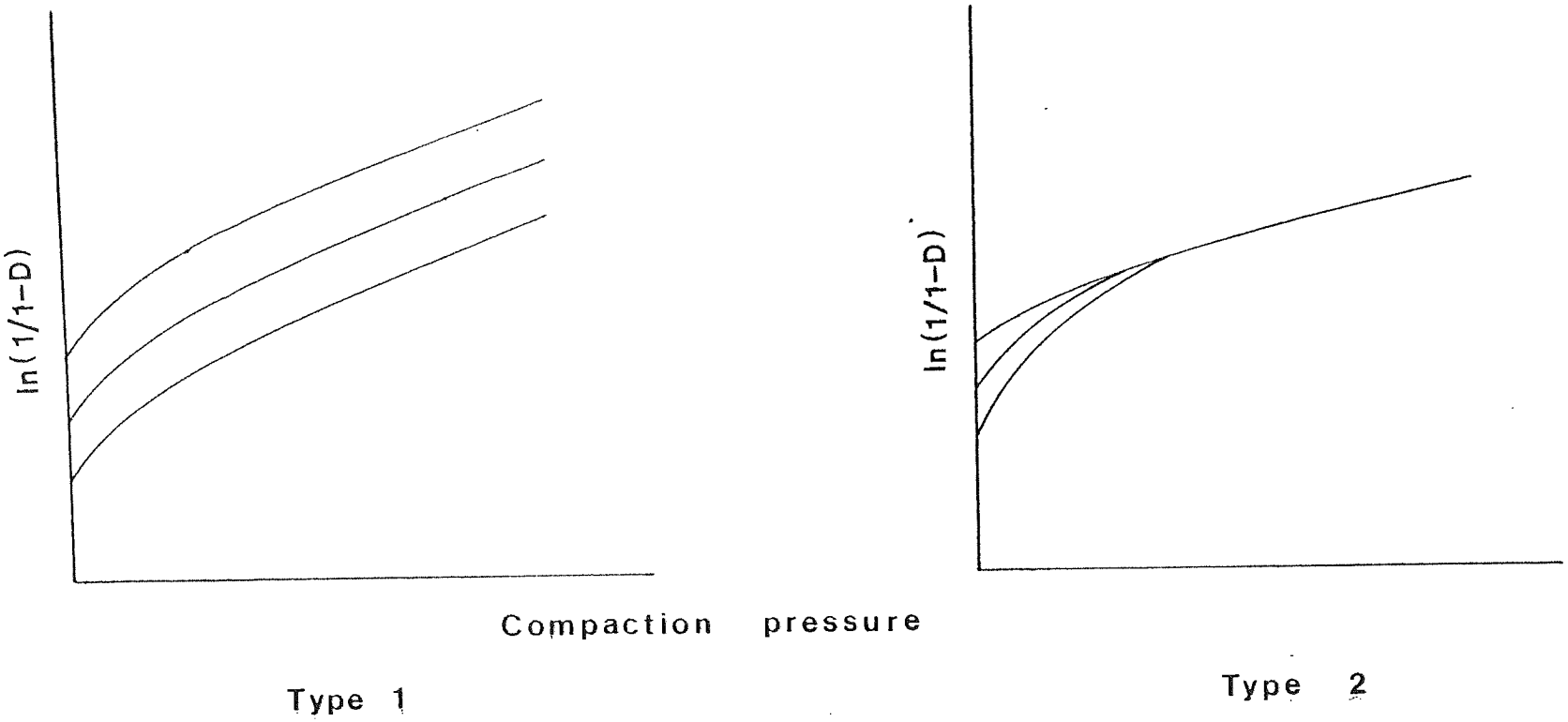

Fig. 1.4 Two types of Heckel plot suggested by Hersey and Rees (1971).

Fig 1.5. This type of plot was seen for some fatty acids and was attributed to the absence of a particle rearrangement stage coupled with plastic deformation and melting of asperities. Despite the work of Hersey, Cole and Rees (1973) and Fell and Newton (1971), which is discussed above and which has shown that the plots obtained will depend on the compaction conditions and the conditions of volume measurement, some workers including Jones (1976) and Esezobo and Pilpel (1977) continue to classify materials as type 1 or 2. This is unsatisfactory since a small change in the experimental procedure, such as a change in the die dimensions, can produce misleading information.

From the conflicting evidence presented here, it appears that inferences, regarding the compaction of materials, drawn from the use of the Heckel equation are only valid for the particular conditions under which the compaction data were obtained.

1.5. Plastic and Brittle Behaviour of Materials

The deformation behaviour of a material greatly influences its failure characteristics. The two types that are generally recognised - brittle and plastic - are characterised by the amount of irreversible deformation which occurs before failure.

1.5.1 Plastic Behaviour

Plastic deformation is characterised by a permanent deformation of the specimen under load. For example, in a true tensile test, a permanent elongation of the specimen is produced. During plastic deformation of crystalline materials, sections of the crystal glide past one another resulting in slip as shown in Fig. 1.6. Each slip is

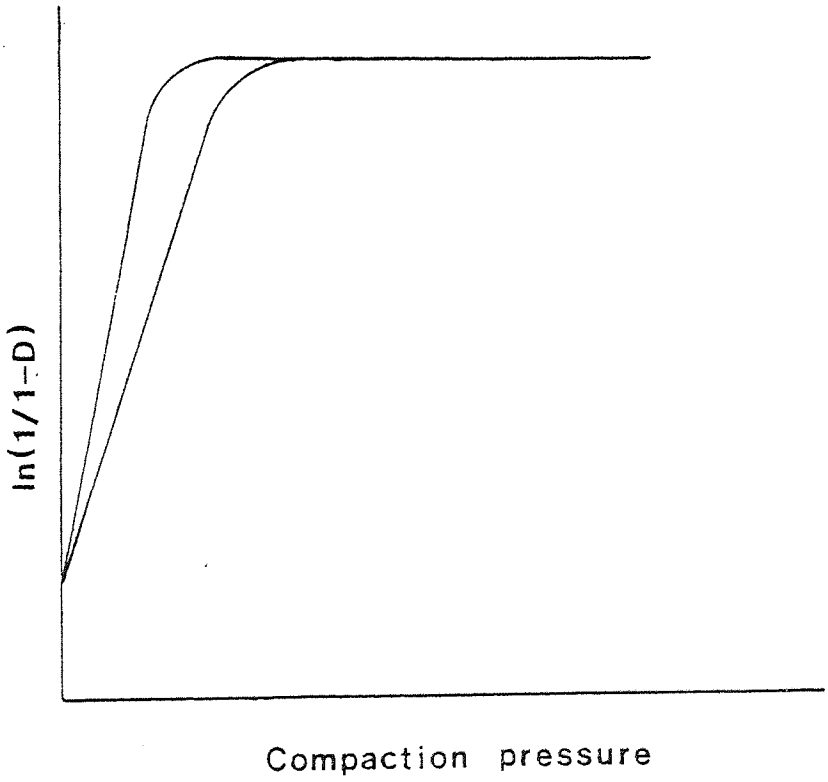

Fig. 1.5 Diagrammatic representation of the Heckel plots found by York and Pilel (1973) for some fatty acids.

a displacement, by a whole number of atomic spacings, in a certain glide direction. The crystal structure is preserved at the glide surfaces between the sections of the crystal, and the slip steps on the crystal's outer surface show the occurrence of glide. A crystal, under stress, can also deform plastically by a process called twinning. The material moves layer-by-layer to bring each deformed slab into mirror-image orientation relative to the un-deformed material. This process is shown diagrammatically in Fig. 1.7. This process is much less common than slip, but both slip and twinning can occur in some materials resulting in a permanent set or plastic deformation.

1.5.2 Dislocation theory

In general the stress required to produce plastic deformation is several orders of magnitude lower than the theoretically calculated values. This discrepancy led to the postulation of the existence of dislocations which are mobile defects in the crystal lattice. The movement of these dislocations requires considerably less stress than the theoretical stress required to deform a perfect crystal.

1.5.2.1 Dislocation types

Two main types of dislocation exist - edge and screw dislocations. An edge dislocation is found when either a row of atoms is removed from a lattice, or a row of atoms is displaced by a unit distance. The structure of an edge dislocation is shown in Fig. 1.8. Under a stress an edge dislocation moves

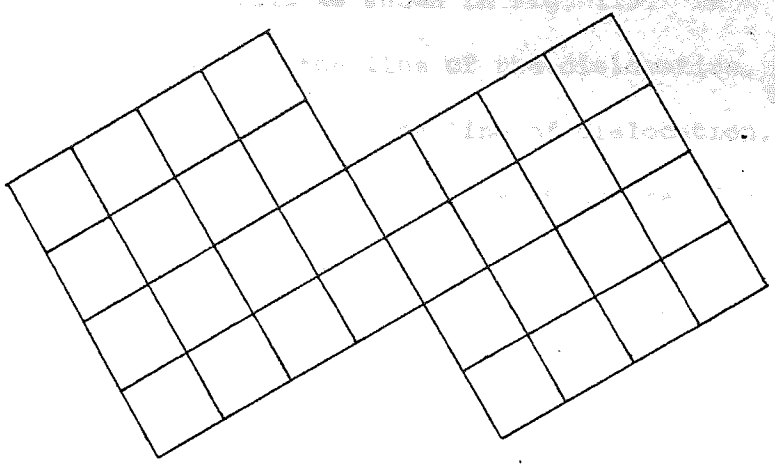

Fig. 1.6 Plastic deformation resulting from slip.

(From Cottrell, 1964.)

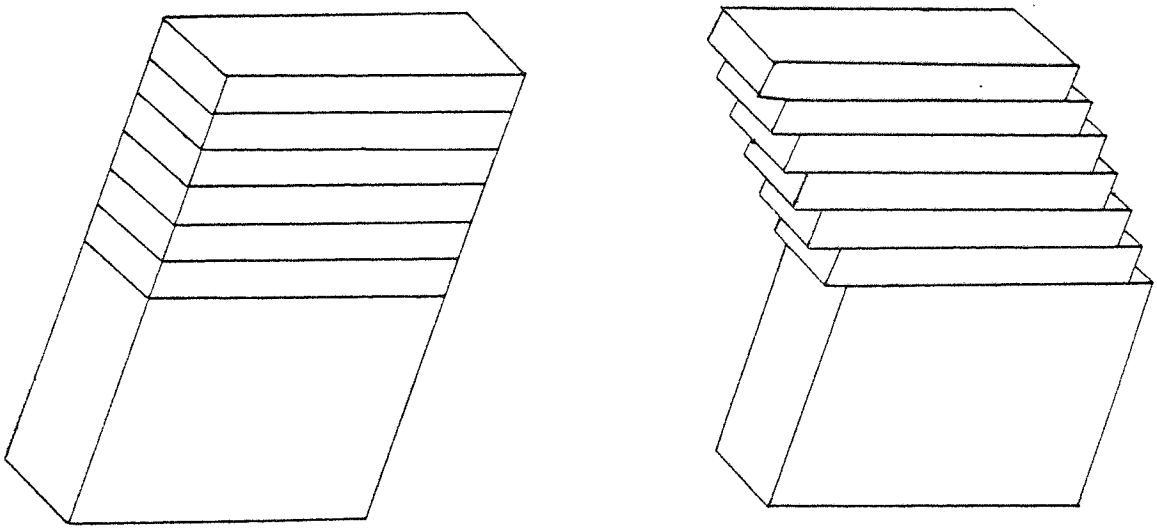

Fig. 1.7 Diagrammatic illustration of the twinning process.

(From Sinnott, 1958.)

through the crystal causing slip as shown in Fig. 1.9. In this case the slip is normal to the line of the dislocation. If, however, the slip is parallel to the line of dislocation, then a screw dislocation is responsible. The structure of a screw dislocation and the slip resulting from its movement are shown in Fig. 1.10.

Slip does not occur on all lattice planes, but is restricted to certain planes which are characteristic of the material. Generally the slip direction is parallel to the direction along which the atomic packing is most dense and the slip planes are those planes which have the largest inter-planar spacing. However, in some materials the critical stress at which slip occurs is such that slip is impossible before the specimen fractures. The effective number of slip planes in such a material is lower than other materials and they thus tend to be brittle.

1.5.2.2 Dislocation movement and inter-actions

Cottrell (1964) states that since inter-atomic bonding conditions can never be exactly the same over the whole of a glide surface, some areas must begin to slip before others. This results in a slip front which is an area of demarcation between a slipped and an unslipped area and which moves across the glide surface as slip continues. The mobility of dislocations is discussed in detail by Smallman (1970) who states that dislocation mobility depends on the width of the dislocation. The width is the number of atomic distances over which the slip front is spread. Wide dislocations are highly mobile; thus materials containing them are intrinsically soft and will undergo plastic deformation. Conversely, narrow dislocations are much less mobile and lead to intrinsic hardness and brittleness.

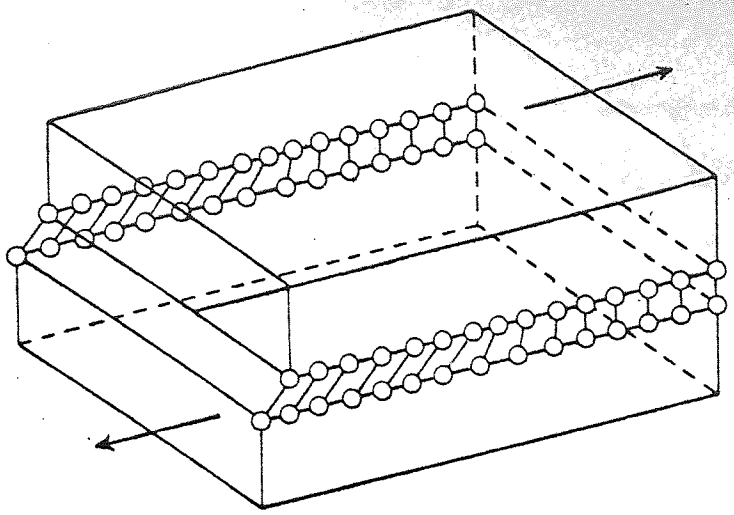

Fig. 1.8 Structure of an edge dislocation. (From Cottrell, 1949).

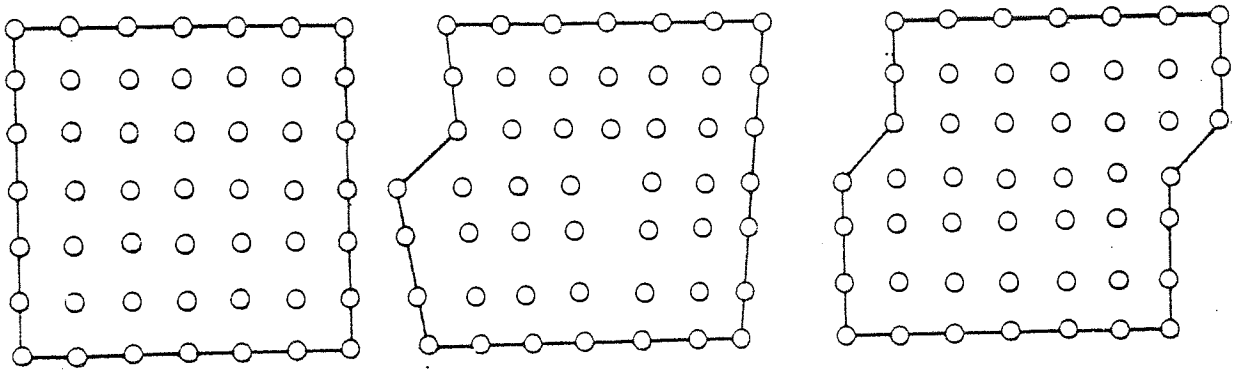

Fig. 1.9 Slip resulting from the movement of an edge dislocation. (From Taylor, 1934).

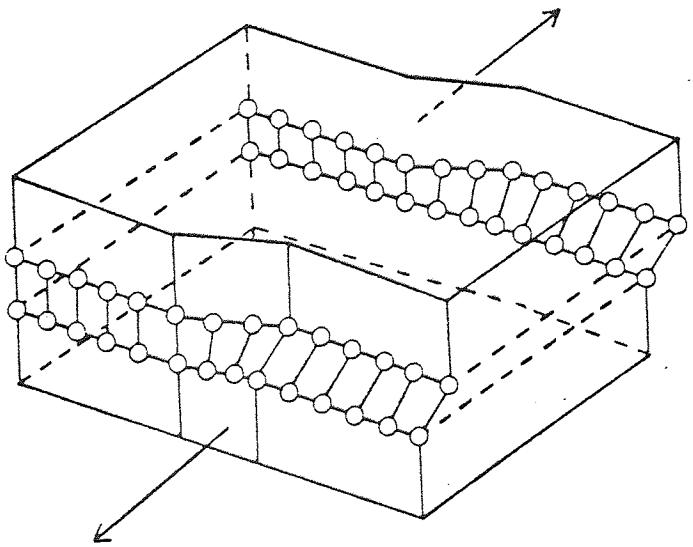

Fig. 1.10 Structure of a screw dislocation and the slip resulting from its movement. (From Cottrell, 1949).

When slip occurs along two intersecting slip planes, the planes will interact to form a sessile dislocation which cannot move. Further dislocations will run along these slip planes and produce an immobile dislocation pile-up. Dislocation pile-ups are also produced in the case of close-spaced, parallel slip planes which are discussed in detail by Hull (1968); the stress required to move one dislocation past another on a parallel slip plane is inversely proportional to the distance between the slip planes. Thus, in a close-spaced arrangement of parallel slip planes, the dislocation will present a strong mutual barrier to dislocation movement resulting in a dislocation pile-up. Other sources of dislocation pile-ups are twin planes and also the grain boundaries in polycrystalline specimens, both of which prevent dislocation movement across the boundaries created. These dislocation pile-ups may produce a cavity dislocation which can cause crack initiation.

1.5.3 Fracture types

Two types of fracture are recognised; (i) brittle and (ii) plastic or ductile. Brittle fracture occurs after little or no plastic deformation whereas ductile fracture occurs after extensive plastic deformation.

1.5.3.1 Brittle fracture

Brittle fracture occurs by the rapid propagation of a crack under an applied stress. Brittle fracture was first explained by Griffith (1920) who assumed the existence of sub-microscopic cracks in a material which concentrate the applied stress at their tips. For an elliptical crack the maximum stress, σ_m at its tip is

given by equation 1.7.

$$\sigma_m = (c/r)^{\frac{1}{2}} . 2\sigma \qquad \text{Eq. 1.7.}$$

where σ = applied stress.

c = half the length of an internal crack.

r = the radius of curvature at the crack tip.

Thus, the maximum stress at the tip of the crack is inversely proportional to the radius of curvature at the crack tip. For a crack with a small radius the stress concentration may be sufficient to exceed the cohesive strength of the material at the tip of the crack, under relatively low applied stresses. For crack propagation to occur, the release of stored elastic strain energy must be greater than the energy required to create the new surface formed. This energy is the surface energy of the material. This concept is referred to as the Griffith criterion for growth of a sharp crack and the Griffith stress for growth, σ_g is given by equation 1.8.

$$\sigma_g = \gamma(E/c)^{\frac{1}{2}} \qquad \text{Eq. 1.8.}$$

where γ = surface energy

E = Young's modulus

Thus, if $\sigma_m > \sigma_g$, crack propagation will occur leading to brittle failure.

The cracks required by the Griffith theory may be impurities present in the material, immobile dislocations or may be nucleated by the dislocation pile-ups discussed in section 1.5.2.2. If the cracks are a result of nucleation by dislocation pile-ups, then a small amount of plastic deformation will be expected prior to brittle

failure since some deformation is produced as the dislocations move into a pile-up.

1.5.3.2 Plastic or ductile fracture

A plastic material is not affected to any great extent by the cracks present in the material since plastic flow at the tip of the crack, caused by the concentrated stress, will blunt the crack and thus reduce the stress concentration. When testing a plastic material in tension, minute cavities are formed at the part of the specimen which has accepted a high strain. This is seen in metal specimens as necking. These cavities coalesce and form a small crack which grows across the specimen until fracture occurs. However, the cracks grow slowly due to the stress relaxing effect of the mobile dislocations which reduce the stress concentration. Continued strain must therefore be applied to increase the stress, in order to allow continued crack growth. Dieter (1961) suggests that the internal cavities are nucleated, at least in some materials, by the dislocation pile-ups discussed in section 1.5.2.2.

1.5.4 Work-hardening

Work-hardening or strain-hardening is related to the strain history of the specimen. During straining of some materials, there is a large increase in dislocation density and a corresponding decrease in dislocation mobility due to dislocation pile-ups. Under these conditions the ability of the material to undergo plastic deformation is greatly reduced and the material tends to become brittle. Thus brittle fracture of a material, which is normally plastic, can take

place if excessive straining has occurred before a fracture test.

1.6 Deformation of Material not containing Dislocations

The theory of dislocations and their movement can be used to explain the deformation and failure properties of some crystalline materials. However, although some polysaccharide materials such as Elcema, a brand of microfine cellulose, may be regarded as crystalline, Gordon (1976) states that there is no dislocation mechanism in these materials. A second polysaccharide material used in this study is Sta-Rx which is a directly compressible starch.

1.6.1 Structure of cellulose and starch

The structure of cellulose is shown in Fig. 1.11. In the case of Elcema, the value of n is approximately 1500. Gordon (1976) states that the cellulose chains are simple thread-like molecules which are unbranched. Natural cellulose consists of up to 40% crystalline material, the remainder being amorphous. The crystalline nature of the material is produced by association of the hydroxyl groups on the sugar rings of the other cellulose chains. This association, or bonding, holds the chains in a solid regular crystal structure. Cross bonding of the cellulose chains in the amorphous regions is prevented by association of water molecules with the hydroxyl groups.

Starch consists of about 20% amylose and 80% amylopectin, the structures of which are shown in Fig. 1.12. The difference between amylose and cellulose is that the glycosidic link between the glucose rings of amylose is in the α configuration, whereas the linkage of

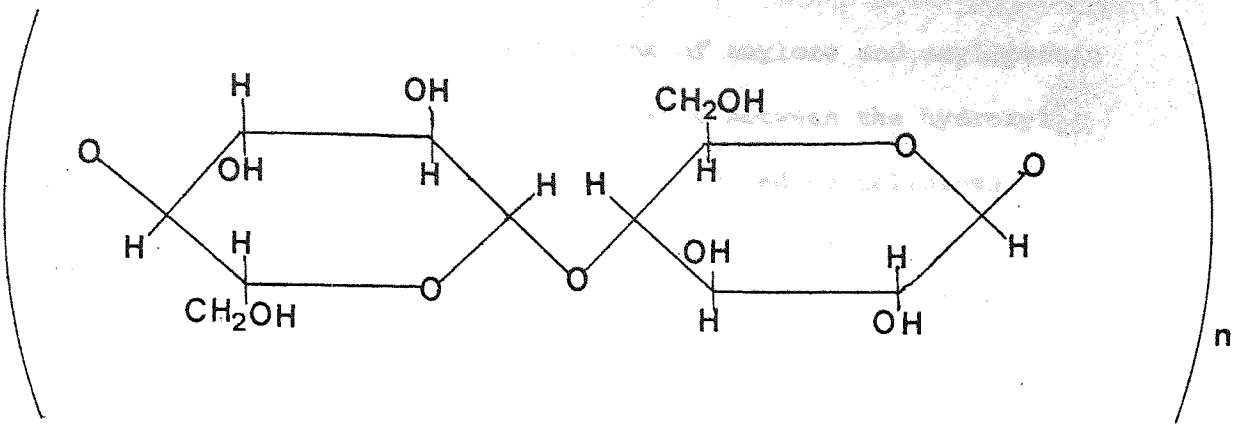

Fig. 1.11 The structure of cellulose.

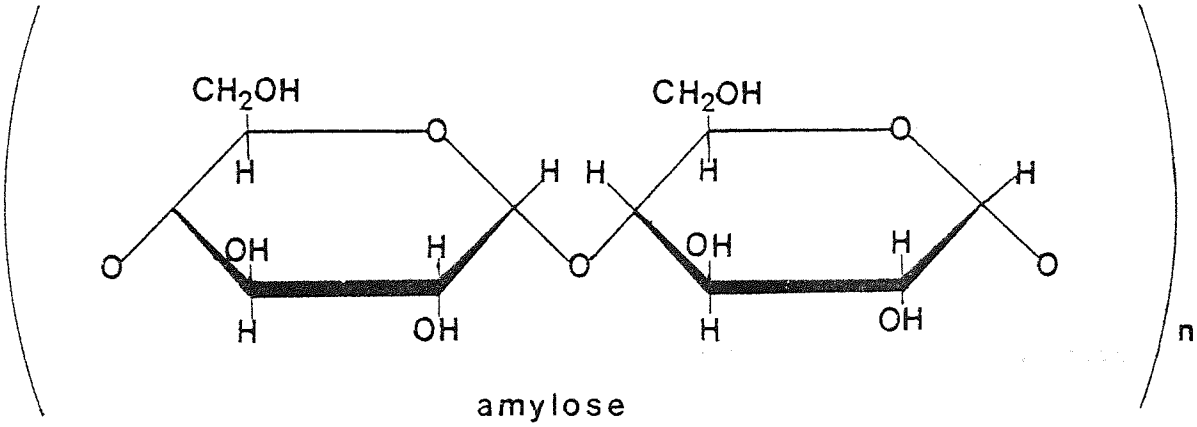

amylose

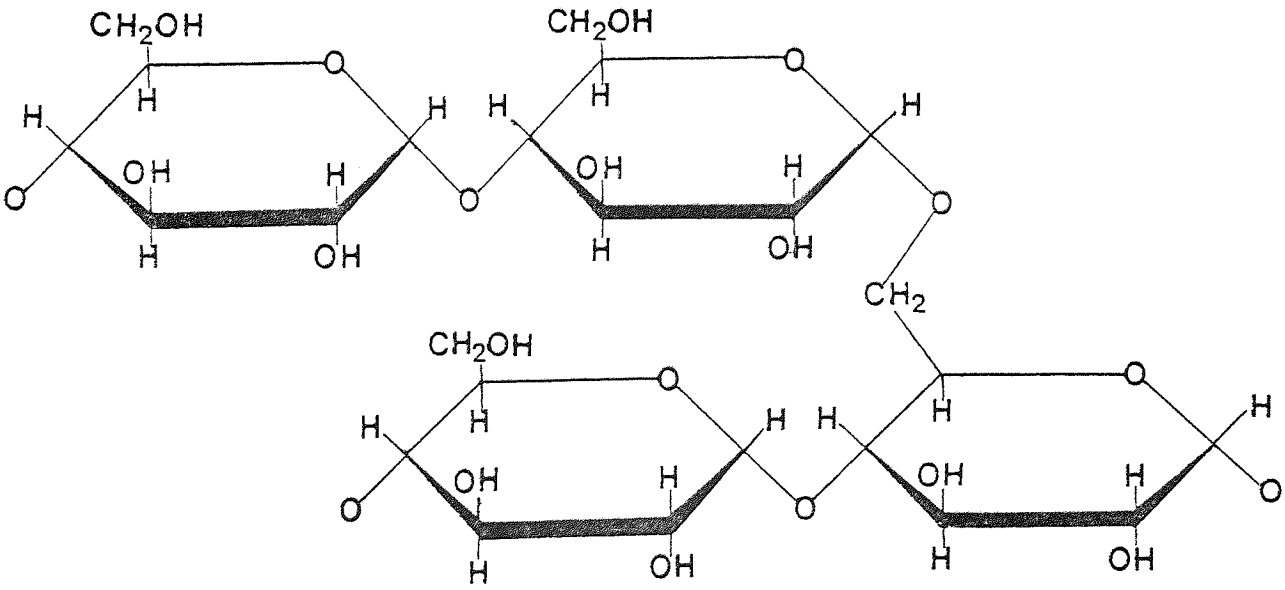

amylopectin

Fig. 1.12 The structure of the two components of starch.

cellulose is β. The α glycosidic link of amylose and amylopectin results in there being a greater distance between the hydroxyl groups on neighbouring polymer chains compared to cellulose. This reduces the hydroxyl association and thus there is no crystalline structure in starch. Each molecule of amylose and amylopectin consists of between 1000 and 4000 glucose units, and, due to the branching of amylopectin, the molecules will become extensively entangled.

1.6.2 Crack propagation in cellulose and starch

From the discussion of crack propagation in section 1.5.3.1, it is clear that unless some mechanism reduces the stress concentrating effect of the cracks, the material will exhibit brittle fracture. Reduction of stress concentration in a metal and in some crystalline materials can occur by plastic deformation caused by dislocation movement. However, since there are no dislocations in polysaccharide materials, some other mechanism must be responsible for the prevention of crack propagation in such materials. Cook and Gordon (1964) proposed a mechanism by which crack propagation is prevented in specimens containing weak interfaces. Such interfaces are regions where the bonding between two sections of the material is weaker than within the sections. In an Elcema tablet, weak interfaces are present both within the particles, between two regions of crystalline material and between the particles where the bonds have been formed during compaction. In a study of microcrystalline cellulose tablets, Reier and Shangraw (1966) found that the disintegration times of tablets increased as the dielectric constant of the disintegration medium decreased. These authors concluded that

microcrystalline cellulose could be visualised as a special form of the cellulose fibril in which the crystal regions of cellulose are inaccessible to water and so the fact that microcrystalline cellulose tablets disintegrate rapidly in water, a medium with a high dielectric constant, suggests that the inter-particulate bonds formed during compaction are weaker than the hydroxyl association of the crystalline region. Similar weak interfaces will also be present in Sta-Rx tablets.

The Cook-Gordon mechanism for preventing crack propagation is shown diagrammatically in Fig 1.13. As the crack approaches the weak interface, the interface breaks ahead of the crack under the stresses concentrated at the crack tip. The T shaped crack so formed has effectively increased the radius of the crack tip and reduces the stress concentration. Although the tip of the crack running along the weak interface may have a small radius, since it is parallel to the applied stress, there is little tendency for this crack to propagate.

1.6.3. Plastic deformation of cellulose and starch

Plastic deformation of cellulose may be due to slip either within the crystalline regions or of the crystalline regions relative to one another. With starch, the plastic deformation is probably due to slip of the polymer chains and straightening of the entangled branched molecules.

Plastic deformation of cellulose and starch will cause a reduction in the stress concentrating effect of any cracks present by increasing the radius of the tip of the crack. Thus, in these materials, there are two mechanisms tending to prevent crack propagation.

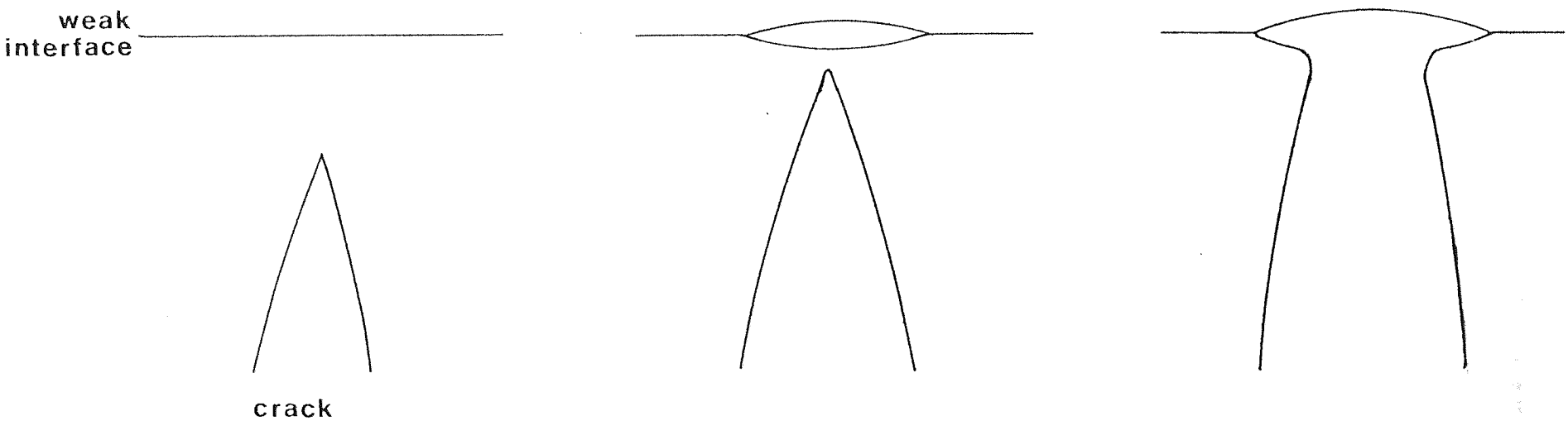

Fig. 1.13 Cook - Gordon mechanism for prevention of crack propagation.

1.7 The Deformation of Pharmaceutical Excipients and Tablets

The mechanical properties of pharmaceutical tablets are influenced by both their formulation and the processes used in their production. However, there are no reports in the literature concerned with the deformation behaviour of tablets during diametral loading. Information regarding such deformation should provide a basis for understanding the physico-mechanical behaviour of tablets. Furthermore, the deformation of tablets may be related to the deformation of their components during compaction. Thus, the study of tablet deformation may allow elucidation of compaction mechanisms.

The work reported in this thesis examines the deformation of tablets during diametral loading and attempts to correlate this deformation behaviour with the compaction mechanisms of several direct compression agents.

2. MATERIALS AND METHODS

2.1 Materials

Four direct compression materials and sodium chloride were used in this study. The four direct compression materials were chosen as representative of the materials, at present, commercially available and sodium chloride was used as a material which is known to behave plastically during compaction.

The materials chosen were:-

Elcema G 250	-	a granular form of microfine cellulose (Degussa, Frankfurt, West Germany);
anhydrous lactose	-	(K. W. Revai Chemicals Ltd., London);
Emcompress	-	a direct compression form of dibasic calcium phosphate (K. K. Greef Ltd., Croydon);
Sta-Rx 1500	-	a modified starch U.S.P. (A. E. Staley Mfg. Co., Illinois, U.S.A.);
sodium chloride	-	analytical reagent grade (Fisons Scientific Apparatus Ltd., Loughborough).

The materials were used as received from the suppliers except sodium chloride which, because of its large particle size, was comminuted using a ball mill and sieved, using a sieve shaker (Endecotts (Test Sieves) Ltd., London), to obtain a 150 to 300 μm fraction.

2.1.1 Characterisation of materials

2.1.1.1 Bulk density measurements

Bulk density measurements of materials may be affected by the diameter of the container in which the measurements are made since this can influence the packing of the particles as they are

introduced into the containers. Prior to the compaction of tablets, the bulk density of the powder will be affected by the diameter of the die and so determination of bulk density was carried out in a 10 cm^3 measuring cylinder having an internal diameter of 12 mm compared to the die diameter of 12.7 mm.

The measuring cylinder was tared and a mass of powder equivalent to about 10 cm^3 was poured from a glass weighing boat into the cylinder held at an angle of about 60° to the horizontal. The exact volume of powder was estimated to the nearest 0.1 cm^3, without levelling the surface of the powder, and the powder was weighed to the nearest 0.01 g. Bulk density was determined by dividing the mass of the powder by its bulk volume. Three determinations were made for each material and the results are shown in Table 2.1.

2.1.1.2 True density measurements

True density of the materials was determined using a helium-air comparative pycnometer (model 1302, Micromeritics Instrument Corporation. From Coulter Electronics Ltd., Harpenden). The operating principle of this instrument is that the change in pressure of a non-adsorbing pure gas (helium) in an enclosed chamber, due to a discrete change in the free space within the chamber, is proportional to the volume of any solid material in the chamber. Thus the volume of the solid material, including the volume of any closed intra-particulate pores, may be determined and the density calculated.

A diagram of the instrument is shown in Fig. 2.1. The movement of the piston, from a zero position, which produces a

MATERIAL	BULK DENSITY $g\ cm^{-3}$ replicate values				TRUE DENSITY $g\ cm^{-3}$ replicate values			
	1	2	3	mean	1	2	3	mean
anhydrous lactose	0.52	0.54	0.58	0.55	1.586	1.592	1.574	1.584
Elcema G250	0.50	0.50	0.50	0.50	1.572	1.556	1.555	1.561
Emcompress	0.82	0.87	0.86	0.85	2.354	2.360	2.363	2.359
Sta-Rx 1500	0.57	0.56	0.58	0.57	1.534	1.521	1.520	1.525
sodium chloride	1.13	1.13	1.14	1.13	* literature value taken 2.17			

Table 2.1 Bulk density and true density values of the five materials

* Hersey, Cole and Rees (1973)

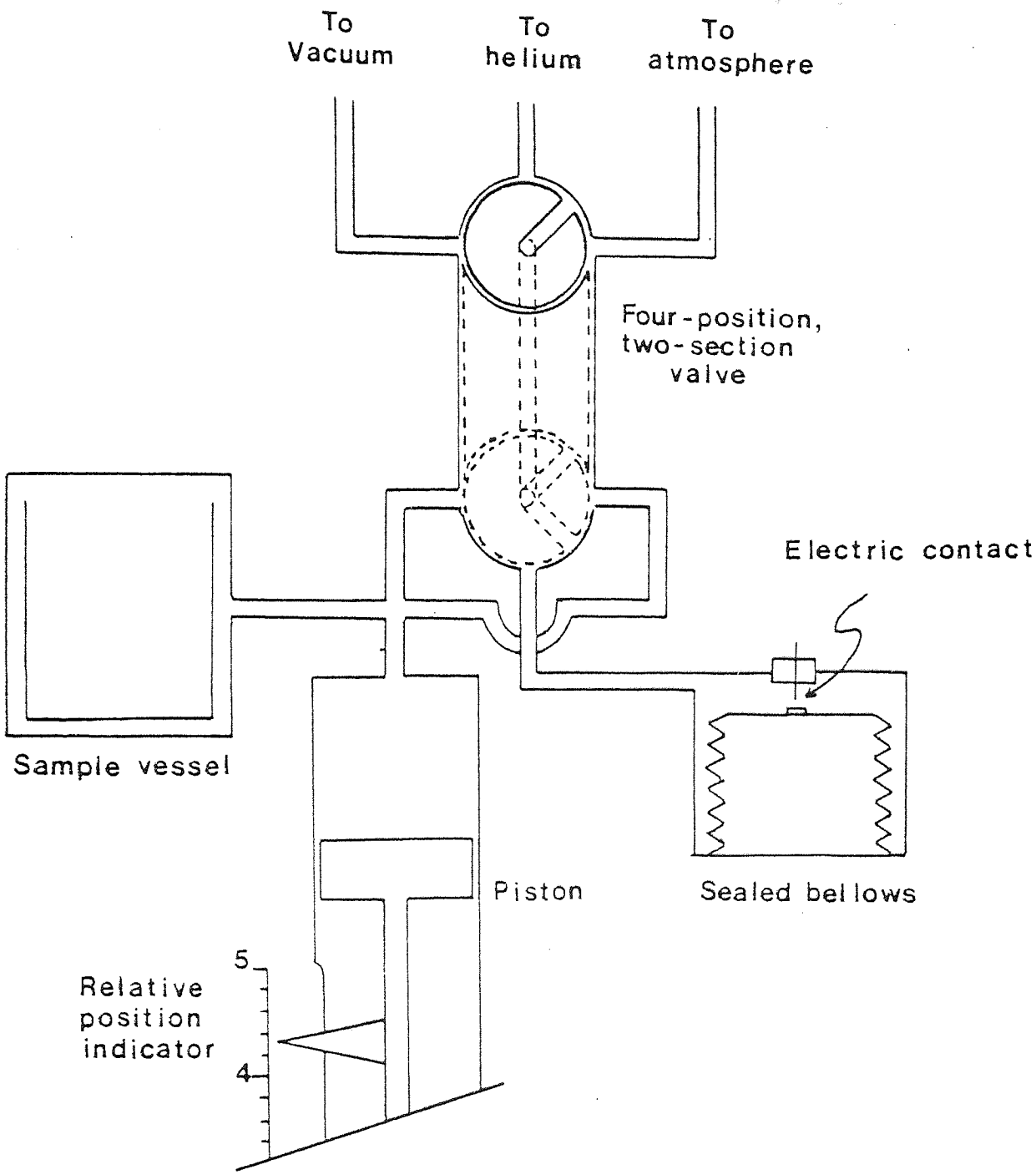

Fig. 2.1 Diagram of the helium comparative pycnometer

pressure in the sample vessel equal to the constant pressure in the sealed bellows is measured by the relative position indicator. This movement is first measured with the sample vessel empty (movement R_2) and then containing a steel sphere of known volume, V_{std} (movement R_1). Since, under the imposed conditions, the ideal gas law applies a calibration factor, α may be calculated using equation 2.1.

$$\alpha = \frac{V_{std}}{R_2 - R_1} \qquad \text{Eq. 2.1}$$

The movement R_s of the piston necessary to produce a pressure in the sample vessel equal to the constant pressure in the sealed bellows is finally measured with a sample of unknown volume, V in the sample vessel and the volume of the sample is calculated from equation 2.2.

$$V = \alpha(R_2 - R_s) \qquad \text{Eq. 2.2}$$

A sample of material weighing about 40 g was dried overnight at 60°C in a hot air oven. The sample volume was determined using the helium-air pycnometer and the mass of the sample was determined accurately to ± 1 mg. The true density of each material calculated by this method is shown in Table 2.1

2.1.1.3 Particle size analysis

The method of particle size analysis of each material was chosen depending on the approximate size of the material. For the coarser materials Elcema and sodium chloride, sieve analysis was chosen using a mechanical sieve shaker. For the finer materials, Emcompress and lactose, the method chosen was air jet sieving.

Efficient separation of particle sizes can be achieved by this method since 'blinding' of the sieve by particles slightly larger than the screen aperture is reduced and fines adhering to coarse particles tend to be separated. For the finest material, Sta-Rx, an optical method was chosen since simple sieving cannot be used unless the main proportion of the material is greater than 75 μm.

The particle size distribution was determined for each of the materials in the following ways:-

a) Elcema:- a 60 g sample of Elcema was obtained from the bulk material by means of a chute sample divider (Endecotts (Test Sieves) Ltd., London). The sample was placed on the top screen of a nest of eight wire mesh sieves assembled on a mechanical sieve shaker (Endecotts (Test Sieves) Ltd., London). The sample was sieved for five minutes as specified in BS 1796; 1952. The material remaining on each sieve was weighed and returned to the sieve. In turn each sieve was shaken separately for a further two minutes using a clean receiver pan and the amount of material passing through the screen determined. If the amount of material passing the screen during the two minutes was less than 0.2% w/w of the initial sample then sieving was considered to be complete. Otherwise the sieve was replaced on the nest and shaken for a further five minutes and the two minute test repeated. When size separation was complete on all the sieves, the amount of material retained by each sieve was determined and the cumulative percent by weight undersize was calculated. The particle size distribution of Elcema is shown in Fig. 2.2.

b) anhydrous lactose:- a 30 g sample of anhydrous lactose was obtained from the bulk material using a chute sample divider.

The sample was placed on a 43 μm wire mesh sieve in an Alpine air jet apparatus (Levino (London) Ltd., London) which was operated for five minutes. The mass of material remaining on the sieve was weighed, replaced on the sieve and the apparatus was operated for a further two minutes. The quantity of material passing through in the two minutes was calculated. If this quantity was less than 0.2% w/w of the sample then sieving was considered to be complete. The oversize material was then placed on a sieve having an aperture $\sqrt[4]{2}$ times larger than the previous sieve and the above procedure repeated. The particle size distribution of anhydrous lactose determined by this method is shown in Fig. 2.2.

A large proportion (about 15% w/w of lactose was finer than 43 μm in size as determined by sieve analysis so further characterisation was carried out using a Fisher sub-sieve sizer (Kek Ltd., Manchester). This instrument is based on the Gooden and Smith (1940) modification of the Lea and Nurse (1939) apparatus. Using this instrument the surface weight mean diameter, d_{sv} can be determined from equation 2.3 (Allen, 1974).

$$d_{sv} = \frac{60,000}{14} \sqrt{\frac{\eta c F \rho_s L^2 M^2}{(V\rho_s - M)^3 (P-F)}} \qquad \text{Eq. 2.3}$$

where c = flowmeter conductance per unit pressure, $cm\ s^{-1}\ g^{-1}$
F = pressure resistance across flow meter, $g\ cm^{-2}$
M = mass of sample, g
ρ_s = density of sample, $g\ cm^{-3}$
V = apparent volume of compacted sample, cm^3
P = overall pressure head, $g\ cm^{-2}$
L = thickness of powder bed, cm
η = viscosity of air

By using a sample weight equal in grams to the true density of the material, d_{sv} may be read directly from a calibration

chart supplied with the instrument.

Assuming spherical particles, the surface area, S_p and volume, V_p of each particle are given by equations 2.4 and 2.5 respectively.

$$S_p = 4\pi(d_{sv}/2)^2 \qquad \text{Eq. 2.4}$$

$$V_p = 4/3\pi(d_{sv}/2)^3 \qquad \text{Eq. 2.5}$$

The specific surface area, S is given by equation 2.6.

$$S = \frac{S_p}{\rho_s V_p} \qquad \text{Eq. 2.6}$$

Thus,

$$S = \frac{4\pi(d_{sv}/2)^2}{\rho_s 4/3\pi(d_{sv}/2)^3} \qquad \text{Eq. 2.7}$$

Equation 2.7 reduces to:-

$$S = \frac{6}{\rho_s d_{sv}} \qquad \text{Eq. 2.8}$$

Since the value of d_{sv} varies with porosity, measurements were made for samples of lactose over a range of porosities. Measurement of d_{sv} was also made for samples of lactose which passed through a 43 μm sieve. The values of d_{sv} together with the calculated specific surface areas are shown in Table 2.2.

c) Emcompress:- the particle size distribution of a sample of Emcompress was determined by air jet sieving using the same method described for anhydrous lactose. The particle size distribution is shown in Fig. 2.2.

(i) Sample:- anhydrous lactose, as received from the supplier

Porosity	d_{sv} µm replicate values 1	2	3	mean	specific surface area $m^2 g^{-1}$
0.607	19.6	19.2	18.6	19.1	1.983×10^{-1}
0.582	20.8	20.2	19.9	20.3	1.866×10^{-1}
0.570	21.2	20.8	20.0	20.7	1.830×10^{-1}
0.560	21.2	21.0	21.0	21.1	1.795×10^{-1}
0.528	21.4	21.2	21.2	21.3	1.778×10^{-1}
0.495	21.2	21.0	20.6	20.9	1.812×10^{-1}
0.467	19.8	20.6	19.8	20.1	1.885×10^{-1}

(ii) Sample:- anhydrous lactose, fraction passing a 43 µm sieve

Porosity	d_{sv} µm replicate values 1	2	3	mean	specific surface area $m^2 g^{-1}$
0.638	8.3	8.4	8.8	8.5	4.466×10^{-1}
0.616	8.5	8.6	8.8	8.6	4.405×10^{-1}
0.600	8.6	9.1	8.9	8.9	4.256×10^{-1}
0.575	9.0	9.4	9.0	9.1	4.163×10^{-1}
0.557	8.9	9.5	9.0	9.1	4.163×10^{-1}
0.535	8.7	9.5	8.8	9.0	4.209×10^{-1}
0.506	9.0	9.5	8.8	9.1	4.163×10^{-1}
0.494	9.0	9.5	8.6	9.0	4.209×10^{-1}
0.475	9.0	9.3	8.6	9.0	4.209×10^{-1}

Table 2.2 The surface weight mean diameter and specific surface area of samples of lactose measured by a Fisher sub sieve sizer.

d) For Sta-Rx:- due to the fine particle size of Sta-Rx, an optical microscopy method of size analysis[1] was used. The Sta-Rx was mounted in liquid paraffin and the particle size was determined according to BS3406 1963 using a X10 objective lens. The particle size distribution is shown in Fig. 2.2.

e) sodium chloride:- the particle size distribution within the 150-300 μm size fraction used was determined by sieving as described in section 2.1.1.3(a), and is shown in Fig. 2.2.

2.2 Preparation of Tablets

2.2.1. Instrumentation of the tablet machine

In order to monitor the force applied to the powder during compression, the upper punch of a reciprocating tablet machine (Model STD 1, S. W. Wilkinson & Co. Ltd., Leicester) was instrumented using a method similar to that described by Rees and Shotton (1969). The shank of a 12.7 mm diameter plane-faced punch and the backing material of a foil strain gauge (Type 3/120/EC, Tinsley Telcon Ltd., London) were lightly abraded using a fine grade emery paper. The abraded surfaces were cleaned using a mixture of 50% v/v chloroform and 50% v/v acetone to remove traces of grease. The gauge was located on the punch using adhesive tape ('Sellotape'). The tape was peeled back to form a hinge thus ensuring the gauge returned to its correct location after application of adhesive to the gauge. A small amount of adhesive (Eastman 910, Emerson and Cuming (U.K.) Ltd., London) was applied to the gauge

[1] Size analysis carried out by Formulation Research Group, Boots Pure Drug Co. Ltd., Nottingham.

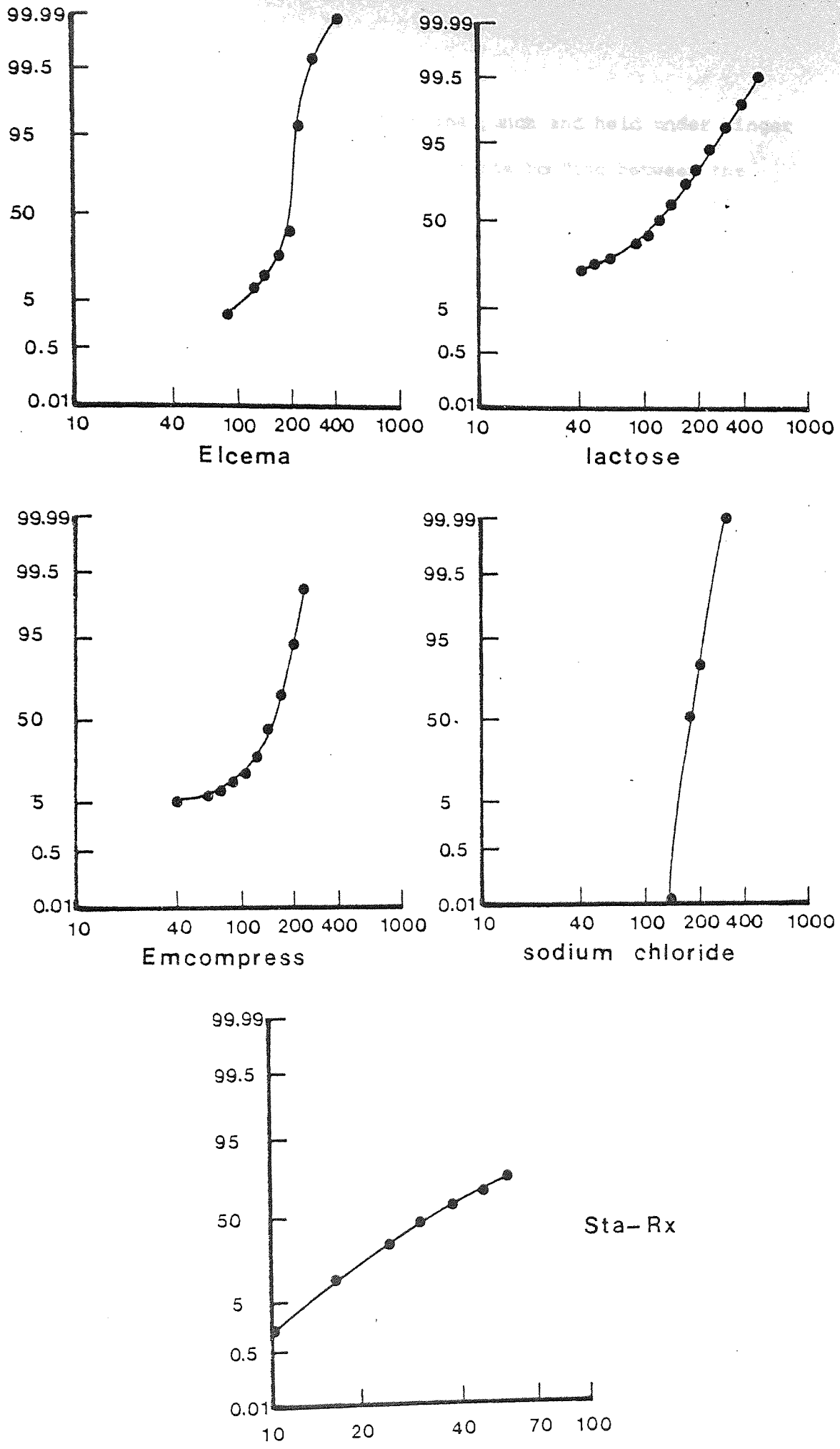

Fig. 2.2 Particle size distribution of the materials expressed as cumulative percent undersize on a probability scale (ordinates) versus the logarithm of sieve aperture diameter in micrometres (abscissae)

backing which was then relocated on the punch and held under finger pressure for two minutes to ensure intimate bonding between the gauge and the punch.

Using this technique two active and two temperature-compensating foil strain gauges were bonded to the shank of an upper punch. The gauges were connected to form the four arms of a Wheatstone bridge which was energised by 3 volts D.C., and balanced using a bridge supply and balance unit (Type FE-492-BBS, Fylde Electronics Ltd., Preston). The signal from the bridge was conditioned using a differential D.C. pre-amplifier (Type FE-251-GA, Fylde Electronics Ltd., Preston), and recorded using a U.V. oscillograph (Model 3006, S. E. Laboratories (Engineering) Ltd., London) fitted with moving coil galvanometers (Type 'A', Manarp Electronic Instruments Ltd., Hayes) which had a frequency response of 0 to 160 Hz.

The instrumented punch and recording system was calibrated using a universal testing instrument (W. H. Mayes and Sons (Windsor) Ltd., Windsor) at forces up to 30 kN. By adjustment of the amplifier sensitivity control a calibration factor was obtained such that 1 kN corresponded to 1 cm movement of the oscillograph at a gain control setting of 500. Calibration graphs for the punch are shown in Fig. 2.3.

2.2.2 Compaction of tablets

The mass of material required to produce a cylindrical compact 12.7 mm diameter and 2.49 mm thick at zero theoretical porosity was calculated from the true density of the material. This mass of material was weighed to ± 2 mg, poured into a 12.7 mm

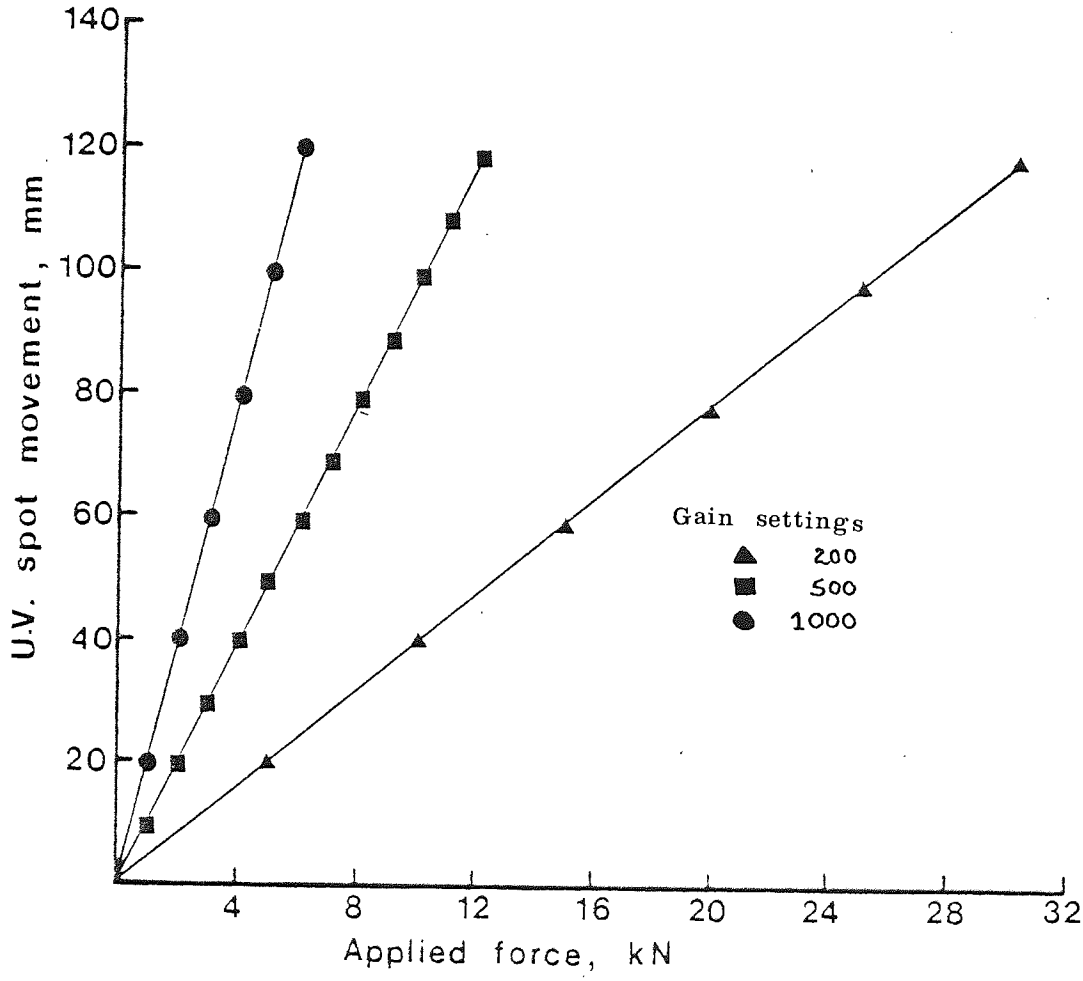

Fig. 2.3 Calibration graph of the instrumented punch

diameter, cylindrical die and compressed, by hand, between plane faced punches using the reciprocating tablet machine. Before each tablet was prepared the die was lubricated by compressing a sample of the same material containing 50% w/w magnesium stearate (Hopkins and Williams Ltd., Chadwell Heath). Applied compression force was monitored using the equipment described in section 2.2.1. In order to standardise the time of the compression cycle the fly-wheel of the machine was turned at the same rate for all materials and compression forces. The time of the compression cycle was 0.17 seconds. All materials and tablets were stored at 24°C and 50% R.H. before use.

2.2.3 Stress relaxation measurements during powder compaction

The technique used for stress relaxation studies during the compaction cycle was similar to that normally used to prepare tablets as described in section 2.2.2, but at an applied force of about 20 kN the movement of the upper punch was stopped, holding the compressed powder under constant strain. The measurement of upper punch force was continued and recorded on the U.V. oscillograph. In this way the decrease in upper punch force, with time, was monitored. The experiment was repeated twice for each material with the die wall lubricated as described in section 2.2.2.

To determine the effect of magnesium stearate on stress relaxation, 0.3% w/w magnesium stearate was mixed with each material by the following method. 50 g of material was accurately weighed and spread on a metal tray. 0.15 g of magnesium stearate was accurately weighed and forced through a 180 µm sieve, to break up large aggregates, onto the surface of the material. The

powders were mixed by hand, using a spatula, for three minutes and then transferred to a plastic bag which was shaken for a further five minutes. Stress relaxation studies were performed on this mixture of material and magnesium stearate in a similar way to that described for the pure materials, except that no additional die wall lubrication was necessary.

2.3 Characterisation of Tablets

2.3.1 Diametral compression test equipment

Fig. 2.4 shows the diametral compression instrument and data logging system. The main frame of the instrument, A is based on a Hounsfield tensiometer (Tensiometers Ltd., Croydon) modified for use in compression. The lower platten of the compression assembly, B shown in more detail in Fig. 2.5, is driven upwards by a high torque synchronous motor, C (Type KLZ-42.60 - 2 - 138D - B200, Papst-Motoren KG, Schwarzwald, West Germany) via two reduction gear boxes, D and E (Type 22A,G and K. Osborne Ltd., Harlow) and a variable ratio reduction gear train, F. Four rates of platten movement are possible by alteration of the gear ratios. The rates are; 0.052, 0.26, 1.3 and 6.5 mm min^{-1}. The force applied to the tablet is measured using an electronic load transducer, G (Interface 1410 AF, Interface Inc., Arizona, U.S.A.) with a range of 0 - 45 kg, a sensitivity of 10 g and a minimum claimed accuracy of 0.01% of full scale deflection. The transducer was energised by 10 volts D.C. using a bridge supply and balance unit, and calibrated by dead weight loading using the calibration weights of an Instron physical testing instrument. The output of the transducer was

Fig 2.4 The diametral compression test instrument and recording system

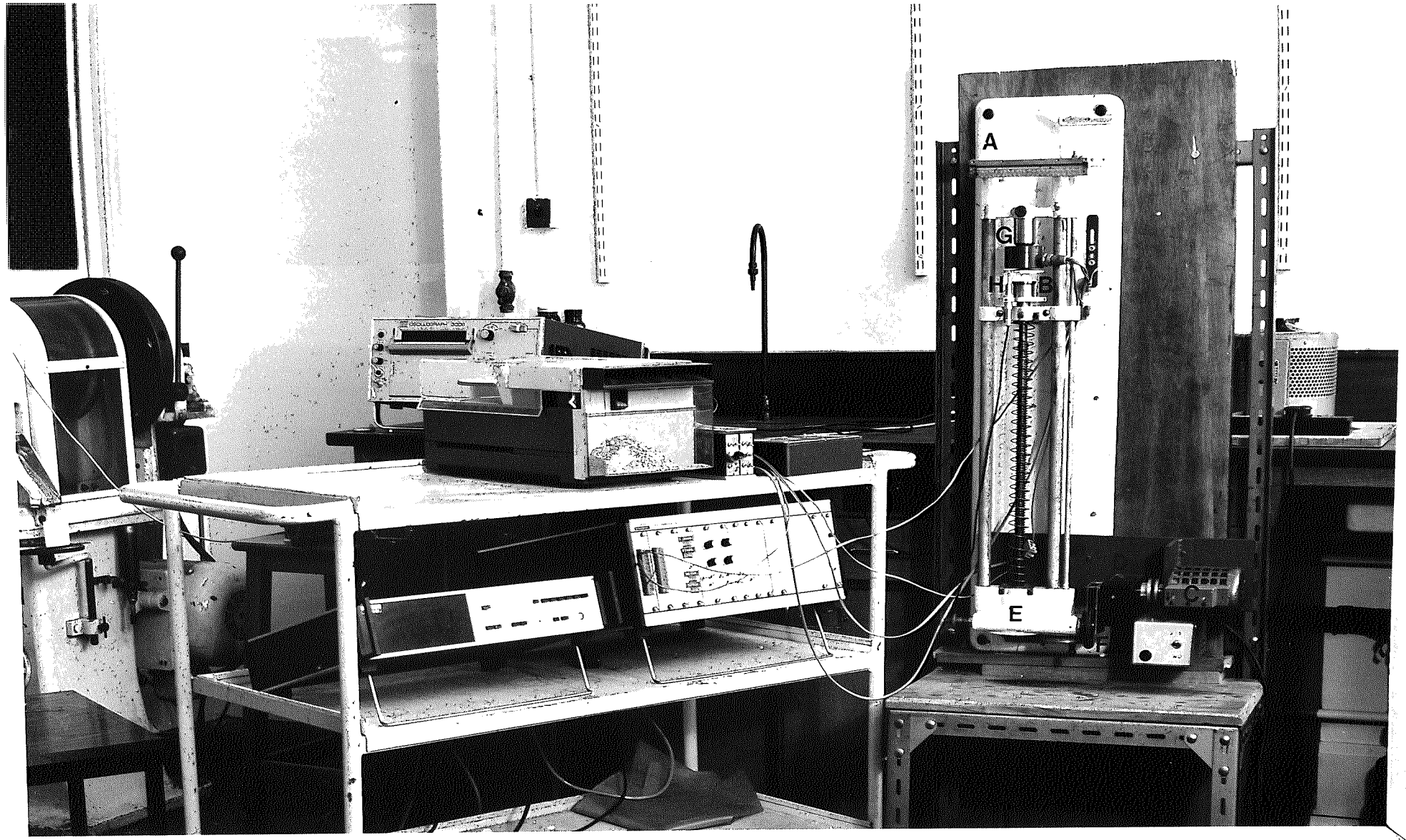
A
G
H
B
E

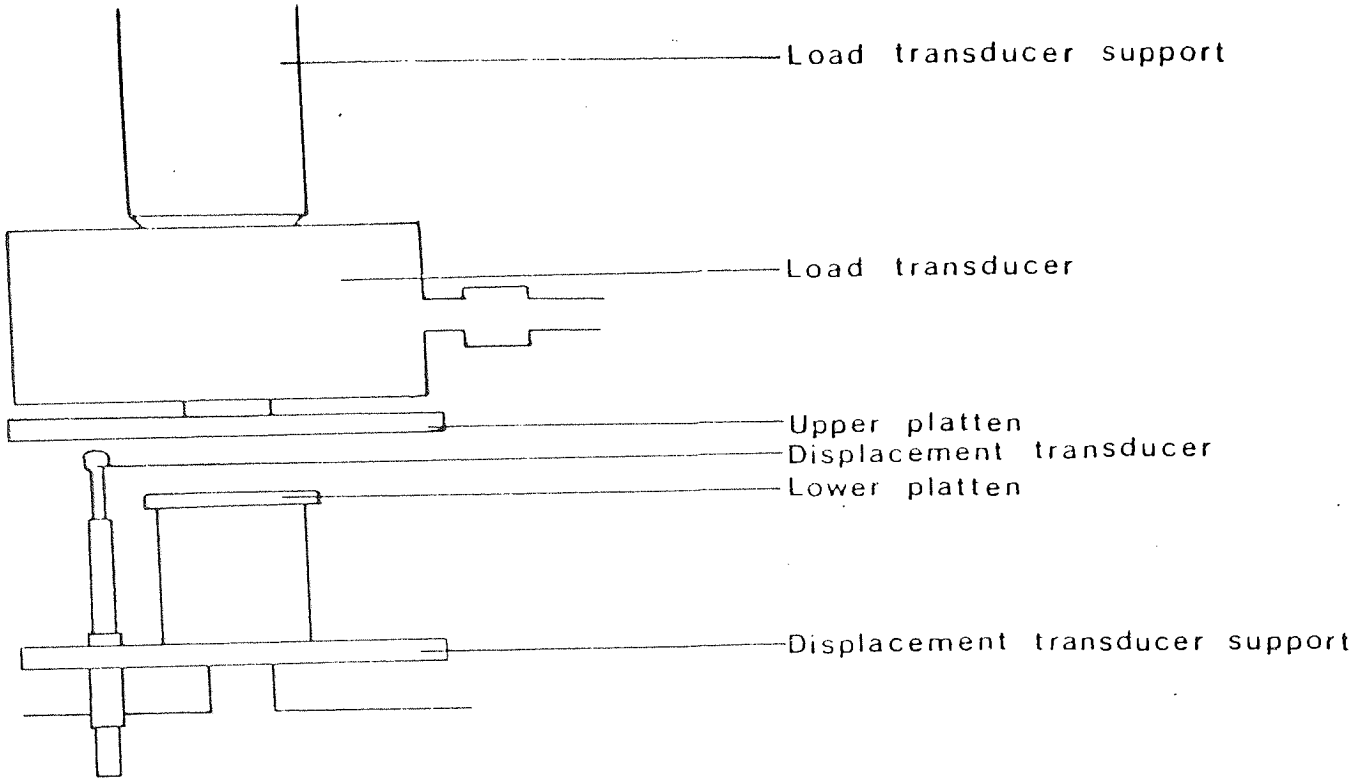

Fig. 2.5 Diagram of the arrangement of transducers on the diametral compression test instrument

Mass applied kg	Digital voltmeter reading mV replicate values 1	2	3	mean
0	0.004	0.000	0.002	0.002
0.878	0.440	0.440	0.438	0.439
5.878	2.943	2.941	2.937	2.940
10.878	5.444	5.441	5.436	5.440
15.878	7.940	7.948	7.936	7.941
20.878	10.450	10.440	10.435	10.442
25.878	12.960	12.942	12.938	12.947
30.878	15.464	15.441	15.438	15.448
35.878	17.969	17.943	17.939	17.950
40.878	20.480	20.450	20.44	20.46
45.878	22.99	22.94	22.94	22.96
40.878	20.48	20.44	20.44	20.45
35.878	17.986	17.945	17.937	17.953
30.878	15.472	15.444	15.440	15.452
25.878	12.968	12.944	12.938	12.950
20.878	10.465	10.443	10.435	10.448
15.878	7.966	7.944	7.938	7.949
10.878	5.460	5.446	5.437	5.448
5.878	2.959	2.946	2.937	2.947
0.878	0.458	0.447	0.438	0.448
0	0.002	0.002	0.002	0.002

Table 2.3 Calibration data for the load transducer obtained by dead weight loading

measured using a digital voltmeter (Type A200, Solartron Electronics Group Ltd., Farnborough). From the calibration data shown in Table 2.3, a calibration factor of 2 kg mV^{-1} was calculated. This value was converted to 1.96×10^{-2} kN mV^{-1} for use in the computer program described in Appendix 1.

A displacement transducer, H (Type D 5100AG, RDP Electronics Ltd., Wolverhampton), with an accuracy of 0.1% of its full scale deflection of 2.5 mm, was used to measure the movement of the lower platten, relative to the upper platten, during diametral loading of tablets. Calibration of the displacement transducer was carried out, using slip gauges, while the transducer was in position on the instrument. The calibration data for the displacement transducer are shown in Table 2.4.

Slip gauge size mm	Digital voltmeter reading Volts replicate values 1	2	3	mean
0	-0.281	-0.282	-0.285	-0.283
1	-1.667	-1.659	-1.659	-1.662
2	-3.143	-3.142	-3.140	-3.142
3	-4.676	-4.667	-4.663	-4.669
4	-6.220	-6.210	-6.206	-6.212
5	-7.763	-7.759	-7.753	-7.758
6	-9.307	-9.302	-9.296	-9.302
7	-10.848	-10.841	-10.837	-10.842
8	-12.389	-12.379	-12.375	-12.381
9	-13.828	-13.833	-13.839	-13.833
10	-13.900	-13.916	-13.916	-13.909

Table 2.4 Calibration data for the displacement transducer

From the calibration data in Table 2.4, the linear range of the displacement transducer was found to be 3 to 8 mm, and a computer program calibration factor of 6.483×10^{-4} mm mV^{-1} was calculated.

2.3.1.1 Diametral compression test procedure

For all tablets prepared at each compression force the following procedure was used during a diametral loading test. Three hours after compression the thickness of a sample of ten tablets was measured using a micrometer. The tablets were then tested in diametral compression, unless otherwise stated at a rate of 0.26 mm min^{-1}, between plane metal plattens on the instrument described in section 2.3.1. The force applied to each tablet during the test was monitored continually using the load transducer and the corresponding distance between the plattens was measured by the displacement transducer. The analogue signals from the two transducers were sequentially scanned and digitised by a data transfer unit (Solartron Electronics Group Ltd., Farnborough) in conjunction with the digital voltmeter. The digital values were recorded on punch paper tape (Facit Model 4070, from Solartron Electronics Group Ltd., Farnborough), and later converted to force and displacement values using the calibration factors. From the values of breaking force, the tensile strengths were calculated using equation 1.1.

The energy expended by the moving platten during a test is the force multiplied by the distance moved. This energy is equivalent to the work done on the tablet during a test, (work of failure) and was calculated by numerical integration of applied force with respect to platten displacement, using the trapezoidal rule. The values of breaking force and work done on the tablet were calculated by a computer using the program shown in Appendix 1.

2.3.2 Multiple diametral impact testing

To simulate conditions to which commercial tablets might be subjected in practice either during coating operations, packaging or transport, a multiple diametral impact test was devised. A modified jolting volumeter, (J. Engelsmann A. G., Ludwigshafen, West Germany) commonly used for determination of tapped bulk density of powders, was modified as shown diagrammatically in Fig. 2.6. A close fitting metal sleeve was attached to the column of the jolting volumeter to provide a plane metal surface for location of the tablet. A holder, to contain the required weights was machined so that its lower edge was parallel to the metal sleeve. This holder was raised and dropped onto the tablet by the motor driven cam and the number of revolutions of the cam was determined by an automatic counter attached to one end of the motor drive shaft.

A mass of 240 g attached to the weights holder by adhesive tape was dropped a distance of 2.4 mm at a frequency of 4 Hz onto the edge of a tablet located diametrally between the metal sleeve and the weights holder. The number of times the load was applied before breakage occurred was counted. The mass of 240 g was selected empirically so that values greater than one were obtained for all tablets tested.

Batches of twenty tablets were compressed from each material at a suitable force to produce tablets of similar tensile strengths. Ten tablets were tested for tensile strength and work of failure, and ten tablets were subjected to multiple impact testing.

Multiple diametral impact tests were also carried out on several placebo tablets supplied by the pharmaceutical industry.

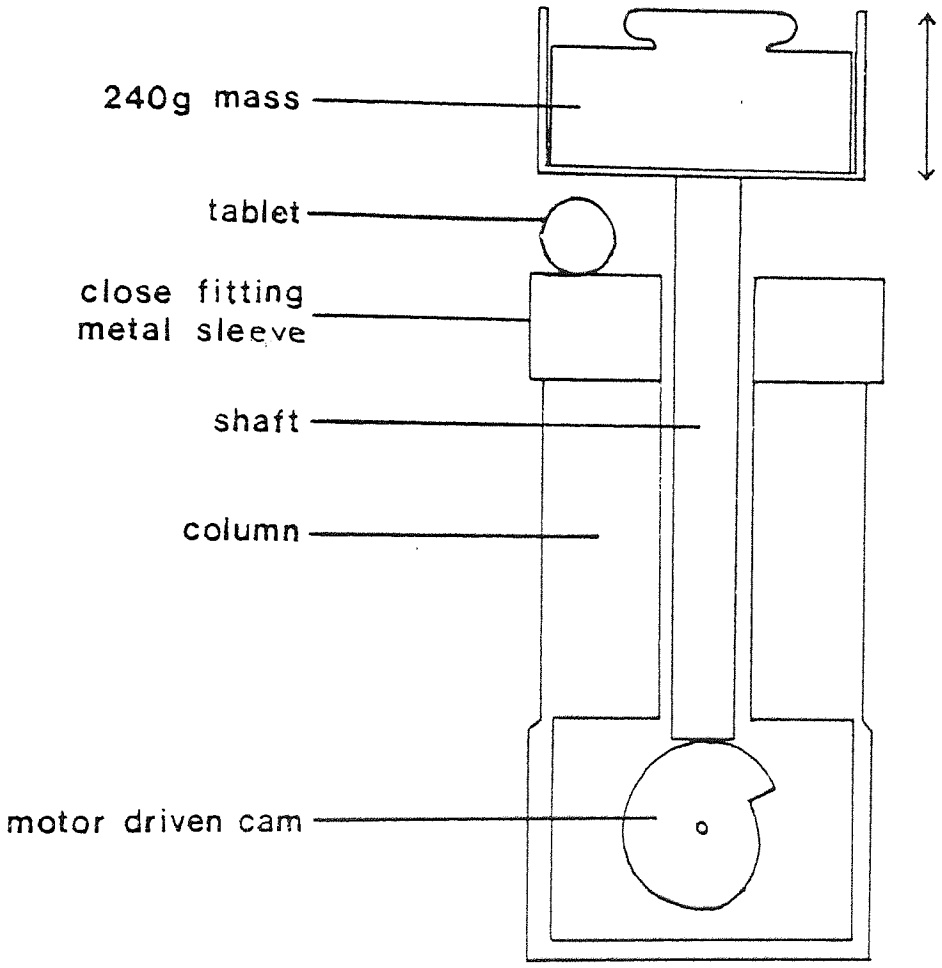

Fig. 2.6 Diagram of the modified jolting volumeter

Although the diameter of these tablets varied between 5 and 12 mm the 2.4 mm drop height was maintained by altering the length of the shaft connected to the weights holder. Ten placebo tablets were tested for tensile strength and work of failure using the instrument described in section 2.3.1 and ten placebo tablets were subjected to multiple diametral impact testing.

2.3.3 Stress relaxation measurements during diametral loading of tablets

Tablets of each material were compressed as described in section 2.2.2 to produce tablets of about 7.8×10^{-2} kN breaking force. The tablets were tested by loading at a rate of platten movement of 0.26 mm min^{-1} up to a force of 5.9×10^{-2} kN which is equivalent to 75% of the breaking load. The platten movement was then stopped so as to maintain the tablet at constant strain. The decrease in force on the upper platten with time was monitored by the U.V. oscillograph for short periods (up to 10 seconds) and by the data logging system for longer time periods. The experiment was repeated for four tablets of each material.

2.3.4 Measurement of non-recoverable deformation (NRD)

During diametral loading, deformation of the tablets occurs as measured by the displacement transducer. Part of this deformation will be elastic and recoverable, and part plastic and non-recoverable. To determine the amounts of deformation of the tablet which was non-recoverable the following procedure was used. Thirty tablets were compressed at a suitable force to produce tablets with a breaking force of about 7.8×10^{-2} kN. Ten tablets

were tested in diametral compression at a rate of platten movement of 0.26 mm min^{-1}, to determine the exact mean breaking force. Knowing this value for a particular batch, five tablets were loaded to 75% of their breaking load and rapidly unloaded by withdrawing the lower platten. The load was then reapplied. This procedure was repeated at each of the four loading rates which were possible using the diametral compression instrument. During each test the analogue signals from the transducers were recorded on an X-Y plotter (Model 26000, Bryans Southern Instruments, Mitcham) with the displacement on the X axis and the diametral force on the Y axis. The NRD was calculated by subtracting the displacement, d_1 when the force rises from zero on the first loading, from the displacement, d_2 when the force rises from zero on the second loading (equation 2.9).

$$NRD = d_2 - d_1 \qquad \text{Eq. 2.9}$$

The total deformation of the tablet, loaded to 75% of its breaking load, $d_{75\%}$ is given by equation 2.10

$$d_{75\%} = d_T - d_1 \qquad \text{Eq. 2.10}$$

where d_T is the total displacement recorded on the X axis of the X-Y plotter.

3. MECHANICAL PROPERTIES OF TABLETS

3.1 The Strength of Tablets

3.1.1. Tensile strength-compaction force profiles

The tensile strength-compaction force profile for each of the materials studied is shown in Fig. 3.1. For all of the materials the relationship is non-linear and, with the exception of lactose, all profiles show a sigmoidal shape. This shape is probably indicative of the different ways in which the energy of compaction, supplied by the tablet press, is utilised during various stages of tablet formation.

The first stage of compaction, as suggested by Seelig and Wulff (1946), involves rearrangement and closer packing of particles, work being done to overcome particle-particle and particle-die wall friction. As the compaction force increases, elastic and plastic deformation of the particles takes place, possibly associated with fragmentation depending on the nature of the material, and inter-particulate bonds are formed. Finally, elastic compression of the bulk compact occurs as shown by Train (1956). These stages of compaction cannot be separated and may occur simultaneously but with one consolidation mechanism predominating, depending on the magnitude of the compaction force.

Considering the shape of the tensile strength-compaction force profile of Elcema, shown in Fig. 3.1, the initial slope of section AB suggests that particle rearrangement and slight distortion of surface asperities cause only small changes in tensile strength for a given increase in compaction force. As compaction proceeds,

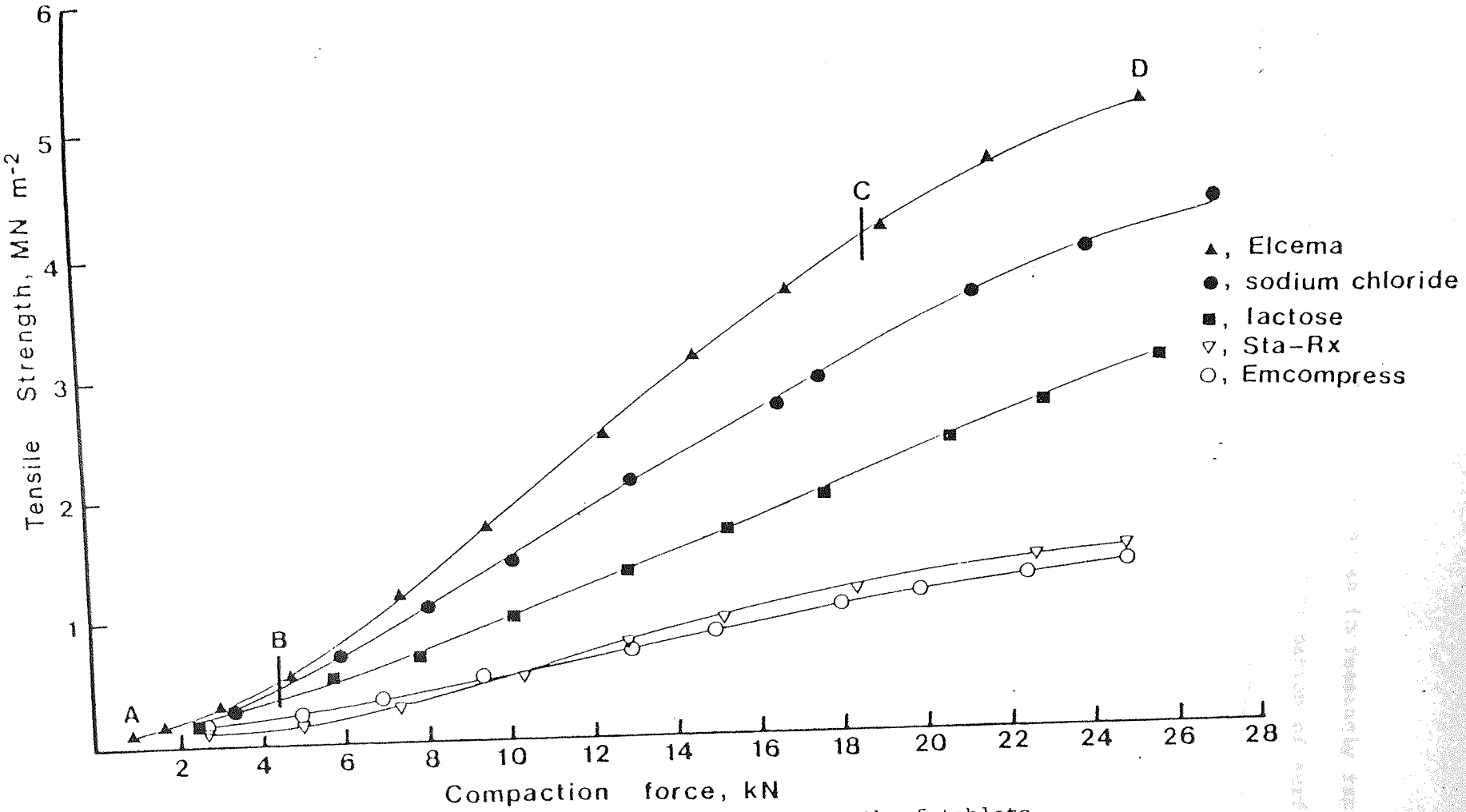

Fig. 3.1 The relationship between tensile strength of tablets and the applied compaction force.

the slope of AB increases, indicating an increasingly rapid change in tensile strength as more extensive deformation of surface asperities and whole particles occurs; this increases the total area of inter-particulate contact which in the materials studied is apparently associated with bond formation. The low values of tensile strength in the region AB cause difficulties in measurement and, together with the relatively large inter-tablet variation, this may explain the conclusions of earlier workers, including Shotton and Ganderton (1960) and Rees and Shotton (1970), that section BC can be extrapolated to the compaction force axis to indicate the force below which a coherent compact cannot be formed. However, this conclusion is not correct since extrapolation of the region BC for Elcema predicts a minimum necessary compaction force of 3kN, whereas it was possible to produce compacts using a compaction force as low as 0.8 kN. This is not unexpected since even a powder bed, in which the only axial force acting is due to the powder's own weight, possesses a small tensile strength. Thus the intercept on the tensile strength axis must have a positive value. For a material which consolidates purely by plastic deformation over the entire compaction force range, the tensile strength must increase with an increasing compaction force due to an increased area of inter-particulate contact. If precise measurement of tensile strength could be performed at low values of compaction force, materials which easily fragment might initially exhibit very small increases in tensile strength, due to closer packing of the particles, followed by a temporary decrease as particle fragmentation predominates and reduces the mechanical interlocking of the particles. Evidence for this might be difficult

to obtain due to the non-isotropic nature of the consolidating material since particles at different levels of the powder bed will be subjected to different stresses. Some particles will be fragmenting causing a reduction in tensile strength, while other particles will be bonding due to the applied compaction force.

During stage BC, extensive deformation of the particles at first causes a rapid reduction in void volume associated with inter-particle bonding, but eventually more work must be done to produce an equivalent increase in the area of surface contact. This is due to the reduction in voidage of the tablet into which the material can deform or, in some materials, due to work hardening which increases the difficulty of deformation of the material as discussed in section 1. At this stage, the slope of section BC starts to decrease. Eventually a state of maximum consolidation is approached and an increasing proportion of the energy is used for elastic compression of the bulk compact; thus during stage CD the gradient of the curve decreases more rapidly showing a smaller rise in tensile strength with compaction force.

An exception to the characteristic sigmoidal curve is anhydrous lactose which does not exhibit an equivalent to stage CD. This is not unexpected since Fell and Newton (1970) found a linear relationship between tensile strength and compaction force for spray dried and crystalline lactose at compaction forces between 5 and 40 kN. It is probable that lactose would show a stage equivalent to CD if the compaction force was increased to a suitably high value.

3.1.2 The effect of porosity on tensile strength

Jones (1976) criticised tensile strength-compaction force profiles as often being misleading since comparison is made at constant compaction pressure rather than constant porosity. For example, differences in the particle size distribution of materials may lead to variation in the number of contact points available for bonding. Even when comparing tablets of different materials at similar porosities, the number of inter-particulate contact points may be different. However, the area of inter-particualate contact in two tablets will probably have a greater similarity if they are compared at equal porosity rather than equal compaction force. Fig. 3.2 shows the relationship between the tensile strength and the % void volume which is calculated from the true density of the material and the tablet dimensions. There are large differences in tensile strengths of different materials, even when comparing tablets of equal porosity. These differences are reduced with an increasing % void volume, which is equivalent to a reduced compaction force. However, it is interesting that the relationship between % void volume and tensile strength for the two brittle materials (see section 3.2) lactose and Emcompress is very similar whereas their tensile strength-compaction force profiles show considerable differences. Generally the mechanical strength of the tablet formed during compaction will depend on failure properties of the materials being compressed and so differences in tensile strength of tablets would be expected even if comparison is made at constant porosity. For lactose and Emcompress the similarity in the relationship between % void volume and tensile strength suggests that the failure properties

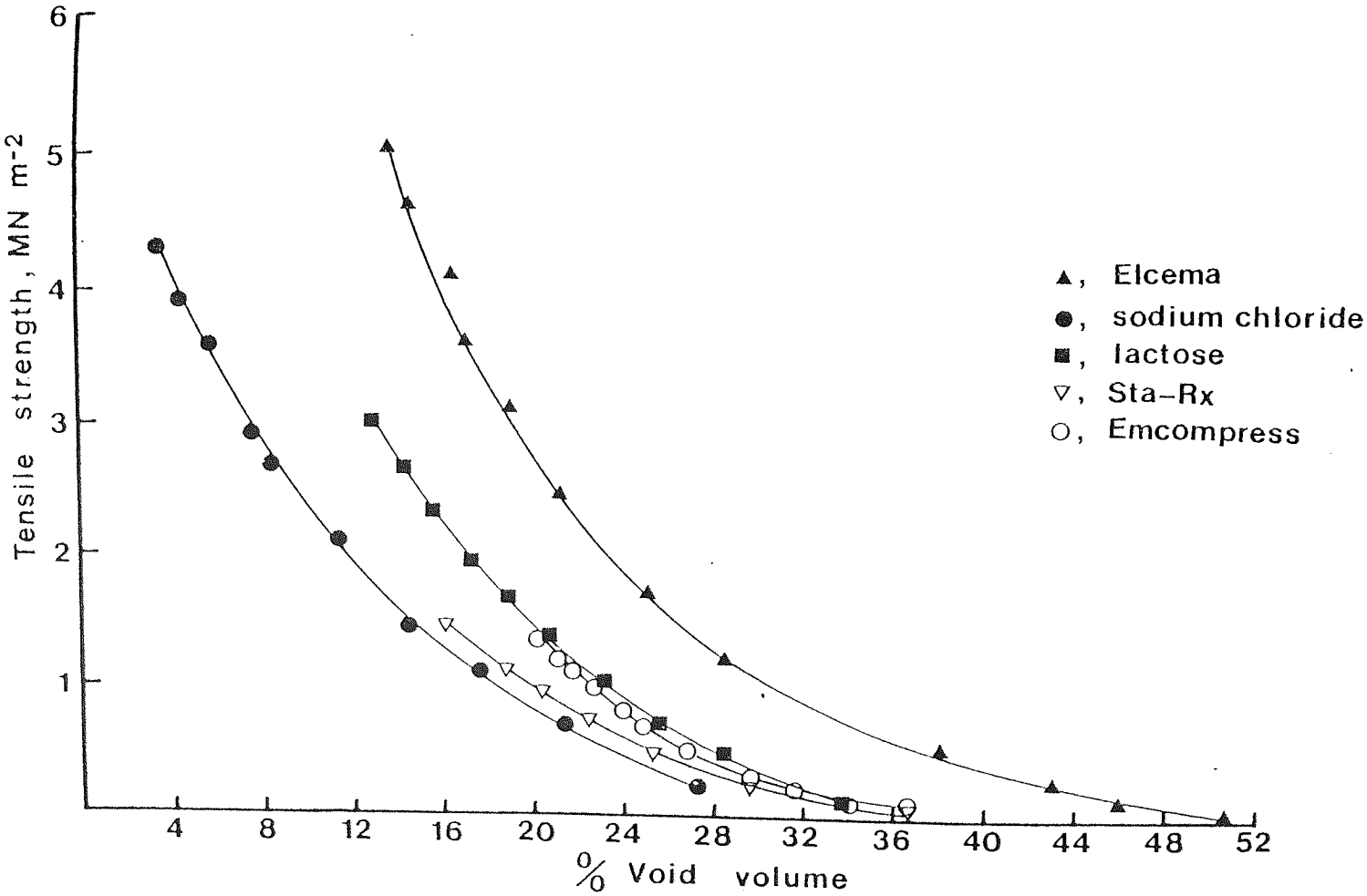

Fig. 3.2 The relationship between the tensile strength and the %void volume of tablets

of these materials are similar and that differences in their tensile strength-compaction force profiles are due to differences in the number of bonds formed by each material at a given compaction force. The effect of compaction force on the % void volume is shown in Fig. 3.3. Increasing the compaction force reduces the % void volume of lactose tablets more rapidly than that of Emcompress tablets and since, at a given compaction force, the tensile strength of lactose tablets is greater than that of Emcompress, this reduction in % void volume appears to cause a greater increase in the number of inter-particulate contact points for lactose than for Emcompress. It appears that there is a greater similarity in the failure properties of lactose and Emcompress than is indicated by their tensile strength-compaction force profiles. However, the differences in the effect of compaction force on % void volume for these two materials indicates that there is a difference in their deformation behaviour during compaction. At a given compaction force Emcompress appears to form less points of inter-particulate contact than lactose. This may be due to less fragmentation of Emcompress occurring than of lactose, or fragments of Emcompress being of a larger particle size. Thus the tensile strength of Emcompress tablets is lower, at a given compaction force, than that of lactose tablets.

For materials which undergo plastic deformation during compaction the actual number of contact points will initially remain constant over a wide range of compaction forces. Nevertheless with increasing compaction force the area of each bond will increase and therefore increase the tensile strength of the tablet.

For pharmaceutical applications the most appropriate

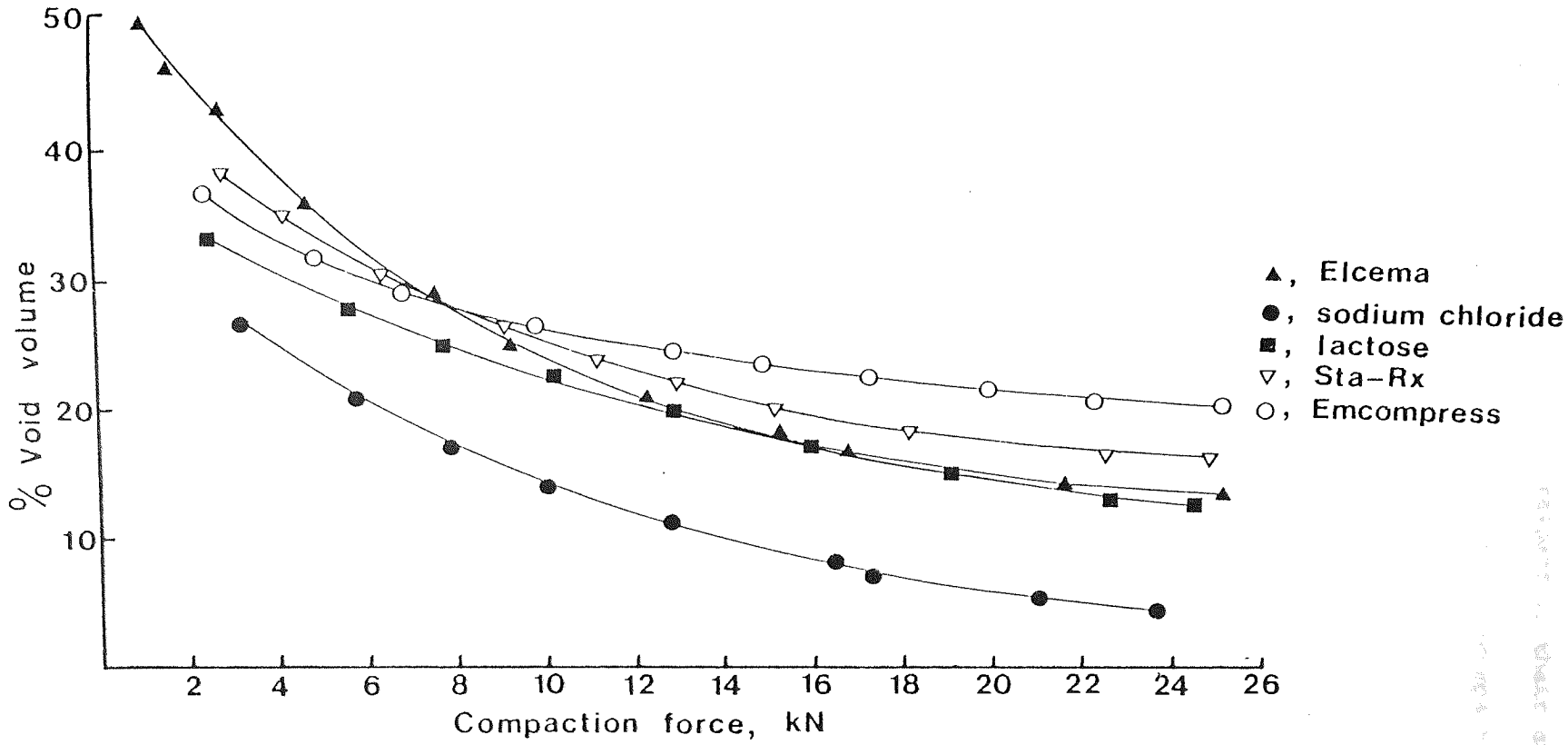

Fig. 3.3 The relationship between the %void volume of tablets and the applied compaction force

characterisation of materials with respect to their compaction properties appears to be the tensile strength-compaction force profile since it is the compaction force which is normally controlled as the independent variable. However, the relationship between % void volume and compaction force and between % void volume and tensile strength can provide useful information regarding the compaction behaviour of materials.

3.2 Load-Displacement Curves

Typical load-displacement curves for tablets of various materials subjected to diametral compression testing are shown in Fig. 3.4. Each curve shows an initial linear section followed by a curve of decreasing slope. One might conclude that this indicates linear elastic behaviour up to a yield point, during which loading and unloading would follow the same line, followed by plastic deformation. However, the apparent elastic behaviour may not be truly elastic for all materials. Dieter (1961), referring to metals, suggests that the true elastic limit may be very low, "if indeed one exists at all". If the behaviour of the tablets is truly elastic, then the rate of platten movement, or strain rate, would have no effect on the linear section of the load-displacment curves. However, if the behaviour is not elastic, for example visco-elastic, then the strain rate would have a marked effect on the linear section of such curves.

Figs. 3.5 and 3.6 show the load-displacement curves for tablets of lactose and Elcema at four rates of platten movement. The rate has little effect on the brittle lactose. In contrast, with the plastic material Elcema, as the rate of loading decreases there

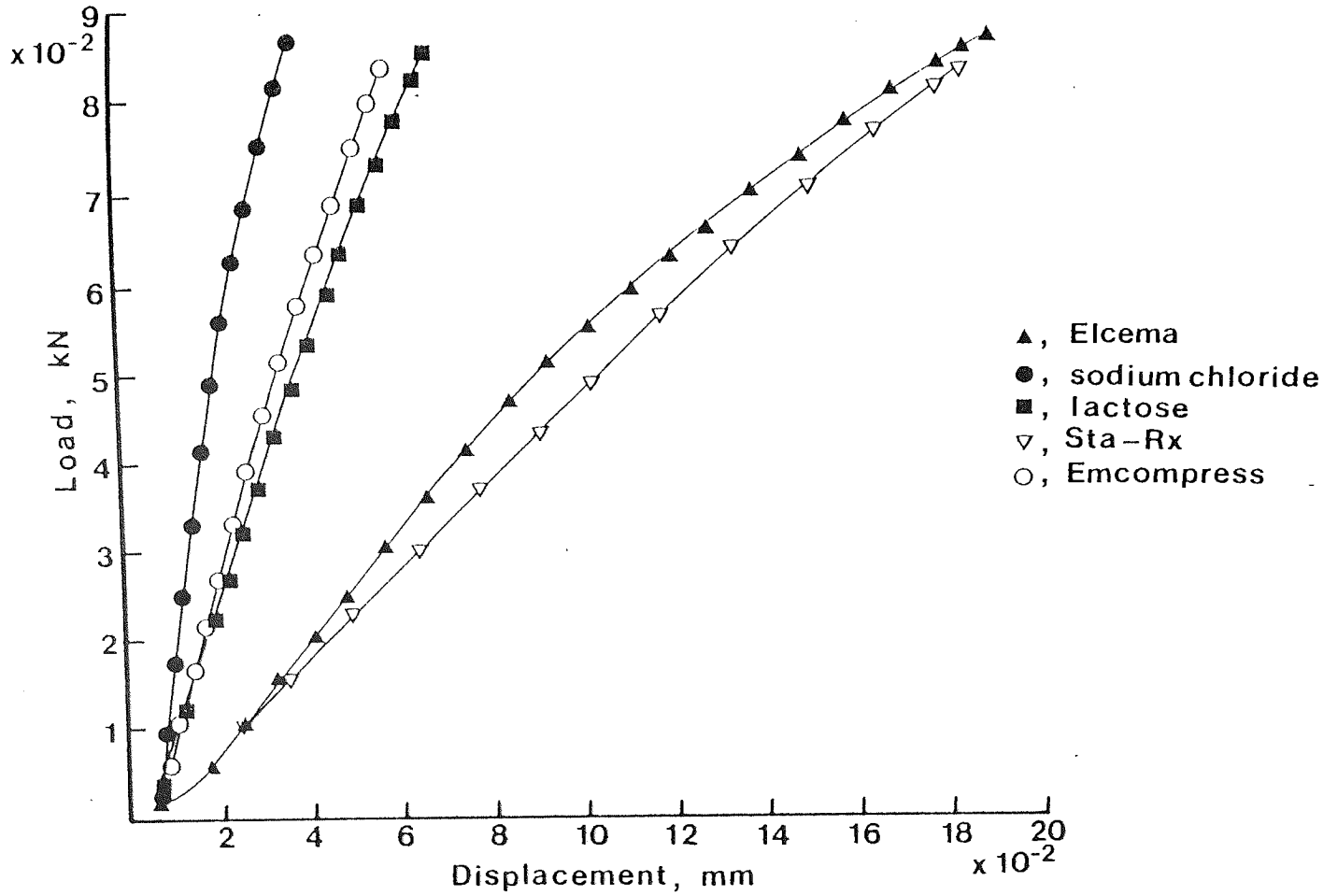

Fig. 3.4 Load-displacement curves for tablets subjected to diametral compression testing at a rate of platten movement of 0.26 mm min^{-1}

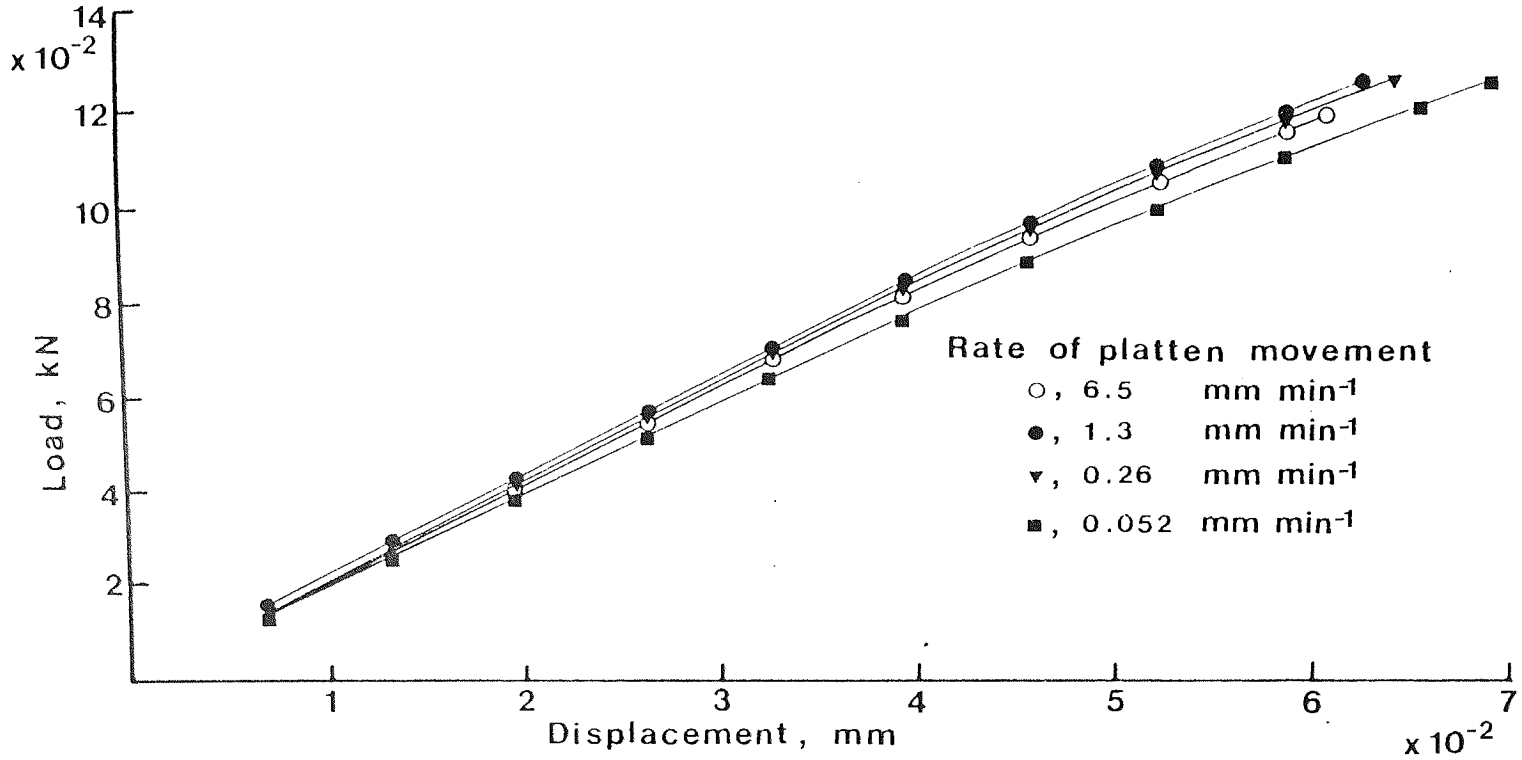

Fig. 3.5 Load-displacement curves for lactose tablets subjected to diametral compression testing at four rates of platten movement until failure

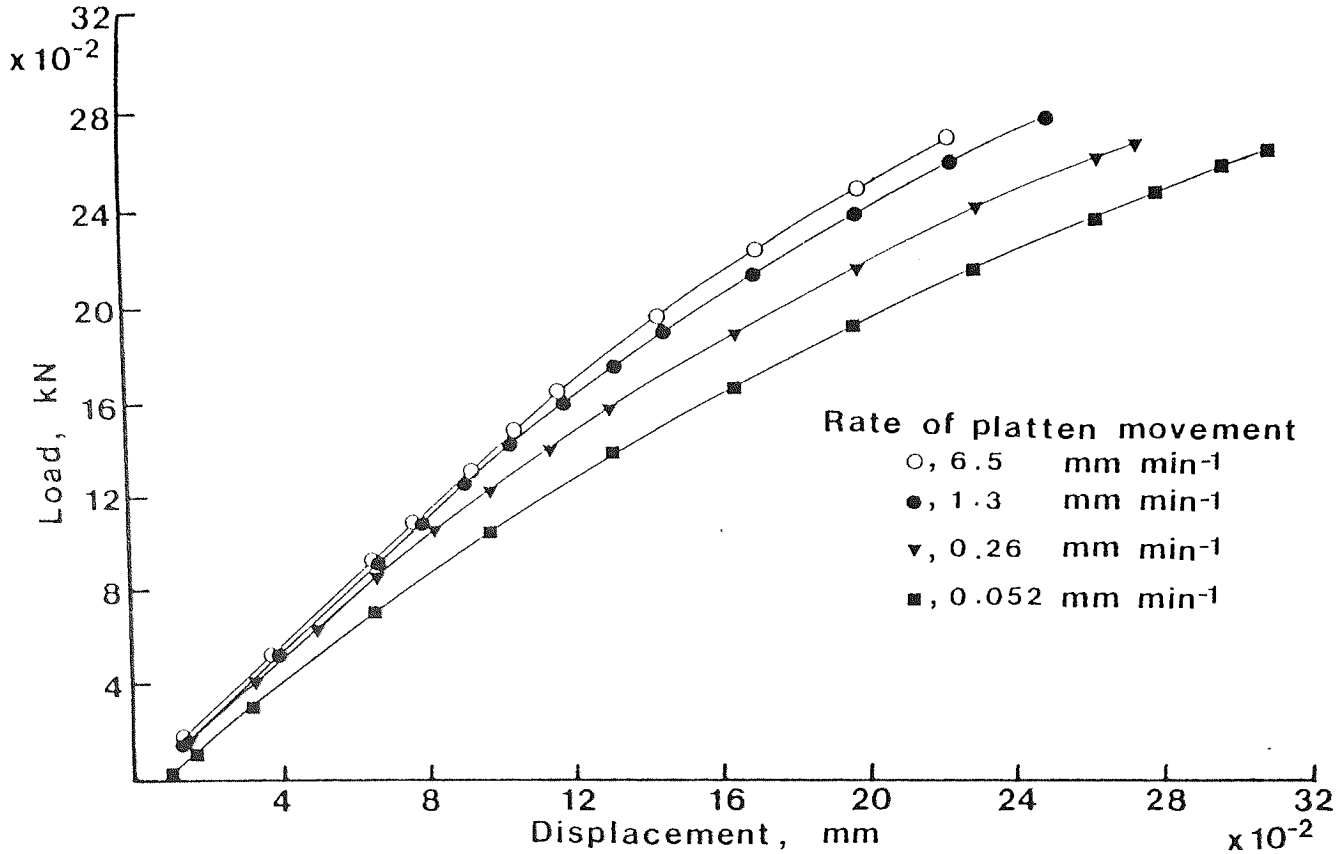

Fig. 3.6 Load-displacement curves for Elcema tablets subjected to diametral compression testing at four rates of platten movement until failure

is a decrease in the 'apparent elastic limit' as represented by the limit of linear behaviour until, at a rate of platten movement of 0.052 mm min^{-1}, there is no discernible linear behaviour during the entire loading line. This time-dependent lowering of the 'apparent elastic limit' suggests that there is no true elastic limit for some plastic materials. This is not unexpected since it is known that high strain rates tend to cause brittle failure (Cottrell, 1964), the stress-strain curve for an ideal brittle material being completely linear to the point of failure.

The effect of increasing the rate of platten movement on the load-displacement curves of Elcema tablets is to reduce the amount of plastic deformation which occurs. At high rates of platten movement the applied diametral load probably causes a high proportion of the total strain to be seen as elastic deformation of the crystalline sections of Elcema. As the rate of platten movement decreases the time available for slip of the sections of Elcema over one another increases and a greater proportion of the total deformation is seen as plastic deformation. At very high rates of platten movement, it is probable that the behaviour of Elcema tablets will tend towards that of a brittle material showing a higher 'apparent elastic limit' and a lower displacement at the point of failure.

For lactose tablets, the changes of strain rate used in this study have little effect on the load-displacment curves. This is because during loading of lactose tablets only very limited slip occurs before the stress is sufficient to satisfy the Griffith criterion discussed in section 1.5.3.1 at which point rapid crack propagation occurs.

It is interesting to consider the effect of strain rate on the load-displacment curves of Elcema in the context of Dieters' (1961) statement that the yield stress of specimens is more sensitive to strain rate than is their tensile strength. This appears to be true in the case of Elcema since the yield stress, which is the equivalent of the 'apparent elastic limit' is affected by the strain rate, but the breaking force is not, as shown in Fig. 3.6.

During this study, no difference was found in the tensile strengths of Elcema tablets tested at different rates. However, Rees, Hersey and Cole (1970), using a formulation containing equal parts of anhydrous lactose and Avicel, which is a material chemically similar to Elcema, found a small but significant increase in the breaking strength of tablets subjected to diametral compression at rates of platten movement increasing from 0.5 to 50 mm min^{-1}. No explanation of this difference between the results shown by Rees, Hersey and Cole (1970) and the results of this study can be suggested, but it is possible that differences in the measured tensile strength, due to changes in the rate of platten movement, may be more easily seen at higher rates of platten movement than used in this study, such as those used by Rees, Hersey and Cole (1970). Further work is necessary using a wider range of rates of platten movement than used in this study to clarify the effect of strain rate on both the tensile strength and failure displacement of tablets.

The classification of failure as brittle or plastic (ductile) generally depends on the amount of plastic deformation preceeding failure (Sinnott, 1958). In Fig. 3.4. the failure of Elcema tablets may be described as plastic, while failure of Emcompress,

sodium chloride and lactose is brittle.

The gradients of the linear section of the load-displacement curves listed in Table 3.1 are a measure of the ease of deformation of the tablet and are related to the modulus of elasticity obtained from the gradient of a true stress-strain curve.

Material	Breaking force kN	Rate of platten movement mm min^{-1}	Gradient kN mm^{-1}
sodium chloride	8.65×10^{-2}	0.26	3.33
Emcompress	8.35×10^{-2}	0.26	1.83
lactose	8.50×10^{-2}	0.26	1.46
Elcema	8.65×10^{-2}	0.26	0.65
Sta-Rx	8.35×10^{-2}	0.26	0.52
Elcema	2.65×10^{-1}	0.052	no linear section
Elcema	2.68×10^{-1}	0.26	1.30
Elcema	2.83×10^{-1}	1.30	1.43
Elcema	2.70×10^{-1}	6.50	1.49
lactose	1.26×10^{-1}	0.052	2.03
lactose	1.26×10^{-1}	0.26	2.19
lactose	1.26×10^{-1}	1.30	2.19
lactose	1.19×10^{-1}	6.50	2.13

Table 3.1 The gradients of the linear sections of load-displacment curves of tablets tested in diametral compression.

The load-displacement curves shown in Fig. 3.4 are, however, based on the diametral displacement in the compressive direction of a non-isotropic, non-homogeneous, cylindrical specimen and so other factors will influence the gradients of such curves. For a true stress-strain curve, the strain is a dimensionless quantity calculated by dividing the change in a dimension by the original dimension, whereas the diametral displacement has the dimensions of mm. The diametral displacement could be modified, by dividing by the tablet diameter, to produce a true compressive strain. However, the resulting curves would be a combination of

a tensile stress and a compressive strain. The compressive strain will have a complex relationship with the tensile strain, the relationship depending on the Poissons ratio of the material, the porosity of the tablet and, for some materials, the rate of platten movement. The true stress-strain curves for tablets, which may provide a more precise characterisation of a tablet's mechanical behaviour, can be determined only if the deformation of the tablet is measured normal to the applied diametral load, or if the relationship between compressive and tensile strains is determined. Both the porosity of the tablet and the deformation of the tablet at its contact surface with the metal plattens will affect the load-displacement curves by altering the stress distribution across the tablet diameter. An increasing porosity will result in a higher tensile force per unit area of bond at any given applied load and will thus increase the displacement at that load. The deformation behaviour of the tablet at the contact surface will alter the stress distribution across the diameter by changing the area of contact through which the compressive load is applied resulting in unwanted compressive and shear stresses of unknown magnitude. Nevertheless load-displacement curves provide a method of quantifying the deformation behaviour of specimens of a standard size (12.7 mm) and equal tensile strengths.

3.3 Distance Moved by the Platten During Testing

The distances moved by the platten during diametral compression tests on the various tablets are compared in Fig. 3.7, with respect to the compaction force used to prepare the tablets.

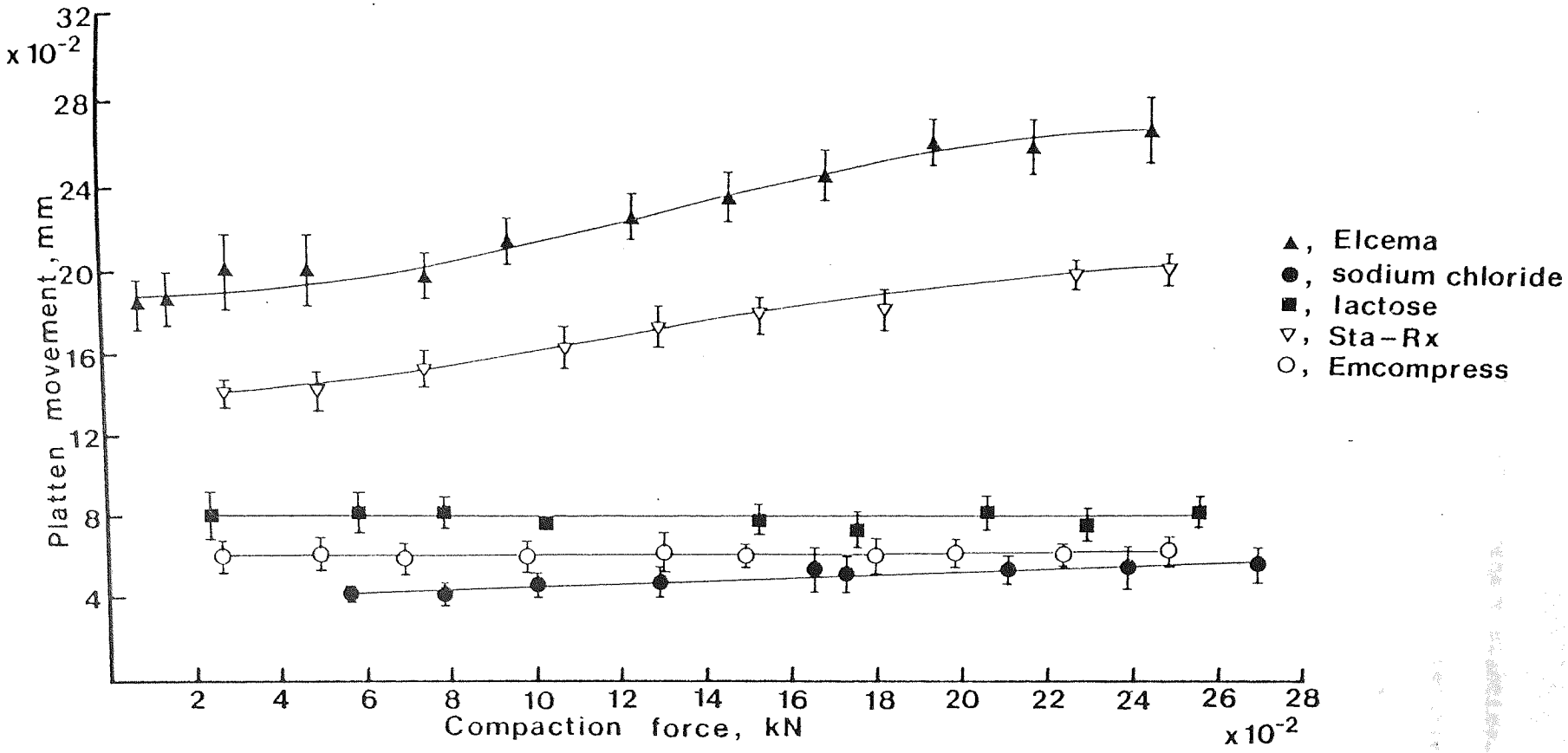

Fig. 3.7 The relationship between the platten movement at the point of failure and the applied compaction force for tablets subjected to diametral compression testing at a rate of platten movement of 0.26 mm min^{-1}.
The bars indicate the standard errors.

Tablets of Elcema and Sta-Rx, which behave plastically as shown by their load-displacement curves (Fig. 3.4) require a relatively large platten displacement before tablet failure occurs. The increase in diametral displacement with increasing compaction force for the materials is thought to be due to the relatively large areas of inter-particulate bonding created at higher compaction forces. Such bonds of large cross-sectional area could undergo greater plastic strain before failure occurs. In contrast tablets of brittle materials such as Emcompress or lactose require only a small diametral displacement to cause failure. In this case compaction force has little effect on the diametral displacement at failure, presumably because for a brittle material the effect of increasing compaction force is primarily to increase the number of brittle inter-particulate bonds rather than to increase the area of existing points of contact as in the case of a plastic material.

Sodium chloride exhibits apparently anomalous behaviour; small diametral displacements were recorded prior to failure and the force-displacement curve for this material shown in Fig. 3.4, exhibits the characteristics of a brittle material. However, extensive plastic deformation is known to occur during compaction of sodium chloride as shown by Hardman and Lilley (1973) and Cole, Rees and Hersey (1975). This phenomenon is probably due to work hardening of the material during compaction when extensive deformation of the particles occurs. Bowden and Tabor (1964) and Hardman and Lilley (1973) have reported that work hardening of sodium chloride can occur.

Work hardening which is discussed in detail in section 1.5.4,

is due to glide dislocations interacting and mutually obstructing one another thus preventing further plastic flow. During compaction of sodium chloride extensive deformation of the particles occurs until large scale entanglement of dislocations has made further particle deformation more difficult. This work hardening during compaction will prevent plastic deformation taking place under diametral loading of tablets of sodium chloride which therefore show brittle failure.

3.4 Work of Failure

The usual method of characterising the mechanical strength of tablets is to measure the tensile strength or crushing force. Such tests, together with friability measurements, are used widely by the pharmaceutical industry as quality control assessments of a tablets resistance to mechanical failure, but it is well known that specifications for different formulations cannot be compared quantitatively. For a particular tablet to withstand mechanical shock or abrasion under specific conditions of processing or transport, it may require a considerably higher breaking strength than tablets of a different drug substance or of the same drug substance formulated differently.

Schubert, Herrman and Rumpf (1975) suggested that it is often necessary to study the stress-strain behaviour of an agglomerate in order to fully characterise its mechanical behaviour. For example, a specimen with a large fracture strain will be less sensitive to cracking than a material with a low fracture strain even though their tensile strengths may be identical. This phenomenon is known in metallurgy as toughness and has been

described by Dieter (1961) as the ability of the material to absorb energy in the plastic range. One way of quantifying toughness is to measure the total area under the stress-strain curve. Theoretical stress-strain curves for two identically sized specimens of different materials are shown in Fig. 3.8. Material I has a higher tensile strength than material II, but material II has a higher fracture strain. The area under the curve for material II is larger and material II is therefore described as being tougher than material I.

It is not possible to obtain true stress-strain curves for tablets using a diametral compression test, but it is possible to calculate the area under the load-displacement curves as described in section 2.3.1.1. This area is a measure of the work done on the tablet by the plattens to cause failure and is related to the toughness of the tablet. Since the area is not based on a true stress-strain curve, the term work of failure is used here rather than toughness. Figs. 3.9 and 3.10 show the effect of increasing the compaction force, used to prepare the tablets, on the work of failure for the five materials studied; the curves show a similar sigmoidal shape to that observed for tensile strength (Fig. 3.1). Fig. 3.10 is included to allow comparison of the complete work of failure/compaction force profile of Elcema with the other materials since the very high values of work of failure of Elcema tablets prevent the complete profile being drawn on Fig. 3.9. Considering the two extreme materials, the tensile strength of Elcema tablets is 3 to 3.5 times greater than for Emcompress tablets, whereas the work of failure for Elcema tablets is 10 to 20 times greater than for Emcompress, these ratios increasing with increasing compaction force. For tablets

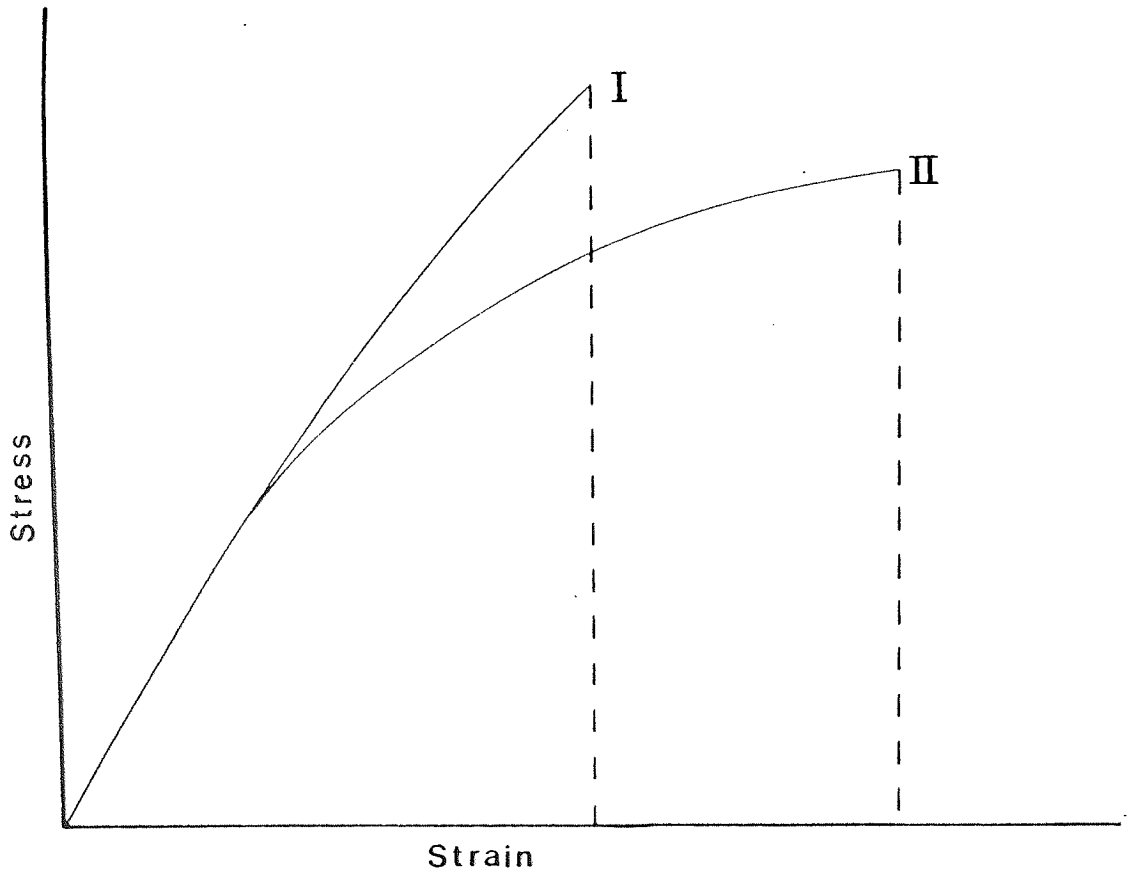

Fig. 3.8 Theoretical stress-strain curve for two identical sized specimens of different materials

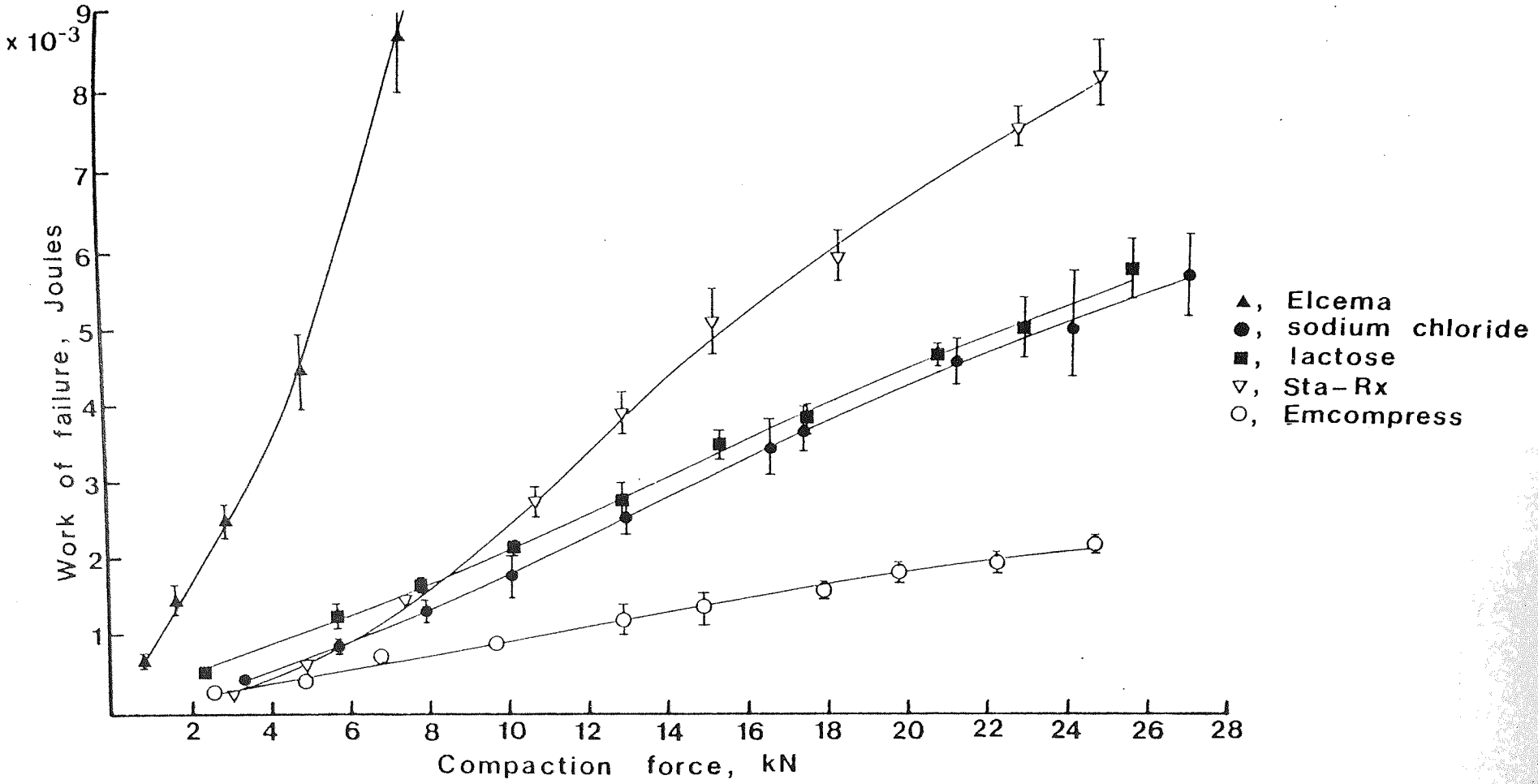

Fig. 3.9 The relationship between the work of failure and the applied compaction force for tablets subjected to diametral compression testing at a rate of platten movement of 0.26 mm min^{-1}. The bars indicate the standard errors.

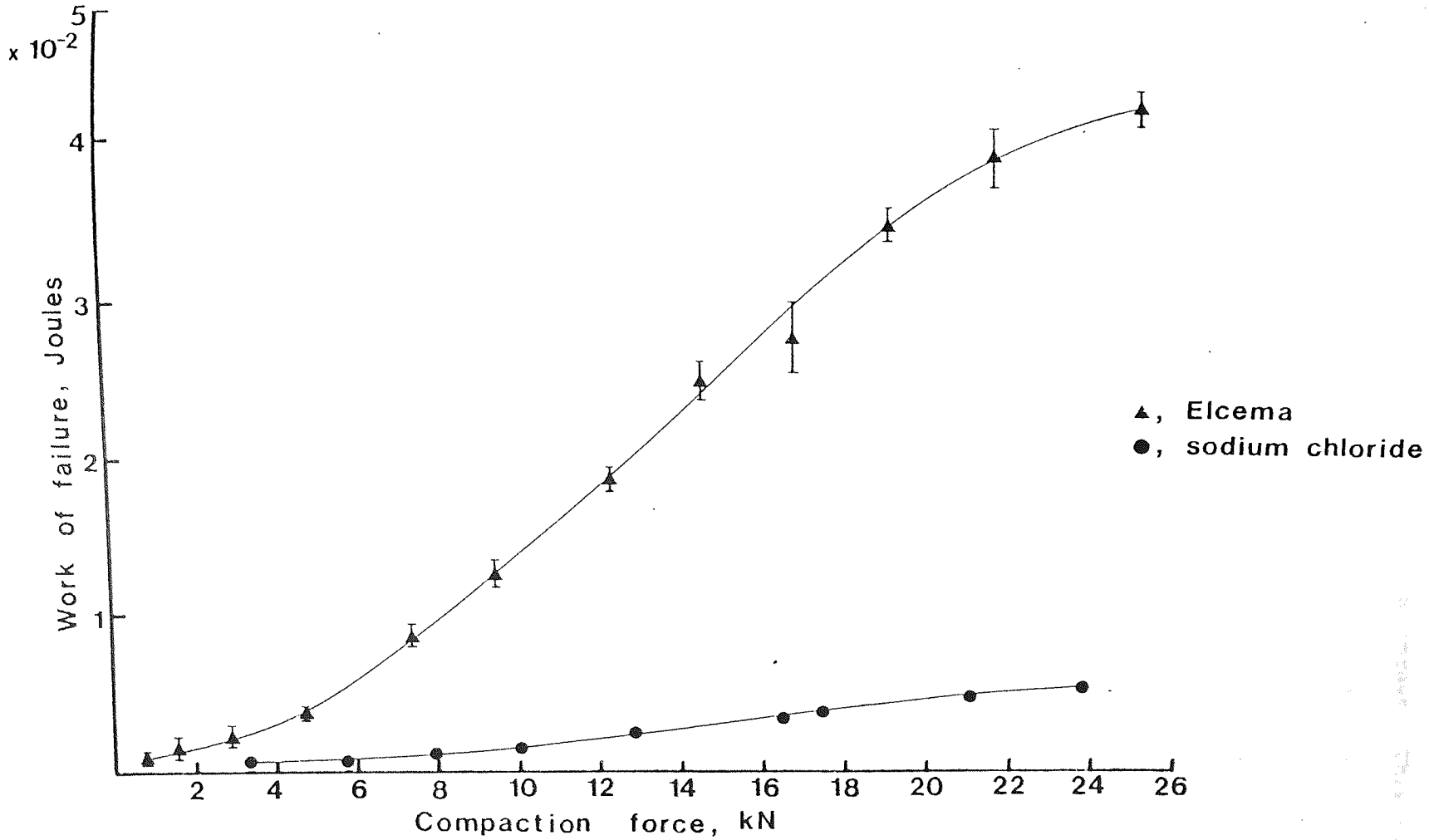

Fig. 3.10 The relationship between the work of failure and the applied compaction force for Elcema and sodium chloride tablets subjected to diametral compression testing at a rate of platten movement of 0.26 mm min^{-1}. The bars indicate the standard errors.

of equal tensile strength, the work of failure for Elcema is therefore considerably higher than for Emcompress. This is because the Elcema tablets show a much higher failure displacement as seen in Fig. 3.7.

Despite the small diametral displacements recorded for sodium chloride tablets, compared with the other materials investigated shown in Fig. 3.7, the values for work of failure are intermediate. This is because of the relatively steep tensile strength-compaction force profile for this material which is shown in Fig. 3.1. Comparing sodium chloride with Sta-Rx, the tensile strength values for Sta-Rx are much lower (Fig. 3.1) but the work of failure values are greater (Fig. 3.9). This is due to the large failure displacement values for Sta-Rx tablets seen during the diametral loading tests. The work of failure values for Elcema are exceptionally high (Fig. 3.10) due to a combination of high tensile strength and large displacement.

In this slow rate diametral compression test, Sta-Rx and Elcema, materials which show plastic failure as defined in section 3.2, have a higher work of failure than materials which show brittle failure. This is due to the greater energy absorbed by a plastic material, relative to a brittle material, which is used to cause slip of the material. For a plastic material, an increase in the rate of platten movement would be expected to cause a reduction in work of failure. No experiments were carried out in this study to determine the effect of rate of platten movement on the work of failure due to the limited range of rates available and the difficulties of calculation of the area under the load-displacement curves at high rates. Further work is necessary to determine this effect and is discussed in section 9.5.

3.5 Multiple Diametral Impact Testing

Generally if a material absorbs relatively large amounts of energy during stressing which is used for plastic work along the slip planes then the material will possess good shock resistance, being able to absorb the energy of impact by plastic deformation. The work of failure values are related to the energy absorbed by a tablet to cause failure in a low strain rate diametral compression test. Cottrell (1964) states, "All crystalline solids in which dislocations move fast only at high stresses appear capable of brittle cleavage under impact loading. Their dislocations cannot move fast enough to relax the stress of a high speed crack". The materials Sta-Rx and Elcema do not contain dislocations, nevertheless the rate of testing has been shown, in section 3.2, to affect the deformation of tablets during diametral compression testing. Some materials may have a latent brittleness which may be seen during very high strain rate testing and so values for work of failure may not reflect the resistance of the tablets to mechanical failure under impact loading. Initially a friabilator (J. Engelsmann A.G., Ludwigshafen, West Germany) was used in an attempt to cause breakage of tablets under the shock conditions of the 15 cm drop which occurs on each revolution. However, the stresses imposed on the tablets were insufficient to cause fracture of tablets other than those of very low tensile strength. For this reason the multiple diametral impact test, described in section 2.3.2., was devised in an attempt to simulate conditions to which tablets might be subjected in practice and which might be responsible for their mechanical failure.

The results of this semi-empirical test, shown in Table 3.2

Material	Diametral compression test			Number of impacts to cause failure	
	Mean tensile strength $MN\ m^{-2}$	Work of failure Joules			
		mean	coefficient of variation %	mean	coefficient of variation %
Elcema G250	1.67	1.51×10^{-2}	5.4	4360	11.8
Sta-Rx 1500	1.36	7.01×10^{-3}	8.8	322	28.3
anhydrous lactose	1.59	3.45×10^{-3}	8.1	41	17.1
Emcompress	1.63	3.05×10^{-3}	3.6	28	17.9
sodium chloride	1.85	2.52×10^{-3}	12.8	5	20.0

Table 3.2 Multiple diametral impact test data for tablets of similar tensile strength

and Fig. 3.11, indicate a relationship between the work of failure for tablets and the number of impacts required to cause failure, N. The effective stress imposed on the tablet is an unknown combination of compressive, shear and tensile stresses and this probably explains the large coefficient of variation for the values of N. For some tablets extensive fragmentation occurred before and during failure, whereas for others, clean tensile failure occurred along a diameter. In general, fragmentation was seen for materials which exhibit brittle failure during diametral compression and clean tensile failure was seen for materials which undergo plastic failure during diametral loading tests. For a brittle material the applied stress is concentrated at the tips of cracks. When a tablet is subjected to impact loading the stress is not instantaneously transmitted to all parts of the tablet; parts of the tablet remote from the impact site remain undisturbed due to the time required for stress-wave propagation and the very short time of stress application. On impact the surface of the tablet in contact with the metal platten is subjected to tensile, compressive and shear stresses which are concentrated by the cracks and this may lead to localised crack propagation in the region near the impact site thus causing the observed fragmentation. Initially the cracks do not propagate across the whole tablet since, under impact loading, the cracks do nct have time to propagate throughout the tablet before the stress changes from a relatively high to a relatively low value. This localised surface crushing weakens the tablet and on repeated impact further crack propagation occurs causing further fragmentation and also failure of bonds until the strength of the tablets is no longer great enough to prevent crack

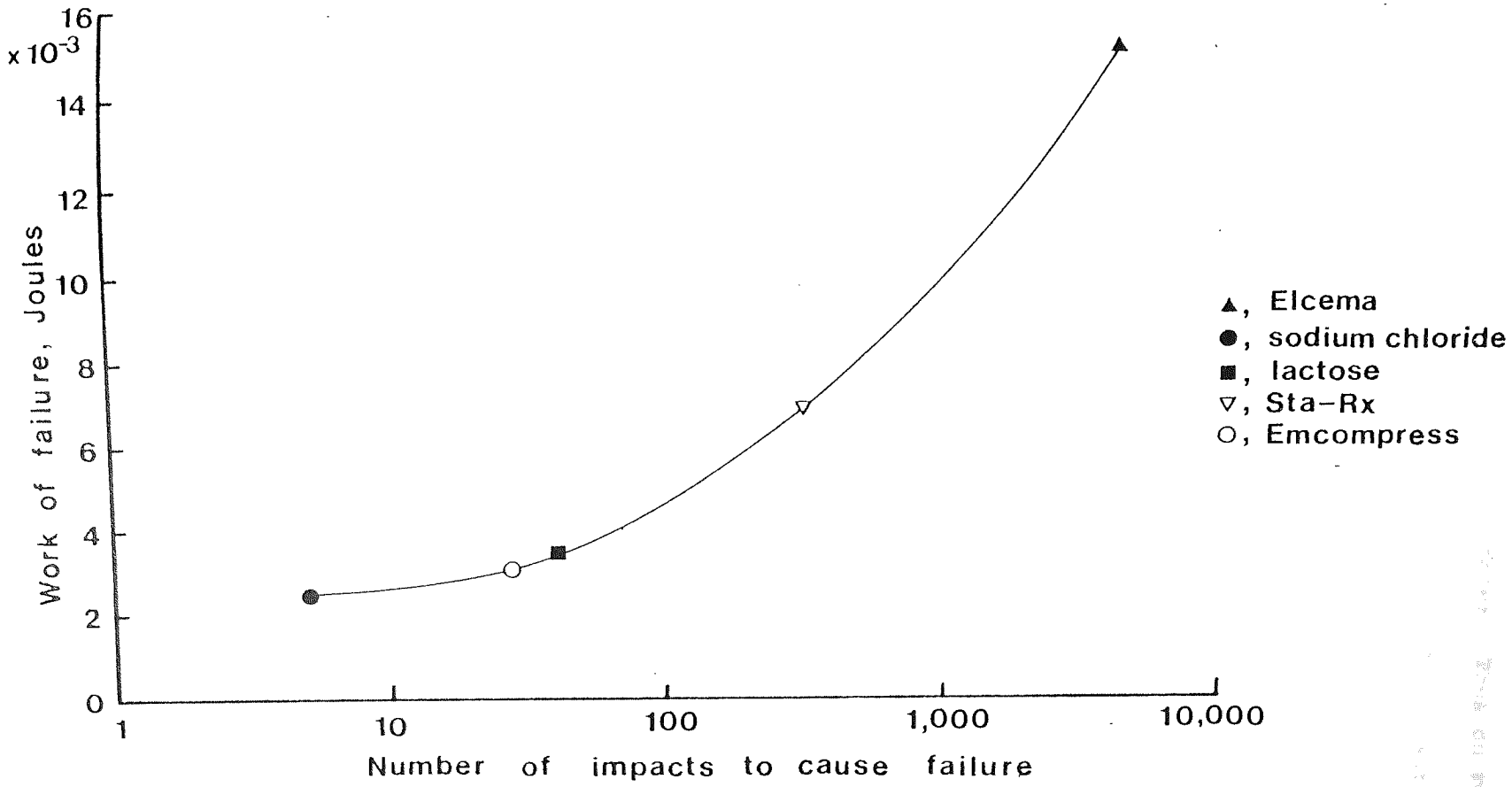

Fig. 3.11 The relationship between the work of failure and the number of impacts required to cause failure for tablets of similar tensile strength

propagation across the tablets' diameter. Thus on repeated impacts, a fatigue-like process leads to failure. For Elcema and Sta-Rx tablets, the large values of N suggest that the materials possess good shock resistance presumably due to absorption of the impact energy by plastic deformation. This plastic deformation will prevent rapid crack propagation, which is characteristic of brittle materials, by reducing the stress concentration effect at the tip of the cracks and so clean tensile failure will occur, without local fragmentation by a fatigue-like process. This process of fatigue crack growth is not well understood. However, it is known that, after crack initiation in a plastic material, the crack may become dormant showing no growth for up to three-quarters of the fatigue life of the specimen (Cottrell, 1964).

For tablets of each material possessing similar tensile strengths the mean value of N is in rank order agreement with the work of failure, suggesting that the work of failure is a more useful quantitative assessment of a tablets mechanical resistance to damage than values of tensile strength. The rank order agreement also suggests that the statement of Cottrell, given at the beginning of section 3.5, relating to latent brittleness does not apply to the two plastic materials since they show high values of N with no brittle fragmentation during impact loading.

Since the multiple impact tests were carried out on single materials with widely different failure properties, the data shown in Table 3.2 suggests that the relationship between the work of failure and N might be independent of the formulation of the tablet. If so, the work of failure values would be a better quality control parameter than tensile strength, since the tensile strength of different formulations cannot be compared quantitatively.

Rees, Rue and Richardson[1] (1977), using the same experimental technique described in section 2.3.2 conducted further studies on the relationship between work of failure and the number of impacts required to cause failure using tablets of the materials described in this study prepared at four different compaction forces and also using fourteen types of placebo tablets of various sizes, formulated with typical diluents, binders and lubricants. The formulated placebo tablets were supplied by various pharmaceutical companies and, although their qualitative composition was known, no further details were requested since the objective of the work was to test the hypothesis that differences in the formulation had no effect on the relationship between work of failure and N. The qualitative composition of the placebo tablets is given in Appendix 2.

Fig. 3.12 shows the regression line of the relationship between work of failure and N for all the placebo tablets and the direct compression materials. A linear correlation coefficient of 0.875 was obtained between work of failure and log N. In contrast the correlation coefficient between tensile strength and log N for the same tablets was 0.378.

The diameter of the placebo tablets was between 5 and 12 mm. To allow for the effect of size of the placebo tablets on the relationship between work of failure and N, a correction factor was used to convert the load applied during diametral compression to a tensile stress. The corrected value for work of failure is given by equation 3.1.

[1] Work carried out as part of a final year undergraduate project by Miss S. C. Richardson under the supervision of Dr. J. E. Rees and P. J. Rue.

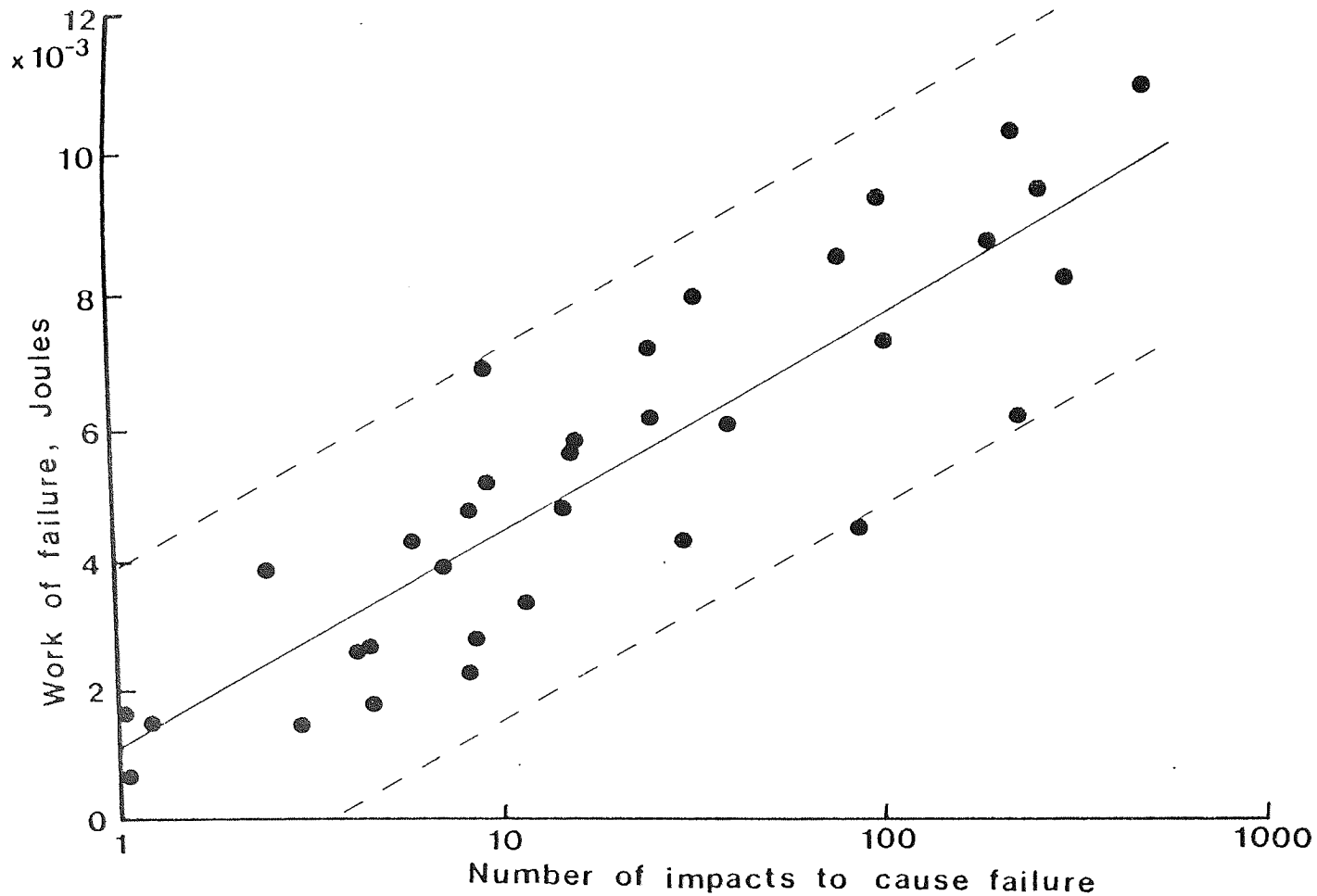

Fig. 3.12 The relationship between the work of failure and the number of impacts required to cause failure for formulated tablets and single direct compression excipient tablets. The dotted lines represent the 95% confidence limits of the regression line

$$Wf = \frac{2}{\pi Dt} \int P \cdot dx \qquad \text{Eq. 3.1}$$

where D = diameter of the tablet
t = thickness of the tablet
x = displacement of the platten.

For bi-convex tablets the area term Dt of equation 3.1 was modified to allow for the increased cross-sectional area created by the tablet shape. The modification is shown in equation 3.2.

$$Wf^* = \frac{2}{\pi (Dt_e + 2A_s)} \int P \cdot dx \qquad \text{Eq. 3.2}$$

where t_e = thickness of the tablet edge
A_s = increased cross-sectional area.

The method of calculation of A_s is shown in Appendix 2. The regression line of the relationship between Wf* and log N, is shown in Fig. 3.13. The linear correlation coefficient between Wf* and log N is 0.869. The critical correlation coefficient, which is the coefficient at which the correlation becomes significantly different from 0, for 30 degrees of freedom and at the 95% confidence level is 0.349. Thus the calculated values of correlation coefficient for the experimental data shows that there is a highly significant linear correlation between work of failure and log N and also between Wf* and log N. However, the correlation between tensile strength and log N, is only slightly significant.

The combined results for the placebo tablets and the direct compression materials obtained by Rees, Rue and Richardson (1977) indicate a linear relationship between work of failure and log N. However, this does not agree with Fig. 3.11 which suggests a non-linear relationship at high values of work of failure. If

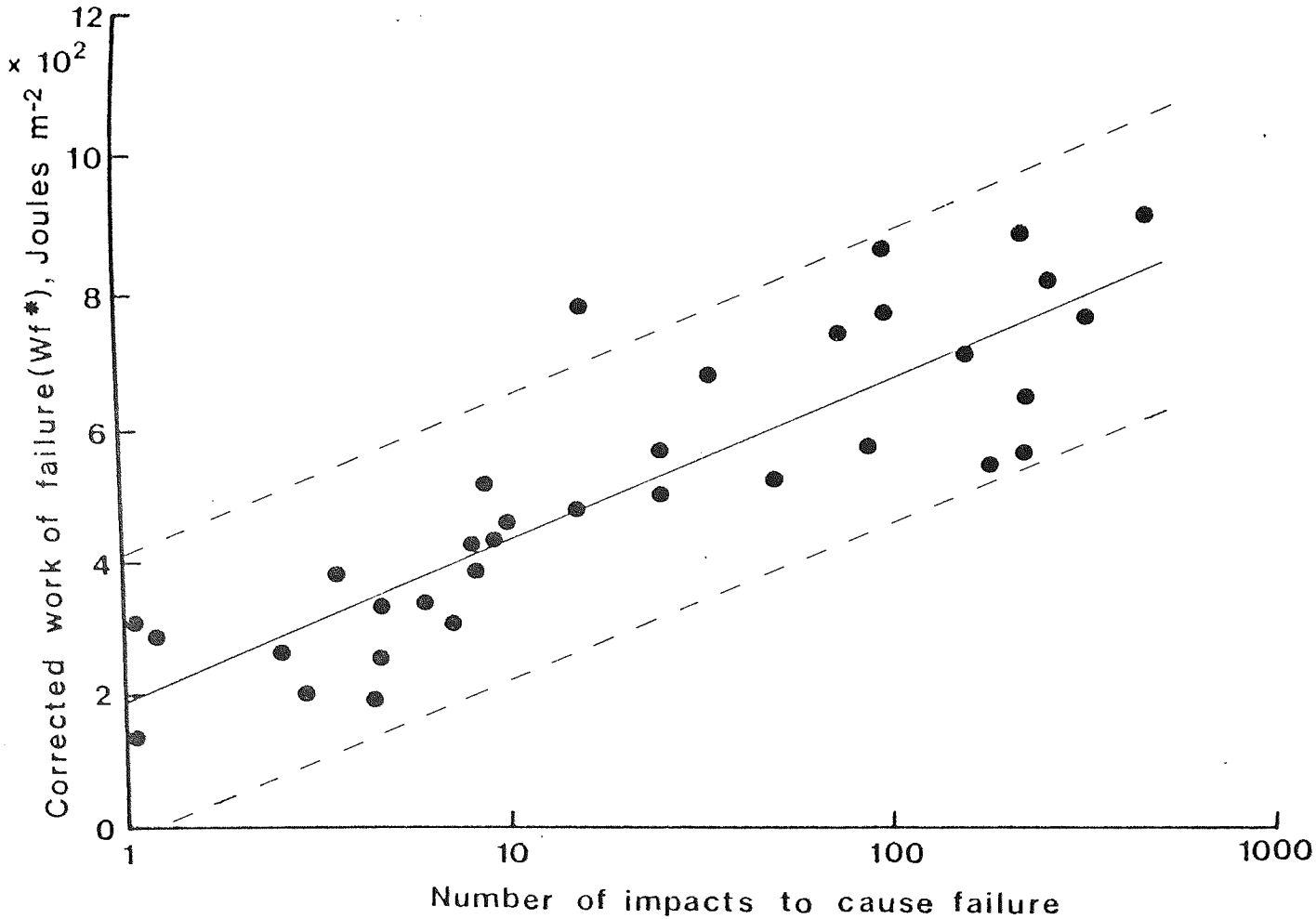

Fig. 3.13 The relationship between the work of failure corrected for tablet size and the number of impacts required to cause failure for formulated tablets and single direct compression excipient tablets. The dotted lines represent the 95% confidence limits of the regression lines

the data in Fig. 3.11 are plotted on Fig. 3.12, the result for Elcema lies outside both the 95% and 99.9% confidence lines, showing a much higher work of failure than expected for tablets which break after a mean number of 4360 impacts. During both impact testing and diametral compression testing, plastic deformation must occur to absorb the energy transferred to the tablet. In slow-rate diametral compression testing of tablets with a very high work of failure, time is available for plastic deformation to occur. However, during impact testing, such tablets cannot absorb the energy supplied by the large number of impacts at a high frequency and thus fatigue failure occurs more rapidly than expected causing a value of N lower than expected for tablets with a high work of failure. This may explain the non-linearity in the relationship between work of failure and log N for such tablets. This problem of non-linearity might be overcome if the values of work of failure were determined at higher rates of platten movement so as to reduce the energy absorbed by the tablet during the diametral compression test.

3.6 Conclusions

Fell and Newton (1970) have suggested that the tensile strength of tablets characterises the bond formation occurring during compaction. Many workers including Shotton and Ganderton (1960), Alpar, Hersey and Shotton (1970) and more recently Khan and Rhodes (1976) and David and Augsburger (1977) have used tensile strength or breaking force to characterise the mechanical properties of tablets or the effect of compaction variables on the mechanical properties. However, the results of multiple impact testing,

discussed in section 3.5, show that tensile strength alone does not fully characterise the mechanical properties of tablets. The deformation behaviour of the tablets must be considered in order to understand the failure properties and mechanical behaviour of tablets.

The area under the force-displacment curves of tablets tested in diametral compression, is related to the resistance of tablets to mechanical failure. During industrial production of tablets, the compressed tablet may be subjected to stress during further processing such as coating, packing and transport. To resist these stresses and to prevent breakage of tablets during these processes, tensile strength or crushing force specifications are established, for each formulation, on an empirical basis. Based on the results of the relationship between work of failure and log N, it may be possible to specify limits for work of failure ensuring that all tablets whose work of failure lies within these limits will withstand the stresses imposed during a particular processing operation without breakage or other mechanical damage.

4. STRESS RELAXATION STUDIES AND CONSOLIDATION BEHAVIOUR OF MATERIALS

4.1 Stress Relaxation During Compaction

During compression of a powder bed, the dwell time which, for a reciprocating tablet machine, may be defined as the time during which the upper punch is in contact with the material, may affect the amount of plastic deformation which occurs, but will have no effect on true elastic deformation or fragmentation caused by brittle failure of the particles. The effect of time on the compression process may be examined by means of stress relaxation measurements of materials maintained at constant strain. In this study, stress relaxation of a tablet was investigated in the die immediately after compression by stopping the rotation of the tablet machine fly-wheel, thus maintaining a constant upper punch displacement. The experimental details of this technique are given in section 2.2.3.

The effect of time on the upper punch force at constant upper punch displacement during powder compaction is shown in Fig. 4.1. Since the maximum compression force for each material varied slightly about the nominal value of 20 kN, the upper punch force is expressed as a percentage of the maximum applied force so as to standardise the values. In this initial study, the die wall was lubricated by compression of a blank compact containing 50% w/w of magnesium stearate, as described in section 2.2.2. The materials, Sta-Rx and Elcema, which show plastic failure during diametral compression testing of ejected tablets, as discussed in section 3.2, also show a large total relaxation

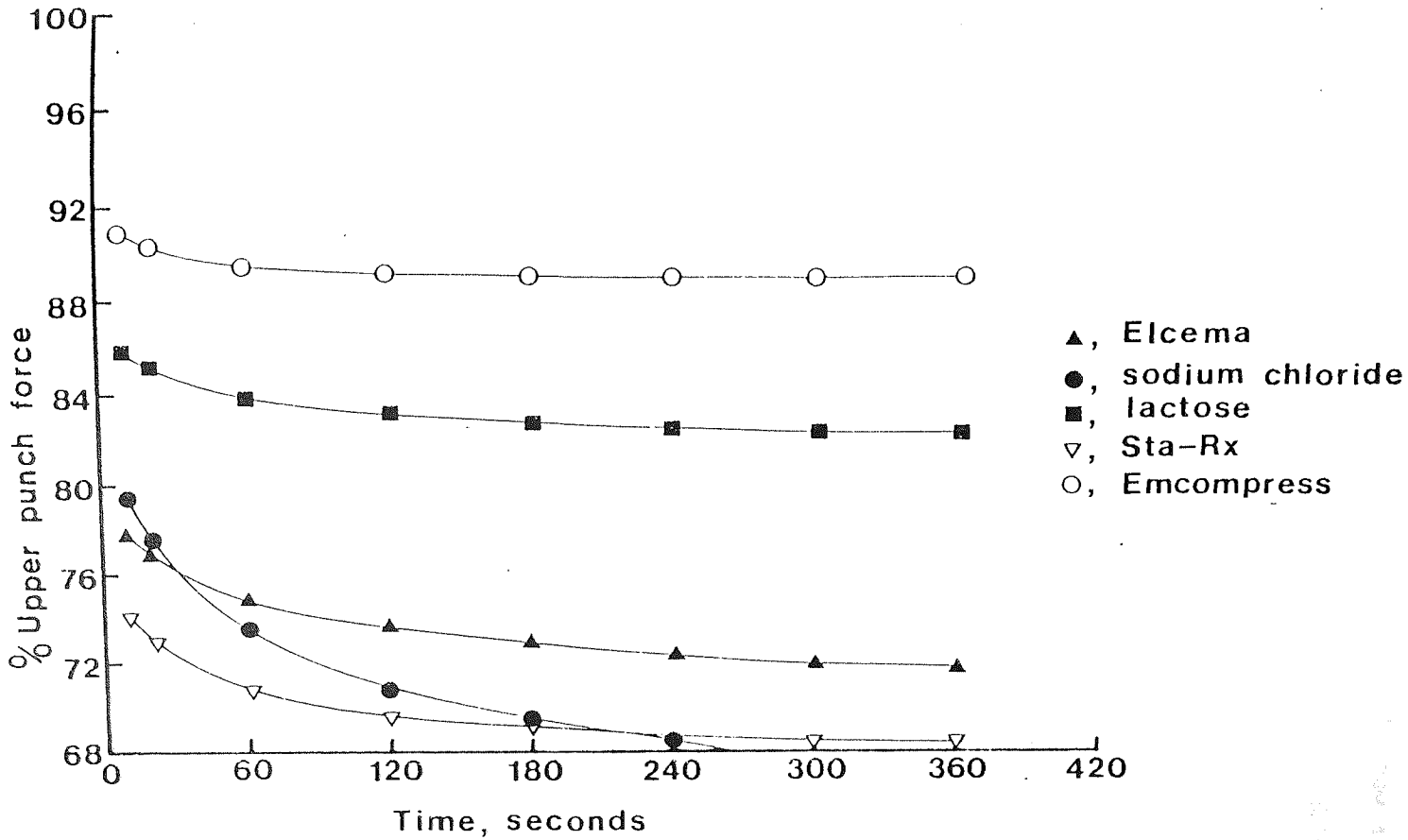

Fig 4.1 Decay of the upper punch force with time at constant upper punch displacement after compaction to about 20 kN

apparently confirming that plastic flow of the particles occurs. Conversely with lactose and Emcompress, which show evidence of brittle failure during diametral compression of tablets, much less stress relaxation is observed.

4.1.1 Mathematical analysis of the relaxation process

A mathematical analysis of the stress relaxation curves is desirable in order to define the mechanical properties of the powders. However, the powder is neither isotropic nor homogeneous and so the slope of the curve at any given time will be related not only to the deformation properties of the material but also to the porosity of the powder bed. A simple method of analysis of stress relaxation data is to test whether the data can be fitted to a Maxwell model. This model has previously been used by Shlanta and Milosovich (1964) and by David and Augsburger (1977), to analyse the stress relaxation of powders during compression.

For a perfectly elastic body, if a strain, S is induced in that body, a state of stress, σ is produced and the relationship between stress and strain is given by equation 4.1.

$$\sigma = kS \qquad \text{Eq. 4.1}$$

where k = modulus of elasticity for the particular type of strain

If the body is free from viscosity, σ will remain equal to kS and equation 4.2 will be applicable.

$$\dot{\sigma} = k\dot{S} \qquad \text{Eq. 4.2}$$

where $\dot{\sigma}$ = rate of change of stress
$\dot{S}$ = rate of change of strain

If, however, the body is viscous, the stress will not remain constant but will disappear at a rate depending on its magnitude and on the nature of the body. The Maxwell model assumes that the rate of disappearance is proportional to the stress and so equation 4.2 may be rewritten to give equation 4.3.

$$\dot{\sigma} = kS - \frac{\sigma}{\tau} \qquad \text{Eq. 4.3}$$

where τ = a constant, with the dimensions of time, known as the relaxation time.

If S is held constant, integration of equation 4.3 gives equation 4.4.

$$\sigma = kSe^{-t/\tau} \qquad \text{Eq. 4.4}$$

If $\dot{S}$ is constant, integration of equation 4.3 gives equation 4.5.

$$\sigma = k\tau\dot{S} + Ce^{-t/\tau} \qquad \text{Eq. 4.5}$$

where C = constant of integration.

In this case, as t tends to infinity, σ tends to a constant value. The term $k\tau$ which, when multiplied by the rate of strain gives the stress, is the coefficient of viscosity and it is possible that, in some cases, τ may be a function of stress (Richardson, 1957). Thus the relaxation time may vary with a decreasing stress during relaxation.

At the point of maximum strain at zero time, S_o equation 4.1 may be rewritten as equation 4.6.

$$\sigma_o = kS_o \qquad \text{Eq. 4.6}$$

where σ_o = maximum stress due to the imposed strain

Substituting equation 4.6 in equation 4.4 gives equation 4.7.

$$\sigma = \sigma_o e^{-t/\tau} \qquad \text{Eq. 4.7}$$

A Maxwell solid will show stress relaxation according to equation 4.7 and the relaxation curve will become asymptotic to the time axis at zero stress. However, in Fig. 4.1, it can be seen that the relaxation curves become asymptotic to a positive value of applied compaction force. Thus, during compaction of these powders, there is a viscous deformation combined with a pure elastic deformation. The Maxwell model is applicable only to the visco-elastic region of the relaxation curve which is the region above the asymptotic value of applied compaction force.

In the present study the area of contact between the punch and the powder is assumed to be constant during relaxation and so equation 4.7 may be rewritten to give equation 4.8.

$$F = F_o e^{-t/\tau} \qquad \text{Eq. 4.8}$$

where F = force on the upper punch.

Equation 4.8, however, ignores the effect of porosity and the non-isotropic nature of the material. A material which behaves as a Maxwellian body will show a linear relationship between the logarithm of the force remaining in the visco-elastic region and time. Fig. 4.2 shows the plots of the logarithm of force remaining in the visco-elastic region against time for the data presented in Fig. 4.1. Each material exhibits an initial curved section which becomes linear after about 30 seconds. Thus, the initial rapid rate of relaxation decreases until all materials assume the first order stress relaxation characteristic of a true

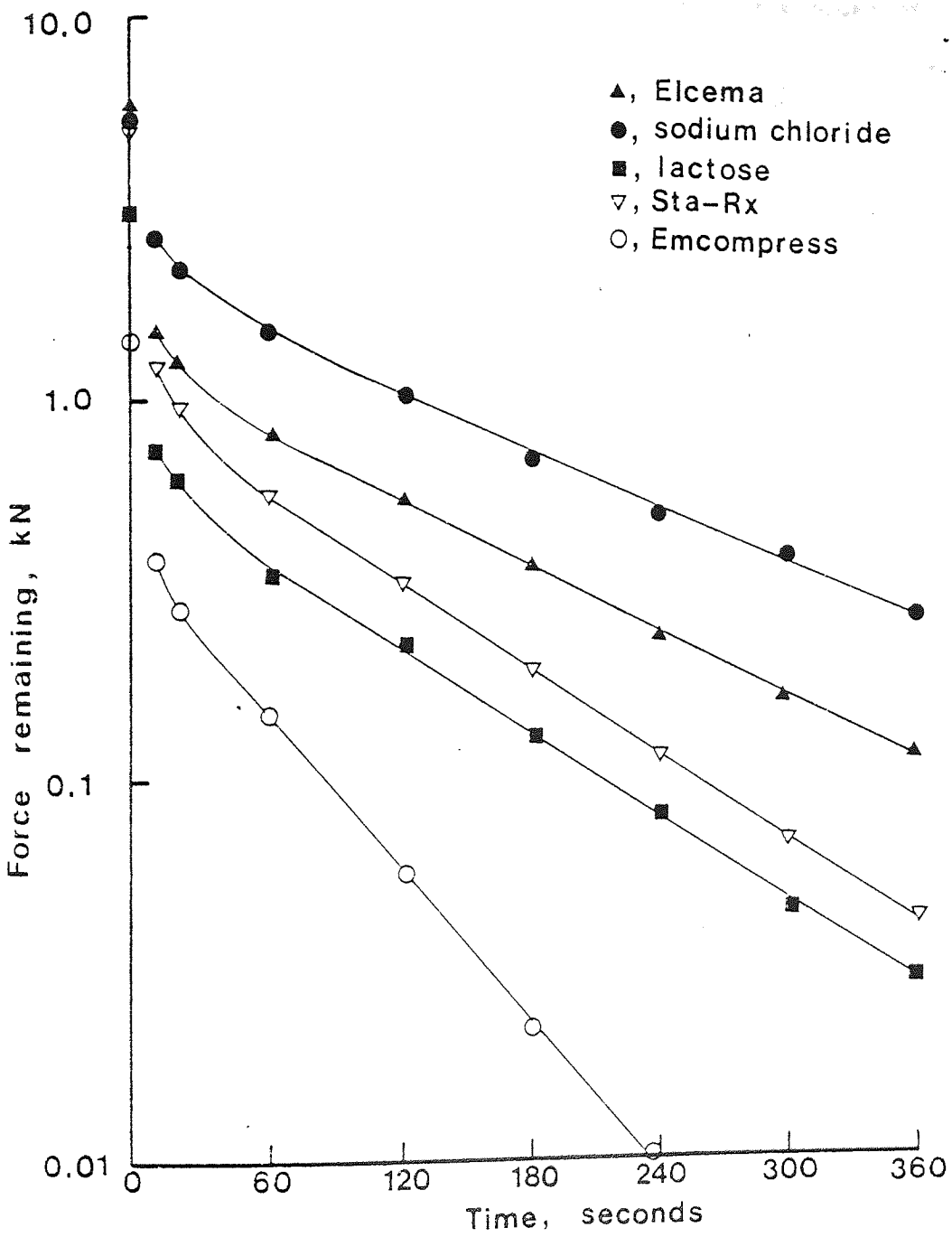

Fig. 4.2 Semi-logarithmic plot of the force remaining in the visco-elastic region with respect to time

Maxwellian body. The visco-elastic slopes calculated between 30 and 360 seconds are shown in Table 4.1, the rank order of these slopes being Emcompress > Sta-Rx > lactose > Elcema > sodium chloride. By using the Maxwell model, the assumption is made that only a single relaxation time exists for each material, the relaxation time being defined as the time required for the force to reach $^{1}/e$ times the maximum force. However, since the data do not fit a Maxwell model, more than one relaxation time must be involved. The curved sections of the semi-logarithmic plots, shown in Fig. 4.2, indicate that there are initially many relaxation times involved until about 30 seconds after the point of maximum force. It is possible that, during the initial 30 second period, the relaxation time, τ is dependent on the stress, σ, or in this case, the force on the upper punch.

A second method of analysis of stress relaxation data is that used by Hiestand, Wells and others (1977), where the stress is plotted against the logarithm of time. Fig. 4.3 shows the plots of upper punch force, as a percentage of the maximum applied force, against the logarithm of time for the same data presented in Fig. 4.1. The use of this logarithm of time plot assumes several relaxation times to be occurring simultaneously as might be expected with a non-homogeneous, non-isotropic system. Hiestand, Wells and others (1977) claim that, "the changes in slope observed in stress versus log time plots suggest that an initially prominent mechanism (of relaxation) soon becomes negligible"; however, they make no proposals as to what mechanisms are operative. The physical significance of the changes in slope in Fig. 4.3 are unknown and this causes difficulties in interpretation of such

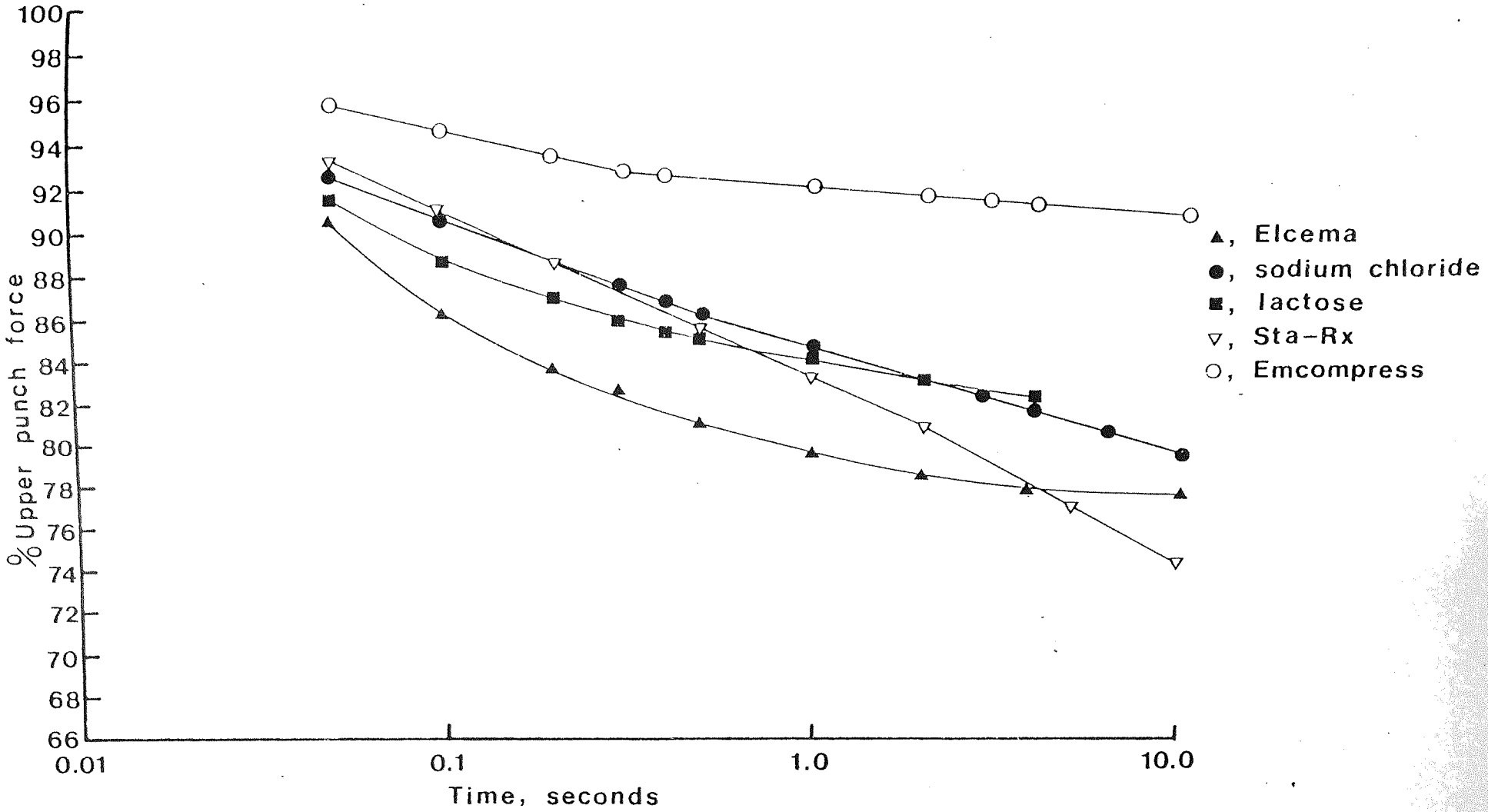

Fig. 4.3 Decay of the upper punch force with the logarithm of time at constant upper punch displacement after compaction to about 20 kN

Material	Maximum compression force kN	Total force decay kN	Force decay as percentage of maximum applied force	Force decay as percentage of maximum applied force in first 10 seconds	Time required to reach 0.1 kN force remaining in visco-elastic region seconds	Visco-elastic slope $seconds^{-1}$
sodium chloride	20.24	7.06	45.62	33.58	545	5.9×10^{-3}
Sta-Rx	19.67	6.27	31.67	25.87	260	8.5×10^{-3}
Elcema	21.92	6.32	28.83	22.12	390	6.3×10^{-3}
lactose	20.25	3.61	17.82	14.12	214	8.3×10^{-3}
Emcompress	20.42	2.25	11.01	9.15	86	1.5×10^{-2}

Table 4.1 Stress relaxation data for five direct compression materials after compression at about 20 kN applied force.

relationships. Using the present experimental system, the relaxation behaviour of the materials during the first 0.05 seconds cannot be determined. Nevertheless a comparison of the logarithm of time plots of the materials reveals certain trends. The brittle material, Emcompress, shows a slower relaxation and also a lower total relaxation than the plastic material, Elcema, which shows a larger and more rapid relaxation. The relaxation of Sta-Rx is initially slower than the brittle lactose, but the total relaxation after 10 seconds is much larger than lactose and also larger than the other plastic material, Elcema.

4.1.2 The effect of magnesium stearate on relaxation

The rank order of visco-elastic slopes listed in Table 4.1 contradicts the results of David and Augsburger (1977) who reported a much lower visco-elastic slope for Emcompress than for Sta-Rx or microcrystalline cellulose (Avicel - a material chemically similar to Elcema). These differences in slope are due to the much longer times required for the materials to undergo relaxation to a given level in the present study, compared with the times reported by David and Augsburger (1977), who state that relaxation was complete for all materials after 10 seconds. The materials used by David and Augsburger (1977) contained 0.3% magnesium stearate whereas in this study pure materials were compressed after lubricating the die wall as described in section 2.2.2. To determine the effect of magnesium stearate on the stress relaxation behaviour, the relaxation experiments were repeated using materials mixed with 0.3% w/w magnesium stearate. The effect of time on the upper punch force during compaction of

each lubricated material is shown in Fig. 4.4 and the plots of the logarithm of the force remaining in the visco-elastic region against time for the same data in Fig. 4.5. The general shape of the semi-logarithmic plots are similar for materials with or without 0.3% w/w lubricant. However, there is a small change in the visco-elastic slopes as shown in Table 4.2; the rank order becomes Emcompress > lactose > Sta-Rx > Elcema > sodium chloride. Both with or without magnesium stearate, the relaxation process continues for a much longer time than found by David and Augsburger (1977). The results for lubricated powders again show an initial relaxation which is more rapid than the first order rate of a true Maxwell body, but this was not reported by David and Augsburger (1977).

A probable explanation of the differences between the results shown in Fig. 4.5 and those of David and Augsburger (1977) is given by a consideration of the strain conditions during the relaxation experiment. Stress relaxation experiments must be carried out at constant strain, which in this case necessitates a constant distance between the upper and lower punch faces. In a reciprocating tablet machine this distance is constant for a given upper punch displacement, assuming that elastic recovery of the punch and other machine components is negligible. However, in a rotary tablet press, as used by David and Augsburger (1977), a small downward movement of the lower pressure roll normally occurs during compression due to movement in the overload spring mechanism as explained by Deer and Finlay (1973) and Deer (1975). This movement will reach a maximum at the point of maximum force and may be in the order of 0.1 mm (Deer, 1977). As the punch

Material	Maximum compression force kN	Total force decay kN	Force decay as percentage of maximum applied force	Force decay as percentage of maximum applied force in first 10 seconds	Time required to reach 0.1 kN force remaining in visco-elastic region seconds	Visco-elastic slope $seconds^{-1}$
sodium chloride	18.82	4.28	22.76	13.00	442	5.9×10^{-3}
Sta-Rx	19.15	5.67	29.65	23.89	260	6.8×10^{-3}
Elcema	18.70	5.80	31.04	22.87	414	5.9×10^{-3}
lactose	19.22	3.59	18.66	14.91	189	9.1×10^{-3}
Emcompress	20.53	2.66	12.94	10.45	77	2.2×10^{-2}

Table 4.2 Stress relaxation data for 5 direct compression materials containing 0.3% w/w magnesium stearate after compression to about 20 kN applied force.

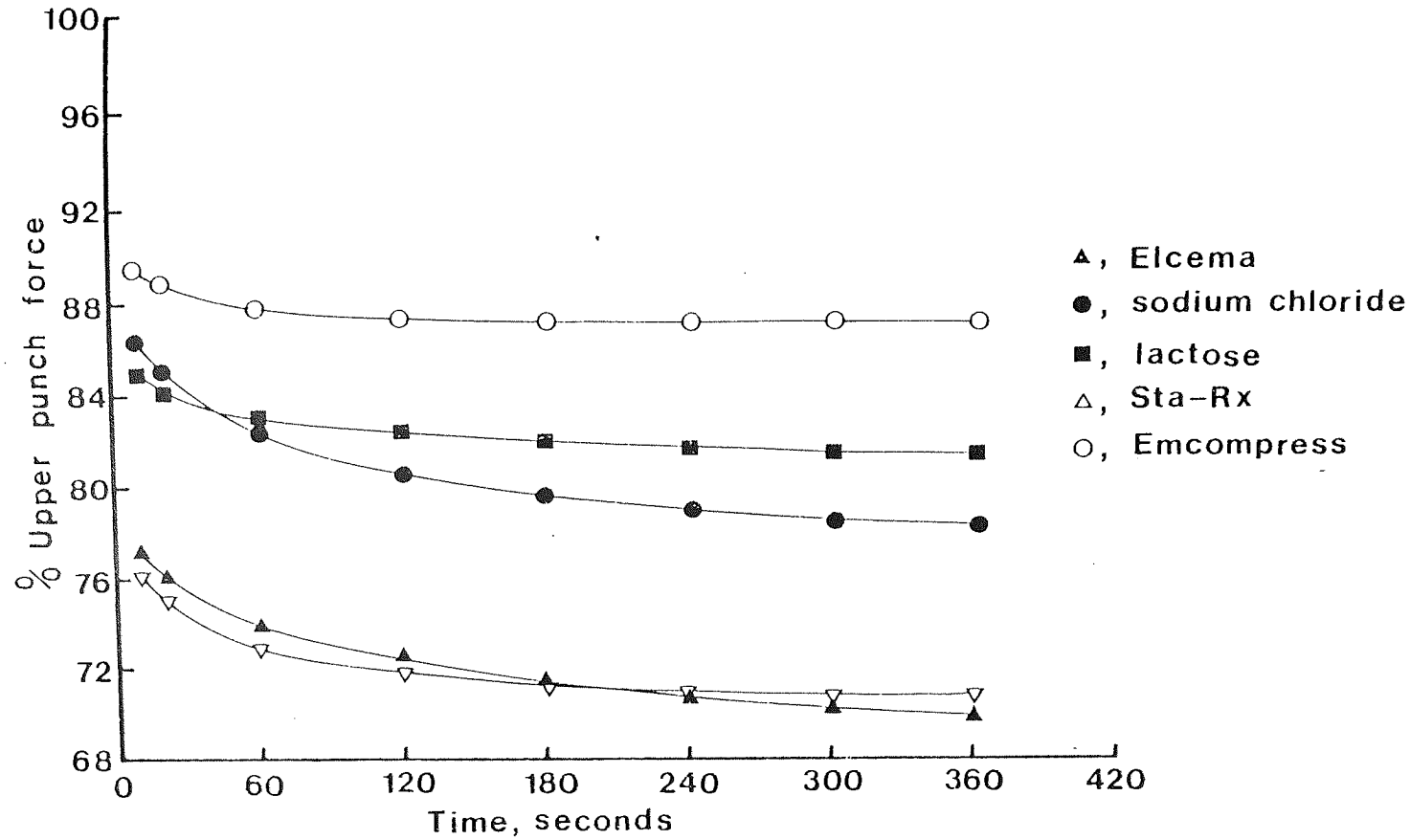

Fig. 4.4 Decay of the upper punch force with time at constant upper punch displacement after compaction to about 20 kN . Materials each containing 0.3% w/w magnesium stearate

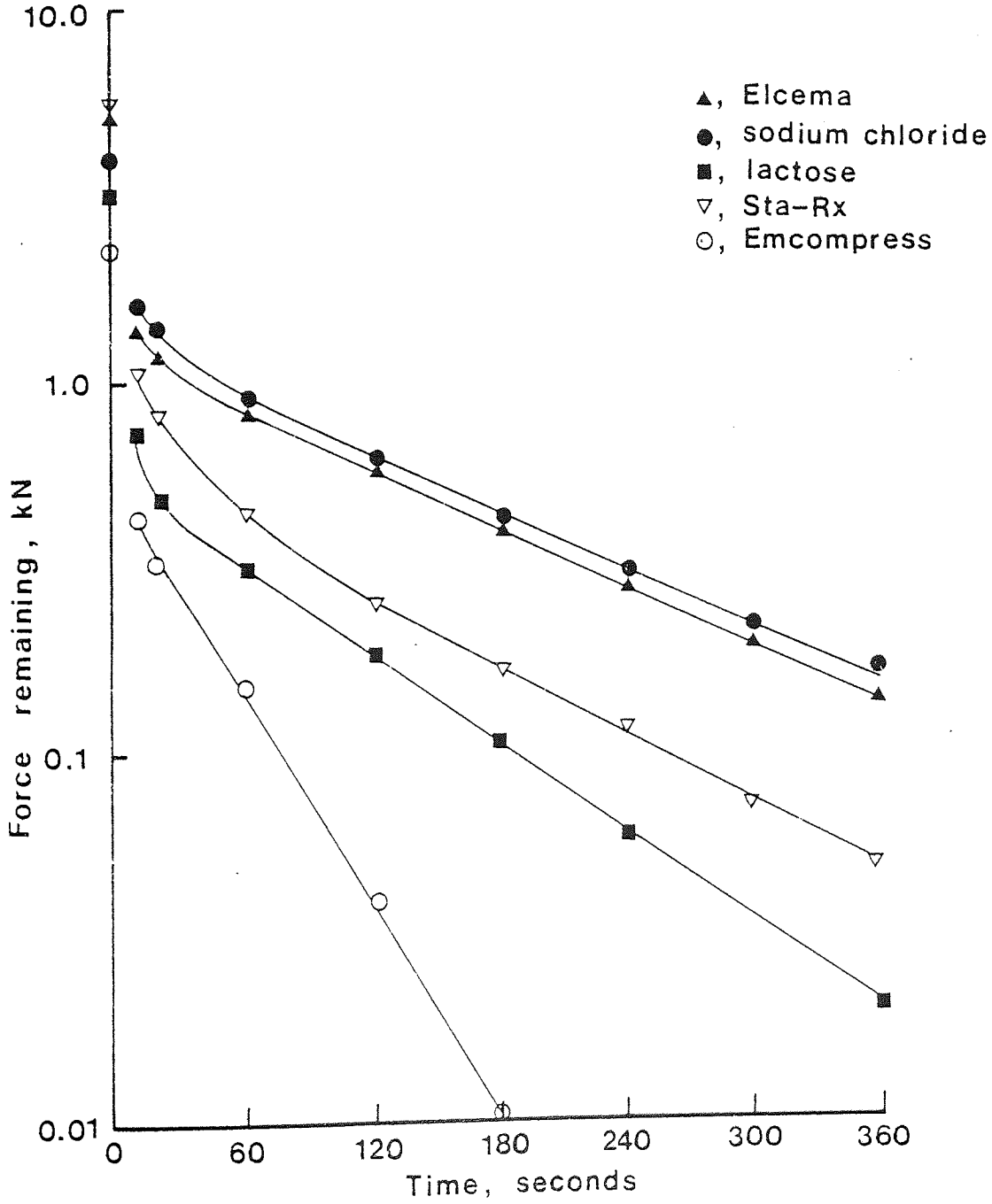

Fig. 4.5 Semi-logarithmic plot of the force remaining in the visco-elastic region. Materials each containing 0.3% w/w magnesium stearate

force decreases, due to relaxation of the compact, the lower pressure roll will move upwards in an attempt to regain its equilibrium position. The effect of this movement will be to maintain a stress on the upper punch higher than that which would be found during relaxation under conditions of true constant strain. Under the experimental conditions which probably applied in David and Augsburger's study (1977), pseudo-equilibrium values of residual punch force may therefore be observed which are higher, at any given time, than under conditions of constant strain. Because of this possible change in strain during stress relaxation studies during compaction, it is better to use an instrumented reciprocating tablet machine, than a rotary machine, for this type of experiment.

The effect of magnesium stearate on the stress relaxation may be seen by comparing Figs. 4.1 and 4.4, and by comparing the percentage force decay shown in Tables 4.1 and 4.2. Magnesium stearate appears to inhibit slightly the relaxation of sodium chloride. Conversely, the presence of magnesium stearate appears to increase slightly the relaxation of Elcema, lactose and Emcompress. However, this is a misleading picture of the relaxation process since the amount of irreversible deformation, and in effect the amount of stress relaxation, which occurs during the time required for application of the compaction force is not considered. During the time required to reach the maximum force, plastic flow of the material will occur as shown by Shlanta (1963), thus reducing the total flow which can occur subsequently at constant strain; this will result in a reduction of the total stress relaxation recorded.

During compression an increase in tablet density will be facilitated if particles which are deforming plastically can slide past one another. This rate of sliding will be increased by reducing inter-particulate friction and it is probable that magnesium stearate, within the tablet, would have this effect. During the application of force to a brittle material, which consolidates by fragmentation, little plastic flow will occur due to fragmentation of the particles. At the point of maximum force fragmentation will stop, since it is not time dependent, and plastic flow may occur at the newly formed points of contact subjected to high stresses. Magnesium stearate will lubricate the inter-particle junctions and allow the plastic flow to occur more easily.

For materials such as Sta-Rx and sodium chloride which consolidate mainly by plastic flow the major effect of magnesium stearate is to increase the sliding of particles relative to one another during loading, thus reducing the relaxation seen after the point of maximum force. Conversely, for materials which consolidate by fragmentation, the major effect of magnesium stearate is possibly to increase the inter-particulate sliding after the point of maximum force, thus increasing the relaxation seen with these materials. Despite the load-displacement curve for Elcema shown in Fig. 3.4 and the relatively high tensile strength of Elcema tablets shown in Fig. 3.1, both of which indicate that consolidation of this material is by plastic flow, the effect of magnesium stearate is to increase slightly the stress relaxation. Fig. 3.3 shows that the % void volume of Elcema tablets at any given compaction force is large compared to the other materials. When magnesium stearate is present within the compact, the strength

of the bonds formed during compaction will be reduced and the formation of some bonds will be prevented. During relaxation of Elcema in the presence of magnesium stearate the amount of inter-particulate sliding, into the large % void volume will be increased thus increasing the observed relaxation.

When determining the deformation behaviour of materials by using stress relaxation measurements, many factors will affect the observed relaxation. The force is not applied instantaneously and so plastic deformation of the particles will occur during the time required for force application. The porosity of the compact, together with the presence or absence of lubricants, can affect the amount of inter-particulate slippage which will be seen as relaxation but which is not necessarily due to true plastic flow of the particles. It appears that conclusions, regarding the deformation behaviour of materials drawn from stress relaxation measurements are only valid for the conditions of that particular experiment. However, useful information may be obtained regarding the comparative behaviour of materials under a particular set of conditions.

4.1.3 Short term stress relaxation during compaction of powders

During tablet manufacture on a reciprocating tablet press the compaction cycle may be complete in less than 0.2 seconds and on a rotary tablet press in less than 0.1 seconds. The deformation behaviour of materials during this short period of time is therefore critical to tablet manufacture but is not specifically considered in section 4.1.2. The results presented in section 4.1.2 clearly show the time-dependent nature of stress relaxation in the

materials studied and also show the difficulties of interpreting the relaxation process in non-homogeneous non-isotropic systems. The calculated visco-elastic slopes shown in Tables 4.1 and 4.2 provide little information about the behaviour of the materials, with respect to their tabletting properties, since values cannot be calculated until 30 seconds after maximum force. Thus it is probably more useful to consider the relaxation behaviour during the initial short period of time after maximum force. This will relate more closely to the deformation behaviour, during the short times available during a compaction cycle, than the relaxation behaviour discussed in section 4.1.2.

Stress relaxation behaviour of the materials during the first 0.5 seconds after maximum force is shown in Fig. 4.6. After 0.5 seconds Elcema shows a relatively high, and Emcompress a relatively low relaxation with sodium chloride, Sta-Rx and lactose showing intermediate relaxation values. This contrasts with the relaxation after 360 seconds (Fig. 4.1) when sodium chloride shows the greatest relaxation followed by Sta-Rx, Elcema, lactose and Emcompress in decreasing order. Within 0.5 seconds Elcema has undergone considerable plastic deformation as shown by its relatively large relaxation, whereas little irreversible deformation occurs in Emcompress even after much longer times. For Sta-Rx, plastic flow is much more time dependent than for other materials as shown by the small relaxation during the first 0.5 seconds compared with the relaxation after 360 seconds. The relaxation data for sodium chloride indicate that plastic flow of this material is also highly time dependent. However, this result is probably due to the very low porosity of sodium chloride tablets at this compaction

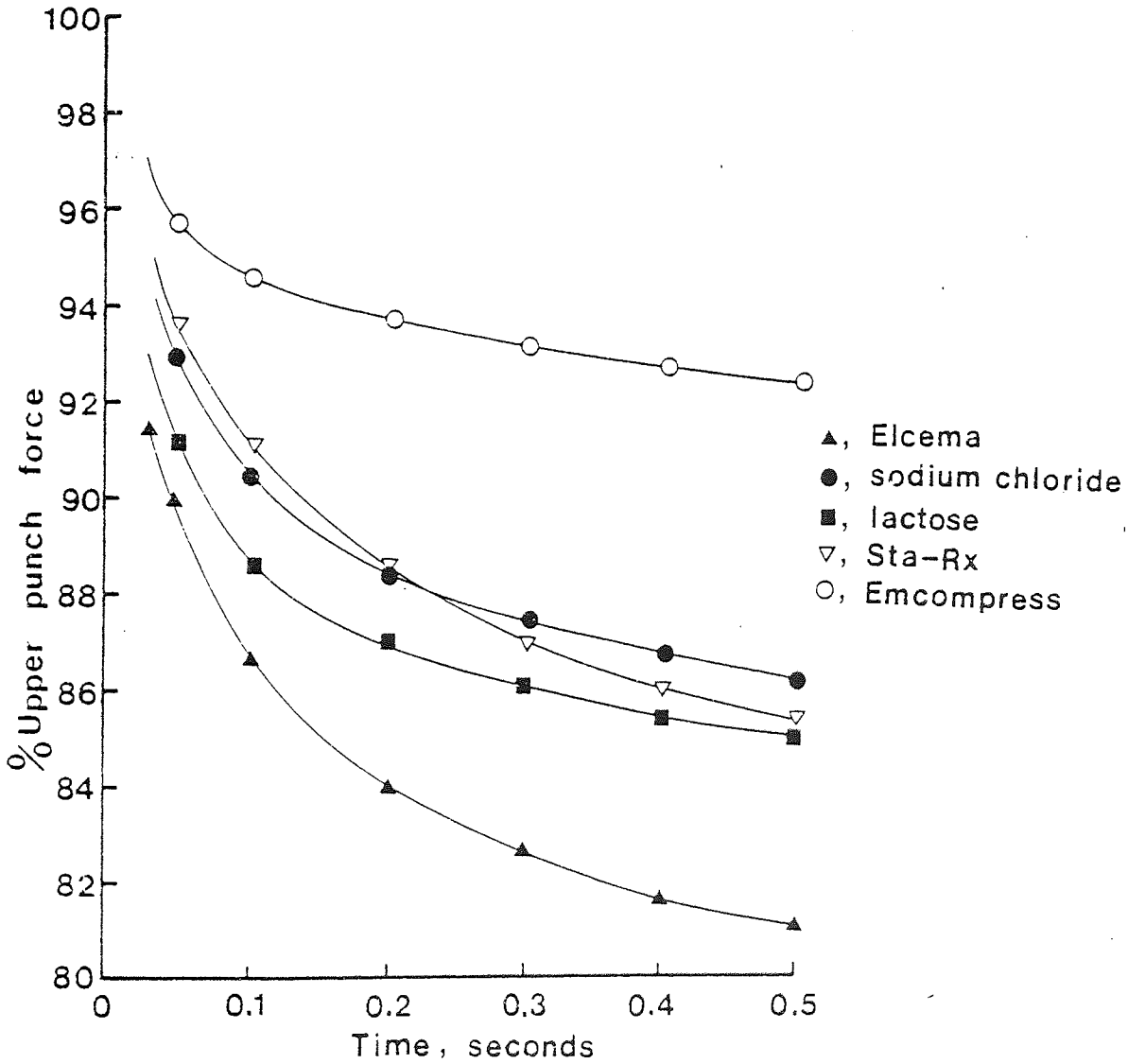

Fig. 4.6 Decay of the upper punch force within the first 0.5 seconds after the maximum force of about 20 kN

force which will reduce the rate of relaxation by inhibiting plastic flow. The relaxation of sodium chloride will be further inhibited by work hardening of the particles.

4.2 Consolidation of Materials During Compaction

In the present experimental system, if stress relaxation occurs while the tablet is held under constant strain before ejection, then the density of the ejected tablet must increase as a result of irreversible deformation. Any increase in density will be related only to the amount of plastic flow which occurs since fragmentation, which causes densification of brittle materials during compaction, cannot occur after the point of maximum force.

Fig. 4.7 shows the effect of increasing the total time of the compaction event on the density of the tablets in the form of Heckel plots which are discussed in section 1.4. Increasing the dwell time from 0.17 to 10 seconds has little effect on the consolidation of Emcompress, lactose or sodium chloride, some effect on Elcema, but markedly increases the consolidation of Sta-Rx at any given compaction force. The Heckel equation predicts a linear relationship between log (1/1-D) and compaction force, but only sodium chloride and lactose show linearity over any part of the range of compaction forces used. Hersey, Cole and Rees (1972) found a completely linear solution when the Heckel equation was applied to the compaction of sodium chloride and also a linear relationship for lactose above a certain minimum applied pressure. These authors used a 33 mm diameter die and measured the volume of the compact under load by monitoring the penetration of the upper punch into the die. The measurement of tablet volume under

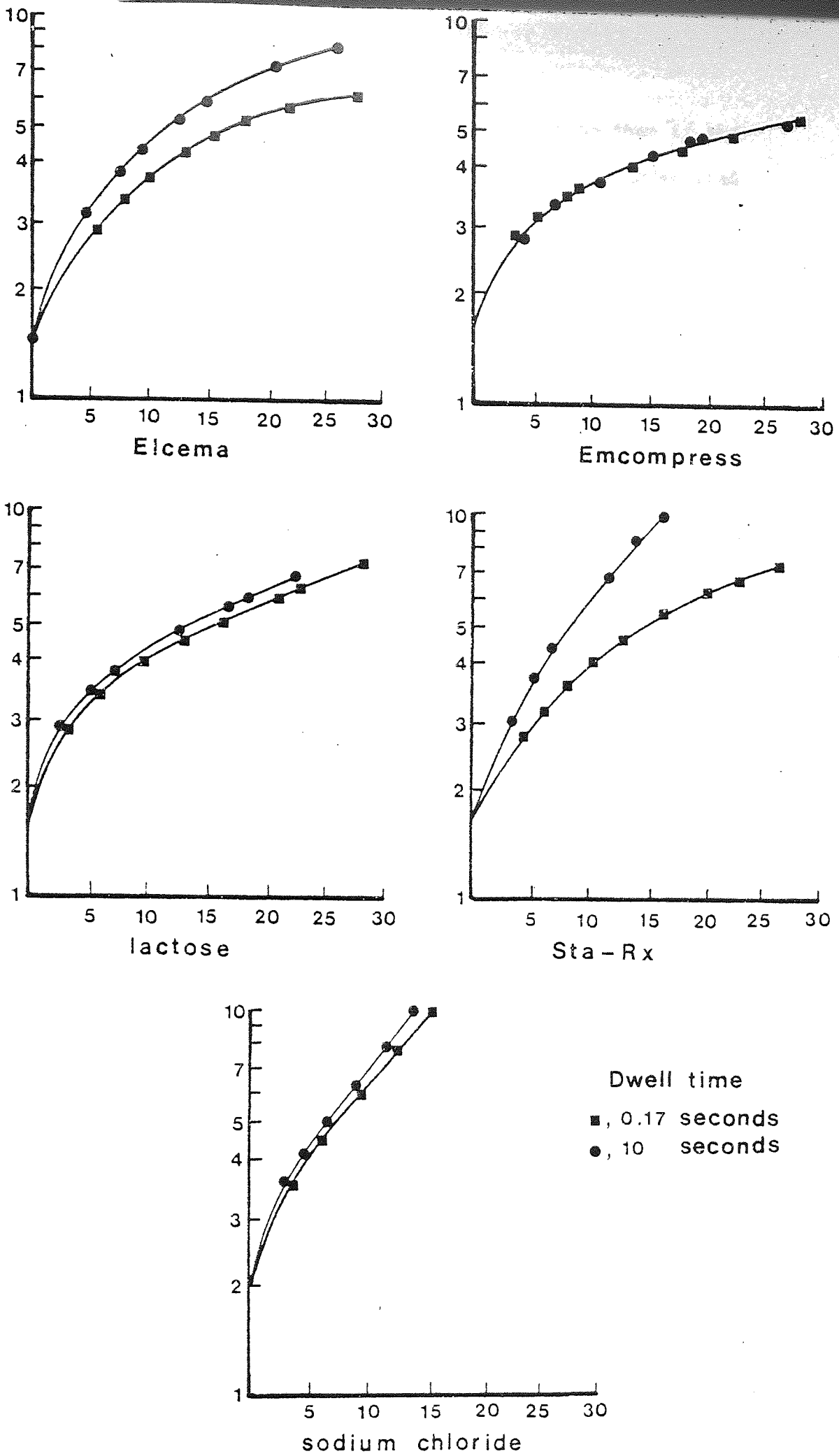

Fig. 4.7 The effect of dwell time on the consolidation behaviour of materials shown by plotting 1/(1-D) on a logarithmic scale (ordinates) against compaction force in kN (abscissae)

load will lead to higher values of tablet density than if the volume is measured after ejection since the values under load will include an elastic component of deformation which will recover on decompression giving larger values of tablet volume and hence lower densities. Hersey and Rees (1970) using the data from Hersey, Bayraktar and Shotton (1967) and Alpar, Hersey and Shotton (1970), which were obtained using a 12 mm diameter die and employing tablet volumes measured after ejection, found non-linear Heckel plots for both sodium chloride and lactose over the same pressure range (up to 50 MN m^{-2}) used by Hersey, Cole and Rees (1972). Thus the deviation from linearity observed in the Heckel plots for materials used in the present study is probably due to measurement of the volume of the tablet after ejection since this allows elastic recovery of the tablet. As the compaction force increases, a greater proportion of the total volume reduction measured under load will be elastic and, after recovery, the value of D will be lower than the corresponding value for D determined under load. The Heckel plots for both lactose and sodium chloride would be expected to deviate from linearity if applied pressures were sufficiently high. This effect has been observed by Fell and Newton (1971b) for crystalline lactose at applied pressures above about 250 MN m^{-2}. Increasing consolidation due to increasing dwell time lies in the rank order Sta-Rx > Elcema > lactose > sodium chloride > Emcompress. This agrees with the results of David and Augsburger (1977) who found that an increasing dwell time increased the strength of Sta-Rx tablets by 135%, microcrystalline cellulose (Avicel) tablets by 37% and lactose tablets by only 15%. For a given material, assuming neither capping nor lamination occurs, an increase in the density of a tablet, as measured after ejection,

will increase its tensile strength. Densification may be a result of either plastic flow or fragmentation. However, since only plastic flow is time dependent and therefore affected by dwell time, it would be expected that tablets which show the greatest increase in density with increasing dwell time would also show the greatest increase in tensile strength. Considering also the stress relaxation behaviour of the materials as shown in Fig. 4.1 and 4.6, the percentage increase in tensile strength of Sta-Rx tablets would be expected to be greater than that of Elcema tablets after a 10 second dwell time since the stress relaxation of Sta-Rx is greater than that of Elcema after 10 seconds. However, if the dwell time was increased by only 0.5 seconds the percentage increase in strength of Sta-Rx tablets would be expected to be less than that of Elcema tablets since Elcema shows the greater relaxation after this shorter time.

The effect of dwell time on the density of the materials confirms the conclusions based on stress relaxation measurements, that Sta-Rx and Elcema both consolidate mainly by plastic flow. However, inferences regarding the tabletting properties of materials drawn from slow rate compaction or long term relaxation studies must be treated with extreme caution, since the behaviour of the materials during the times available for plastic flow during normal high speed compaction may be very different from their behaviour during longer times.

4.3 Stress Relaxation During Diametral Compression of Tablets

As explained in section 3.4, the ability of a tablet to withstand mechanical shock during, for example, pan coating or

transport depends on its toughness. For tablets of a given tensile strength the work of failure, which is related to their toughness, is controlled by the relative platten movement before failure. Tablets will be tougher and possess a high work of failure if plastic flow occurs during stressing, thus relaxing the forces imposed on the particles and bonds and resulting in a large failure strain. If plastic flow occurs during stressing of tablets in diametral compression, stress relaxation should be observed if the tablet is held under constant strain prior to failure.

To examine the stress relaxation of tablets after ejection from the die, tablets were loaded in diametral compression to 75% of their breaking load as described in section 2.3.3. Fig. 4.8 shows the stress relaxation observed with tablets of each of the materials subjected to a diametral loading test during which platten movement was arrested prior to tablet failure. The two plastic materials, Elcema and Sta-Rx, show large values of stress relaxation as expected from their load displacement curves, shown in Fig. 3.4, and from relaxation measurements during powder compaction. The relaxation of tablets of Emcompress and lactose is relatively small and is completed more quickly. The relaxation of sodium chloride tablets, although relatively small, continues for a long period of time (480 minutes). This is probably due to a combination of work hardening of the particles and bonds during compression and the very low porosity of sodium chloride tablets; both phenomena will reduce the rate and magnitude of relaxation. During compaction of sodium chloride powder, the inter-particulate contact areas will be subjected to greater deformation, or strain, than the interior of each particle. Thus the region of the particle

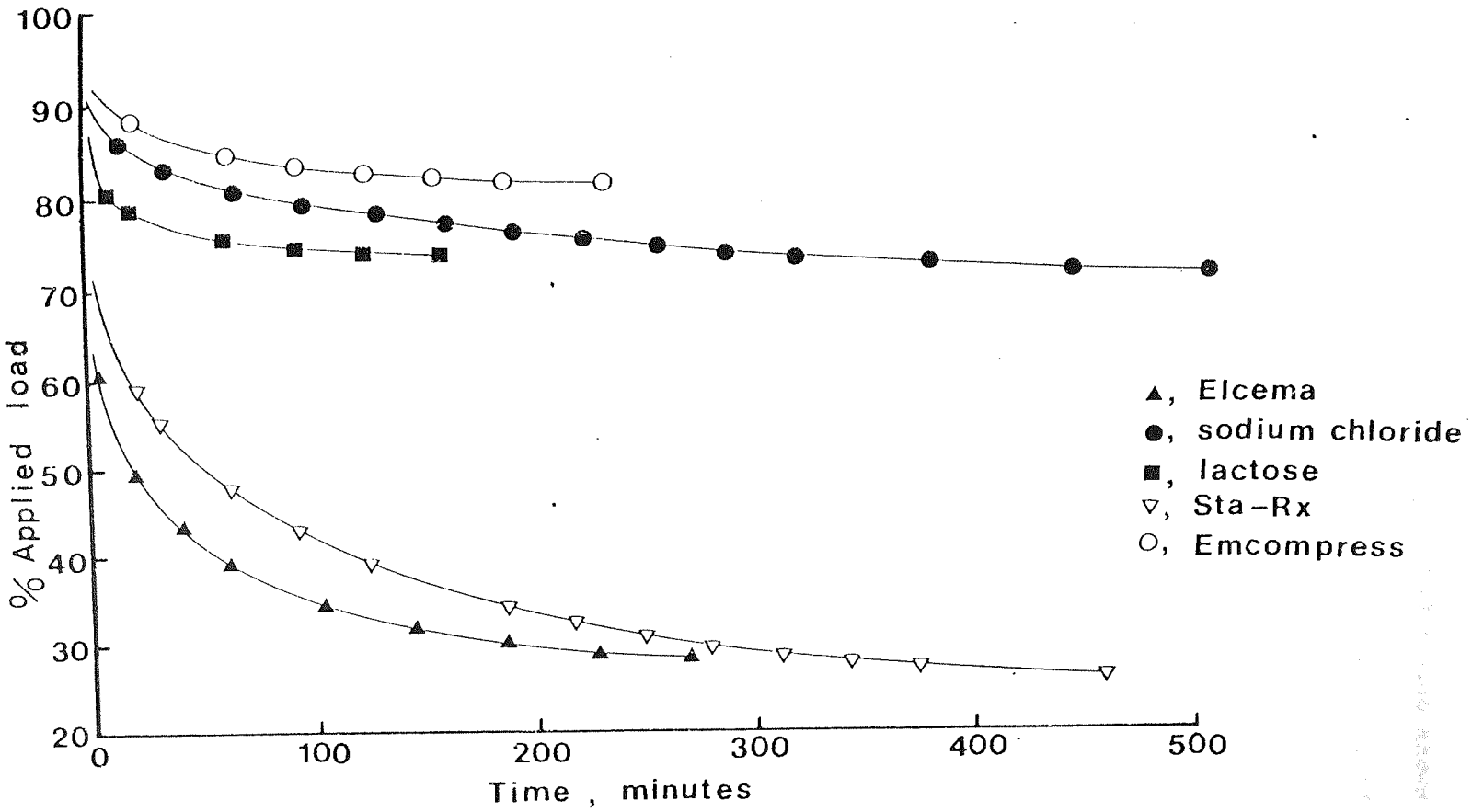

Fig. 4.8 Decay of the applied diametral load with time for tablets loaded to 75% of their breaking load at a rate of platten movement of 0.26 mm min^{-1} in a diametral compression test

around the bond will have work hardened - also known as strain hardened - to a greater extent than the remainder of the particle. During diametral compression there will be a high stress on the inter-particulate bonds but, since these bonds have become difficult to deform due to work hardening, little plastic flow will occur in the region of the bonds. Owing to the larger cross-sectional area of the particles, compared to the bonds, the stress on the particles will be lower than on the bonds. Since the particles have undergone less work hardening than the bonds, the particles are still capable of plastic deformation. However, this deformation will occur more slowly due to the lower stress on the particles. The total relaxation of Sta-Rx tablets is greater than that of Elcema tablets, but takes 480 minutes to complete compared with 260 minutes for Elcema.

The relaxation of tablets within the first second after the peak diametral load is shown in Fig. 4.9. The rank order of relaxation is Elcema > Sta-Rx > lactose > sodium chloride > Emcompress. This order is that which would be expected from the fracture strain data shown in Fig. 3.7 and from stress relaxation measurements during powder compaction. The relaxation data for tablets during diametral loading shows that both Elcema and Sta-Rx tablets are capable of extensive plastic flow and are thus able to absorb more energy than a brittle material. This effect is reflected in the work of failure values (Fig. 3.9) and in the multiple diametral impact test results (Fig. 3.11) of these two materials.

During the application of the diametral load, plastic flow will occur in a manner analogous to the effect of the rate of

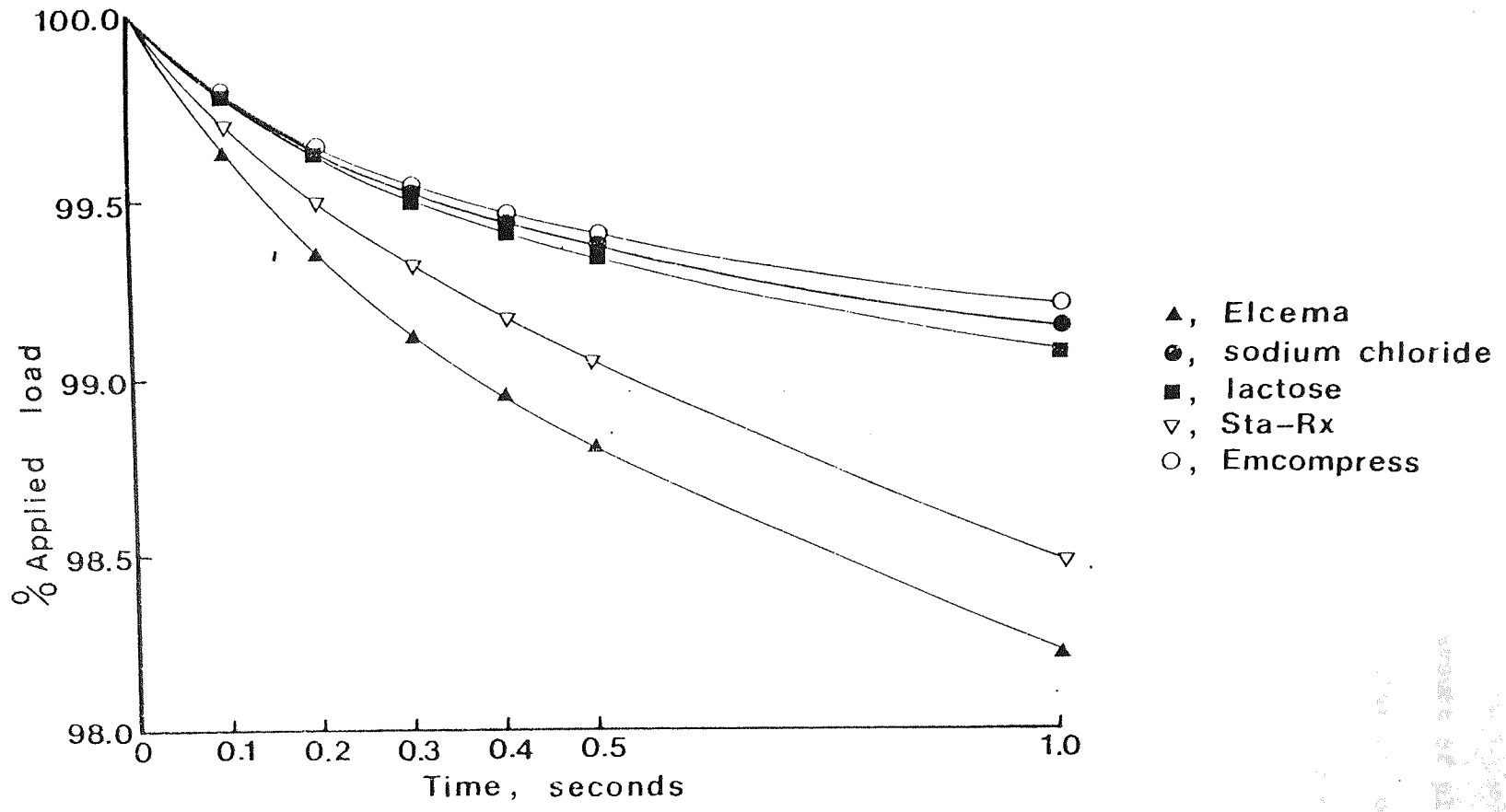

Fig. 4.9 Decay of the applied diametral load within the first second after maximum load for tablets loaded to 75% of their breaking load at a rate of platten movement of 0.26 mm min^{-1} in a diametral compression test

loading during powder compaction. Thus the amount of plastic flow, and hence stress relaxation, occurring after the peak load will be reduced. The effect of the rate of platten movement on the stress relaxation of Elcema and Emcompress tablets after loading at four rates of platten movement is shown in Fig. 4.10. As the rate of platten movement increases the stress relaxation, at a given time increases showing that a smaller percentage of the total irreversible deformation occurs during the loading event at higher rates of loading. This trend was seen with all materials, but was most marked with Elcema and Sta-Rx and least with Emcompress. The greater effect of increasing rate of loading on Elcema tablets compared with Emcompress tablets would be predicted from the nature of failure of these materials, Elcema showing plastic and Emcompress brittle failure.

4.4 Evaluation of Stress Relaxation and Consolidation Studies

The use of stress relaxation to examine the deformation behaviour of materials is subject to severe limitations. However, it can provide some indication of the extent to which plastic flow of powders occurs during the compaction process. The initial fast rate of relaxation means that the Maxwell model cannot be used to characterise the behaviour of the materials since the plots of the logarithm of the force remaining in the visco-elastic region against compaction force, shown in Figs. 4.2 and 4.5, do not become linear until 30 seconds after the point of maximum force. However, the critical time period of relaxation relevant to tablet compaction would appear to be the initial 0.1 seconds, after maximum force is applied. Comparison of relaxation values

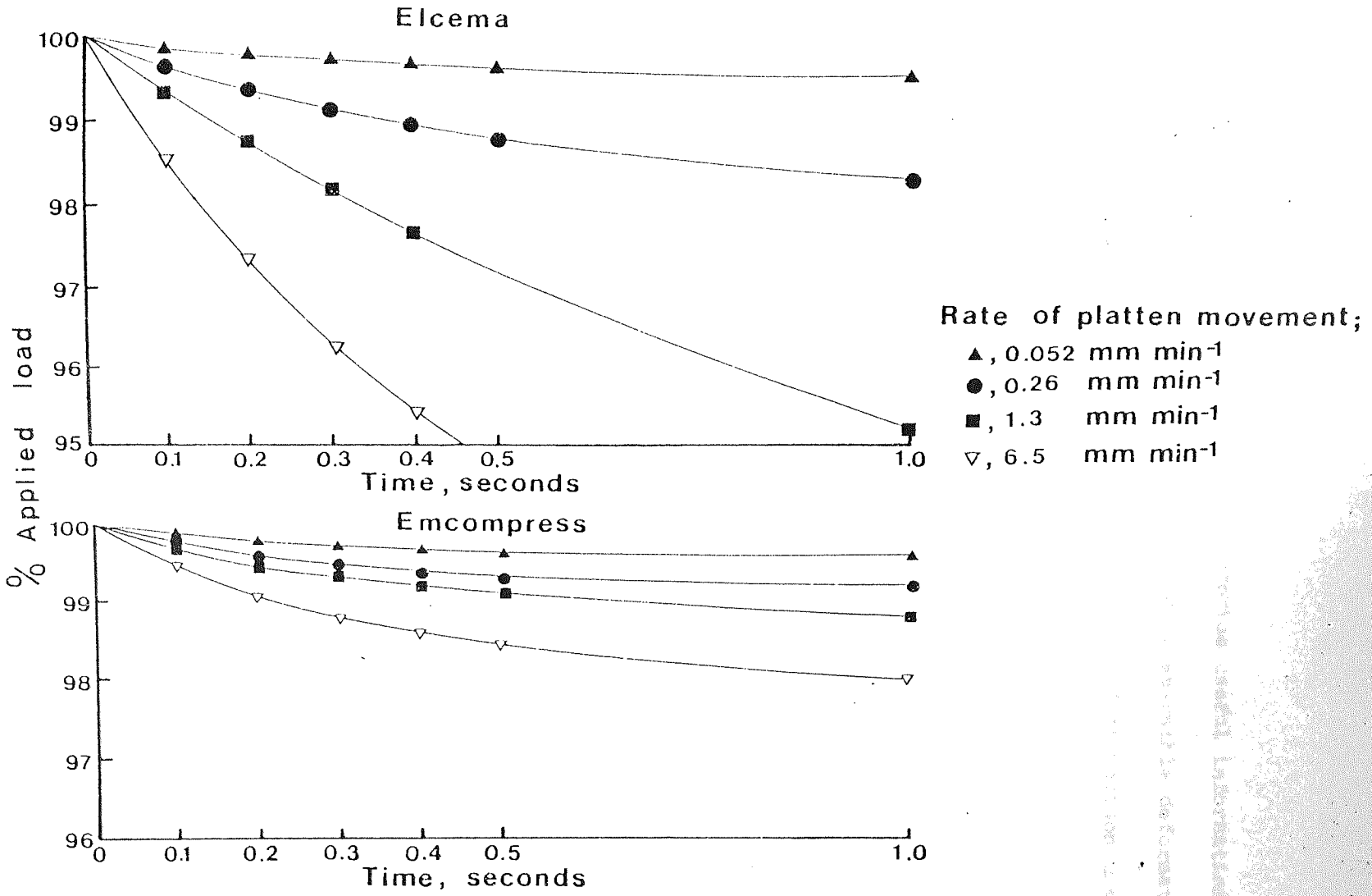

Fig. 4.10 Decay of the applied diametral load with time for tablets of Elcema and Emcompress loaded to 75% of their breaking load at four rates of platten movement

after short and long time periods can provide useful information regarding the time dependent nature of the irreversible deformation during powder compaction. A convenient method of comparison uses the plot of upper punch force against the logarithm of time, shown in Fig. 4.3, which allows both short and long term relaxation to be compared directly on the same graph. However, the changes in slope of the lines and, in the case of lactose and Elcema, the curved plots cause difficulty in interpretation of the data. Thus plots of this type are useful only for comparative purposes.

Plastic flow will occur during the application of compaction force, but this flow cannot be detected by simple relaxation measurements and time consuming interpolation techniques are required such as used by Shlanta (1963). For valid results the type of instrument used to obtain relaxation data must be carefully chosen so that a true constant strain is maintained throughout the experiment.

The density of a compressed tablet is determined by the amount of fragmentation and plastic flow during the compaction event but, since fragmentation is not time dependent, alteration of the dwell time will only affect plastic flow. Considering the previous criticisms of stress relaxation measurements, a better method of examining the plastic properties of materials may be to consider the effect of dwell time on the tablet density as represented by the Heckel plots. In this way plastic flow during the entire compaction event is considered without the need for interpolation techniques.

Stress relaxation measurements on tablets during diametral compression are useful and should provide more informative data

if the initial rate of relaxation is determined after a high rate of loading. This will give an indication of the ability of the tablet to undergo plastic deformation which, if high, results in a tough tablet with a high work of failure.

5. DEFORMATION BEHAVIOUR OF TABLETS PRIOR TO FAILURE DURING DIAMETRAL COMPRESSION TESTING

5.1 The Non-recoverable Deformation of Tablets During Diametral Loading

During diametral compression testing, tablets of different materials deform by different amounts before failure, both at the region of contact with the metal plattens and in a direction normal to the applied load due to the tensile stresses developed in this type of test as discussed in section 1.3.1.2. Part of this deformation will be non-recoverable due to plastic flow, or possibly due to local fracture, and part will be elastic and hence recoverable when the compressive load is removed. The failure deformation of tablets, shown in Fig. 3.7, indicates the total deformation at the point of failure but gives no indication as to what proportion of the deformation would be recoverable if failure had not occurred.

To examine the deformation behaviour of tablets before failure, the tablets were loaded to 75% of their breaking force and the non-recoverable deformation (NRD), as well as the total deformation, was measured as described in section 2.3.4. By plotting the logarithm of NRD expressed as a percentage of the total deformation (% NRD) against the log of rate of platten movement, a linear relationship was observed of the form of equation 5.1.

$$\log \% \text{NRD} = K (\log \text{rate}) + \log C \qquad \text{Eq. 5.1}$$

where K = the gradient of the line
C = % NRD at a rate of platten movement equal to 1 mm min^{-1}

This relationship is shown in Fig. 5.1 for tablets of each of the materials, all tablets having similar diametral breaking strengths. Tablets of Elcema and Sta-Rx, materials which exhibit plastic failure in diametral compression tests, show a decrease in % NRD as the rate of platten movement increases indicating that at higher strain rates a greater proportion of the deformation is elastic and hence recoverable. For tablets of materials which exhibit brittle failure during diametral compression testing, there is no change in % NRD as the rate of platten movement increases.

The gradients of the lines shown in Fig. 5.1 are an indication of the effect of strain rate on the deformation of the materials. The larger the negative gradient, the greater the strain rate sensitivity. The gradients for Elcema and Sta-Rx are -0.082 and -0.159 respectively, indicating that Sta-Rx has a greater strain rate sensitivity than Elcema. The fact that plastic flow of Sta-Rx is more time dependent than that of Elcema has previously been shown by the stress relaxation measurements both on tablets, and during compaction of the powders; these were discussed in sections 4.1.3 and 4.3. For example in Figs. 4.6 and 4.9, the stress relaxation of Sta-Rx, immediately after the maximum load is applied, occurs more slowly than that of Elcema even though the total relaxation of Sta-Rx is greater.

Fig. 5.1, showing the % NRD, can lead to misleading conclusions since it gives no information about the total deformation which occurs when tablets are loaded to 75% of their breaking load. The values of total deformation and % NRD are given in Table 5.1 for tablets of each material loaded to 75% of their breaking force. The effect of rate of platten movement on

Material	Rate of platten movement mm min^{-1}	Total deformation mm	Recoverable deformation mm	Non-recoverable deformation mm	% NRD	Total deformation divided by applied force mm kN^{-1}	Non-recoverable deformation divided by applied force mm kN^{-1}	Applied force kN
Elcema	0.052	0.144	0.109	0.035	24.31	2.510	0.605	0.058
"	0.26	0.140	0.108	0.033	23.57	2.384	0.545	0.059
"	1.30	0.141	0.113	0.027	19.15	2.285	0.444	0.062
"	6.50	0.121	0.101	0.020	16.53	2.085	0.345	0.058
Sta-Rx	0.052	0.110	0.094	0.016	14.55	1.874	0.274	0.059
"	0.26	0.102	0.091	0.011	10.78	1.722	0.190	0.059
"	1.30	0.099	0.091	0.009	9.09	1.690	0.150	0.058
"	6.50	0.093	0.087	0.006	6.46	1.511	0.103	0.062
lactose	0.052	0.034	0.029	0.005	14.71	0.569	0.086	0.059
"	0.26	0.034	0.029	0.005	14.71	0.574	0.089	0.059
"	1.30	0.035	0.029	0.005	14.28	0.579	0.082	0.058
"	6.50	0.036	0.030	0.005	14.28	0.574	0.087	0.062
Emcompress	0.052	0.035	0.027	0.007	20.00	0.554	0.118	0.063
"	0.26	0.033	0.026	0.007	21.21	0.563	0.117	0.059
"	1.30	0.036	0.028	0.008	22.22	0.603	0.133	0.059
"	6.50	0.037	0.029	0.008	21.62	0.589	0.132	0.063
sodium chloride	0.052	0.023	0.011	0.012	52.17	0.379	0.190	0.059
"	0.26	0.023	0.012	0.011	47.83	0.386	0.187	0.059
"	1.30	0.023	0.011	0.012	52.17	0.384	0.199	0.059
"	6.50	0.024	0.013	0.011	45.83	0.396	0.186	0.061

Table 5.1 Deformation data obtained during diametral compression of tablets of five materials to 75% of their breaking load.

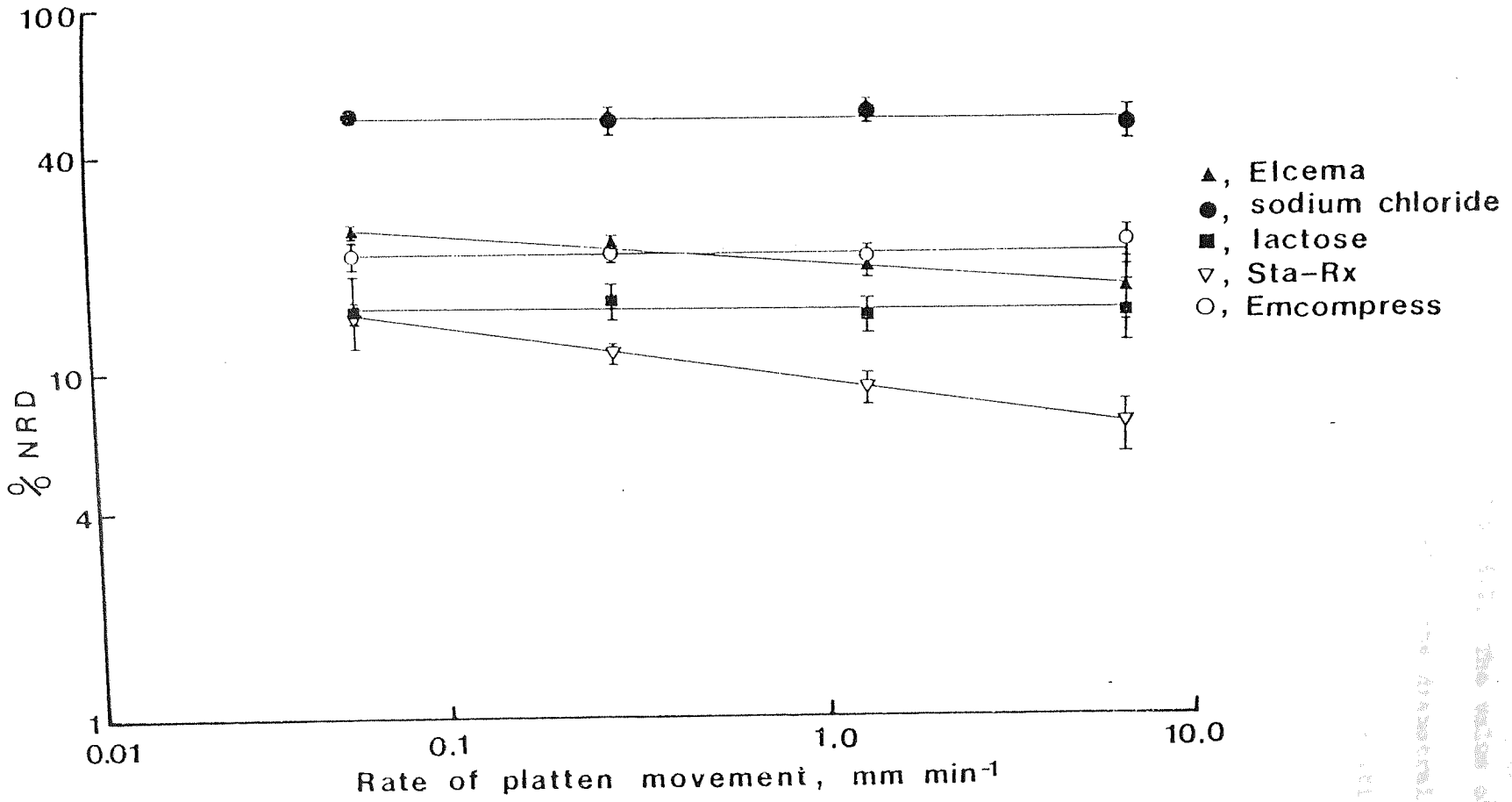

Fig. 5.1 The effect of rate of platten movement on the non-recoverable deformation (NRD) of tablets, expressed as a percentage of the total deformation, when loaded to 75% of their breaking load in a diametral compression test. The bars indicate the standard errors

the total deformation is shown in Fig. 5.2. The value of total deformation for each tablet was divided by the diametral load applied to the tablet to give a value of total deformation per unit force, thus removing the effect of slight differences in the diametral load applied to individual tablets. Comparing Figs. 5.1 and 5.2, shows that, although the % NRD for sodium chloride tablets is about 50%, the total deformation per unit force is relatively small. Conversely, Elcema shows an intermediate % NRD but has a relatively high total deformation. At a given rate of platten movement the total deformation of tablets is in the same rank order as their failure deformation shown in Fig. 3.7, tablets of plastic materials showing a greater total deformation per unit force than tablets of brittle materials. Despite the fact that sodium chloride consolidates by plastic flow, tablets of this material show a relatively low total deformation per unit force, due to the effect of work hardening which prevents deformation of the tablets as explained in section 3.3. The total deformation per unit force of tablet of plastic materials is affected by the rate of platten movement as was the % NRD of these materials. There is a statistically significant difference, at the 99% confidence level, between the total deformation at rates of platten movement of 0.052 and 6.5 mm min^{-1} for both Elcema and Sta-Rx, the Student t values being 6.39 and 4.86 respectively, compared to the critical value of 4.60.

Fig. 5.3 shows the relationship between the logarithm of absolute values of NRD and the logarithm of rate of platten movement. As with the total deformation, since the NRD values will be affected by small differences in the diametral load

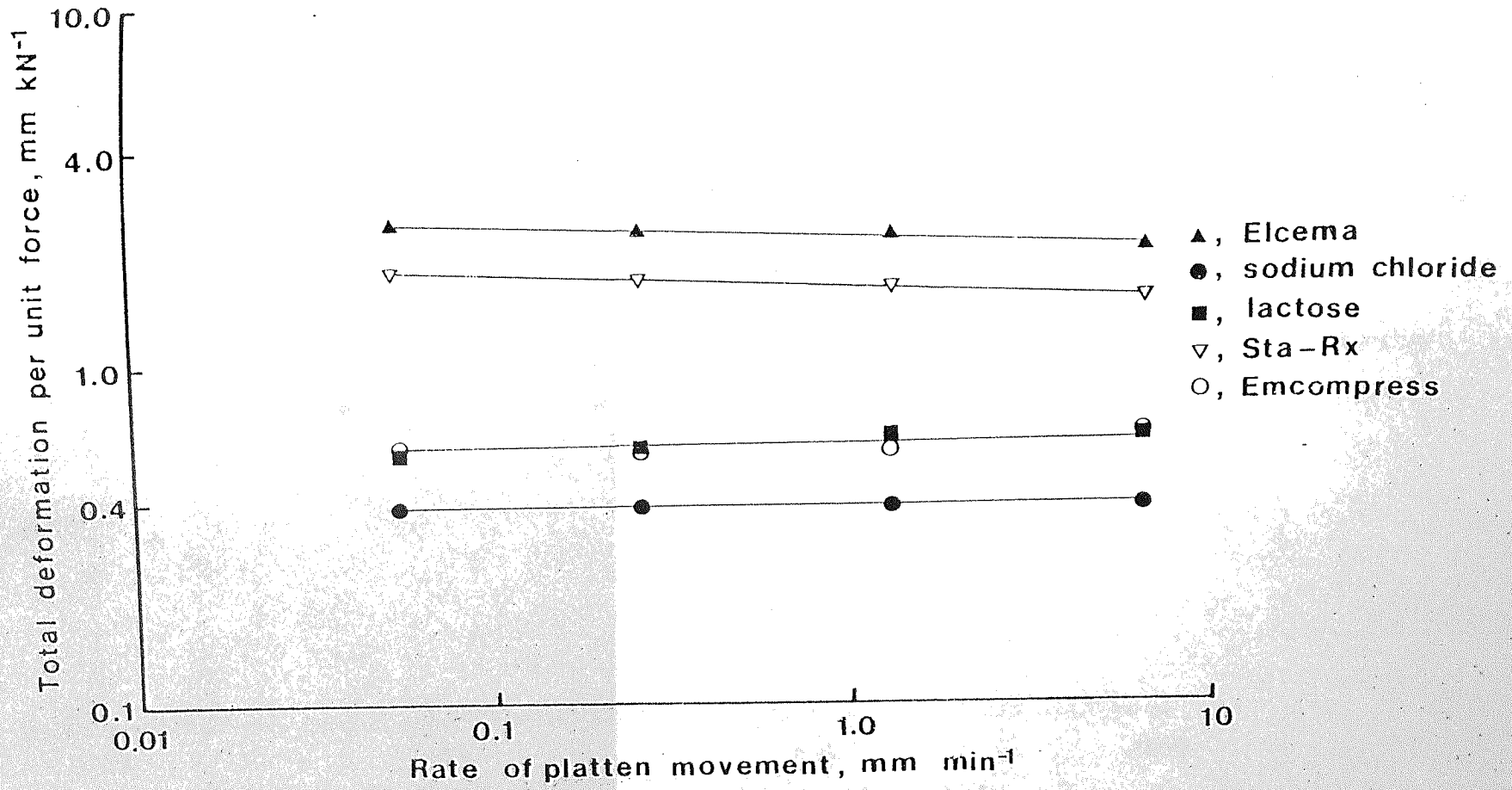

Fig. 5.2 The effect of rate of platten movement on the total deformation per unit force of tablets loaded to 75% of their breaking load in a diametral compression test

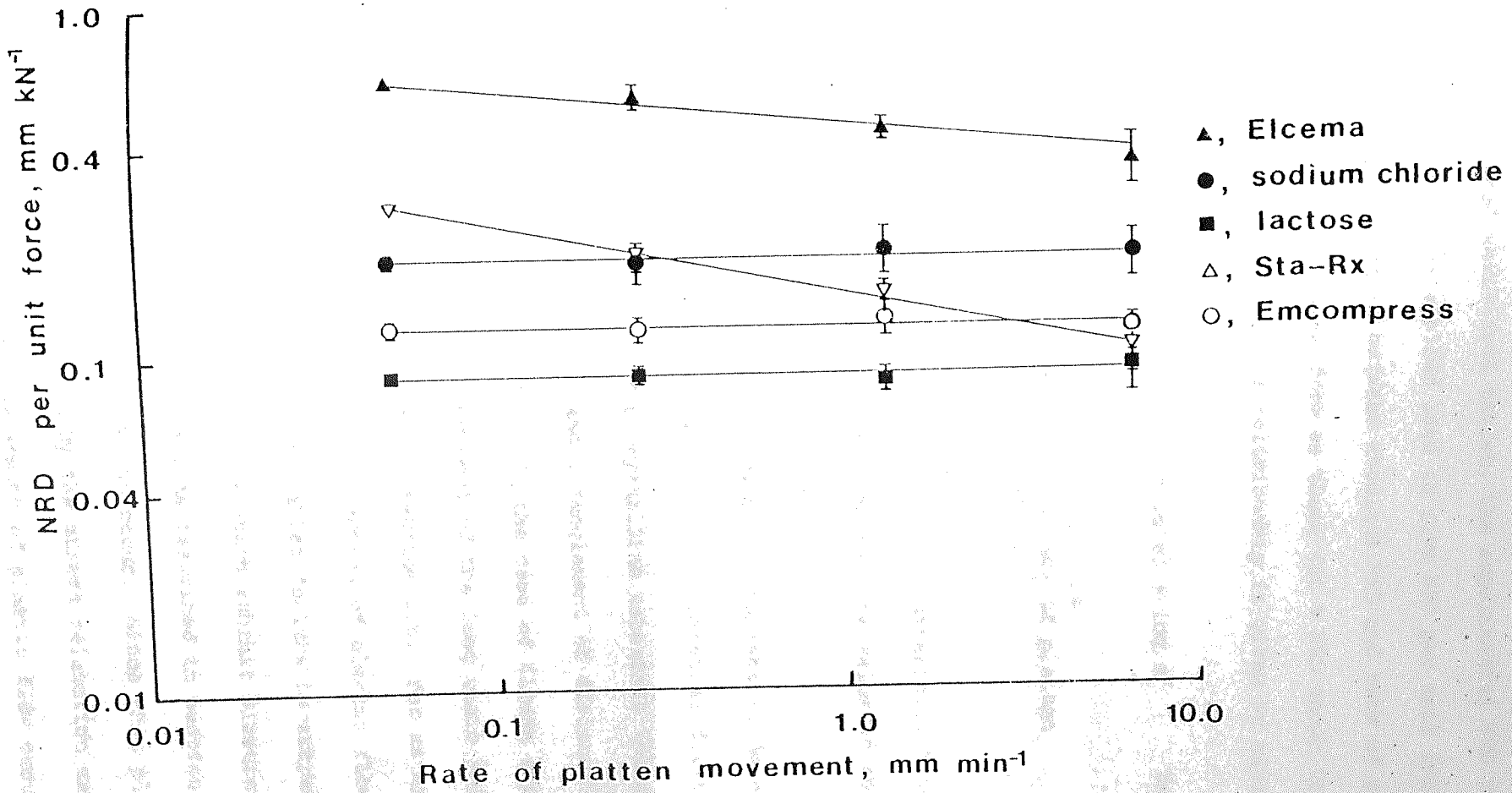

Fig. 5.3 The effect of rate of platten movement on the NRD per unit force of tablets loaded to 75% of their breaking load in a diametral compression test. The bars indicate the standard errors

applied to each individual tablet, the experimental NRD values were divided by the applied load to give NRD per unit force. The observed relationships between absolute NRD and rate of platten movement are of the same form as those for % NRD shown in Fig. 5.1, and the general form of the relationship is given by equation 5.2.

$$\log \text{absolute NRD} = K' (\log \text{rate}) + \log c' \qquad \text{Eq. 5.2}$$

where K' = the gradient of the line
c' = absolute NRD at a rate of platten movement of 1 mm min^{-1}

The value of absolute NRD for the plastic materials, Elcema and Sta-Rx, is strain rate dependent whereas the value of absolute NRD for the brittle materials is not.

The non-recoverable deformation of tablets is determined by the amount of slip which occurs in the material during diametral loading of the tablets. For crystalline materials the slip is controlled by the movement and entanglement of dislocations as discussed in section 1.5.2.2. In the case of Elcema and Sta-Rx, the slip is controlled by movement of the long chain molecules over one another as discussed in section 1.6. For materials which exhibit brittle failure the amount of plastic flow occurring before crack propagation causes tablet failure is extremely limited. For Elcema and Sta-Rx, materials which exhibit plastic failure, crack propagation is prevented, as described in section 1.6.2, and considerable plastic flow can occur. Since this plastic flow is time dependent, as shown by the stress relaxation measurements discussed in section 4, the amount of plastic flow occurring during diametral compression testing will depend on the rate of

platten movement. As the rate of platten movement increases, the time available for plastic flow decreases thus increasing the proportion of the total deformation which is elastic and hence recoverable. The larger negative gradient of Sta-Rx tablets, compared to that of Elcema tablets, shown in Fig. 5.1, shows that the slip which occurs in Sta-Rx and which is responsible for the non-recoverable deformation occurs more slowly than in Elcema.

There are certain anomalies apparent from Fig. 5.3; the absolute value of NRD for Emcompress is greater than that of lactose whereas, on the basis of stress relaxation measurements for tablets discussed in section 4.3, the reverse order would be expected. However, there are two possible mechanisms responsible for non-recoverable deformation of tablets during diametral loading. One mechanism is plastic flow of particles and bonds under the imposed stresses and the second is surface crushing of brittle materials at the points of contact with the platten. The load-displacement diagrams (Fig. 3.4) show that, during diametral compression testing, tablets of brittle materials are more difficult to deform than tablets of plastic materials. Thus, during such testing, the area of contact between the platten and the tablets will be smaller with brittle materials than with plastic materials. This small area of contact will result in a high compressive stress at the surface of the tablets in the region of contact with the plattens. Thus, in a brittle material, a relatively high proportion of the absolute NRD may be due to surface crushing, whereas, with tablets of a plastic material which are easily deformed to produce larger areas on contact between the tablet and plattens, little or no surface crushing occurs. The

greater absolute NRD of Emcompress tablets compared to that of lactose tablets is probably due to the relative amounts of surface crushing in these materials.

The gradients of the relationship between the absolute NRD and the rate of platten movement will be a measure of the strain rate sensitivity of the material to deformation, as is the gradient of the relationship shown in Fig. 5.1 between the % NRD and the rate of platten movement. As before, the negative gradient of the relationship between absolute NRD and rate of platten movement is greater for Sta-Rx than for Elcema, the gradients being -0.191 and -0.090 respectively.

5.2 The Effect of Tensile Strength on the Non-recoverable Deformation of Tablets During Diametral Loading

To determine the effect of increasing tensile strength of tablets on the absolute NRD, the same diametral load used in the previous experiments (5.88×10^{-2} kN) was applied to several batches of tablets of increasing tensile strength. For each successive sample this results in a lower load ratio which is defined as the applied diametral load expressed as a percentage of the mean breaking load.

The effect of reducing the load ratio on the relationship between the total deformation and the rate of platten movement for Elcema tablets is shown in Fig. 5.4. There is a linear relationship between the logarithm of total deformation and the logarithm of rate of platten movement, for each of the load ratios, of the form shown in equation 5.3.

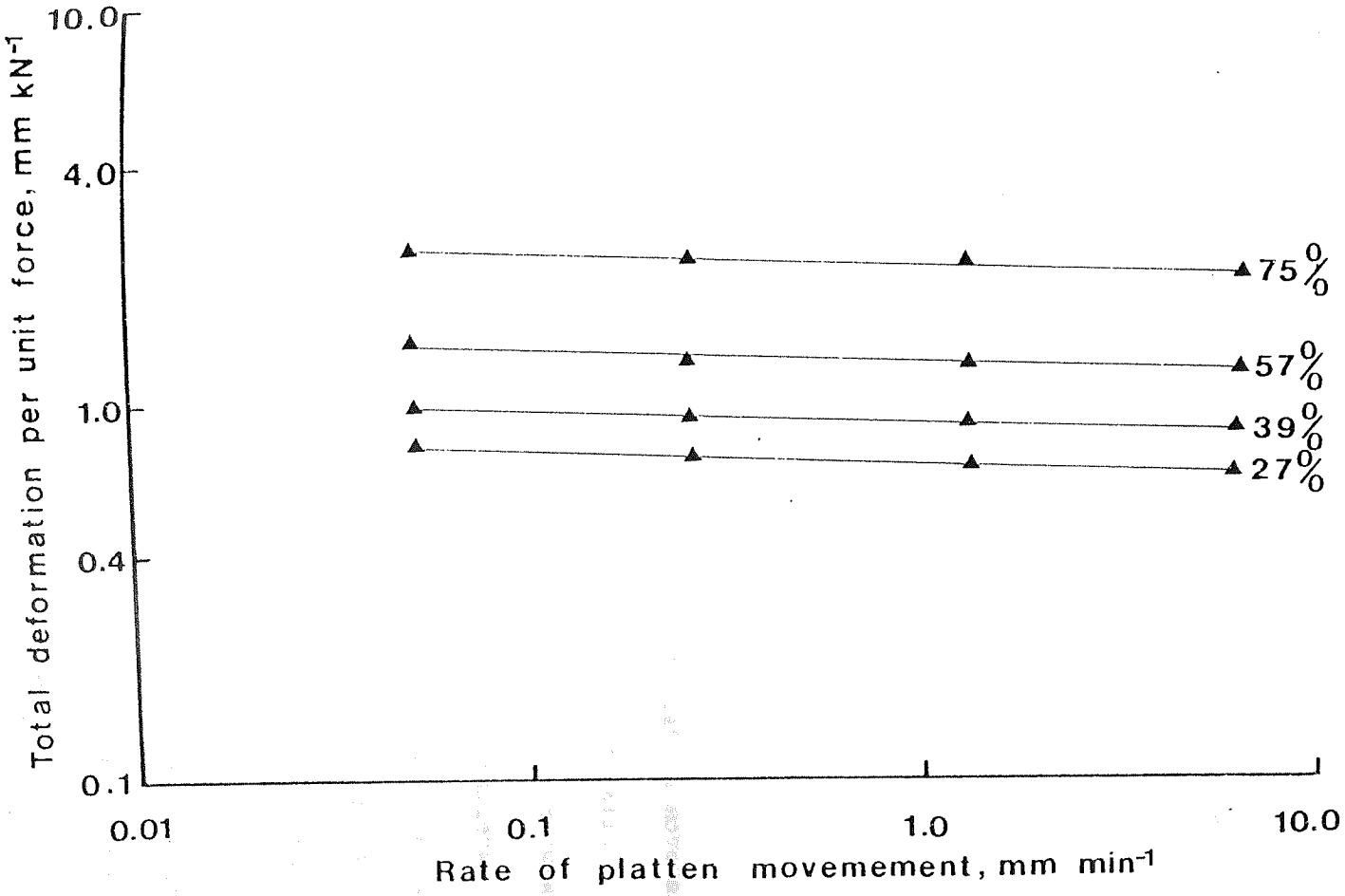

Fig. 5.4 The effect of rate of platten movement on the total deformation per unit force of Elcema tablets at four load ratios. The load ratios are indicated as a percentage for each line

$$\log \text{total deformation} = k(\log \text{rate}) + \log C \qquad \text{Eq. 5.3}$$

where k = gradient of the line
C = total deformation at a rate of platten movement of 1 mm min^{-1}

Table 5.2 shows the values of k and C for each load ratio.

Load ratio %	k	C
75	-3.3×10^{-2}	2.20
57	-3.4×10^{-2}	1.25
39	-3.1×10^{-2}	0.87
27	-3.1×10^{-2}	0.68

Table 5.2 The slope, K and the intercept, C of the linear relationship between the logarithm of total deformation and the logarithm of rate of platten movement for Elcema tablets at four load ratios

From Fig. 5.4 and Table 5.2 it can be seen that, at each load ratio, the total deformation decreases with an increasing rate of platten movement and that, for a given rate of platten movement the total deformation decreases with a decreasing load ratio. The effect of reducing the load ratio on the relationship between absolute NRD and rate of platten movement for Elcema tablets is shown in Fig. 5.5. There is a decrease in the absolute NRD with an increasing rate of platten movement at each load ratio and, at a given rate of platten movement, there is a decrease in the absolute NRD with a decrease in load ratio. The decrease in both total deformation and absolute NRD with decreasing load ratio may be attributed to the larger areas of inter-particulate bonding created at the higher compaction forces used to prepare higher strength tablets. As the total area of bonding increases, the force per unit area of bond (bond stress) developed during the diametral compression of tablets decreases for a given diametral load; this decreases both

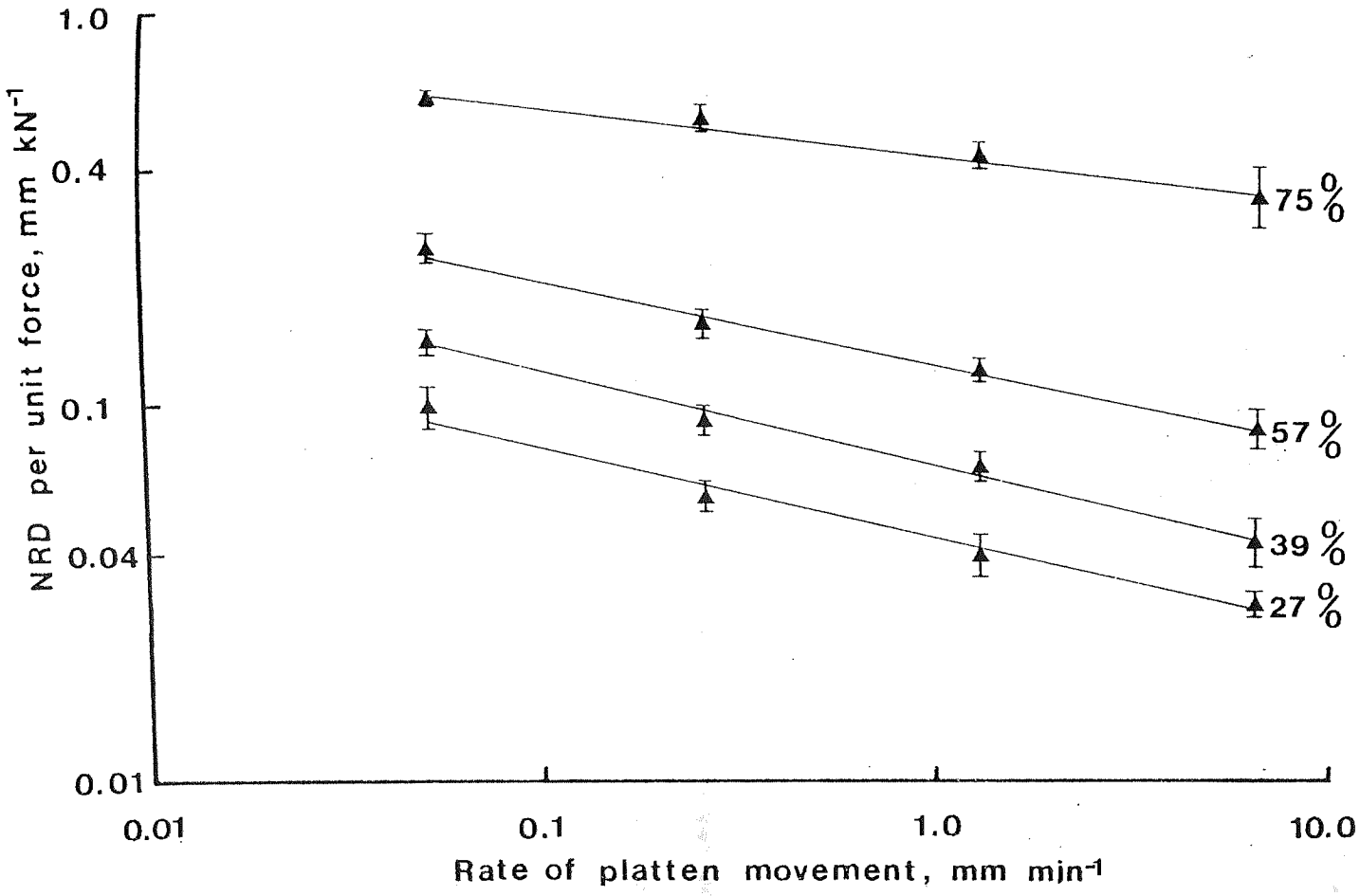

Fig. 5.5 The effect of rate of platten movement on the NRD per unit force of Elcema tablets at four load ratios. The load ratios are indicated as a percentage for each line. The bars indicate the standard errors

the total deformation and the amount of plastic flow which occurs as represented by the NRD.

The effect of reducing the load ratio on the relationship between total deformation and rate of platten movement for lactose tablets is shown in Fig. 5.6. As with Elcema tablets, a decrease in the load ratio decreases the total deformation. The absolute NRD also decreases with a decrease in the load ratio as shown in Fig. 5.7. However, with lactose tablets, the rate of platten movement has no effect on either the total deformation or the absolute NRD. When the load ratio for lactose tablets was 45% or less, there was no measurable NRD and the load-displacement diagrams were completely linear indicating that, under these conditions of loading, the tablets were behaving as Hookean elastic solids. The reduction in the total deformation and absolute NRD of lactose tablets with an increasing tablet tensile strength is caused by the larger total area of inter-particulate bonding in the higher strength tablets. The larger area of bonding will reduce the bond stress for a given diametral load thus reducing the total deformation. The larger area of bonding, which for a brittle material will be due to an increased number of bonds, will be of particular importance in the regions of contact between the tablet and plattens since it will enable the tablet to resist surface crushing. For load ratios of 45% or less the relatively small total deformation, shown in Fig. 5.6, is completely elastic and recoverable since the surface of the tablet is sufficiently strong to resist surface crushing under these loading conditions.

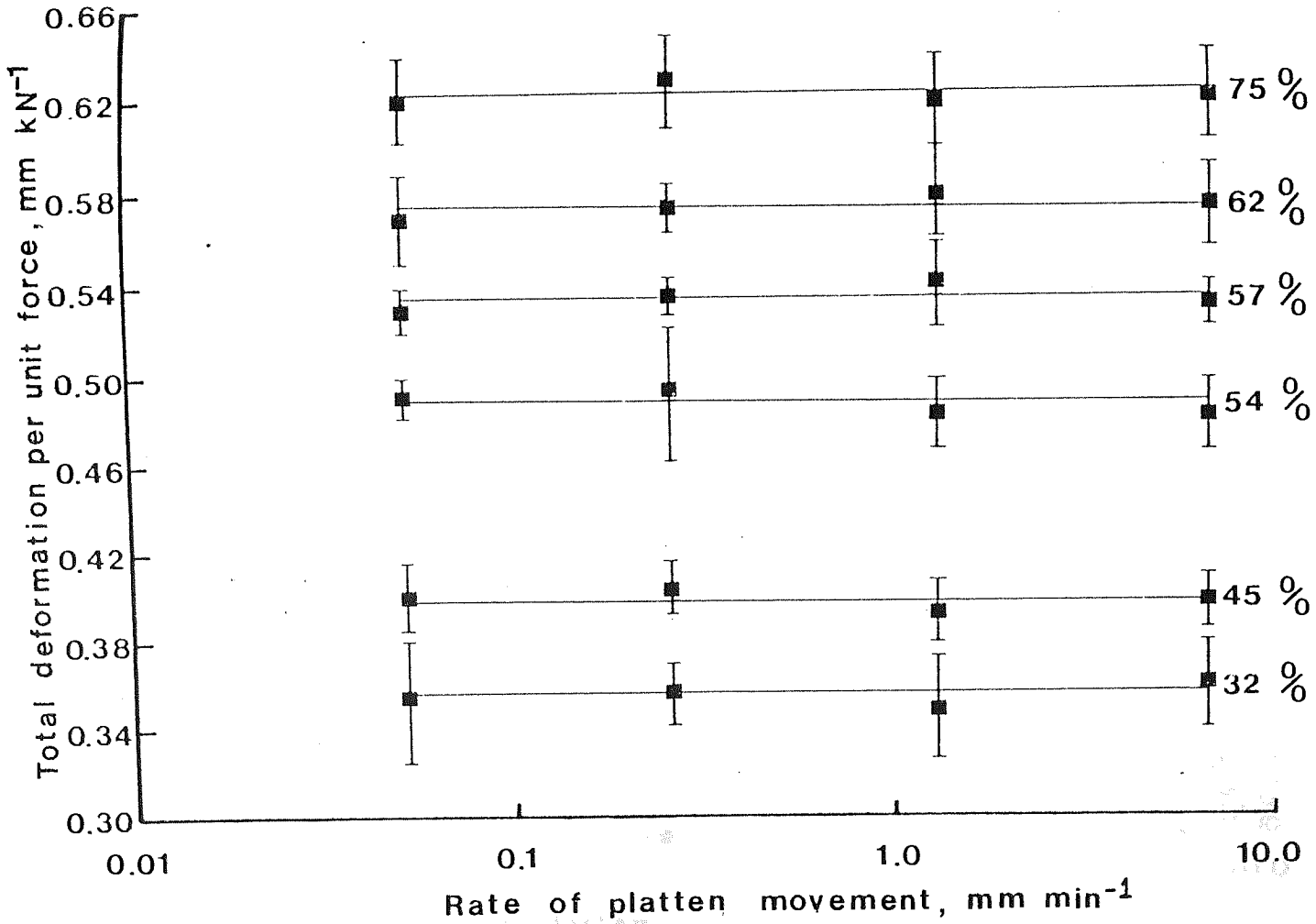

Fig. 5.6 The effect of rate of platten movement on the total deformation per unit force of lactose tablets at six load ratios. The load ratios are indicated as a percentage for each line. The bars indicate the standard errors

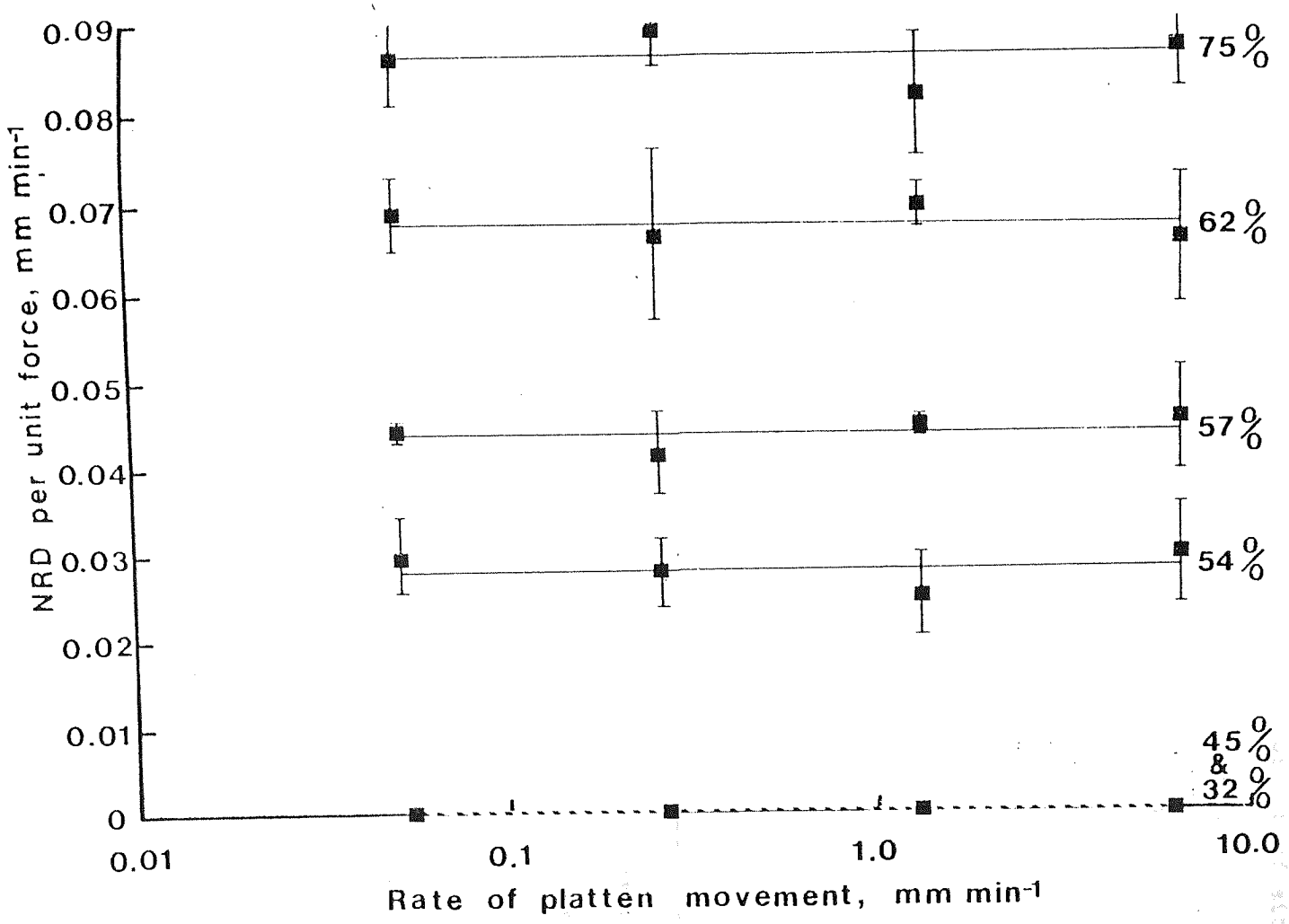

Fig. 5.7 The effect of rate of platten movement on the NRD per unit force of lactose tablets at six load ratios. The load ratios are indicated as a percentage for each line. The bars indicate the standard errors

5.3 Applications of NRD Measurements

NRD measurements are a simple method of quantifying the deformation behaviour of tablets. For example, the effect of strain rate on the deformation of tablets may be evaluated by considering the gradient of the plot of the logarithm of either % NRD or the absolute NRD against the logarithm of rate of platten movement. If the rate of platten movement affects the NRD then the deformation of the material is strain rate sensitive and, the larger the negative gradient, the greater the strain rate sensitivity. A zero gradient indicates that little or no plastic flow is occurring during diametral loading of the tablets and that the deformation is elastic or mainly due to surface crushing.

The effect of strain rate on the NRD of tablets is a characteristic of the compacted material and may facilitate prediction of the effect of compaction variables, such as rate of compaction, during manufacture of tablets. Such predictions may not however be valid for materials which work harden during compaction, such as sodium chloride, since deformation properties of such materials will be different before and after compaction. In particular, the high strain rate sensitivity of Sta-Rx, shown by the effect of rate of platten movement on NRD and by the effect of dwell time on its consolidation behaviour during compaction shown in Fig. 4.7, may explain the relatively low strength of tablets formed from this material as shown in Fig. 3.1. Sta-Rx is capable of considerable plastic flow during a slow rate diametral compression test as shown by its relatively high failure deformation seen in Fig. 3.7. However, at the high strain rates during powder

compaction in a tabletting machine, a greater proportion of the deformation of particles will be elastic and recoverable. During powder compaction, particles are brought into intimate contact allowing surface forces to act thus forming inter-particulate bonds. The importance of plastic flow in the production of high strength tablets has been discussed by Cole, Rees and Hersey (1975) and by David and Augsburger (1977). During the high strain rate operation of compaction the amount of plastic flow occurring in Sta-Rx is relatively small and so a low strength compact is formed. Furthermore, a high proportion of the total deformation of Sta-Rx particles will be elastic and will recover rapidly during decompression and on ejection of the tablet, rupturing bonds and further decreasing the strength of the tablet.

The gradient of the relationship between NRD and rate of platten movement, shown in Fig. 5.3, for Elcema indicates that the deformation of Elcema tablets is also strain rate dependent. However, this effect is less for Elcema than for Sta-Rx. The stress relaxation data shown in Figs. 4.6 and 4.9 indicate that plastic flow of Elcema is initially much more rapid than that of Sta-Rx both during compaction of the powders and presumably during diametral loading of tablets. Considering the compaction of Elcema particles during tabletting, considerable plastic flow occurs as force is applied thus facilitating intimate inter-particulate contact and bonding between large areas of particle surfaces. Only a relatively small proportion of the deformation of Elcema particles is elastic compared with Sta-Rx. Considering also the rapid plastic flow of Elcema relative to Sta-Rx, shown in Fig. 4.6, it is probable that the elastic deformation of Elcema which recovers during

decompression will be accommodated by further plastic flow thus minimising the failure of bonds which would otherwise occur during decompression and on ejection. This may account for the observation of Esezobo and Pilpel (1977), that microcrystalline cellulose reduces the tendency of oxytetracycline compacts to laminate and cap when elastic recovery occurs during decompression and ejection. In the formulation, containing 7.2% w/w of microcrystalline cellulose and 2.6% w/w of alginic acid HED, used by Esezobo and Pilpel (1977), the elastic recovery of oxytetracycline will be accommodated by plastic flow of the microcrystalline cellulose, and possibly the alginic acid, thus preventing bond failure and maintaining a strong compact which did not cap or laminate. Esezobo and Pilpel (1977) explain their observation regarding capping by suggesting that the microcrystalline cellulose, in particular, and also alginic acid counteract the elastic recovery of the oxytetracycline. This is probably incorrect since the elastic recovery of the oxytetracycline will still occur and the microcrystalline cellulose does not counteract this recovery but accommodates it by plastic flow.

Although Fig. 4.6 shows that a small amount of plastic flow occurs during compaction of lactose, the NRD of lactose tablets does not appear to be strain rate dependent within the rates of platten movement used in this study. This suggests that during compaction of lactose, fragmentation is primarily responsible for consolidation of the powder. This fragmentation will produce new, clean surfaces of lactose which, when brought into intimate contact, form inter-particulate bonds. The fragmentation of lactose particles during compaction has been shown by Hersey, Cole and Rees (1973) who photographed a sample of lactose before and after

compaction. The particle size of lactose after compaction was considerably reduced with the appearance of many fine particles. During compaction of a brittle material fragmentation will occur as the compaction force is applied, but will be associated with considerable elastic deformation of the fragmented particles. Once the maximum applied force is reached, and also during decompression, no further fragmentation will occur and little plastic flow is possible. Neglecting die wall friction, which would otherwise prevent some axial recovery of the tablet in the die, during decompression there will be instantaneous and virtually complete recovery of the axial elastic deformation of the particles. If stresses within the tablet, due to elastic recovery, are sufficiently large to rupture the bonds formed during compaction, then the strength of the tablet will be severely reduced and capping may occur either during decompression or on ejection, due to radial elastic recovery.

For brittle materials, such as lactose and Emcompress which show little stress relaxation during powder compaction and in which the primary mechanism of consolidation is particle fragmentation, the tablet strength should be less dependent on dwell time than more plastic materials. This hypothesis is supported by the results of David and Augsburger (1977) who increased the duration of the compression cycle from 0.1 to 10 seconds and found an 8.7% increase in the strength of Sta-Rx tablets, a 4.4% increase for microcrystalline cellulose, but no increase in the strength of lactose tablets.

In addition to the rapid axial elastic recovery of tablets which occurs in the die before ejection as shown by DeBlaey (1972) and the rapid radial elastic recovery which occurs during ejection,

there is also a time-dependent, so-called anelastic recovery of tablets after ejection. This anelastic strain recovery may be due to either the residual stresses within the tablet after compaction shown by Rees and Shotton (1970) or elastic recovery which is constrained by the surrounding inter-particulate bonds which retard the strain recovery. Aulton, Travers and White (1973) suggested that time-dependent changes in tablet dimensions are associated with a deterioration of mechanical properties. Table 5.3 shows the percentage increase in thickness of tablets of the materials during the first 3 hours after ejection from the die. The values of percentage increase in thickness are in the same rank order as the values of strain recovery of tablets of some similar materials found by Baba and Nagafuji (1965) which are also shown in Table 5.3. The larger values of strain recovery found by Baba and Nagafuji (1965) compared to the present study may be due to the higher compaction pressures and to the thicker tablets used by these authors. The thickness of tablets used by Baba and Nagafuji (1965) was 15 mm and they used a compaction pressure about 40% higher than used in this study. If the comment of Aulton, Travers and White (1973) that time dependent changes in tablet dimensions are associated with deterioration of mechanical properties is correct, then the strength of both Elcema and particularly Sta-Rx tablets would be expected to be reduced by the anelastic strain recovery after ejection, as well as by the elastic strain recovery during decompression in the die. Rees and Shotton (1970) found an increase in the strength of sodium chloride tablets after ejection from the die. They attributed this to continued plastic flow of the material within the constraint

of a rigid skin of sodium chloride formed by shear at the die wall. Thus, with sodium chloride tablets, since there is no anelastic strain recovery which might cause rupture of bonds or particles, especially in the presence of work hardening, the strength of the tablets may increase, rather than decrease as would be expected for tablets which exhibit considerable anelastic strain recovery. This may account for the absence of strain rate sensitivity of sodium chloride tablets during a diametral compression test as shown in Fig. 5.3. If the deformation of such tablets is restricted by a work hardened rigid skin, the tablets will behave as brittle specimens rather than as plastic specimens expected on the basis of the compaction behaviour of sodium chloride observed by Hardman and Lilley (1970). Train and Hersey (1960) have shown that large shear forces are exerted on the particles at the die wall during compaction of lead spheres and these forces create an outer "skin" of sheared lead enclosing deformed, but unbonded, lead particles. If work hardening occurs during deformation of the particles, as with sodium chloride, the outer "skin" will be rigid and brittle.

Material	Measured thickness on ejection mm	Measured thickness after 3 hours mm	Percentage increase in thickness	Percentage axial strain recovery of tablets after ejection (from Baba and Nagafuji, 1965)
Sta-Rx	2.991	3.021	1.51	
Elcema	2.955	2.972	0.58	
microcrystalline cellulose	-	-	-	6.7
lactose	2.926	2.929	0.11	3.2
Emcompress	3.180	3.180	0	
sodium chloride	2.642	2.642	0	0.9

Table 5.3 Anelastic axial strain recovery of tablets compressed to 20 kN applied force

6. INTER-BATCH VARIATION OF THE COMPACTION PROPERTIES OF ELCEMA

During the period of study a second batch of Elcema G250 was obtained from the suppliers for use in further studies on multiple diametral impact testing. Using this second batch of material, referred to as new Elcema, unexpected results were obtained for tensile strength of tablets. It was therefore decided to investigate the inter-batch variation in the properties of Elcema G250.

6.1 Comparison of the Properties of Tablets Compressed from Two Batches of Elcema.

6.1.1 Tensile strength-compaction force profiles

The tensile strength-compaction force profiles of the two batches of Elcema are shown in Fig. 6.1. The extent of the variation may be seen by comparing Fig. 6.1 with the strength profiles of the other materials which are shown in Fig. 3.1. The profile for new Elcema shows a similar sigmoidal shape to that of old Elcema, but at any compaction force the tensile strength of new Elcema is only about 25% of the strength of old Elcema tablets. Assuming the intrinsic strength of the material is the same for both batches, the reduced strength of new Elcema tablets suggests that, for a given amount of energy supplied by the tablet press during compaction, less bonding occurs in new Elcema than old Elcema.

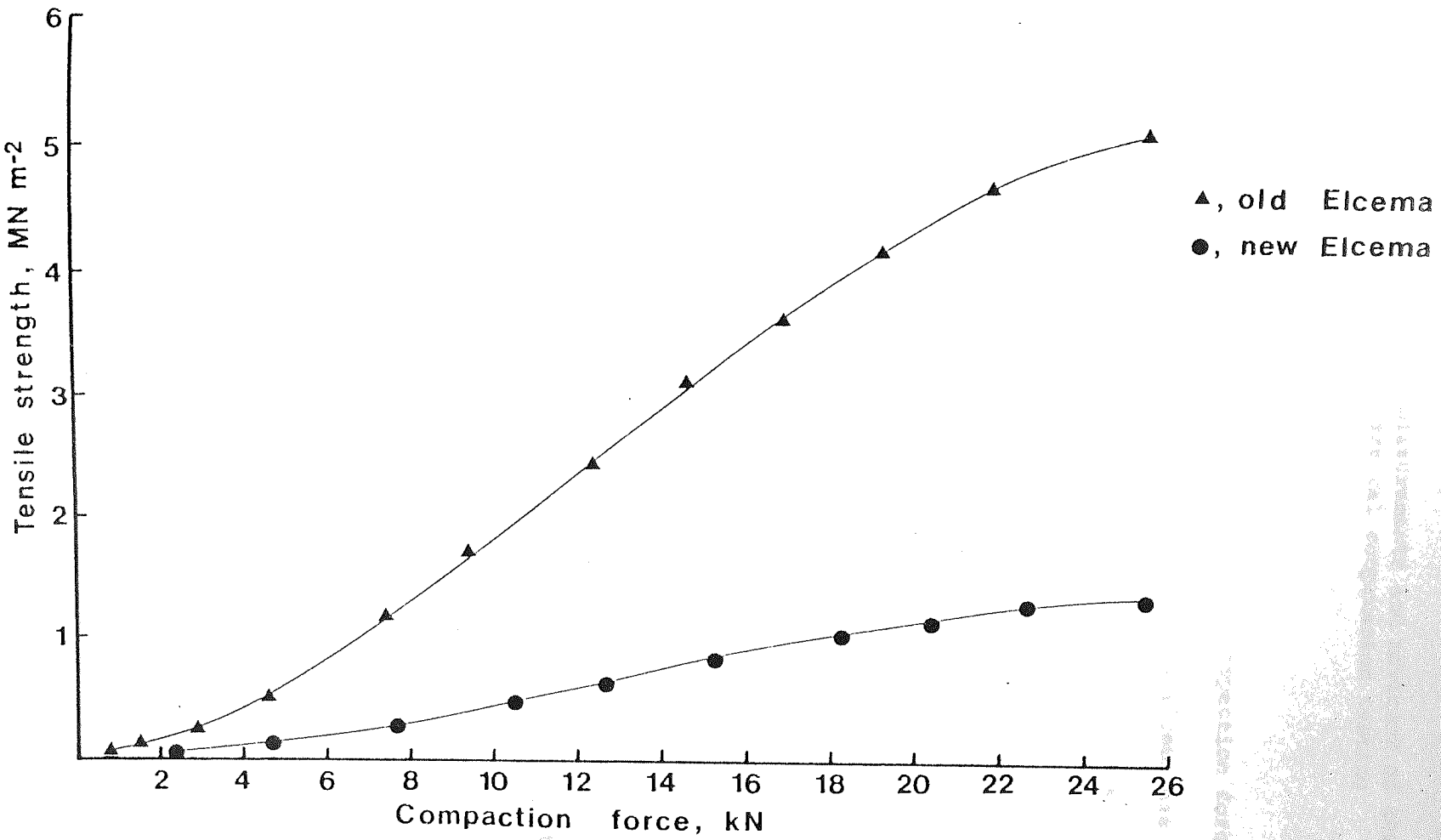

Fig. 6.1 The relationship between the tensile strength of tablets and the applied compaction force for two batches of Elcema

6.1.2 Work of failure measurements and movement of the platten during diametral compression testing.

Fig. 6.2 shows the work of failure-compaction force profiles for the two batches of Elcema. New Elcema has a relatively low work of failure compared with old Elcema indicating that the toughness of new Elcema tablets is much lower than that of old Elcema tablets, and that the resistance of new Elcema tablets to mechanical damage is lower than that of old Elcema tablets. This is confirmed by the results of the multiple diametral impact test carried out on new Elcema tablets as shown in Table 6.1.

Material	Tensile strength	Number of impacts required to cause failure	
		mean	coefficient of variation %
old Elcema	1.67	4360	11.8
new Elcema	1.60	364	32.9
Sta-Rx	1.36	322	28.3
lactose	1.59	41	17.9

Table 6.1 Multiple diametral impact test results for two batches of Elcema. The results for Sta-Rx and lactose are included for comparison.

Although the tablets of both batches had very similar tensile strengths, the mean number of impacts required to break new Elcema tablets is very much lower than for old Elcema tablets.

The lower work of failure of new Elcema tablets compared to old Elcema tablets prepared at the same compaction force, is due to a combination of the lower tensile strength and the smaller platten movement required to cause failure, in a diametral compression test, shown in Fig. 6.3. This smaller platten movement

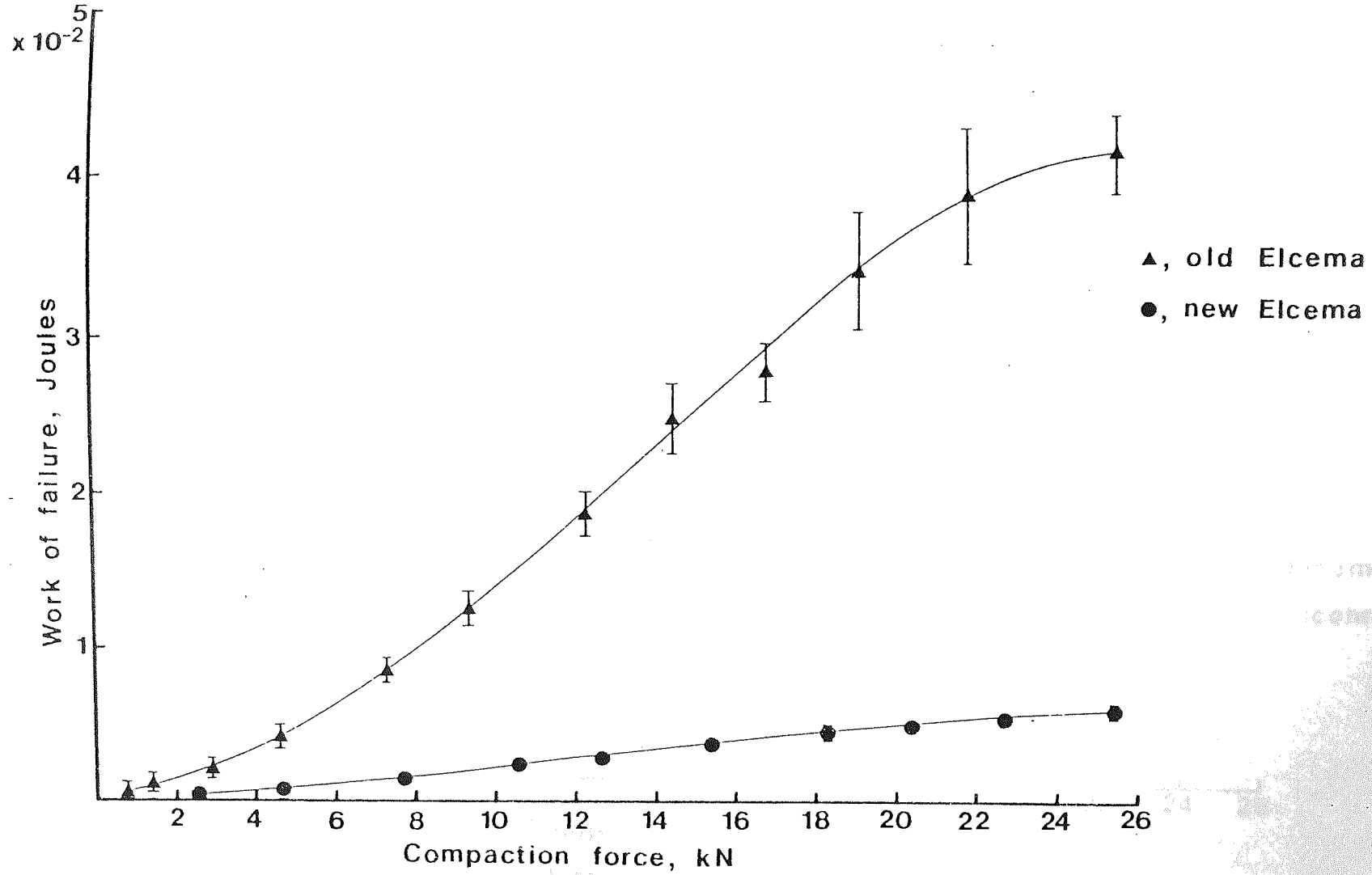

Fig. 6.2 The relationship between the work of failure and the applied compaction force for tablets of two batches of Elcema subjected to diametral compression testing at a rate of platten movement of 0.26 mm min^{-1}. The bars indicate the standard errors

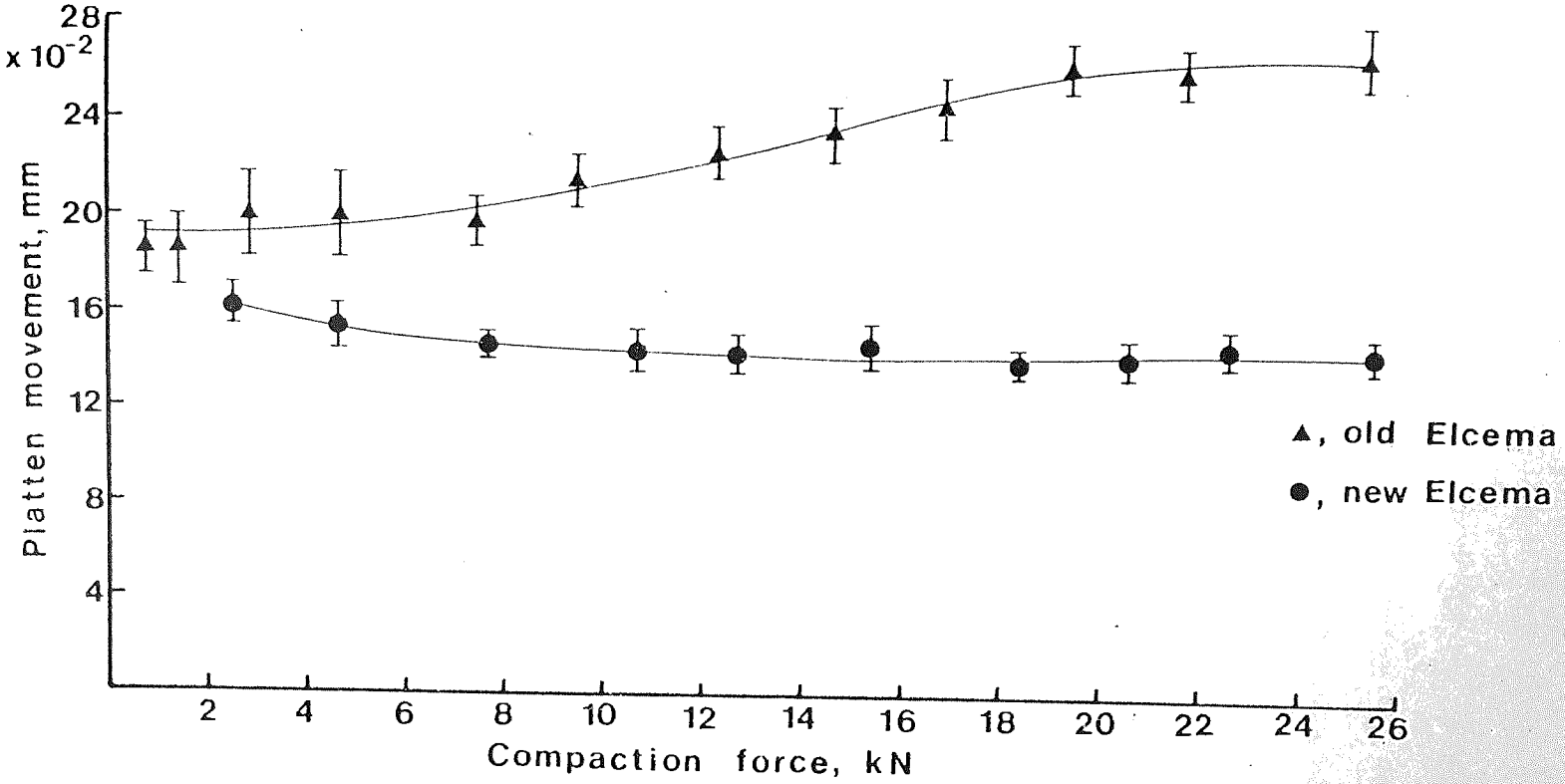

Fig. 6.3 The relationship between the distance moved by the platten at the point of failure and the applied compaction force for tablets of two batches of Elcema subjected to diametral compression testing at a rate of platten movement of 0.26 mm min^{-1} . The bars indicate the standard errors

indicates that new Elcema tablets accept less plastic strain before failure than old Elcema tablets. The increase in platten movement at failure with an increase in compaction force, for plastic materials, was discussed in section 3.3 and was attributed to an increase in the area of inter-particulate bonding created at higher compaction forces. Thus, the initial decrease in platten movement with increasing compaction force shown by new Elcema is unexpected. This decrease in platten movement may be due to inter-action between the surface of the tablet and the metal plattens. The surface of tablets prepared at low pressures from new Elcema was observed to be loose and many particles became detached from the surface during even the most careful handling. Thus, the initial large platten movement may be due to surface deformation of these loose particles.

The load-displacement curves for Elcema tablets are shown in Fig. 6.4. Although new Elcema tablets still exhibit plastic failure, as shown by the relatively high failure deformation compared to the brittle materials lactose and Emcompress shown in Fig. 3.4 and by the deviation from linearity at the higher diametral loads, the amount of plastic deformation is reduced compared to old Elcema. The displacement values at any given diametral load are smaller for new Elcema tablets than for old Elcema showing that new Elcema tablets are more difficult to deform.

6.2 Chemical and Physico-chemical Characterisation of Two Batches of Elcema

6.2.1 Chemical nature of Elcema.

It was thought that differences in the properties of the

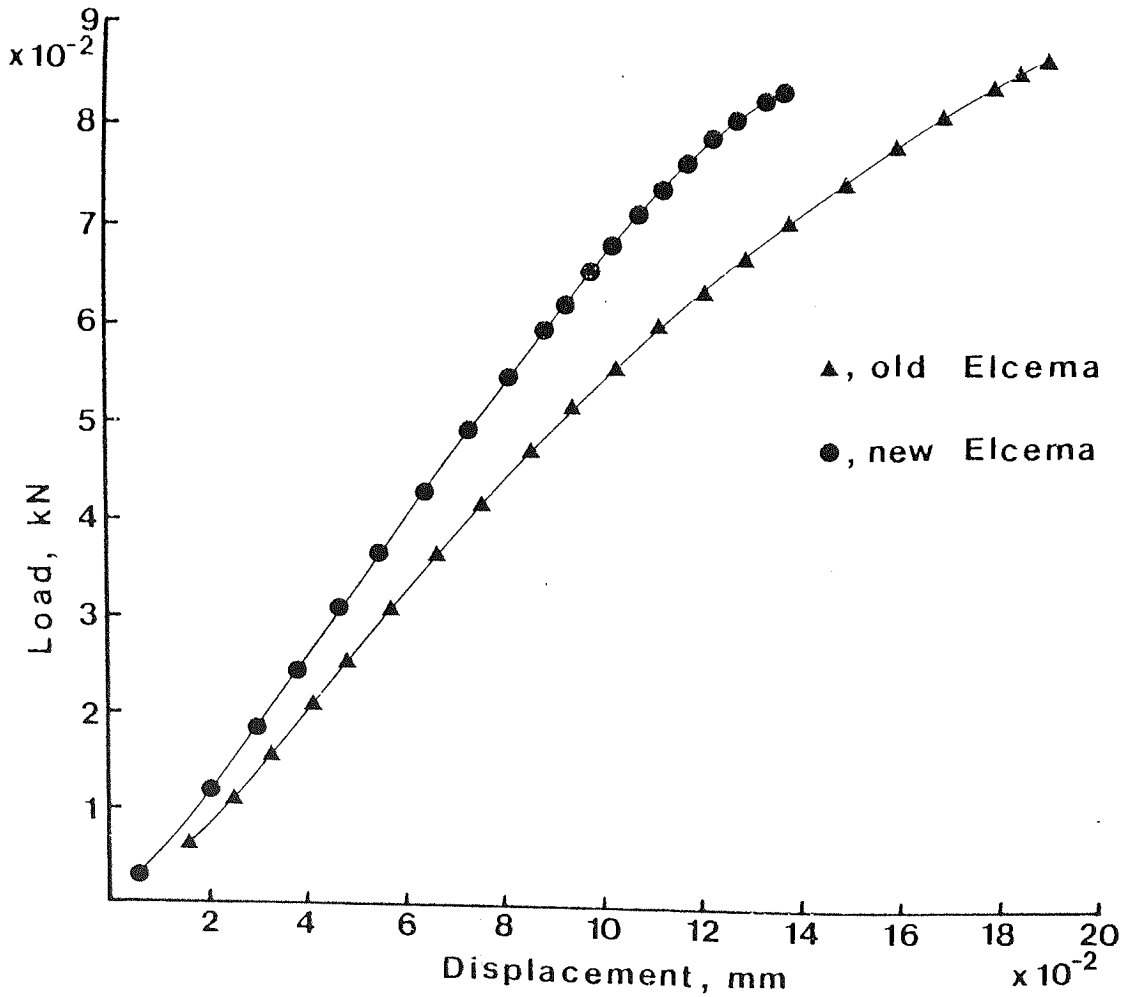

Fig. 6.4 Load-displacement curves for tablets of two batches of Elcema subjected to diametral compression testing at a rate of platten movement of 0.26 mm min^{-1}

tablets prepared from the two batches of Elcema might be due to differences in the chemical nature of the two samples.

To determine the chemical nature of these samples a carbon and hydrogen analysis was performed (Butterworth Microanalytical Consultancy Ltd., Teddington). An infra-red spectrum of each sample was also obtained by grinding a small amount of the sample to a fine powder and compressing the powder in a potassium bromide disc.

No difference was found in the elemental composition of the two batches by chemical analysis, nor was there any difference in the infra-red spectra of the samples. From these results it appears there was no difference in the chemical composition of the batches of Elcema.

6.2.2 Manufacturer's specification

Tests were carried out to ensure that both batches of Elcema conformed to the manufacturer's specification given on the sample container of each batch.

6.2.2.1 Proof of identity

0.25g of each sample was added to 3 ml of ammoniacal copper oxide solution. Both samples of Elcema dissolved slowly to produce a clear solution. An aqueous dispersion of 0.5g in 10 ml distilled water showed no blue colouration when treated with iodine solution showing the absence of starch.

6.2.2.2 Loss on drying

The manufacturer's specification for loss on drying of Elcema is that when dried for 2 hours at 105°C, less than 6% loss will occur. However, the moisture content of the sample will be affected by the relative humidity conditions during storage of the sample and these conditions are not listed in the specifications. In order to standardise the storage conditions, the samples were stored at 50% R.H. for 24 hours before drying. After storage a sample of about 10g was accurately weighed and then dried at 105°C for 2 hours in a hot air oven. The loss in weight was calculated as a percentage of the sample weight.

The losses in weight of new and old Elcema were 5.2% and 4.9% respectively which comply with the specification of less than 6% loss.

6.2.2.3 Residue on ignition

A sample of about 10g of each batch of Elcema was accurately weighed and poured into a tared crucible. The crucible was heated in a Bunsen burner flame until the Elcema was reduced to ash and reached constant weight. The weight of the ash remaining was calculated as a percentage of the initial sample weight.

The ash values for new and old Elcema were 0.080% and 0.079% respectively, thus complying with the specification of less than 0.1%.

6.2.2.4 Water soluble substances

A sample of about 20g of each batch of Elcema was accurately

weighed and shaken with 50 ml of distilled water. The suspension was filtered through a Whatman No. 42 filter paper and the solid material was washed with a further 50 ml of distilled water. The filtrate was evaporated to dryness. The weight of dissolved solids in the filtrate was calculated as a percentage of the initial weight.

The percentage for new and old Elcema was 0.62% and 0.60% respectively compared to the specification of less than 1.0%.

These results show that both batches of Elcema conform to the manufacturer's specifications.

6.2.3 Physical properties of Elcema

6.2.3.1 Particle size distribution

Alpar, Hersey and Shotton (1970) comment that there is a tendency for the crushing strength of lactose tablets to increase as the particle size decreases and Fell and Newton (1971a) have shown that differences in particle size can affect the tensile strength of lactose tablets. Hersey, Bayraktar and Shotton (1967) found that the strength of sodium chloride tablets is also dependent on particle size. For this reason it was decided to compare the particle size distributions of the two batches of Elcema.

The particle size distributions, determined by sieve analysis as described in section 2.1.1.3 (a) are presented in Fig 6.5. There is little difference in the particle size distribution of the two batches of Elcema, the new Elcema containing slightly less particles under about 200μm than old Elcema. It is unlikely that the small differences in particle size distribution

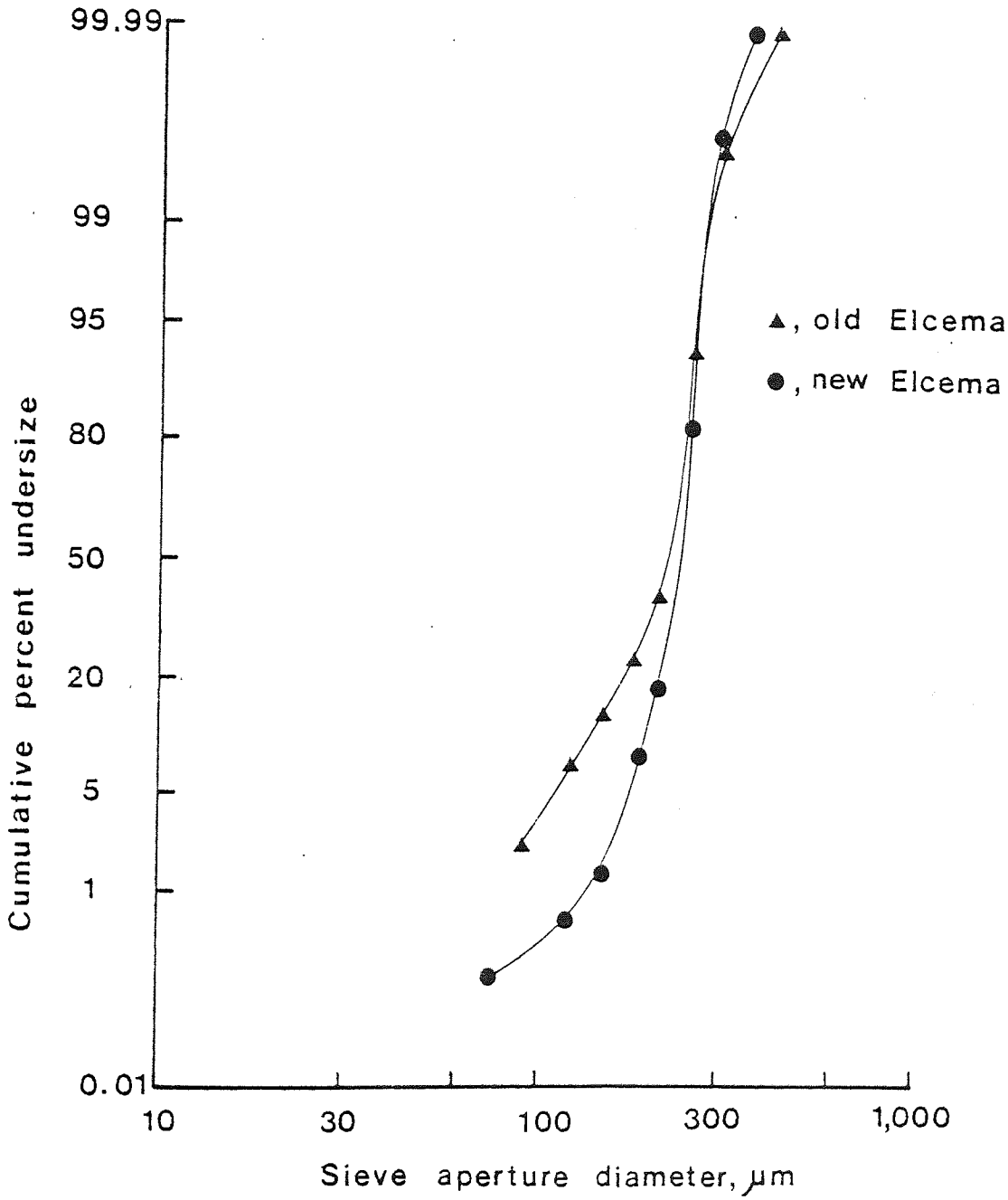

Fig. 6.5 Particle size distribution of two batches of Elcema expressed as cumulative percent by weight undersize on a probability scale (ordinate) versus the logarithm of sieve aperture diameter in micrometers (abscissa)

of the two batches of Elcema would cause the large observed differences in the tensile strength of the tablets.

6.2.3.2 Surface properties

To examine the surface properties of the two batches of Elcema, scanning electron photomicrographs were taken of samples of each batch. These are shown in Fig. 6.6; there is little difference in the surface structure of the two batches.

6.3 Physico-mechanical Characterisation of New and old Elcema.

Although no differences could be found in either the chemical or the physico-chemical nature of the two batches of Elcema, there is a marked difference in the ability of the batches to form strong compacts. Since the force-displacement diagrams (Fig. 6.4.) indicate that new Elcema is more difficult to deform plastically than old Elcema, it appears that the differences in tensile strength may be due to differences in the deformation properties of the two batches.

6.3.1 Stress relaxation measurements

The stress relaxation of new Elcema, during compaction, was measured as described in section 2.2.3. Fig. 6.7. shows the decrease in force on the upper punch of the tablet machine, with time, for both batches of Elcema for times between 10 and 360 seconds after the maximum applied compaction force. The new Elcema shows less total relaxation than old Elcema, indicating

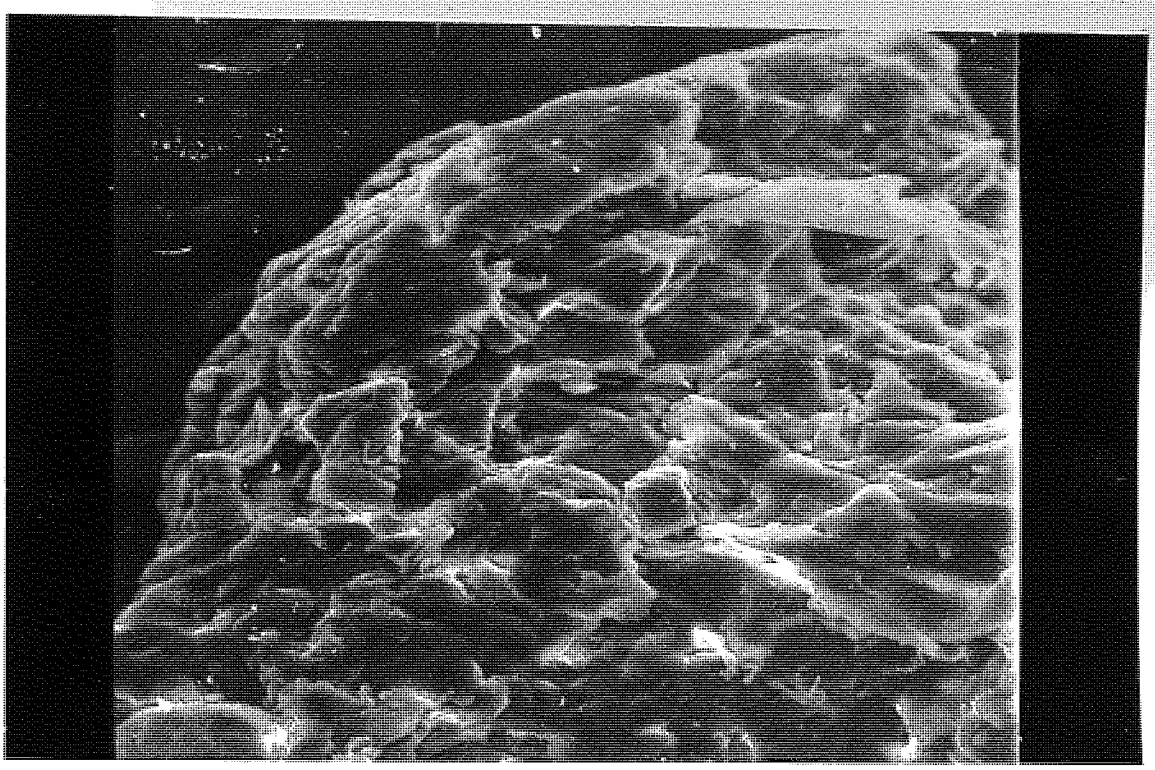

old Elcema x 500

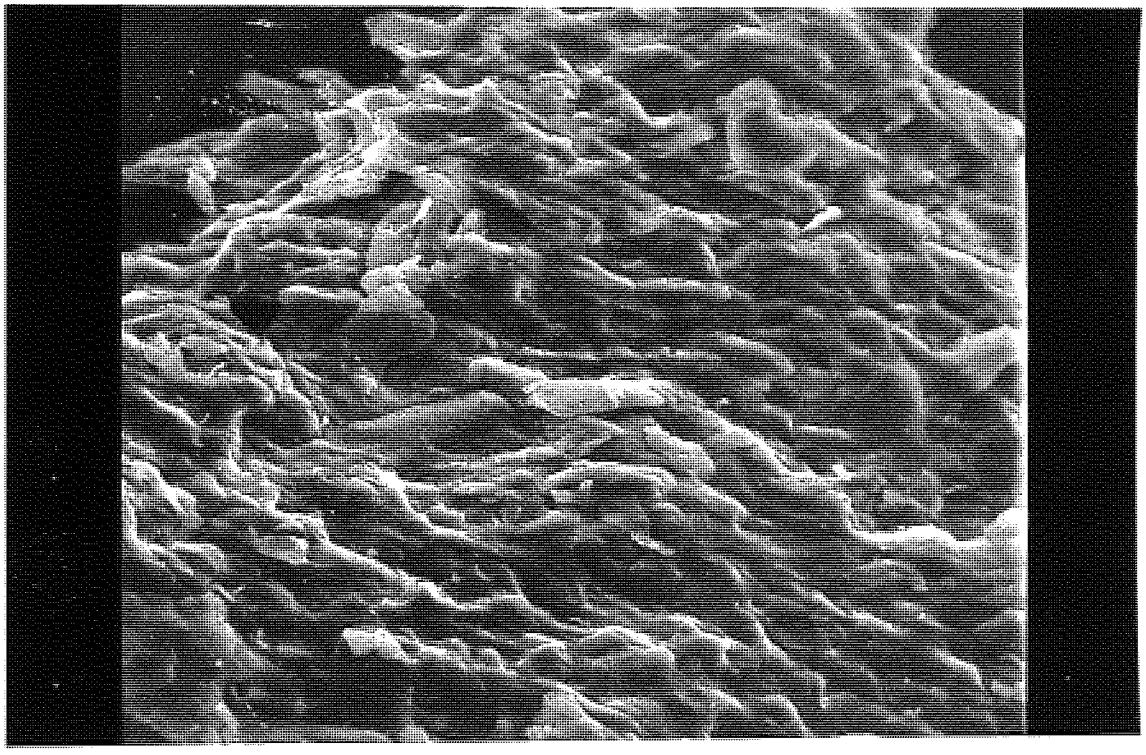

new Elcema x 500

Fig. 6.6 Scanning electron photomicrographs of two batches of Elcema at a magnification of 500

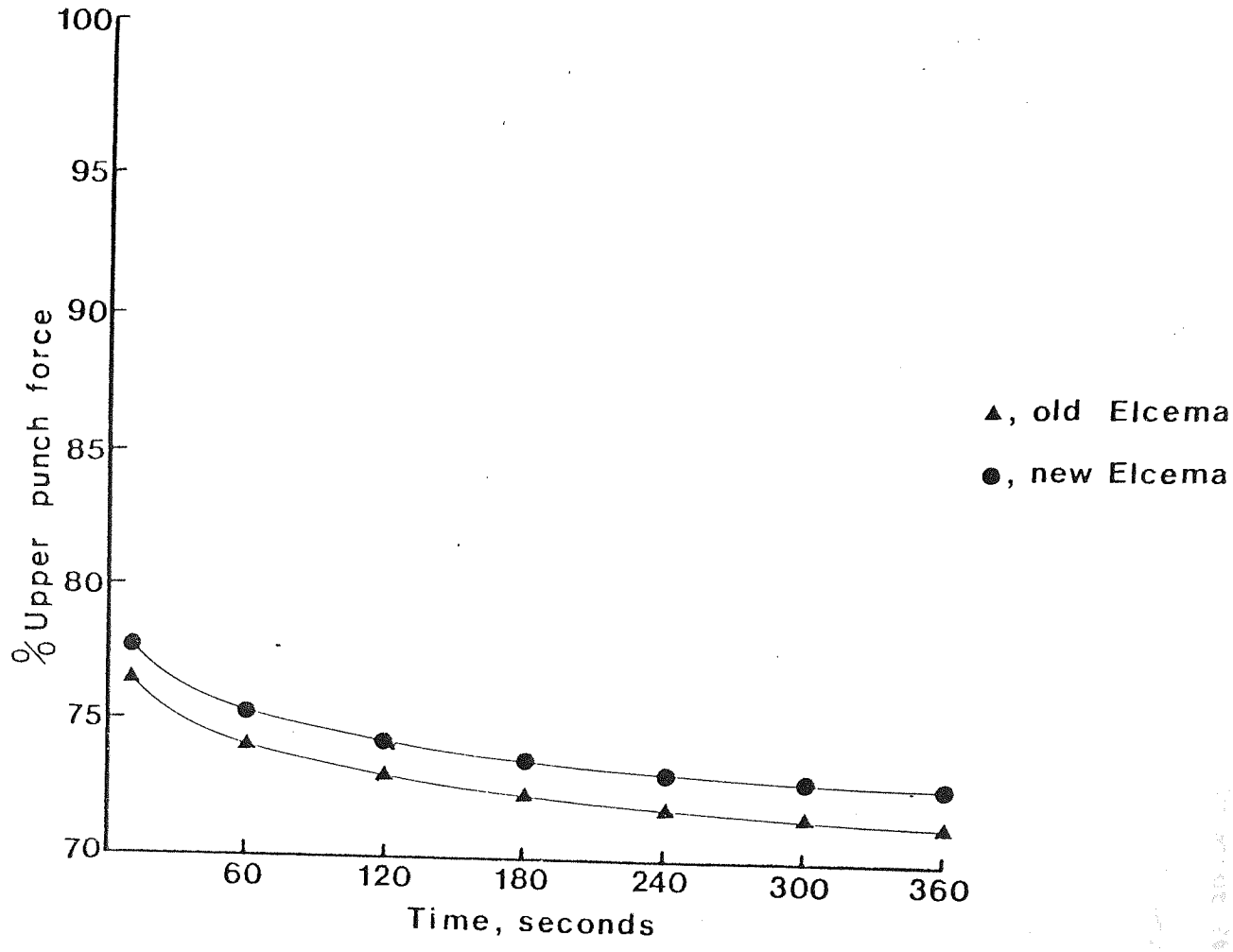

Fig. 6.7 Decay of the upper punch force with time at constant upper punch displacement for two batches of Elcema after compaction to about 20 kN

that a greater proportion of the total deformation of new Elcema is elastic. The difference in upper punch force, at any time between 10 and 360 seconds is only about 2% of the peak force and it is doubtful if the small difference in plastic flow, indicated by the small difference in relaxation, could cause such a large difference in the tensile strength of the tablets. However, as discussed in section 4.4., the stress relaxation occurring during the first 0.1 seconds after the application of maximum force will be more indicative of the behaviour of materials during tablet compaction. The decrease in force on the upper punch during the initial 0.5 seconds after the application of maximum force is shown for both batches of Elcema in Fig. 6.8. The difference in stress relaxation of the two batches is greater during this shorter time than during the longer times shown in Fig. 6.7., the initial rate of relaxation of new Elcema being much slower than that of old Elcema. This suggests that plastic flow of new Elcema is slower than old Elcema. Thus, during the compaction event, less plastic flow of new Elcema will occur than of old Elcema, resulting in less inter-particulate bonding and weaker tablets.

6.3.2 NRD measurements

To investigate the strain rate sensitivity of new Elcema, and to determine the amount of plastic deformation occurring before failure during a diametral compression test, the NRD and total deformation were measured for tablets of new Elcema as described in section 2.3.4., when the tablets were loaded to 75% of their breaking force. The data from these experiments are shown in Table 6.2.

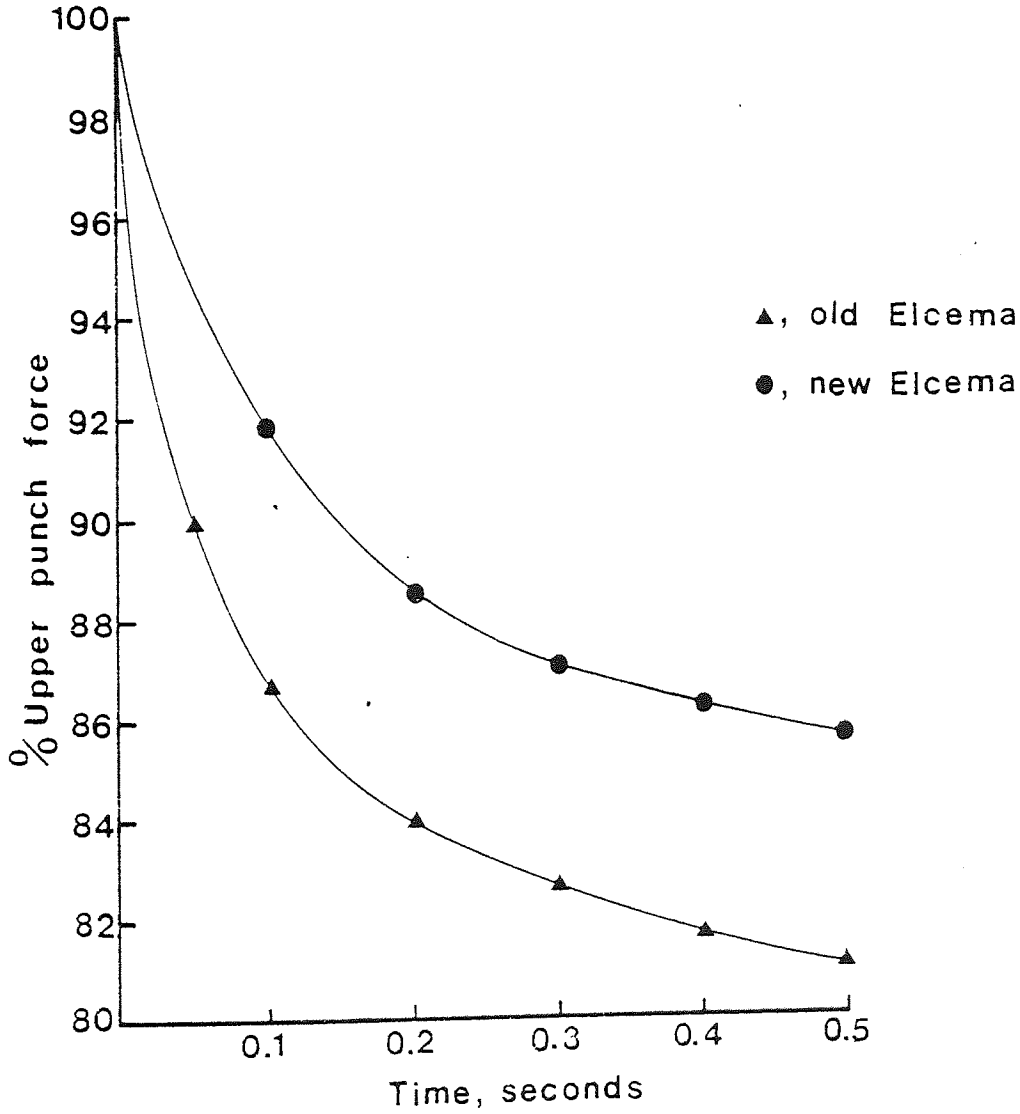

Fig. 6.8 Decay of the upper punch force within the first 0.5 seconds after maximum force for two batches of Elcema after compaction to about 20 kN

Material	Rate of platten movement	Total deformation	Recoverable deformation	Non-recoverable deformation	% NRD	Total deformation divided by applied force	Non-recoverable deformation divided by applied force	Applied force
	mm min^{-1}	mm	mm	mm		mm kN^{-1}	mm kN^{-1}	kN
new Elcema	0.052	0.101	0.077	0.024	23.99	1.703	0.409	0.059
"	0.26	0.093	0.076	0.017	18.43	1.565	0.289	0.059
"	1.3	0.088	0.076	0.013	14.20	1.490	0.212	0.059
"	6.5	0.086	0.077	0.011	11.99	1.478	0.177	0.059
old Elcema	0.052	0.144	0.109	0.035	24.31	2.510	0.605	0.058
"	0.26	0.140	0.108	0.033	23.57	2.384	0.545	0.059
"	1.3	0.141	0.113	0.027	19.15	2.285	0.444	0.062
"	6.5	0.121	0.101	0.020	16.53	2.085	0.345	0.052

Table 6.2. Deformation data obtained by diametral compression of tablets prepared from two batches of Elcema loaded to 75% of their breaking load. Each value is the mean of five replicates.

The effect of rate of platten movement on the total deformation per unit force is shown in Fig. 6.9. The total deformation of new Elcema tablets is less than that of old Elcema tablets as expected on the basis of their load-displacement curves shown in Fig. 6.4. The relationship between absolute NRD and rate of platten movement for new Elcema and old Elcema tablets, shown in Fig. 6.10, shows a larger negative gradient for new Elcema indicating that the deformation of new Elcema tablets is more dependent on strain rate than that of old Elcema tablets.

The effect of the rate of platten movement on the NRD expressed as a percentage of the total deformation (% NRD) is shown in Fig. 6.11. At any given rate of platten movement studied, above 0.052 mm min^{-1}, the %NRD of new Elcema is lower than the % NRD of old Elcema indicating that the percentage of the total deformation which is elastic and recoverable is higher for new Elcema than for old Elcema. As discussed in section 5.1., the gradients of both the relationship between % NRD and rate of platten movement and between NRD and rate of platten movement are a measure of the sensitivity of tablet deformation to strain rate. However, since the total deformation of the tablets of new and old Elcema is different under identical loading conditions, it is better to compare their strain rate sensitivity by considering the relationship between % NRD and rate of platten movement, shown in Fig. 6.11. The gradients for new and old Elcema are -0.145 and -0.082 respectively, indicating that the deformation of new Elcema is more sensitive to strain rate than that of old Elcema.

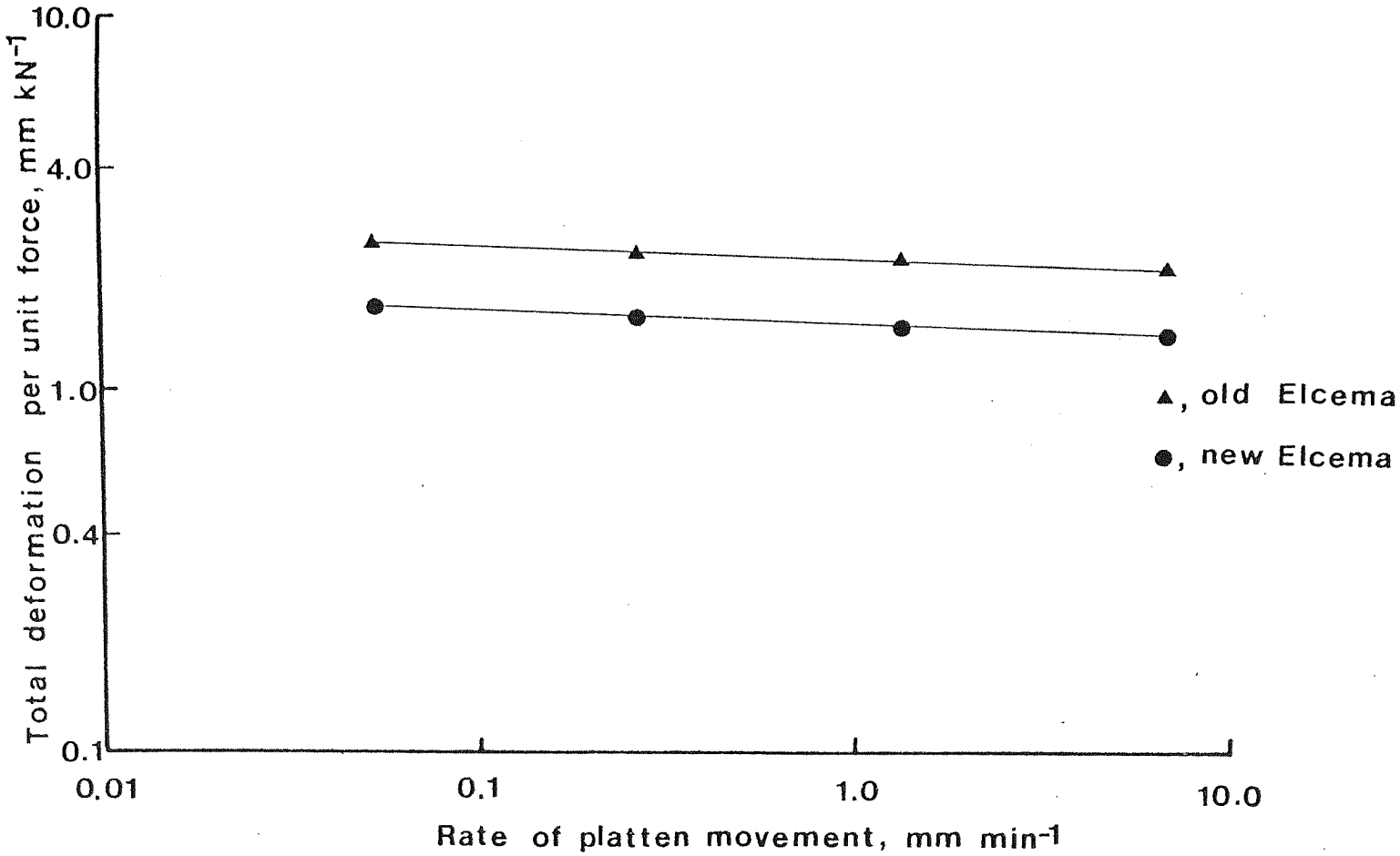

Fig. 6.9 The effect of rate of platten movement on the total deformation per unit force of tablets of two batches of Elcema loaded to 75% of their breaking load in a diametral compression test

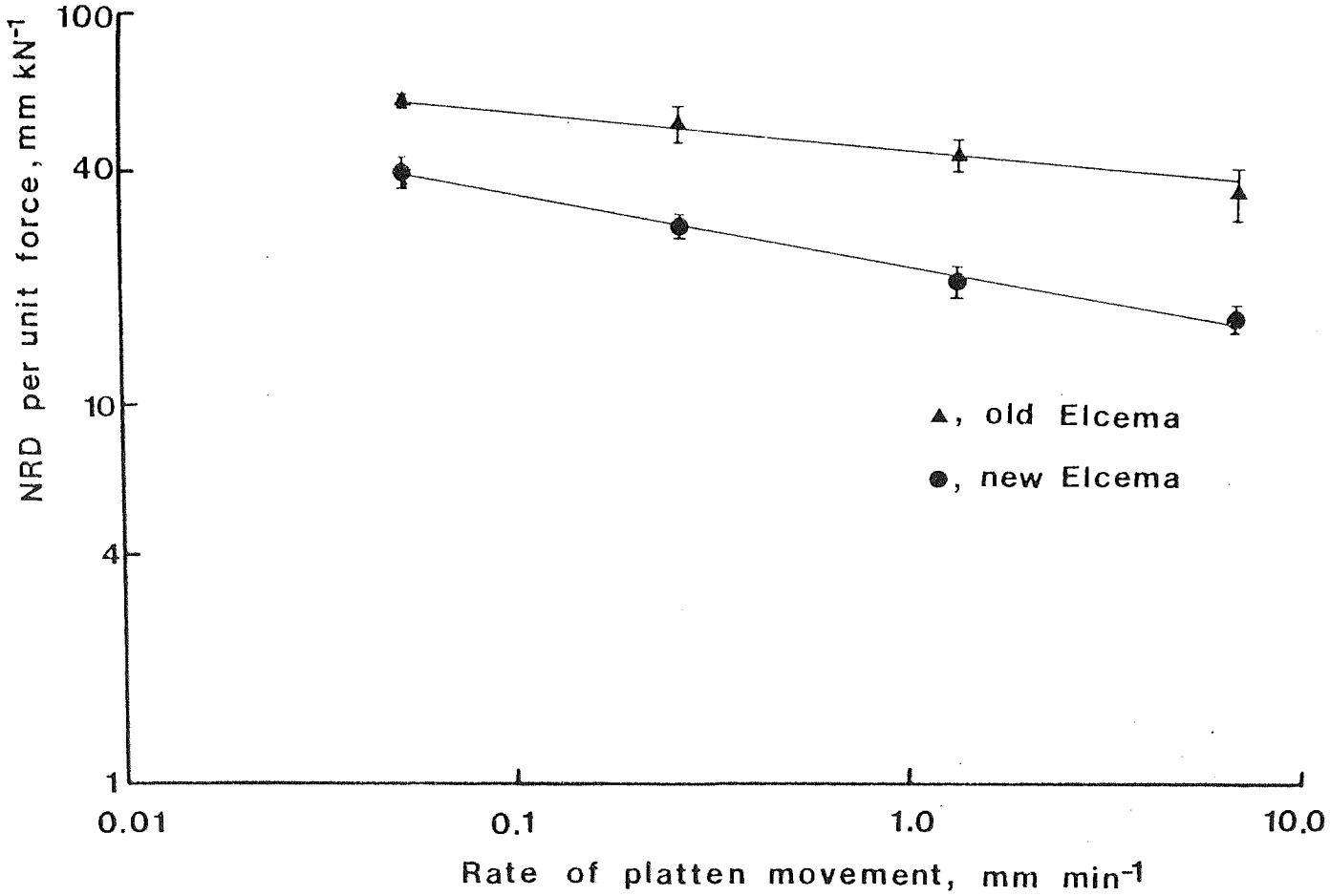

Fig. 6.10 The effect of rate of platten movement on the NRD per unit force of two batches of Elcema tablets loaded to 75% of their breaking load in a diametral compression test

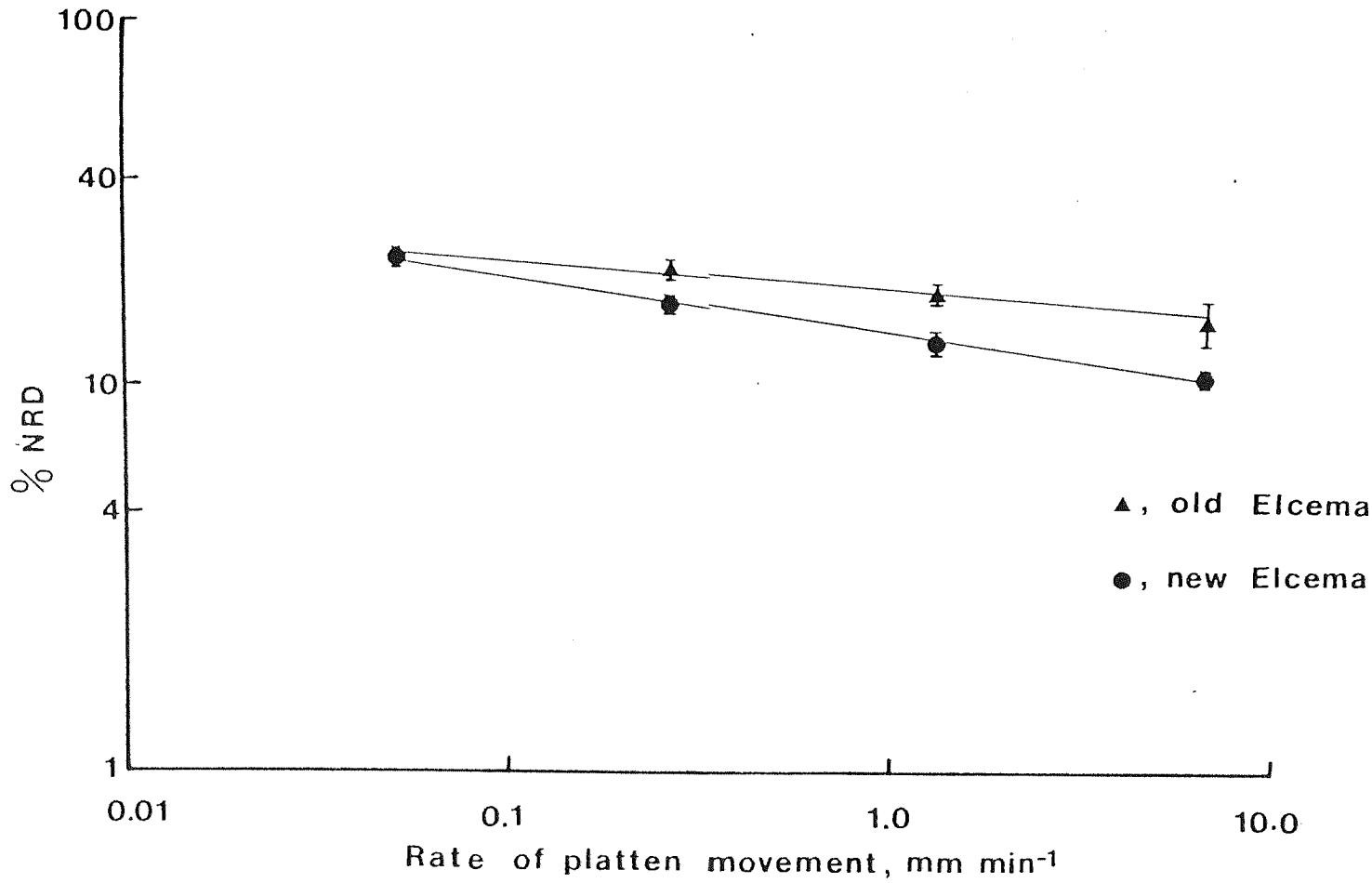

Fig. 6.11 The effect of rate of platten movement on the %NRD of tablets of two batches of Elcema loaded to 75% of their breaking force in a diametral compression test

6.4 Comparison of the Two Batches of Elcema

As the strain rate employed during diametral compression testing increases, the proportion of elastic deformation exhibited by both new and old Elcema tablets increases. This is shown by the lower values of non-recoverable deformation expressed as a percentage of the total deformation shown in Table 6.2. However, since the plastic deformation of new Elcema tablets is more sensitive to strain rate than that of old Elcema, one might expect that at the very high strain rates operating during compaction of the powders to form tablets, a much higher proportion of the total deformation of new Elcema will be elastic compared to that of old Elcema. Recovery of this elastic deformation during decompression and on ejection will cause bond rupture. This bond rupture, combined with the reduced plastic flow during compaction which results in less extensive bonding, will lower the tensile strength of new Elcema tablets compared to that of old Elcema tablets.

During diametral compression testing the failure deformation of new Elcema tablets is less than that of old Elcema tablets due to the reduced plastic flow. Together with the reduced tensile strength of new Elcema tablets, the reduced failure deformation greatly reduces the work of failure of new Elcema tablets. Thus, new Elcema tablets have a lower resistance to mechanical damage than old Elcema tablets.

7. GENERAL DISCUSSION

The results presented in this thesis show how investigation of the deformation behaviour of materials and tablets can provide information regarding the compaction properties and mechanical stability of tablets. Some advantages of physico-mechanical characterisation of drugs and excipients during pre-formulation studies have been considered earlier by Rees (1973) and the influence of physico-mechanical properties on tablet design has been discussed by Jones (1976). Evaluation of such properties of materials as reported here may help the formulation scientist to select systematically the optimum excipient for a particular formulation.

7.1 Characterising the Mechanical Properties of Tablets - Possible Benefits

The results presented in section 3.4. show that neither breaking force nor tensile strength completely characterise the mechanical behaviour of tablets prepared from a given material. In particular, these properties provide no information about the deformation behaviour of the finished tablet. The mechanical behaviour of a tablet depends not only on the strength of the inter-particulate bonds, but also on the deformation characteristics of the bulk material and the stress-strain behaviour of the bonds. A better assessment of a tablet's ability to resist damage is given by the area under the diametral load-displacement curves shown in Fig. 3.4. This area, termed work of failure in this thesis, is related to the toughness of the tablet. Furthermore,

the results of the multiple diametral impact test show that the work of failure values correlate well with the resistance of a tablet to mechanical failure.

The presence of a plastically deforming material should prevent crack propagation through tablets of a brittle material by increasing the radius of curvature at the crack tip by plastic flow. Increasing the radius of curvature of a crack decreases the stress concentrating effect and as a result the Griffith criterion is not satisfied. Thus, despite possible crack initiation in such a tablet, crack propagation cannot occur. This effect would explain the results of Esezobo and Pilpel (1977) who showed that as little as 7% w/w of microcrystalline cellulose prevents the capping of oxytetracycline tablets. It is possible that incorporation of plastic materials into a formulation consisting of brittle materials could increase the toughness of tablets without increasing the tensile strength. This effect could be confirmed by examining the load-displacement curve of a tablet and quantified by evaluating work of failure.

During the industrial development stage of a compressed tablet, breaking force specifications are established on an empirical basis to ensure that a satisfactory tablet is formed during production. However, such specifications must be established for each individual formulation depending on the subsequent mechanical treatment which the tablet must withstand during processing, such as pan coating and packaging. By measuring displacement during diametral loading of tablets it appears that it may be possible to determine a limiting value for the work of failure for all tablets, irrespective of formulation, which would enable them to withstand a particular process. For example, tablets may require

a higher work of failure to resist damage in a coating pan than in a fluid bed coating apparatus. After establishing a work of failure specification for a particular coating technique, tablets which are to be coated by that technique could therefore be formulated to an already established specification for work of failure.

The values of work of failure presented in this thesis were measured using complex and costly equipment. However, it may be possible to simplify measurement by attaching a displacement measuring device, such as a dial gauge, to a commercially available strength measuring instrument such as the Schleuniger[1]. As a first approximation, the work of failure could be calculated by measuring the breaking strength and failure displacement and assuming a linear relationship between force and displacement. Despite the errors incurred by this assumption, the calculated values would approximate to work of failure and allow comparison of different formulations.

7.2 Deformation Behaviour of Materials and Tablets

An understanding of the deformation behaviour of materials is important in determining the compaction properties of powders and in predicting the characteristics of the compressed tablet. For example, work of failure values for tablets of a given tensile strength are influenced by the amount of deformation occurring before failure. One method of studying the deformation of tablets under load is to examine the load-displacement curves. Such curves provide useful information about the ability of a material, in the compressed state, to undergo plastic flow; a large failure

[1] Available from Manesty Machines Ltd., Liverpool

deformation is evidence for plastic flow, whereas a small failure deformation indicates a brittle material. It is the extensive deformation of plastic components which enables tablets of even relatively low tensile strength to accept the stresses and resultant strains during impact testing without total failure. Comparison of the load-displacement curves and the Heckel plots for each of the materials shows that by examining the deformation of a tablet during diametral loading it is often possible to infer details of the consolidation behaviour of the particulate material itself during compaction. For example, particulate materials such as Sta-Rx and Elcema, tablets of which show a large failure deformation, would be expected to consolidate mainly by plastic flow with little or no fragmentation. Conversely tablets of lactose or Emcompress having the same breaking load as Elcema tablets and showing a relatively small failure deformation would be expected to consolidate mainly by fragmentation. However, care must be taken when predicting the compaction behaviour of a material from load-displacement curves. For example, such curves indicate that tablets of sodium chloride are brittle; one would therefore expect sodium chloride crystals to fragment during powder compaction. However, it has been shown conclusively both by Hardman and Lilley (1973) and by Hersey, Cole and Rees (1973) that sodium chloride consolidates mainly by plastic flow. This apparent contradiction has been attributed in section 3.3, to the effect of work hardening which leads to the formation of extensive brittle regions within the compressed tablet. Consequently tablets of sodium chloride have a low resistance to damage, as shown by multiple impact testing, despite their relatively high tensile strength which results from

plastic flow during powder compression. The low resistance to impact loading is characteristic of a brittle material which cannot accommodate the imposed stresses by plastic flow.

Another problem associated with the prediction of consolidation behaviour from load-displacement measurement arises from the relatively low strain rates used during this test. At low strain rates certain materials such as Sta-Rx show a large amount of plastic deformation but, if the deformation is highly strain rate dependent, at the high strain rates encountered during powder compaction, a greater proportion of the total deformation will be elastic. It is probable that little fragmentation of Sta-Rx occurs during compaction to relieve the stress associated with this elastic deformation. As a result, during decompression and on ejection, the elastic strain recovers causing bond rupture and therefore weakening the tablet. A further reduction in the strength of the tablet may occur after ejection due to time dependent elastic, or so-called anelastic, recovery shown by the results in Table 5.3. However, this longer-term, anelastic effect is probably less important than the rapid elastic recovery during decompression since anelastic recovery is much slower than elastic recovery and so time is available for plastic flow of the material to accommodate the anelastic strain recovery.

7.3 Strain Rate Sensitivity of Material Deformation

7.3.1 Quantifying plastic flow

The amount of plastic flow which occurs during compaction is important since it has a marked influence on the amount of

bonding which occurs within the tablet during consolidation. Plastic flow is usually examined using stress relaxation techniques. Although, for the reasons discussed in section 4.4, stress relaxation measurements are of limited value, they can provide an indication of the deformation behaviour of materials during compaction. A large total relaxation indicates plastic flow whereas a small amount of relaxation is usually characteristic of a brittle material. However, in the context of powder compaction, the total relaxation is less important than the initial rate at which relaxation occurs since total relaxation may take several hours and yet, when using a reciprocating tablet machine, the compression cycle is complete within about 0.2 seconds.

An attempt to fit stress relaxation data to the Maxwell visco-elastic flow model failed since the relaxation time constant of the material was continually changing during the first 30 seconds after the time of maximum applied force. The use of this model is therefore of doubtful value since the period of time most relevant to tablet compression is of the order of 0.2 seconds after maximum force. The method of analysing stress relaxation data used by Hiestand, Wells and others (1977), whereby the decrease in upper punch force is plotted against the logarithm of time (Fig. 4.3), provides a simple means of comparing the short and long term relaxation of materials. However, since the physical significance of changes in slope of these graphs is unknown, they provide little additional information about the consolidation behaviour of the material. All the materials show at least one change in slope, Elcema and lactose showing a continually changing slope during the time period studied. Comparison of the short and long term relaxation of powders shows that the initial rate

of plastic flow is extremely important in relation to the consolidation of materials. If the initial rate of relaxation is slow and the total amount of relaxation is relatively large, this suggests that the deformation of the material is strain rate dependent.

7.3.2 Quantifying strain rate sensitivity

As discussed in section 5, the strain rate sensitivity of a material can be determined by measuring the non-recoverable deformation (NRD) of tablets at several rates of platten movement in a diametral compression test. The gradient of the linear relationship between the logarithm of the NRD and the logarithm of platten rate (Fig. 5.3) is a characteristic value for a given material which indicates its strain rate sensitivity. The larger negative gradient of -0.191 for Sta-Rx, compared to the value of -0.090 for Elcema, indicates that the strain rate affects the deformation of Sta-Rx tablets more than the deformation of Elcema tablets.

The effect of increasing tablet strength on the relationship between absolute NRD and rate of platten movement is shown in Fig. 5.5 for Elcema tablets tested at equal diametral loads. At each rate of platten movement, as the load ratio decreases there is less plastic flow measured as NRD. There is also a tendency for the negative gradient to increase with a decrease in load ratio which suggests that the deformation of stronger tablets is more time dependent than that of weaker tablets. This may be due to the larger area of bonding in the higher strength tablets. For a given diametral load, the larger the area of bonding, the lower the stress per unit area

of bond. Thus a greater proportion of the deformation will be elastic and since the rate of plastic flow is proportional to the stress, the rate of plastic flow will decrease.

7.4 Effect of Strain Rate Sensitivity on Consolidation Behaviour

The strain rate sensitivity of a material will affect its compaction behaviour; for example the relatively high strain rate sensitivity of Sta-Rx explains why low strength tablets are formed from this material even though it is capable of extensive plastic flow. The large total stress relaxation following compaction of Sta-Rx shows that this material can deform plastically but, owing to its high strain rate sensitivity, during the high strain rate compaction event there is a considerable reduction in the proportion of the total deformation which is plastic and therefore non-recoverable. This fact, together with the elastic strain recovery after compaction which will rupture bonds results in a decrease in the strength of the tablets.

7.4.1 The effect of dwell time

Decreasing the rate of application of force during compaction prolongs the time available for plastic flow. For highly strain rate sensitive materials, decreasing the rate of compaction should have a considerable effect on the consolidation behaviour of powders and on the strength of the tablets produced. Hersey and Rees (1971) suggested that it is possible to differentiate between consolidation by plastic flow or by fragmentation using the Heckel equation to compare results for different particle size fractions

of a material. However, as discussed in section 1.4, there are many difficulties associated with the interpretation of these Heckel plots. For example Hersey, Cole and Rees (1973) found that potassium chloride consolidates by plastic flow. However, at high applied pressures their results for a large particle size fraction of potassium chloride exhibit a significant deviation from linearity, showing a curve of increasing gradient above 40 MN m^{-2}. They attributed this to work hardening causing embrittlement of the contact areas within the compact and presumably leading to further consolidation of particles by brittle fracture. This explanation may be incorrect since one might expect deformation to become increasingly more difficult in the presence of work hardening which would tend to increase the yield pressure of the material. The yield pressure is related to the reciprocal of the gradient of the Heckel plot. Thus any deviation from linearity due to work hardening would be expected to reduce the gradient of the Heckel plot.

The effect of strain rate on plastic flow is clearly shown by the effect of dwell time on the Heckel plots in Fig. 4.7. Of the materials studied, Sta-Rx shows the highest strain rate sensitivity as determined by measurement of NRD and also shows the greatest increase in consolidation due to increased dwell time. There is a smaller increase in the consolidation of Elcema with increasing dwell time, but the least effect is shown by the brittle materials lactose and Emcompress. This confirms that the consolidation of the two brittle materials, which occurs by fragmentation, is not time dependent.

This experimental technique of increasing the dwell time might possibly be used to quantify the role of plastic flow in the compaction process for example, by measuring the area under the Heckel plots. For a plastic material, as the dwell time

increases, the area under the curve will also increase; by measuring the change in area as a function of dwell time it may be possible to quantify the amount of plastic flow occurring at any given compaction rate. This would be a valuable technique since it would facilitate the prediction of problems associated with rate of compression such as the effect of "scale-up" from single punch reciprocating to fast rotary tabletting machines and the transfer of a formulation from one type of rotary machine to another.

The preceeding discussion emphasises the importance of strain rate dependence, particularly with materials such as Sta-Rx. However, all materials so far examined by stress relaxation techniques have shown some evidence of plastic flow; their compaction behaviour would therefore be expected to be sensitive to strain rate or dwell time. Newton and Rowley (1972) found that changes in the dwell time on a reciprocating machine, due to differences in the depth of the powder bed, could be quantified by calculating the area under the force time profiles. Using this force time integral a common regression equation, relating the area to the tensile strength of tablets, could be fitted to four weight ranges of lactose. Previously Newton, Rowley and others (1971) had found it impossible to obtain a common regression equation relating compaction force to the tensile strength for all tablet weights. In the present study, the deformation of lactose tablets in a diametral loading test was found to be independent of strain rate. Several factors may account for these apparently conflicting observations. During the compaction of lactose powder, the force on each point contact will be relatively high causing plastic flow as well as fragmentation but, during diametral compression testing of finished tablets at lower applied loads, the force per

unit area of bond will be relatively small so that only very limited plastic flow occurs. In this latter case, the effect of strain rate on the non-recoverable deformation may be negligible and therefore not detectable, especially in view of the inter-tablet variation. As previously indicated by the effect of increasing dwell time on the Heckel plot, the consolidation of lactose powder at high compaction loads is only very slightly sensitive to strain rate. Thus Fig. 5.1 is correct in showing that loading rate has little effect on the non-recoverable deformation of lactose tablets. Both of these results confirm that the consolidation of lactose is mainly by fragmentation. It is probable that strain rate dependence would be seen if a wider range of platten rates were used and if the tablets were loaded to a higher percentage of their breaking force.

7.5 Effect of Strain Rate Sensitivity on Capping

Capping is a problem frequently encountered during the production of tablets, especially on high speed tablet machines. Hiestand, Wells and others (1977) explain capping by considering elastic recovery of the tablet in a radial direction during ejection from the die as proposed earlier, by Train (1956). The stresses created by the radial elastic recovery are concentrated by the small radius of curvature at the edge of the die cavity. In brittle materials these concentrated stresses cannot be relieved by plastic flow and a crack is initiated at the edge of the die. The Griffith criterion is satisfied and the crack propagates across the tablet causing capping. Neither capping nor lamination was seen in either of the brittle materials, lactose

or Emcompress, used in this study. Thus the amount of recoverable elastic deformation of these materials at applied compaction forces up to 25 kN was apparently insufficient to cause crack initiation and propagation during ejection. A possible explanation is as follows. The stress applied to individual particles during compaction presumably exceeded the elastic limit and caused fragmentation which relieved the elastic stresses. As consolidation proceeded, continuing fragmentation reduced the mean particle size of the powder. This would tend to raise the yield pressure of the material since, as the particle size decreases, the probability of a particle containing a stress concentrating crack decreases. As consolidation continued, fragmentation would therefore become more difficult, thus increasing the recoverable elastic deformation of the tablet. However, at applied forces up to 25 kN, elastic deformation of lactose or Emcompress was apparently insufficient to cause capping probably due to continued fragmentation up to this force and the production of strong bonds which resisted excessive elastic recovery.

This explanation of capping however does not consider the effect of time dependent plastic flow or strain rate sensitivity. In the present study tablets of lactose and Emcompress exhibited brittle failure during diametral loading. Lactose is known to fragment during compression as shown by Hersey, Cole and Rees (1973). Nevertheless, some stress relaxation during powder compaction was seen with both of these materials indicating a limited amount of plastic flow. Shlanta (1963), Cole, Rees and Hersey (1975), David and Augsburger (1977) and Hiestand, Wells and others (1977) have performed stress relaxation experiments on several pharmaceutical materials, all of which showed some

degree of relaxation due to plastic flow. It would therefore be expected that the strength and capping tendency of all these materials would be altered by varying the dwell time and rate of ejection. Certainly this effect has been seen by Newton, Cook and Hollebon (1977) for phenacetin, a material which does not easily form tablets by direct compression and which is frequently involved in capping problems. These authors state that by slow removal of the applied pressure and by slow ejection from the die tablets could be prepared over a limited pressure range. The rate of movement of the upper punch and the rate of ejection was 1 mm min^{-1}. Similarly, for a formulation containing phenacetin, microcrystalline cellulose and lactose, Hiestand, Wells and others (1977) have shown that reducing the strain rate by decreasing the tablet machine speed increased the maximum compaction force which could be applied before lamination was observed.

For a strain rate sensitive material such as Sta-Rx, the amount of elastic strain recovery will depend not only on the maximum force applied, but also on the total time of the compaction event. Since the phenomenon of capping is related to the amount of elastic strain recovery which occurs following the compaction event, the capping tendency of Sta-Rx will depend on both maximum force and compaction rate. As the compaction rate is reduced, the amount of plastic flow of Sta-Rx increases leading to increased bonding and reduced elastic strain. This concept is supported by the results of David and Augsburger (1977) for the increased strength of Sta-Rx tablets with increasing dwell time, and also by the effect of dwell time on the compaction behaviour of Sta-Rx discussed in section 4.2.

In addition to the radial elastic strain recovery of materials there is also an axial elastic strain recovery which can lead to a reduction in tablet strength before actual capping or lamination is observed. Working on the formulation of a new compound, deBlaey, Weekers-Anderson and Polderman (1971) used a formulation consisting of between 49 and 82% w/w of a lactose granulation, which itself contained 2% w/w amylopectin as a binding agent, 1% w/w magnesium stearate and between 17 and 50% w/w of drug. In all cases they found a maximum in the strength-compaction force profile and also an increase in the elastic deformation with increasing compaction force. However, contrary to expectation, there was no change of slope in the relationship between elastic deformation and compaction force at the force which produced the maximum strength tablet. Nevertheless it is probable that recovery of this elastic deformation was responsible for the reduction in strength of the tablets as the compaction force increased. As the percentage of the new compound in the formulation was increased, there was a decrease in the maximum elastic deformation that the tablets could withstand before a reduction in strength occurred. This presumably indicates that there was a limit to the amount of elastic recovery of the drug which could be accommodated by plastic flow of the polymeric binder in the granulation. In the work of deBlaey, Weekers-Anderson and Polderman (1971) the lactose granulation was probably more plastic than might be expected on the basis of the present results, due to the incorporation of a polymeric binding agent.

7.6 Pre-formulation and the Standardisation of Material Properties

Rees (1973) states, "An important factor which must be standardised if successful processing predictions are to be made is the physico-mechanical behaviour of the excipients. Unless the relevant physical properties of different excipients are defined as quality control standards, it is difficult to control adequately the processing behaviour of a dosage form". This type of problem was clearly demonstrated by the inter-batch variation in compression properties of Elcema G250 discussed in section 6. Both batches of Elcema conformed to the manufacturer's specifications, but the tablets produced at a given compaction force possessed widely differing strengths. In this case the specification for the excipient did not include any parameter which would standardise the time-dependence of its plastic flow characteristics. Examples of parameters which might be used to quantify this property include relaxation values during the first 0.5 seconds after maximum force or the strain rate sensitivity of the deformation of tablets. It may be necessary to include specifications for this type of property of a material to ensure reproducability of tablet properties when different successive batches of an excipient are used in production.

Several of the experimental techniques developed during the present work can provide useful information regarding the compressive behaviour of materials and may be useful in preformulation studies. For example, if it is shown that the deformation of tablets of a pure drug substance is not strain rate sensitive and that increasing compaction dwell time has little or no effect on the Heckel plot, then it may be assumed that the drug consolidates

mainly by fragmentation with little plastic flow. If the dose of this drug constitutes a high proportion of the intended total weight of a tablet and if the drug is formulated with a brittle diluent then a capping tendency may be anticipated. In this case it might be possible to minimise the possibility of capping by careful control of processing variables, such as compaction force and rate, within accurate limits. However, such rigid restrictions are highly undesirable, and often impractical, and therefore usually unacceptable to production personnel. A better approach would be to improve the formulation by the addition of a plastically deforming direct-compression agent or by granulation with a polymeric binder capable of plastic flow.

The investigations described in this thesis provide a basis for systematic selection of materials and formulations. Such systematic tablet design may reduce both the cost and time involved in the development of a new product.

8. CONCLUSIONS

Tensile strength does not completely characterise the physico-mechanical behaviour of tablets. A better method of characterisation is to measure the area under the diametral load-displacement curves which, in this thesis, is termed work of failure. Work of failure values are related to the resistance of tablets to damage, which depends on both the tensile strength and the deformation behaviour of the tablets. Tablets of the plastic materials Elcema and Sta-Rx possess a higher work of failure and greater resistance to damage than tablets of the brittle materials lactose and Emcompress due to their ability to deform plastically.

The ability of powders to deform plastically during compaction may be inferred from the deformation behaviour of tablets during diametral loading. However, factors such as work hardening of crystalline materials may lead to misleading inferences. For example, although sodium chloride is known to consolidate by plastic deformation, the deformation behaviour of tablets of sodium chloride is characteristic of a brittle material. This brittle behaviour is a result of work hardening of the material at the inter-particulate contact junctions and at the die wall due to the high strain during compaction.

Stress relaxation experiments show that plastic deformation of both powders and finished tablets is time dependent. Thus, for a particulate material which exhibits extensive plastic flow, the compaction behaviour and the physico-mechanical properties of a tablet compressed from it depend on both the dwell time and

the strain rate during compaction. Stress relaxation measurements provide useful information regarding the relative amount of plastic deformation in different materials. For example Elcema and Sta-Rx show a relatively large relaxation whereas lactose and Emcompress, which consolidate mainly by fragmentation, show relatively little relaxation. However, quantitative interpretation of the relaxation was not possible using a simple Maxwell model due to changes of the relaxation time constant within the first 30 seconds after the point of maximum force.

In diametral compression tests a linear relationship was observed between the logarithm of the non-recoverable deformation of a tablet and the logarithm of the rate of platten movement. The extent to which plastic deformation of a tablet of a given material is strain rate dependent may be quantified by calculating the gradient of this relationship. A large negative gradient, such as that seen for Sta-Rx indicates a high strain rate sensitivity and is characteristic of a material on which compaction dwell time has a considerable effect. Conversely a zero gradient indicates a low strain rate sensitivity which is characteristic of a material such as lactose or Emcompress which consolidates by fragmentation.

The large differences in tensile strength and work of failure of tablets prepared from two batches of Elcema is attributed to differences in the physico-mechanical properties of the powders, in particular to their strain rate sensitivity. Specifications for the physico-mechanical properties of materials, such as tablet diluents, should be included as quality control parameters. In particular some property which describes the time dependency

of plastic deformation should be defined and standardised in order to minimise variability in tablet properties when different batches of excipients are used during the routine production of a compressed tablet formulation. For example the relative amount of stress relaxation at a given time after the maximum force or the gradient of the relationship between the non-recoverable deformation and the rate of platten movement during diametral compression testing may be used as such quality control parameters.

9. SUGGESTIONS FOR FURTHER WORK

The techniques described in this thesis have been used to examine the deformation and compaction behaviour of some direct compression excipients and the properties of tablets compressed from such materials. Listed below are some suggestions for further work based on the results discussed in this thesis.

9.1 The Effect of Dwell Time on Tablet Density

The strength of compressed lactose tablets has been shown by Newton and Rowley (1972) to depend on the dwell time during compaction. David and Augsburger (1977) have shown a similar effect for some other direct compression excipients, the effect being greater for plastic materials than brittle materials. This effect may be examined by using the Heckel equation to consider the effect of small increases in dwell time on the density of tablets prepared at a range of compaction forces. The increase in the area under the graph of log (1/1-D) plotted against compaction force, due to increasing dwell time, will be caused by increasing plastic flow. The relationship between the increase in area and the dwell time will indicate the role of plastic flow during compression.

9.2 The Effect of Particle Size

During this study the materials, with the exception of sodium chloride, were used as received from the suppliers and no attempt was made to standardise particle size. Hersey and Rees (1970) have shown that the particle size affects the compaction

behaviour of powders and other workers (Alpar, Hersey and Shotton, 1970 ; Fell and Newton, 1971a) found that particle size affects the strength of tablets. It would be expected that both the deformation behaviour of tablets during diametral compression and the work of failure values will be affected by the initial particle size of the powders due to variation in yield stress and tensile strength. Thus further information regarding the compaction of materials may be obtained if the effect of particle size on the load-displacement curves of tablets is examined.

9.3 The Compaction Behaviour of Multicomponent Systems

Although Fell and Newton (1970) have shown that it is possible to predict the strength of tablets consisting of mixtures of different types of lactose, Newton, Cook and Hollebon (1977) found that this was not possible for mixtures of lactose and phenacetin. They suggest that it is not possible to predict the strength of tablets prepared from mixtures if the components consolidate by different mechanisms. York and Pilpel (1977) also suggest that such predictions are not possible if the formulation contains several different components or if it has been wet granulated. The multiple impact test results discussed in section 3.5 show that the resistance of tablets to mechanical failure is not related to tensile strength but to their work of failure which is dependent on both their tensile strength and deformation behaviour. The resistance to failure of multi-component tablets will thus depend on inter-particulate bonding and the deformation behaviour of the individual materials. Thus the addition of a relatively small amount of a plastically deforming material should increase a tablet's resistance to failure without necessarily

increasing the tensile strength. On the basis of the work of Newton, Cook and Hollebon (1977) and York and Pilpel (1977), quantitative predictions of work of failure would not appear possible. However, it should be possible to qualitatively select a suitable mixture of excipients, to produce a formulation with the desired characteristics, by comparing the work of failure measurements of the separate components.

9.4 The Effect of Strain Recovery on the Tensile Strength of Tablets

Continued strain recovery occurs after ejection of the tablets from the die as shown by Baba and Nagafuji (1965), Aulton, Travers and White (1973) and by York and Baily (1977). This strain recovery may affect properties of the tablets such as tensile strength. Rees and Shotton (1970) showed that the crushing resistance of sodium chloride tablets increases by approximately 100% during the first hour after ejection. However, these authors reported no measurements of dimensional changes of the tablets. The other authors, mentioned previously in this section, monitored the time-dependent dimensional changes of tablets but made no measurements of tensile strength. The need to standardise a time between ejection and testing has been recognised by many workers who have measured tensile strength. For example, Higuchi, Rao and others (1953) state that tablets were prepared and tested on the same day and Shotton, Deer and Ganderton (1963) measured the crushing force of tablets 6 hours after ejection. In the present study the time between ejection and testing was 3 hours. On the basis of the preceeding discussion, it would appear useful to examine the effect of the time dependent strain recovery on the

tensile strength of tablets.

9.5 The Effect of Rate of Platten Movement on Work of Failure

Rees, Hersey and Cole (1970) have shown that the rate of platten movement employed during diametral compression testing can affect the measured values of breaking force. The effect of increasing rate of platten movement on the deformation of tablets is discussed in both section 3.4 and section 5. However, no measurements were made on the effect of rate on the work of failure. Determination of work of failure at high rates of platten movement may provide more information regarding the resistance of tablets to damage.

Appendix 1. The Computer Program for Calculating Breaking Force and Work of Failure.

A1.1 The Calculation of Co-ordinate Values of Force and Displacement.

Due to the large number of tablets tested and the time consuming nature of the calculations involved in determining the area under a curve, a Fortran computer program was written to perform calculations of breaking force and work of failure on each tablet. In order to fully explain the program it is necessary to describe, in detail, the recording system referred to in section 2.3.1.1.

The two analogue signals representing force and diametral displacement are sequentially scanned, digitised and recorded on punch paper tape. Each displacement reading is taken between two force readings, thus a corrective calculation is required to give a value of "force-equivalent displacement", - the displacement corresponding to a given value of force. The sequence of recording on the paper tape is:-

Force 1, Disp. 1, Force 2, Disp. 2,..... Force n, Disp. n.

Force 1 is ignored since this corresponds to the last reading taken before any force is applied to the tablet and is thus zero. The displacement which is equivalent to Force 2 is then calculated from equation A1, assuming a linear relationship between displacement and time during the short time period concerned.

$$(\text{Equivalent displacement})_{\text{Force 2}} = \text{Disp. 1} + 0.5(\text{Disp.2} - \text{Disp.1}) \quad \text{Eq. A1}$$

This calculation is repeated for all displacement values on the ascending slope of the force-displacement curve and results in a set of co-ordinate values for force and displacement.

A1.2 Correction of the Breaking Force and Failure Displacement Values.

Since the two signals are scanned sequentially on an alternating basis at finite time intervals of approximately 0.1 seconds, the time between successive force readings is approximately 0.2 seconds. It is therefore unlikely that the final recorded value of force is equal to the true breaking force which will be slightly higher than the recorded value. A calculation to correct the values of breaking force and failure displacement was devised based on the movement of the load cell platten during a test. As the force on the tablet increases, strain in the mechanical components of the test instrument will cause upward movement of the upper platten attached to the load cell. When failure occurs the stress on the upper platten rapidly decreases allowing strain recovery and causing the upper and lower plattens to move toward each other; this will be recorded as a large increase in the recorded displacement. In order to correct for the errors caused by the scanning procedure the following calculation was devised:-

Consider the sequence of readings:-

Force(n-2), Disp.(n-2), Force(n-1), Disp.(n-1), Force(n), Disp.(n).

<u>Condition A:</u>

If failure occurred between Force(n) and Disp.(n):-

(Disp.(n) - Disp.(n-1) > (Disp.(n-1) - Disp.(n-2)) and

Force(n) > Force(n-1)

Condition B:

If failure occurred between Disp.(n-1) and Force(n):-

(Disp.(n) - Disp.(n-1) > Disp.(n-1) - Disp.(n-2) and

Force(n) < Force(n-1).

If condition A was recognised by the computer then a pair of co-ordinate values of theoretical breaking Force(n*) and failure Disp.(n*) was calculated using equation A2 and A3.

Force(n*) = Force(n) + 0.25 (Force(n) - Force(n-1)) Eq. A2

Disp.(n*) = Disp.(n-1) + 0.75 (Disp.(n-1) - Disp.(n-2)) Eq. A3

If condition B was recognised by the computer, equations A4 and A5 were used to calculate a pair of co-ordinate values of theoretical breaking Force(n') and theoretical failure Disp.(n').

Force(n') = Force(n-1) + 0.75 (Force(n-1) - Force(n-2)) Eq. A4.

Disp.(n') = Disp.(n-1) + 0.25 (Disp.(n-1) - Disp.(n-2)) Eq. A5

Using the corrected values for breaking force and failure displacement, the maximum error in calculated work of failure due to errors caused by the scanning procedure is about 3% since a minimum of 30 force data points and the equivalent number of displacement data points were recorded for each force-displacement curve.

A1.3 Calculations Performed by the Program

The program was written to work with batches of ten tablets

and to calculate and print out the following information:-

a) Co-ordinate pairs of values of force and diametral displacement at each point on the force displacement curve for each tablet.

b) The breaking force in kg and kN of each tablet

c) The work of failure in joules (area under the force-displacement curves) of each tablet.

d) The mean, standard deviation and standard error of breaking force in kg and kN for each batch of ten tablets.

e) The mean, standard deviation and standard error of work of failure in joules for each batch of ten tablets.

A1.4 The Flow Chart and Fortran Program Used for the Calculations.

A1.4.1 The flow chart

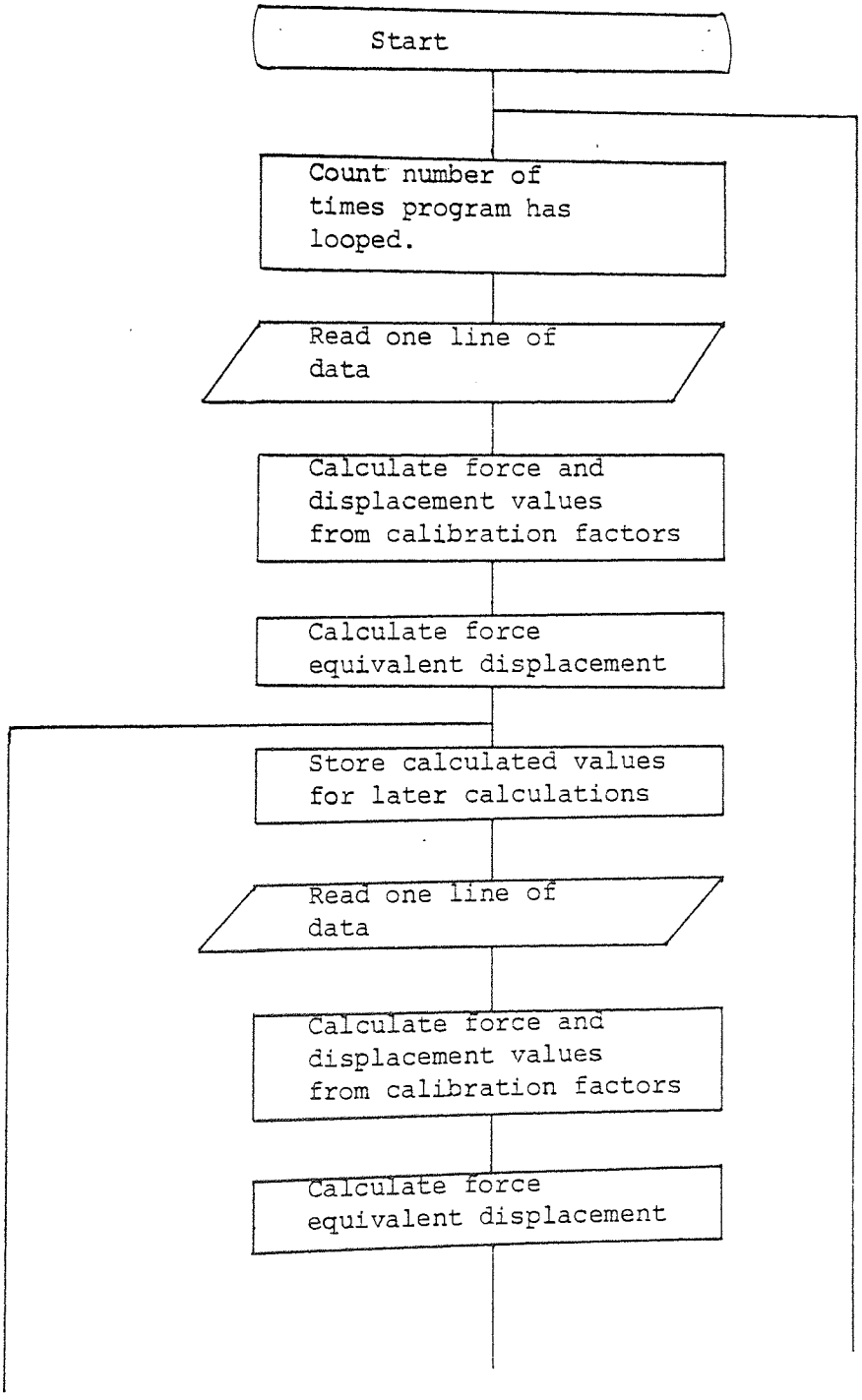

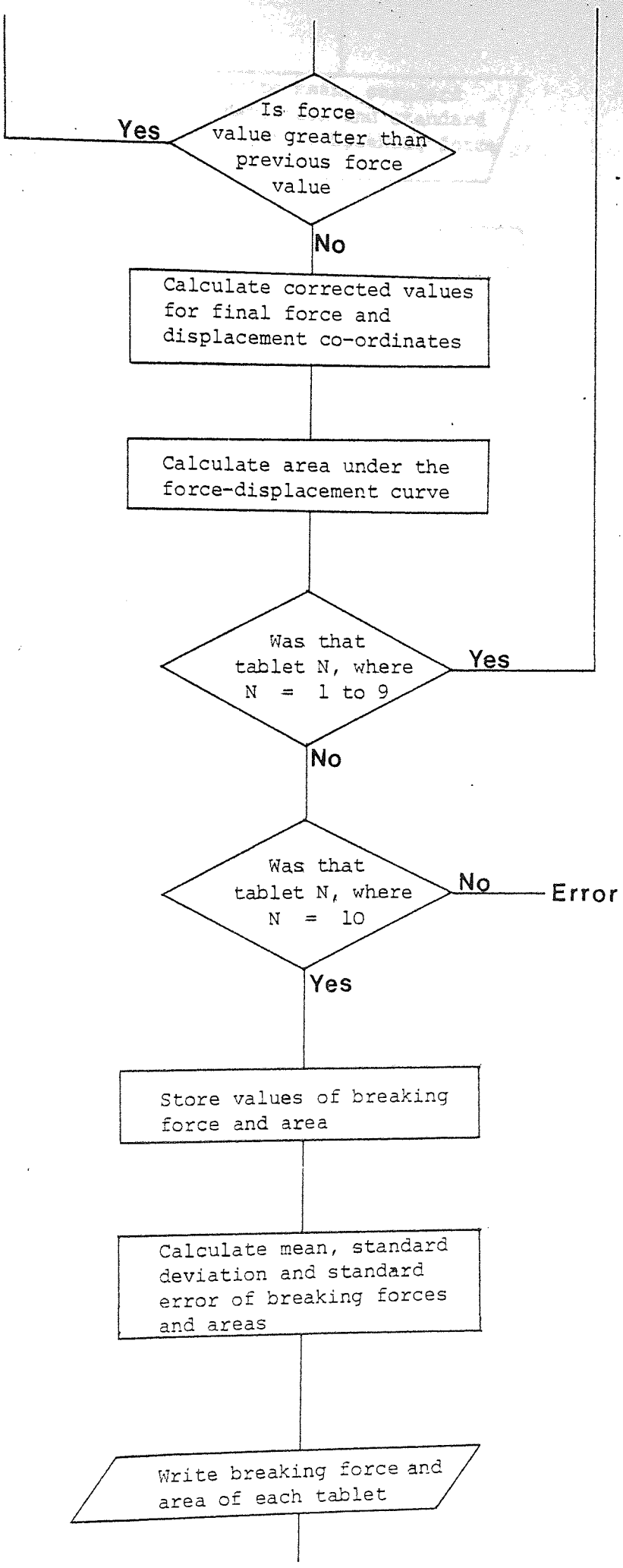
Is force value greater than previous force value
Yes
No
Calculate corrected values for final force and displacement co-ordinates
Calculate area under the force-displacement curve
Was that tablet N, where N = 1 to 9
Yes
No
Was that tablet N, where N = 10
No
Error
Yes
Store values of breaking force and area
Calculate mean, standard deviation and standard error of breaking forces and areas
Write breaking force and area of each tablet

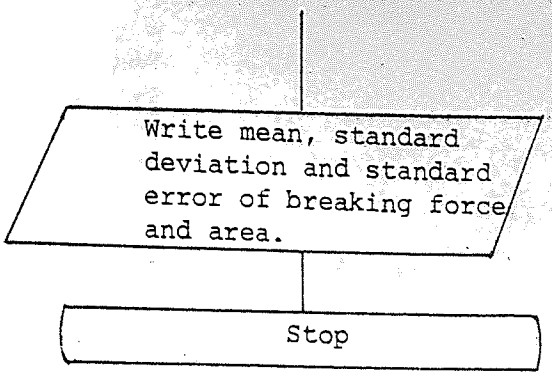
Write mean, standard deviation and standard error of breaking force and area.
Stop

A1.4.2 The Fortran computer program

```
 0          SHORTLIST (LP)
 1          PROGRAM (FXXX)
 2          INPUT  1 = CR0
 3          INPUT  3 = TR0
 4          INPUT  5 = LP0
 5          OUTPUT 2 = LP0
 6          OUTPUT 6 = LP1
 7          COMPRESS INTEGER AND LOGICAL
 8          EXTENDED DATA
 9          TRACE 0
10          END
11          MASTER
12          DIMENSION TIME(2),RESULT(2,1000)
13          REAL MEANA,MEANB,MEANC7N
14          DATA BLANK/4H    /
15          DO 1 J=1,2
16    1     TIME(J)=BLANK
17          READ(3,999)IGNORE
18    999   FORMAT(A4)
19          COUNT=0
20    998   READ(3,2)(TIME(J),J=1,2)
21    2     FORMAT(2A4)
22          COUNT=COUNT+1
23          DO 3 I=1,1000
24          RESULT(1,I)=0.0
25    3     RESULT(2,I)=0.0
26    996   READ(3,4)CHANID1,FOR1,RANGE1,CHANID2,DIS1,RANGE2
27          IF(CHANID1.EQ.01)GOTO 995
28          GOTO997
29    995   READ(3,2)(TIME(J),J=1,2)
30          GOTO 996
31    997   READ(3,2)(TIME(J),J=1,2)
32          READ(3,4)CHANID3,FOR2,RANGE3,CHANID4,DIS2,RANGE4
33    4     FORMAT(6F0.0)
34          IF(RANGE1.EQ.6)GOTO 5
35          IF(RANGE1.EQ.5)GOTO 6
36          IF(RANGE1.EQ.4)GOTO 7
37    5     FOR1=FOR1/1000.0
38          GOTO 8
39    6     FOR1=FOR1/100.0
40          GOTO 8
41    7     FOR1=FOR1/10.0
42    8     IF(RANGE2.EQ.6)GOTO 9
43          IF(RANGE2.EQ.5)GOTO 10
44          IF(RANGE2.EQ.4)GOTO 11
45          IF(RANGE2.EQ.3)GOTO 12
46    9     DIS1=DIS1/1000.0
47          GOTO 12
48    10    DIS1=DIS1/100.0
49          GOTO 12
50    11    DIS1=DIS1/10.0
51    12    IF(RANGE3.EQ.6)GOTO 13
52          IF(RANGE3.EQ.5)GOTO 14
53          IF(RANGE3.EQ.4)GOTO 15
54    13    FOR2=FOR2/1000.0
55          GOTO 16
56    14    FOR2=FOR2/100.0
57          GOTO 16
58    15    FOR2=FOR2/10.0
59    16    IF(RANGE4.EQ.6)GOTO 17
60          IF(RANGE4.EQ.5)GOTO 18
61          IF(RANGE4.EQ.4)GOTO 19
```

```
      IF(RANGE4.EQ.3)GOTO 20
17    DIS2=DIS2/1000.0
      GOTO 20
18    DIS2=DIS2/100.0
      GOTO 20
19    DIS2=DIS2/10.0
20    F=0.0196
      D=-0.0005957
      FOR1C=FOR1*F
      FOR2C=FOR2*F
      DIS1C=DIS1*D
      DIS2C=DIS2*D
      D1=DIS1C+0.5*(DIS2C-DIS1C)
25    FORMAT('0',4X,'TIME',12X,'FORCE',12X,'DISP')
      DO 21 I=1,IC
      RESULT(1,I)=0
21    RESULT(2,I)=0
      IC=1
265   RESULT(1,IC)=FOR2C
      RESULT(2,IC)=D1
      DIS1C=DIS2C
      FOR1C=FOR2C
      READ(3,2)(TIME(J),J=1,2)
      READ(3,4)CHANID3,FOR2,RANGE3,CHANID4,DIS2,RANGE4
      IF(RANGE3.EQ.6)GOTO 27
      IF(RANGE3.EQ.5)GOTO 28
      IF(RANGE3.EQ.4)GOTO 29
27    FOR2=FOR2/1000.0
      GOTO 30
28    FOR2=FOR2/100.0
      GOTO 30
29    FOR2=FOR2/10.0
30    IF(RANGE4.EQ.6)GOTO 31
      IF(RANGE4.EQ.5)GOTO 32
      IF(RANGE4.EQ.4)GOTO 33
      IF(RANGE4.EQ.3)GOTO 34
31    DIS2=DIS2/1000.0
      GOTO 34
32    DIS2=DIS2/100.0
      GOTO 34
33    DIS2=DIS2/10.0
36    FOR2C=FOR2*F
      TEST=FOR2C+(0.25*FOR2C/100)
      IF(FOR1C.GT.TEST.AND.FOR1C.GT.0.00196)GOTO 70
      IC=IC+1
      DIS2C=DIS2+D
      D1=DIS1C+0.5*(DIS2C-DIS1C)
      GOTO 265
70    AREA=0.0
      CHEK1=(RESULT(2,IC))-(RESULT(2,IC-1))
      CHEK2=((RESULT(2,IC-1))-(RESULT(2,IC-2)))*2
      IF(CHEK1.GT.CHEK2)GOTO 2920
      GOTO 2910
2920  RESULT(2,IC)=RESULT(2,IC-1)+((RESULT(2,IC-1))-
      (RESULT(2,IC-2)))
      RESULT(1,IC+1)=RESULT(1,IC)+0.25*((RESULT(1,IC))-
      (RESULT(1,IC-1)))
```

```
117          RESULT(2,IC+1)=RESULT(2,IC)+0.75*((RESULT(2,IC))-
118          GOTO 2930
             (RESULT(2,IC-1)))
119    2910  RESULT(1,IC+1)=RESULT(1,IC)+0.75*((RESULT(1,IC))-
             (RESULT(1,IC-1)))
120          RESULT(2,IC+1)=RESULT(2,IC)+0.25*((RESULT(2,IC))-
             (RESULT(2,IC-1)))
121          IC=IC+1
122    2930  DO 120 I=1,IC-1
123          AREAB=((RESULT(2,I+1))-(RESULT(2,I)))*0.5*
124         1((RESULT(1,I+1))+(RESULT(1,I)))
125    120   AREA=AREA+AREAB
126          WRITE(6,25)
127          WRITE(6,26)(TIME(J),J=1,2),(RESULT(1,1)),(RESULT(2,1))
128    26    FORMAT('0',2A4,5X,E13.6,5X,E13.6)
129          DO 2950 I=2,IC,2
130          WRITE(6,2960)(TIME(J),J=1,2),(RESULT(1,I)),(RESULT(2,I)),
131         1(RESULT(1,I+1)),(RESULT(2,I+1))
132    2960  FORMAT(' ',2A4,5X,E13.6,5X,E13.6,15X,E13.6,5X,E13.6)
133    2950  CONTINUE
134          WRITE(6,130)
135    130   FORMAT(' ',6X,'AREA=')
136          WRITE(6,160)AREA
137    160   FORMAT('+',13X,E13.6)
138          WRITE(6,151)
139    151   FORMAT('0',8X,'FORCE(KN)',9X,'FORCE(KG)')
140          DO 160 I=1,IC
141          BKFOR=(RESULT(1,I))*101.972
142          WRITE(6,155)(RESULT(1,I)),BKFOR
143    155   FORMAT(' ',5X,E13.6,5X,E13.6)
144    160   CONTINUE
145          IF(COUNT.EQ.1)GOTO 210
146          GOTO 220
147    210   BKFORN1=(RESULT(1,IC))
148          BKFOR1=BKFOR
149          AREA1=AREA
150          GOTO 165
151    220   IF(COUNT.EQ.2)GOTO 230
152          GOTO 240
153    230   BKFORN2=(RESULT(1,IC))
154          BKFOR2=BKFOR
155          AREA2=AREA
156          GOTO 165
157    240   IF(COUNT.EQ.3)GOTO 250
158          GOTO 260
159    250   BKFORN3=(RESULT(1,IC))
160          BKFOR3=BKFOR
161          AREA3=AREA
162          GOTO 165
163    260   IF(COUNT.EQ.4)GOTO 270
164          GOTO 280
165    270   BKFORN4=(RESULT(1,IC))
166          BKFOR4=BKFOR
167          AREA4=AREA
168          GOTO 165
169    280   IF(COUNT.EQ.5)GOTO 290
170          GOTO 2900
171    290   BKFORN5=(RESULT(1,IC))
172          BKFOR5=BKFOR
173          AREA5=AREA
```

```
      GOTO 165
2900  IF(COUNT.EQ.6)GOTO 2901
      GOTO 2902
2901  BKFORN6=(RESULT(1,IC))
      BKFOR6=BKFOR
      AREA6=AREA
      GOTO 165
2902  IF(COUNT.EQ.7)GOTO 2903
      GOTO 2904
2903  BKFORN7=(RESULT(1,IC))
      BKFOR7=BKFOR
      AREA7=AREA
      GOTO 165
2904  IF(COUNT.EQ.8)GOTO 2905
      GOTO 2906
2905  BKFORN8=(RESULT(1,IC))
      BKFOR8=BKFOR
      AREA8=AREA
      GOTO 165
2906  IF(COUNT.EQ.9)GOTO 2907
      GOTO 2908
2907  BKFORN9=(RESULT(1,IC))
      BKFOR9=BKFOR
      AREA9=AREA
      GOTO 165
2908  IF(COUNT.EQ.10)GOTO 2909
      GOTO 295
2909  BKFORN10=(RESULT(1,IC))
      BKFOR10=BKFOR
      AREA10=AREA
      GOTO 300
295   WRITE(6,296)
165   READ(3,170)(TIME(J),J=1,2)
170   FORMAT(2A4)
      READ(3,180)CHANID3,FOR,RANGE3
      IF(CHANID3.EQ.01)GOTO 185
      IF(RANGE3.EQ.6)GOTO 171
      IF(RANGE3.EQ.5)GOTO 172
171   FOR=FOR/1000.0
      GOTO 175
172   FOR=FOR/100.0
175   FOR=FOR*F
      IF(FOR.LT.FOR2.AND.FOR.GT.0.0006)GOTO 165
      IF(FOR.LT.FOR2.AND.FOR.LT.0.0006)GOTO 998
180   FORMAT(3F0.0)
185   READ(3,190)(TIME(J),J=1,2)
190   FORMAT(2A4)
      READ(3,200)CHANID3,FOR,RANGE3
200   FORMAT(3F0.0)
      IF(RANGE3.EQ.6)GOTO 171
      IF(RANGE3.EQ.5)GOTO 172

300   SUMA=BKFORN1+BKFORN2+BKFORN3+BKFORN4+BKFORN5
     1+BKFORN6+BKFORN7+BKFORN8+BKFORN9+BKFORN10
      SUMB=BKFOR1+BKFOR2+BKFOR3+BKFOR4+BKFOR5
     2+BKFOR6+BKFOR7+BKFOR8+BKFOR9+BKFOR10
      SUMC=AREA1+AREA2+AREA3+AREA4+AREA5
     3+AREA6+AREA7+AREA8+AREA9+AREA10
      MEANA=SUMA/10
      MEANB=SUMB/10
      MEANC=SUMC/10
```

```
C        USOS=UNCORRECTED SIM OF SQUARES
       USOSA=BKFORN1**2+BKFORN2**2+BKFORN3**2+
       BKFORN4**2+BKFORN5**2
      4+BKFORN6**2+BKFORN7**2+BKFORN8**2+BKFORN9**2+BKFORN10**2
       USOSB=BKFOR1**2+BKFOR2**2+BKFOR3**2+BKFOR4**2+BKFOR5**2
      1+BKFOR6**2+BKFOR7**2+BKFOR8**2+BKFOR9**2+BKFOR10**2
       USOSC=AREA1**2+AREA2**2+AREA3**2+AREA4**2+AREA5**2
      2+AREA6**2+AREA7**2+AREA8**2+AREA9**2+AREA10**2
C        CT =CORRECTION TERM
       CTA=(SUMA**2)/10
       CTB=(SUMB**2)/10
       CTC=(SUMC**2)/10
C        CSOS=CORRECTED SUM OF SQUARES
       CSOSA=USOSA-CTA
       CSOSB=USOSB-CTB
       CSOSC=USOSC-CTC
       VARIANCEA=CSOSA/9
       VARIANCEB=CSOSB/9
       VARIANCEC=CSOSC/9
       SDA=SQRT(VARIANCEA)
       SDB=SQRT(VARIANCEB)
       SDC=SQRT(VARIANCEC)
       T=2.26
       N=9
       SEA=(T*SDA)/SQRT(N)
       SEB=(T*SDB)/SQRT(N)
       SEC=(T*SDC)/SQRT(N)
       WRITE(6,400)
  400  FORMAT('0','STATISTICAL ANALYSIS, TABS 1 TO 10
       IN SAME ORDER')
         WRITE(6,410)
  410  FORMAT('0','WORK OF FRACTURE',10X,
       'BREAKING FORCE(KN)',10X,
      1'BREAKING FORCE(KG)')
       WRITE(6,420)AREA1,BKFORN1,BKFOR1
  420  FORMAT('0',2X,E13.6,13X,E13.6,13X,E13.6)
       WRITE(6,430)AREA2,BKFORN2,BKFOR2
  430  FORMAT(' ',2X,E13.6,13X,E13.6,13X,E13.6)
       WRITE(6,430)AREA3,BKFORN3,BKFOR3
       WRITE(6,430)AREA4,BKFORN4,BKFOR4
       WRITE(6,430)AREA5,BKFORN5,BKFOR5
       WRITE(6,430)AREA6,BKFORN6,BKFOR6
       WRITE(6,430)AREA7,BKFORN7,BKFOR7
       WRITE(6,430)AREA8,BKFORN8,BKFOR8
       WRITE(6,430)AREA9,BKFORN9,BKFOR9
       WRITE(6,430)AREA10,BKFORN10,BKFOR10
       WRITE(6,310)
  310  FORMAT('0','MEAN BREAKING FORCE(KN)=',18X,'S.D.=',22X,
      2'S.E. AT P EQ 0.95=')
       WRITE(6,320)MEANA,SDA,SEA
  320  FORMAT('+',26X,E13.6,12X,E13.6,25X,E13.6)
       WRITE(6,330)
```

```
330  FORMAT('0','MEAN BREAKING FORCE(KG)=',18X,'S.D.=',22X,
    3'S.E. AT P EQ 0.95=')
     WRITE(6,320)MEANB,SDB,SEB
     WRITE(6,340)
340  FORMAT('0','MEAN WORK OF FRACTURE(J)=',18X,'S.D.=',22X,
    4'S.E. AT P EQ 0.95=')
     WRITE(6,320)MEANC,SDC,SEC
     STOP
     END
     FINISH
****
```

Appendix 2. THE PLACEBO TABLETS

A2.1 Details of Formulated Placebo Tablets

Formula number	Components	Process Wet Granulation/ Direct Compression	Diameter mm	Shape
1	Lactose	WG/starch paste	7	Flat, Bevel edge single score line
2	"	"	8	"
3	"	"	9	"
4	"	"	10	"
5	"	"	11	"
6	Spray-dried lactose	DC	5	Flat, Bevel edge
7	Lactose, starch, silica	WG/starch paste	12	Flat, bevel edge single score line
8	Anhydrous lactose, Sta-Rx, Avicel PH 102.	DC	11	"
9	Dipac, Aerosil 200, Magnesium Stearate.	DC	7	Convex single score line
10	Lactose, Dipac, Aerosil, mag. stearate.	DC	7	"
11	Lactose, mannitol Aerosil, mag. stearate.	DC	7	"
12	S.D. lactose, Dipac, Aerosil, mag. stearate.	DC	7	"
13	Kollidon VA 64, Aerosil mag. stearate.	DC	7	"
14	Starch, lactose Aerosil, mag. stearate.	DC	7	"

A2.2 Calculation of the Cross-sectional Area of Bi-convex tablets.

Fig. A2.1 shows the cross-sectional area of a bi-convex tablet. The total cross-sectional area of the tablet is the sum of the area of the rectangle ABCD and the area of the sections either side of this rectangle. Assuming the convex surfaces of the tablet form part of the circumference of a circle, the area, A_s of the section outside the rectangle can be calculated from equation A2.1

$$A_s = \frac{\pi r^2 \theta}{360} - \frac{r^2 \sin \theta}{2} \qquad \text{Eq. A2.1}$$

where θ = the angle subtended, at the centre of the circle, by the chord BC.

Fig. A2.2 shows the cross-section of a bi-convex tablet with the complete circle of which the convex surface forms a part. The angle, $\theta/2$ may be calculated from equation A2.2.

$$\sin \theta/2 = \frac{D/2}{r} \qquad \text{Eq. A2.2}$$

where r = radius of the circle.
D = diameter of the tablet

r may be calculated by applying Pythagorus's theorem to the triangle OBE.

$$r^2 = (D/2)^2 + P^2 \qquad \text{Eq. A2.3}$$

since $p = r - s$

$$r^2 = (D/2)^2 + (r - s)^2$$

$$\therefore r^2 = (D/2)^2 + r^2 - 2rs + s^2$$

$$\therefore 2rs = (D/2)^2 + s^2 \qquad \text{Eq. A2.4}$$

$$\therefore r = \frac{(D/2)^2}{2s} + \frac{s}{2}$$

Substituting equation A2.4 in equation A2.2, the angle $\theta/2$ is given by equation A2.5

$$\theta/2 = \sin^{-1} \frac{2s\ (D/2)}{(D/2)^2 + s^2} \qquad \text{Eq. A2.5}$$

By substituting the calculated values of θ into equation A2.1, the cross-sectional area of the regions outside the rectangle ABCD may be calculated and the total cross-sectional area of the tablet, A is given by equation A2.6.

$$A = Dt_e + 2A_s \qquad \text{Eq. 2.6}$$

where D = diameter of the tablet

t_e = edge thickness of the tablet

A_s = area of the convex section.

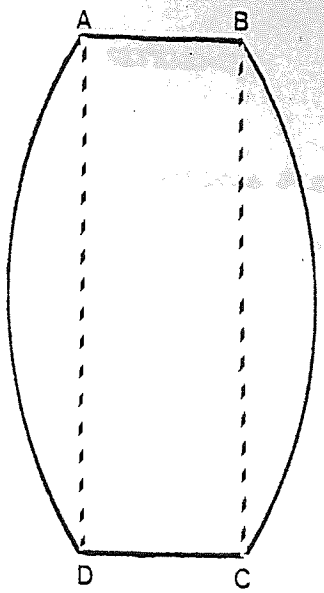

Fig. A2.1 The cross-section of a bi-convex tablet

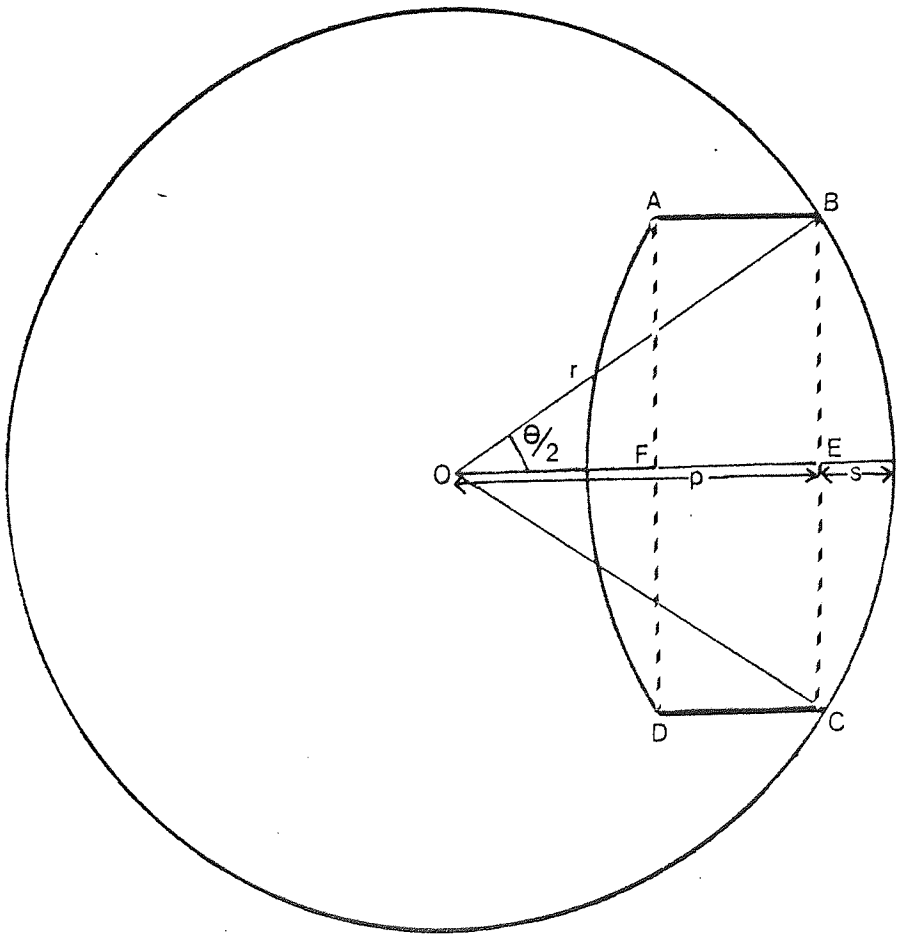

Fig.A2.2 The cross-section of a bi-convex tablet enclosed in the circle forming the convex surface. D is the diameter of the tablet and r is the radius of the circle.

$$s = \frac{\text{crown thickness} - \text{edge thickness}}{2}$$

REFERENCES

Allen, T. 1974 "Particle Size Measurement ". Chapman and Hall, London, 2nd Edition.

Alpar, O., Hersey, J.A. and Shotton, E. 1970 J. Pharm. Pharmac. 22 1S The compression properties of lactose.

Armstrong, N.A. and Griffiths, R.V. 1970. Pharm. Acta Helv. 45 583. Surface area measurement in compressed powder systems.

Aulton, M.E. 1977. Mfg. Chem. Aerosol News 48 (5) 28 Micro-indentation tests for pharmaceuticals.

Aulton, M.E., Travers, D.N. and White, P.J.P. 1973. J. Pharm. Pharmac. 25 79P Strain recovery of compacts on extended storage.

Baba, M. and Nagafuji, N. 1965 Annu. Rep. Shionogi Res. Lab. No. 15 147 Studies on tablet compression II. The stress relaxation and the strain recovery of tablets.

Barenbaum, R. and Brodie, I. 1959 J. Inst. Fuel 32 320 The tensile strength of coal.

Batuyios, N.H. 1966 J. Pharm. Sci., 55 727 Anhydrous lactose in direct tablet compression.

Birks, A.H. and Muzzaffar, A. 1971

Proceedings of Powtech '71: International Powder Technology and Bulk Granular Solids Conference. Harrogate, May 1971. Compaction of powders at low stresses.

Bockstiegel, G. 1973a.

Proceedings of the First International Conference on the Compaction and Consolidation of Particulate Matter. Brighton, October 1972. A.S. Goldberg Editor, Powder Advisory Centre, London, 1973. Probability aspects in powder compaction.

Bockstiegel, G. 1973b.

Reported discussion of the paper by Hersey, Cole and Rees, (1973).

Bolhuis, G.K., Lerk, H.T., Zalustra, A.H. and DeBoer, A.H. 1975

Pharm. Weekblad 110 317

Film formation by magnesium stearate and its effect on tabletting.

Bowden, F.P. and Tabor, D. 1964 "Friction and Lubrication of Solids. Vol 2". Clarendon Press, Oxford 1964.

Brook, D.B. and Marshall, K. 1968 J. Pharm. Sci. 57 481

"Crushing strength" of compressed tablets 1. Comparison of testers.

Carless, J.E. and Sheak, A. 1975 J. Pharm. Pharmac. 28 17
Changes in the particle size distribution during tabletting of sulphathiazole powder.

Carneiro, F.L.L.B and Barcellos, A. 1953.
R.I.L.E.M. Report No 13 97
Tensile strength of concretes

Cole, E.T., Rees, J.E. and Hersey, J.A. 1975
Pharm. Acta Helv. 50 28.
Relations between compaction data for some crystalline pharmaceutical materials

Cook, J. and Gordon, J.E. 1964. Proc. Roy. Soc.A. 282 508
A mechanism for the control of crack propagation.

Cooper, J. and Rees, J.E. 1972 J. Pharm. Sci. 61 1511
Tabletting research and technology.

Cottrell, A.H. 1949 "Progress in Metal Physics. Vol. 1"
Pergamon Press, London. 1949.

Cottrell, A.H. 1964. "The Mechanical Properties of Matter".
John Wiley and Son, New York 1964.

David, S.T. 1973. Ph.D. Thesis, University of Maryland.
Some physical and mechanical properties of direct compression fillers.

David S.T. and Augsburger, L.L. 1974. J. Pharm. Sci. 63 933
Flexure test for determination of tablet tensile strength.

David, S.T. and Augsburger, L.L. 1977. J. Pharm. Sci. 66 155
Plastic flow during compression of directly compressible fillers and its effect on tablet strength.

Deer, J.J. 1975. Chemist and Druggist 204 660
Misconceptions in tablet machine instrumentation.

Deer, J.J. 1977. Private communication.

Deer, J.J. and Finlay, P. 1973
Chemist and Druggist 200 110
The measurement of compaction force.

DeBlaey, C.J. 1972. Ph.D. Thesis, University of Leiden.
Measurement of the work involved in compression of pharmaceuticals.

Deblaey, C.J. and Polderman, J. 1970.
Pharm. Weekblad 105 241.
The quantitative interpretation of F-D curves.

DeBlaey, C.J., Weekers-Anderson, A.B. and Polderman, J. 1971
Pharm. Weekblad 106 893.
Formulation of a new compound with the aid of force-displacement curves.

Dieter, G.E. 1961 "Mechanical Metallurgy".
McGraw-Hill Hogakushi, International Students Edition, Tokyo, 1961.

Doelker, E. and Shotton, E. 1977. J. Pharm. Pharmac. 29 193
The effect of some binding agents on the mechanical properties of granules and their compression properties.

Endicott, C.J., Lowenthal, W. and Gross, H.M. 1961
J. Pharm. Sci. 50 343
New instrument and method for evaluating tablet fracture resistance.

Esezobo, S. and Pilpel, N. 1977. J. Pharm. Pharmac. 29 75
Compression behaviour of oxytetracycline formulations.

Fell, J.T. 1972. Ph.D. Thesis, University of Manchester
A comparative study of the properties of spray dried and crystalline lactose with special reference to their tabletting characteristics.

Fell, J.T. and Newton, J.M. 1968. J. Pharm. Pharmac. 20 657
The tensile strength of lactose tablets.

Fell, J.T. and Newton, J.M. 1970. J. Pharm. Pharmac. 22 247
The prediction of the tensile strength of tablets.

Fell, J.T. and Newton, J.M. 1970. J. Pharm. Sci. 59 688
Determination of tablet strength by the diametral compression test.

Fell, J.T. and Newton, J.M. 1971a. J. Pharm. Sci. 60 1428
Assessment of compression characteristics of powders.

Fell, J.T. and Newton, J.M. 1971b. J. Pharm. Sci. 60 1866
Effect of particle size and speed of compaction on density changes in tablets of crystalline and spray dried lactose.

Fox, C.D., Richman, M.D., Reier, G.E. and Shangraw, R.F. 1963.
Drug and Cosmet. Ind. 92 161
Microcrystalline cellulose in tabletting.

Goetzel, C.G. 1949. "Treatise on Powder Metallurgy"
Interscience Publishing Inc., New York, 1949.

Gooden, E.L. and Smith, C.M. 1940.
Ind. Eng. Chem. Analytical Ed. 12 479.
Measuring average particle diameter of powders.

Goodhart, F.W., Draper, J.R., Dancz, D. and Ninger, F.C. 1973.
J. Pharm. Sci. 62 297
Evaluation of tablet breaking strength testers.

Gordon, J.E. 1976. "The New Science of Strong Materials".
Walker and Co., New York, 2nd Edition, 1976.

Gregory, H.R., Rhys-Jones, D.C. and Phillips, J.W. 1959.
Nature 184 120
Compaction of briquettes.

Griffith, A.A. 1920. Phil. Trans. Roy. Soc. A221 163
The phenomena of rupture and flow in solids.

Gunsel, W.C. and Kanig, J.L. 1976. In "The Theory and Practice of Industrial Pharmacy". L. Lachman, H.A. Lieberman and J.L. Kanig - editors, Lea and Febiger, Philadelphia, 2nd Edition, 1976.

Hanus, E.J. and King, L.D. 1968. J. Pharm. Sci. 57 677
Thermodynamic effects in the compression of solids.

Hardman, J.S. and Lilley, B.A. 1973. Proc. Roy. Soc. Lond.
A333 183.
Mechanisms of compaction of powdered materials

Heckel, R.W. 1961a. Trans. Met. Soc. AIME 221 671
Density-pressure relationships in powder compaction.

Heckel, R.W. 1961b. Trans. Met. Soc. AIME 221 1001
An analysis of powder compaction phenomena.

Hersey, J.A., Bayraktar, G. and Shotton, E. 1967.
J. Pharm. Pharmac. 19 24S
The effect of particle size on the strength of sodium chloride tablets.

Hersey, J.A., Cole, E.T. and Rees, J.E. 1973.
Proceedings of the First International Conference on the Compaction and Consolidation of Particulate Matter.
Brighton, October, 1972.
A.S. Goldberg - Editor, Powder Advisory Centre, London, 1973. Powder consolidation during compaction.

Hersey, J.A. and Rees, J.E. 1970. Second Particle Size Analysis Conference, Society for Analytical Chemistry, Bradford, 1970.
The effect of particle size on the consolidation of powders during compaction.

Hersey, J.A. and Rees, J.E. 1971.
Nature Physical Science 230 96
Deformation of particles during briquetting.

Hersey, J.A., Rees, J.E. and Cole, E.T. 1973.
J. Pharm. Sci. 62 2060.
Density changes in lactose tablets.

Hiestand, E.N., Wells, J.E. Peot C.B. and Ochs, J.F. 1977.
J. Pharm. Sci. 66 511
Physical processes of tabletting.

Higuchi, T., Arnold, R.D., Tucker, S.J. and Busse, L.W. 1952
J. Am. Pharm. Ass. Sci. Ed. 41 93
The physics of tablet compression I.A
preliminary report.

Higuchi, T., Rao, A.N., Busse, L.W. and Swintosky, J.V. 1953
J. Am. Pharm. Ass. Sci. Ed. 42 194
The physics of tablet compression II.
The influence of degree of compression
on properties of tablets.

Higuchi, T., Shimamoto, T., Erikson, S.P. and Yoshiki, T. 1965.
J. Pharm. Sci. 54 11.
Physics of tablet compression XIV.
Lateral die wall pressure during and
after compression.

Hull, D. 1968. "Introduction to Dislocations". Pergamon Press,
Oxford, 1968.

Jaffe, J. and Foss, N.E. 1959.
J. Am. Pharm. Ass. Sci. Ed. 48 26
Compression of crystalline substances.

Jensen, A., Chenoweth, H.H. and Parker, B. 1974.
"Applied strength of Materials". McGraw-
Hill, Sydney, Metric Edition, 1974.

Jones, T.M. 1976. Paper presented to the International Pharmaceutical Federation, 1976. To be published in Die Pharmazeutische Industrie.
The influence of physical characteristics of excipients on the design and preparation of tablets and capsules.

Kanig, J.L. 1970. Paper presented to the Emcompress symposium. London. 1970.
New techniques in the direct compression of pharmaceutical tablets.

Kawakita, K., and Ludde, K.H. 1970/71 Powder Tech. 4 61
Some considerations on powder compression equations.

Kawakita, K. and Tsutsumi, Y. 1966. Bull. Chem. Soc. Jap. 39 1364.
A comparison of equations for powder compression.

Khan, K.A. and Rhodes, C.T. 1973.
Can. J. Pharm. Sci. 8 1
The production of tablets by direct compression.

Lazarus, J. and Lachman, L. 1966. J. Pharm. Sci. 55 1121.
Experiences in development of directly compressible tablets containing potassium chloride.

Lea, F.M. and Nurse, R.W. 1939. J. Soc. Chem. Ind. 58 277
The specific surface of fine powders.

Lerk, C.F.,Bolhuis, G.K. and DeBoer, A.H. 1974.
Pharm. Weekblad 109 945.
Comparative evaluation of excipients for direct compression, II.

Manudhane, K.S.,Contractor, A.M.,Kim, H.Y. and Shangraw, R.F.
1969. J. Pharm. Sci. 58 616.
Tablet properties of a directly compressible starch.

Newton, J.M. 1974. J. Pharm. Pharmac. 26 215.
The calculation of the tensile strength of tablets.

Newton, J.M.,Cook, D.T. and Hollebon, C.E. 1977.
J. Pharm. Pharmac. 29 247
The strength of tablets of mixed components.

Newton, J.M. and Rowley, G. 1972. J. Pharm. Pharmac. 24 256
A method of characterising tablet formation.

Newton, J.M.,Rowley, G.,Fell, J.T.,Peacock, D.G. and Ridgway, K.
1971. J. Pharm. Pharmac. 23 195S.
Computer analysis of the relation between tablet strength and compaction pressure.

Nutter-Smith, A. 1949a. Pharm. J. 109 194
Compressed tablets. 1, Resistance to "wear and tear".

Nutter-Smith, A. 1949b. Pharm. J. 109 227.
Compressed tablets. 2, Resistance to "wear and tear".

Okada, J. and Fukumori, Y. 1974. Chem. Pharm. Bull. 22 493
Compaction of powders 1. Compression under constant upper punch pressure and behaviour of particles filling in void.

Peltier, R. 1954. R.I.L.E.M. Report No 19.

Rankell, A.S. and Higuchi, T. 1968. J. Pharm. Sci. 57 574
Physics of tablet compression XV. Thermodynamic aspects of adhesion under pressure.

Rees, J.E. 1973. Boll. Chim. Farm. 112 216.
Physico-mechanical pre-formulation studies.

Rees, J.E. 1978. "Compaction of Particulate Material". Chapter in "Pharmaceutical Powder Technology", Marcel Dekker Inc., New York, 1978.
To be published.

Rees, J.E., Hersey, J.A. and Cole, E.T. 1970.
J. Pharm. Pharmac. 22 64S
The effect of rate of loading on the strength of tablets.

Rees, J.E., Rue, P.J. and Richardson, S.C. 1977.
J. Pharm. Pharmac. To be published.
Work of failure measurements on formulated tablets.

Rees, J.E. and Shotton, E. 1969. J. Pharm. Pharmac. 21 731
The effect of dimensions on the compaction properties of sodium chloride.

Rees, J.E. and Shotton, E. 1970. J. Pharm. Pharmac. 22 175.
Some observations on the ageing of sodium chloride compacts.

Rees, J.E. and Shotton, E. 1971. J. Pharm. Sci. 60 1704.
Effect of moisture in compaction of particulate material.

Reier, G.E. and Shangraw, R.F. 1966. J. Pharm. Sci. 55 510.
Microcrystalline cellulose in tabletting.

Richardson, E.G. 1957. "Relaxation Spectrometry".
North Holland, Amsterdam, 1957.

Ritschel, W.A.,Skinner, F.S. and Schlumpf, R. 1969.
Pharm. Acta Helv. 44 547.
Vergleichende untersuchungen mit verschiedenen geräten zur bestimmung der druckfestigkeit von tabletten.

Rowe, R.C.,Elworthy, P.H. and Ganderton, D. 1973.
J. Pharm. Pharmac. 25 12P
The effect of sintering on the pore structure and strength of plastic matrix tablets.

Rowe, R.C.,Elworthy, P.H. and Ganderton, D. 1974.
J. Pharm. Pharmac. 26 568
The calculation of the tensile strength of tablets.

Rudnick, W.C.,Hunter, A.R. and Holden, F.C. 1963.
Materials Res. and Standards 283 1963
An analysis of the diametral compression test.

Sakr, A.M. and Kassem, A.A. 1972.
Mfg. Chem. Aerosol News. 43 (11) 51 1972
Factors affecting tablet hardness and friability.

Schubert, H., Herrmann, W. and Rumpf, H. 1975.
Powder Tech. 11 121.
Deformation behaviour of agglomerates under tensile stress.

Seelig, R.P. and Wulff, J. 1946. Trans. Am. Min. Metall. Engrs.
166 492.
The pressing operation in the fabrication of articles by powder metallurgy.

Shlanta, S. 1963. Ph.D. Thesis, University of Michigan.
Time dependent effects in powder compaction

Shlanta, S. and Milosovich, G. 1964. J. Pharm. Sci. 53 563.
Compression of pharmaceutical powders 1. Theory and instrumentation.

Shafer, E.G., Wollish, E.G. and Engel, C.E. 1956.
J. Am. Pharm. Ass. Sci. Ed. 45 114
The "Roche" friabilator.

Shotton, E., Deer, J.J. and Ganderton, D. 1963.
J. Pharm. Pharmac. 15 106 T
The instrumentation of a rotary tablet machine.

Shotton, E. and Ganderton, D. 1960. J. Pharm. Pharmac. 12 87 T
The strength of compressed tablets. Part 1. The measurement of tablet strength and its relation to compression force.

Shotton, E. and Rees, J.E. 1966. J. Pharm. Pharmac. 18 160S
The compaction of sodium chloride in the presence of moisture.

Sinnott, M.J. 1958. "The Solid State for Engineers". John Wiley and Sons, New York, 1958.

Smallman, R.E. 1970. "Modern Physical Metallurgy". Butterworths, London, 3rd Edition, 1970.

Stewart, A. 1950. Engineering 169 203.
The pelleting of granular materials.

Summers, M.P., Enever, R.P. and Carless, J.E. 1976.
J. Pharm. Pharmac. 28 9
The influence of crystal form on the radial stress transmission characteristics of pharmaceutical materials.

Taylor, G.I. 1934. Proc. Roy. Soc. 145 1934.
The mechanism of plastic deformation of crystals.

Timoshenko, S.P. and Goodier, J.N. 1970.
"Theory of Elasticity". McGraw-Hill, New York, 3rd Edition, 1970.

Train, D. 1956. J. Pharm. Pharmac. 8 845.
An investigation into the compaction of powder.

Train, D. and Hersey, J.A. 1960. Powder Met. 6 20.
Some fundamental studies in the cold compaction of plastically deforming solids.

Travers, D.N. and Merriman, P.H. 1970. J. Pharm. Pharmac. 22 11S.
Temperature changes occurring during the compression and recompression of solids.

Windheuser, J.J., Misra, J., Erikson, S.P. and Higuchi, T. 1963. J. Pharm. Sci. 52 767. Physics of tablet compression XIII. Development of die wall pressure during compression of various materials.

York, P. and Baily, E.D. 1977. J. Pharm. Pharmac. 29 70 Dimensional changes of compacts after compression.

York, P. and Pilpel, N. 1972, J. Pharm. Pharmac. 24 47P The effect of temperature on the mechanical properties of some pharmaceutical powders in relation to tabletting.

York, P. and Pilpel, N. 1973. J. Pharm. Pharmac. 25 1P The tensile strength and compression behaviour of lactose, four fatty acids and their mixtures in relation to tabletting.